Investigating the migraine premonitory phase neural networks regulating migraine initiation

Sureda I Gibert, Paula

Awarding institution:
King's College London

Investigating the migraine premonitory phase: neural networks regulating migraine initiation

Doctor of Philosophy in Clinical Neuroscience Research

Paula Sureda Gibert
Student ID: 1309897

Abstract

Migraine is a highly disabling neurological disorder, with a prevalence of 15-18% worldwide, with a significantly higher incidence in women over men. It is characterised by a periorbital throbbing pain, together with a set of sensory disturbances; known as the premonitory phase, which can start up to 72 hours prior to the pain, and remain up to 48 hrs after pain resolution (postdrome phase). Clinical imaging data has shown central structures such as the hypothalamus and the locus coeruleus to be altered throughout the premonitory phase and in between attacks during resting conditions.

Orexinergic networks emerging from the lateral hypothalamus have demonstrated a differential modulatory action over migraine-associated nuclei such as the trigeminocervical complex in *in vivo* anaesthetised animal models. In this project we sought to further investigate the role of the orexinergic system in the regulation of trigeminal nociception and migraine-related symptoms using cre-dependent AAV-approaches. We observed a significant decrease in periorbital mechanical withdrawal thresholds in orexin-ablated mice, which is reflective of a sensitisation of the trigeminovascular system. This sensitisation was normalised by chronic intranasal orexin A, while further studies identified a potential mechanism of action of orexin A acting via the orexin 1 receptors in the locus coeruleus.

Downstream from the hypothalamus; orexinergic projections are known to densely innervate the locus coeruleus, which is the main source of noradrenaline in the central nervous system. Given the potential action of orexin A via the locus coeruleus and its ability to modulate trigeminal nociception we next sought to optimise a novel retrograde canine-adenovirus 2 (CAV2) vector to permit chemogenetic activation of locus coeruleus noradrenergic neurons in freely behaving rats. Clozapine-N-oxide-mediated activation of these noradrenergic neurons inhibited trigeminal nociception, while pilot work in awake rats highlighted increased mechanical withdrawal thresholds following locus coeruleus activation.

Together, the data in this thesis highlights the potential importance of hypothalamic orexinergic and locus coeruleus noradrenergic mechanisms in trigeminal nociception and migraine associated symptomatology (premonitory symptoms). Our data specifically

highlights the therapeutic potential of orexin A, targeted activation of the orexin 1 receptor and noradrenergic signalling as potential therapeutic strategies that have the potential to modulate migraine-related neural circuits likely responsible for increased attack susceptibility.

Table of Contents

Figures and Tables

Tables:

Figures:

Published papers and abstracts

Editorials:

Holland PR, Saengjaroentham C, Sureda Gibert P, Strother LC (2020) Medication overuse headache: Divergent effects of new acute antimigraine drugs. Cephalalgia, Aug;40(9):889-891

Holland PR, Sureda Gibert P, Vila Pueyo M (2020) Rapid uptake of sumatriptan into the brain: An ongoing question of blood-brain barrier permeability. Cephalalgia, Apr;40(4):327-329

Published abstracts:

Sureda Gibert P, M. Vila-Pueyo, S. Hirschberg, T. Pickering, P. J. Goadsby, P. R. Holland (2021). Noradrenergic networks modulating migraine-associated nociception. IHC 2021 Late breaking abstracts. *Cephalalgia*. 2021;41(1_suppl):228-287.

Sureda Gibert P, Strother LC, Goadsby PJ, Vincent M, Wafford KA, Gilmour G Holland PR (2020) Orexinergic networks regulating migraine initiation. Cephalalgia 40:1, 3-17

Sureda Gibert P, Goadsby PJ, Holland PR (2019) Investigating the migraine premonitory phase: orexinergic networks regulating migraine initiation. Cephalalgia, 39(1S) 1–337

Sureda Gibert P, Goadsby PJ, Holland PR (2018) Characterisation of an orofacial pain assessment device (OPAD) to measure facial allodynia. Cephalalgia 38:1 –115

Acknowledgements

Throughout the course of this PhD I have received great support and guidance. First and foremost, I would like to thank my main supervisor Dr. Philip Holland, for his endless guidance and reassurance at every step. His honest support inspired me to become an independent researcher and motivated me to pursue new perspectives by 'thinking outside the box'. Many thanks also to my other supervisors: Professor Peter Goadsby for his always insightful feedback, and Dr. Samuel Cooke for his expertise and helpful advice.

I would like to give a special thanks to Dr. Marta Vila-Pueyo, for her great mentorship both at a professional and personal level, and for the many hours of training in electrophysiological recordings. Many thanks to Dr. Lauren Strother for her huge help with the behavioural assessments and training. Thank you also to all my colleagues in the laboratory for their inspiring team work ethic. This really allowed us to bring out the best of each other and persevere during these especially challenging past few years.

I would also like to express my gratitude to my parents for their support and my sister Carla for her continued affection and encouragement despite the miles of distance between us. Finally, I would have not been able to complete this PhD without the encouragement and uplifting energy from my friends with whom I have had the joy to share my passion for science as well as my interests outside of research. They would often kindly remind me that is often how adaptable (and flexible) we are to change, that will ultimately make us thrive even in constantly changing and challenging circumstances, like those we have all experienced in the last few years. I am thus very grateful to have had the opportunity to adapt and learn, both academically and personally, and hope to continue to do so in the future.

I would also like to extend my thanks to our collaborators Professor Tony Pickering, Dr. Alessio Delogu, and Dr. Milena de Felice for their technical advice and expert suggestions. As well as the Medical Research Council Doctoral Training Partnership (MRC DTP) for their financial support throughout the years.

COVID-19 statement

As it will be briefly mentioned in this thesis; the COVID-19 pandemic has had an inevitable impact over the scope and presentation of this PhD work. Significant proportions of the planned work had to be removed due to an initial 6-month long pause in the research and posteriorly no access to animal resources due to an enforced loss of breeding (orexin-cre+ mouse line) and experimental (CAV-injected rats) cohorts. This did not allow us to finalise future planned work on retrograde targeting of orexinergic networks with the orexin-cre+ mouse line, as well as the implementation of a novel behavioural assay (OPAD) on both cohorts.

While some of the experiments were unable to be fully replicated within the time available; great efforts were made to alter the project plans to finalise achievable studies with the then-available resources. With this in mind; some preliminary data on these two promising studies on retrograde labelling and the OPAD-application have been included in the discussions of the thesis.

1. Chapter 1 – Introduction

1.1. Background

Migraine represents the most disabling of all neurological disorders, with respect to disability adjusted life years- and the 6th most disabling of all disorders globally (Collaborators 2019). It has a prevalence of 15-18% worldwide (Lipton, Bigal et al. 2007) and costs the UK economy approximately 6 billion per annum (McCrone, Seed et al. 2011). Patients are classically divided into two categories; migraine with aura (approximately 25-30% of cases) and the more common migraine without aura (2018, Headache Classification Committee of the International Headache Society (IHS)). However, more recently the complexity of migraine attacks has started to be defined (Goadsby, Holland et al. 2017). Individual attacks consist of severe debilitating, often unilateral headache with associated symptoms, including sensory hypersensitivity to light (photophobia), sound (phonophobia) and touch (allodynia). More recently a number of distinct attack phases have emerged, leading to novel insights into the potential mechanisms that predispose individuals to attack initiation (Bose, Karsan et al. 2018, Karsan, Bose et al. 2018, Karsan and Goadsby 2020, Karsan and Goadsby 2021). As such, it is now clear that migraine attack symptomatology can commence up to 48-72 hours before the onset of headache (Giffin, Ruggiero et al. 2003) and significantly outlast the headache phase (Karsan, Perez-Rodriguez et al. 2021).

Migraine attacks can be divided into several phases, the severity of which will differ from patient to patient. The earliest identifiable phase can commence hours to days before the onset of the headache phase and is termed the premonitory phase, or when combined with aura, alternatively termed the prodromal phase. Migraine sufferers often report increased fatigue, nausea, loss of appetite, yawning, neck stiffness, photophobia and phonophobia (Giffin, Ruggiero et al. 2003). The aura phase can precede the headache phase or occur after the onset of pain in approximately 30% of cases. Consisting of transient neurological features that are considered to result from an underlying cortical spreading depression (CSD) and commonly reported as visual disturbances, but they can be sensory or motor in nature (Charles and Brennan 2009, Charles and Baca 2013, 2018). The most salient feature of the attack is commonly the severe unilateral throbbing, head pain (headache phase) that can last for between 4 and 72 hours, and can be exacerbated

by movement. Following cessation of the headache phase migraine sufferers often report feeling “washed out”, with symptoms of marked fatigue and difficulty concentrating, termed the postdromal phase (Bose, Karsan et al. 2018, Karsan, Perez-Rodriguez et al. 2021).

The presence of a premonitory phase that consists of several neurological symptoms suggests a central rather than peripheral vascular-dependent dysregulation and thus highlights migraine as a complex disorder of brain sensory processing (Goadsby, Holland et al. 2017). This hypothesis is supported by several neuroimaging studies that have identified alterations in key cortical, diencephalic and brainstem regions prior to and during the headache phase (Afridi, Kaube et al. 2005, Afridi, Giffin et al. 2005, Afridi, Matharu et al. 2005, Afridi and Goadsby 2006, Maniyar, Sprenger et al. 2014, Schulte and May 2016). Observed alterations in diencephalic and brainstem brain regions (Afridi, Giffin et al. 2005, Afridi, Matharu et al. 2005, Maniyar, Sprenger et al. 2014) suggest a dysfunctional integration of trigeminal afferent signals and consequentially increased susceptibility to trigger an attack (Stankewitz, Aderjan et al. 2011). Migraine is therefore a multisensory system disorder (Schwedt 2013, O'Hare 2017, Brennan and Pietrobon 2018), likely resulting from imbalances in CNS homeostatic mechanisms, that set a threshold for attack triggering, experienced as a diverse array of premonitory symptoms that can predict ensuing headache onset (Giffin, Ruggiero et al. 2003). Imaging studies during this premonitory phase has revealed increased activation of the hypothalamus, periaqueductal gray (PAG) and dorsal pons (Maniyar, Sprenger et al. 2014), key migraine-related nuclei in which their functional coupling is further altered in the days preceding an attack (Schulte and May 2016), highlighting key underlying alterations to CNS neural networks/function prior to migraine-related head pain.

1.2. MIGRAINE EPIDEMIOLOGY AND HEADACHE PAIN

1.2.1. Epidemiology

With over one billion worldwide sufferers, migraine is currently ranked as the second most disabling condition per life adjusted years (Collaborators 2019), with a 2:1 greater prevalence in women compared to men (Pavlovic, Akcali et al. 2017, Vetvik and MacGregor 2017). This prevalence is highest between the ages of 20-50, resulting in

migraine being ranked as the most disabling condition worldwide in terms of years lost to disability in young females (Steiner, Stovner et al. 2020). An issue that is complicated by poor patient awareness and misdiagnosis, within several countries (Viana, Khaliq et al. 2020), leading to an unnecessary increase in socioeconomic cost and disease burden. This burden impacts individual sufferers across their lifespan, with direct impacts on academic performance and social interactions (Buse, Lipton et al. 2018), again becoming more frequent in females after the onset of puberty. While in adulthood, decreased work productivity, loss of career potential and effects over relationships are increasingly reported (Steiner, Stovner et al. 2014).

There is a high socioeconomic impact on healthcare services; with 50-111€ billion spent in Europe (in 2011) and 23$ billion in the US (in 2007). Contrary to other neurological conditions, around two thirds of these expenses are associated to indirect costs that include lost productivity and absenteeism from work. Direct costs instead include; outpatient care, acute medications and hospitalizations. While these expenses have been largely quantified; the financial impact from effects over career potential, family impact and personal relationships remain significantly underreported, suggesting an even larger economic impact (Ashina, Katsarava et al., 2021). The complexity of migraine and the fact that migraine-related pain is exacerbated by everyday tasks such as movement and exposure to lighting (2018, Headache Classification Committee of the International Headache Society (IHS)) highlight the detrimental impact it can have on an individual, with the most common abortive strategy to withdraw to a dark quiet room to allow the headache pain to resolve. This, together with the general lack of awareness from non-sufferers; has caused an often undervalued effect of loneliness and sense of helplessness for the sufferer; making the disorder even more disabling overall. Not surprisingly, this is directly correlated to the frequency of headache attacks with a substantially greater impact in those suffering from high frequency or chronic migraine, defined as more that 15 headache days per month, with at least 8 of these are migraineous in nature (2018, Lui, Young et al. 2020).

1.2.2. Migraine Therapy (acute and preventive)

Migraine therapy has undergone somewhat of a revolution over the past decade with significant advances in drug approval during my PhD studies. This has heralded the

arrival of several novel acute and preventive therapies, with further blurring of the boundaries between these two classical treatment strategies. Prior to this, many therapies were orphaned from other conditions, used off license and had the potential for considerable side effects or limited efficacy. As noted, these therapies were often divided into two categories; those administered to treat the individual attack (acute therapies, **table 1.1**) and those taken regularly to reduce attack frequency (preventive therapies, **table 1.2**).

Table 1.1. Acute therapies for migraine.

Non- specific therapies	**Specific medications**
Analgesics (non-steroidal anti-inflammatory drugs and combination analgesics) Antiemetics Opioids Corticosteroids Dopamine antagonists	Ergotamine Dihydroergotamine (DHE) Triptans (5-$HT_{1B/D}$ receptor agonists) Lasmiditan (5-HT_{1F} receptor agonists) Rimegepant, Atogepant, Ubrogepant (Calcitonin gene-related peptide receptor antagonists)

Acute treatments include non-specific analgesics, non-steroidal anti-inflammatory drugs (NSAIDS), the triptans: specific 5-$HT_{1B/1D}$ receptor agonists, lasmiditan: 5-HT_{1F} receptor agonist and the newly approved gepants: small molecule calcitonin gene-related peptide (CGRP) receptor antagonists (Diener, Charles et al. 2015). When considering acute therapies, it is critical to consider attack frequency and potential medication overuse, as the frequent use of acute anti-migraine therapies including the triptans (> 10 days per month) or certain NSAID's (>15 days per month) is known to increase the risk of developing a state termed medication overuse headache, characterised by a transition to more frequent attacks and a greater risk of migraine chronification (2018, Headache Classification Committee of the International Headache Society (IHS)). Importantly, recent preclinical studies have suggested that lasmiditan shares a potential medication overuse risk, while the novel CGRP receptor antagonist drugs have a significantly reduced risk (Navratilova, Behravesh et al. 2020, Rau, Navratilova et al. 2020, Saengjaroentham, Strother et al. 2020).

As noted previously, the vast majority of preventive treatments have been repurposed for migraine from other indications such as epilepsy, arterial hypertension or depression, explaining the heterogeneity highlighted in **Table 1.3**. These include Beta-adrenergic blockers (propranolol, metropolol), anticonvulsants (Topiramate, valproate), antidepressants (amitryptiline, fluoxetine) or calcium channel blockers (Flunarizine) (Sprenger, Viana et al. 2018). Given the variability in which migraine manifests in each patient; with high variability in headache attack frequency even throughout the lifespan, and the increasing need to develop personalized therapies, these drug targets are slowly being complemented with, but not replaced, by more novel therapies (Moreno-Ajona, Perez-Rodriguez et al. 2020). These therapies which target CGRP signalling, a key neuropeptide released during migraines (Goadsby, Edvinsson et al. 1990), are rewriting the classical distinction between acute and preventive therapies, with both Rimegepant and Atogepant approved for both. While recent unpublished studies have highlighted a rapid onset of effect for the preventative CGRP antibody Eptinezumab, suggesting it has significant potential as an acute-anti-migraine therapy.

Currently available CGRP-targeted approaches act by blocking CGRP or its receptor in a highly specific manner, leading to few side effects and importantly, no vasoconstriction. The first line of CGRP-blocking compounds developed were small molecules known as gepants, which act as acute migraine treatments by blocking the CGRP receptor (Brain & Grant, 2004, Russo & Dickerson, 2006). Despite their high efficacy; first generation gepants (olcegepant, telcagepant, MK-3207 and BI 44,370 TA) were discontinued due to liver toxicity and issues with the oral solution. However, recent efforts have focused on developing alternate gepants (rimegepant, ubrogepant and atogepant) with increased compound solubility and no toxic side effects. These were initially developed for the acute treatment of migraine, but are being evaluated for their prophylactic properties as preventive; Rimegepant (Croop, Lipton et al., 2021) and Atogepant (Ailani, Lipton et al., 2021) (Schwedt, Lipton et al., 2022) **(Table 1.2).**

In total four monoclonal antibodies have been developed, these are human immunoglobin monoclonal antibodies which block the receptor (Erenumab, Galcanezumab and Fremeenezumab) or CGRP (Eptinezumab) to prevent its binding to the CGRP receptor **(Table 1.2.).** Targeting of the CGRP pathway has proven highly effective in both episode and chronic migraine sufferers, having shown significant

reduction in monthly headache days, as well as reduction in disabling symptoms. CGRP receptors are expressed both peripherally in almost every organ in the body, including the smooth muscle of the arterial system, and extensively throughout the CNS (Brain & Grant, 2004, Russo & Dickerson, 2006, Recober & Russo, 2009, Raddant & Russo, 2011). As such; CGRP release from afferent sensory neurons over the dural vasculature is thought to underlie the characteristic sensitisation of the trigeminovascular system during migraine headache. Similarly, central CGRP action likely contributes to enhanced sensitivity to sensory stimuli (i.e. to light: photophobia), as well as central sensitisation of pain-associated structures (Recober et al., 2009) (Recober et al., 2010).

Table 1.2. CGRP-based therapies for migraine. EM: Episodic Migraine, CM: Chronic Migraine

Monoclonal antibodies	Type	Target	Phase	References
Erenumab	Human	CGRP receptor	Phase 3/4: EM	Ferrari, Reuter at al., 2021 Goadsby, Reuter et al., 2021 Reuter, Ehrlich et al., 2022
Galcanezumab	Humanized	CGRP receptor	Phase 3: EM	Stauffer, Dodick et al., 2018 Skljarevski, Matharu et al., 2019 Detke, Goabsby et al., 2018
Fremenezumab	Humanized	CGRP receptor	Phase 3: EM and CM	Ferrari, Diener et al., 2019 Goadsby, Silberstein et al., 2020 Ashina, Cohen et al., 2021
Eptinezumab	Humanized	CGRP ligand	Phase 3: CM and EM	Lipton, Goadsby et al., 2020 Ashina, Saper et al., 2020 Kudrow, Cady et al., 2021
Gepants				
Rimegepant		CGRP receptor	Phase 2/3: preventive Phase 3: acute	Croop, Lipton et al., 2021 Marcus et al., 2014 Croop, Goabdsby et al., 2019 Lipton, Croop et al., 2019
Atogepant		CGRP receptor	Phase 3: preventive	Ailani, Lipton et al., 2021

Despite the emerging potential of inhibiting this pathway as a migraine-specific preventive treatment, the mechanisms of action of these therapies, and whether they might preferentially act peripherally or centrally, remains unclear. Monoclonal antibodies have a low permeability ratio of 1:1000 (Felgenhauer, 1974), making it unlikely to cross the Blood Brain Barrier (BBB), thus suggesting a preferential peripheral CRGP action. However, clinical imaging data has identified decreased central functional responses in response to trigeminal stimulation; two weeks after the administration of Erenumab; a CGRP mAb. These reported a decrease in activity in the thalamus, the middle temporal gyrus and right lingual gyrus and interestingly; a decrease in hypothalamic activity in Erenumab responders compared to non-responders (Ziegeler, Mehnert et al., 2020). With this; and having identified CGRP-expressing thalamic neurons which are able to respond to; and converge dural and light-incoming information and potentially be involved migraine-associated photophobia; a partial central action through less permeable brain regions such as the area postrema (Shapiro and Miselis, 1985) or the choroid plexus (Johnson, Morin et al., 2019) is also plausible (Summ, Charbit et al. 2010) (Noseda, Kainz et al. 2010). Interestingly, preclinical models have reported a degree of penetrance of other CGRP mAbs such as Galcanezumab into the CNS; with 0.34% found in the hypothalamus (Johnson, Morin et al., 2019).

Table 1.3. Preventative therapies for migraine by drug class. Based upon (Goadsby, Lipton et al. 2002, Sprenger, Viana et al. 2018).

Drug Class	**Agents**
Anticonvulsants	Valproate, Topiramate, Gabapentin
Antidepressants	Amitriptyline, Fluoxetine, Dosulepin (dothiepin), Nortriptyline, Venlafaxine
β-blockers	Propranolol, metoprolol
Calcium channel blocker	Flunarizine
Serotonin antagonists	Pizotifen, Methysergide
Other compounds	Lisinopril, Candesartan
Nutraceuticals	Riboflavin, Coenzyme Q10, Feverfew, Butterbur
Calcitonin gene-related peptide (CGRP) antibodies	Galcanezumab, Eptinezumab, Fremanezumab

Calcitonin gene-related peptide (CGRP) receptor antibodies	Erenumab
CGRP receptor antagonists	Rimegepant, Atogepant

1.2.3. Clinical phenotype

Migraine attacks are characterized by an often unilateral throbbing headache pain that can vary from moderate to severe and are commonly localized in the periorbital area behind the eye. Importantly, prior to the headache arising, patients can also suffer from a set of sensory disturbances including photophobia, phonophobia, allodynia, and osmophobia in conjunction with difficulty concentrating and marked fatigue (2018, Headache Classification Committee of the International Headache Society (IHS)). Importantly, as noted earlier, these symptoms can commence up to 72 hours before the headache attack and when carefully monitored can prove predictive of an ensuing attack of head pain in approximately 70% of cases (Giffin, Ruggiero et al. 2003). As such, they represent the earliest currently identifiable markers of acute attack onset, with important implications for understanding the underlying mechanisms of attack initiation and novel therapies that have the potential to act prior to the headache phase. The timing of treatment, especially in the case of the triptans has shown to be of key importance to increase their efficacy, resulting in the "treat when mild" recommendation (Cady, Sheftell et al. 2000).

The migraine cycle is therefore organized into different phases (**Figure 1.1**): interictal (in between attacks), premonitory (or ictal); comprising the emerging neurological symptoms, headache (ictal) and the postdrome (post-ictal); in which symptoms can persist up to 48 hours after headache resolution.

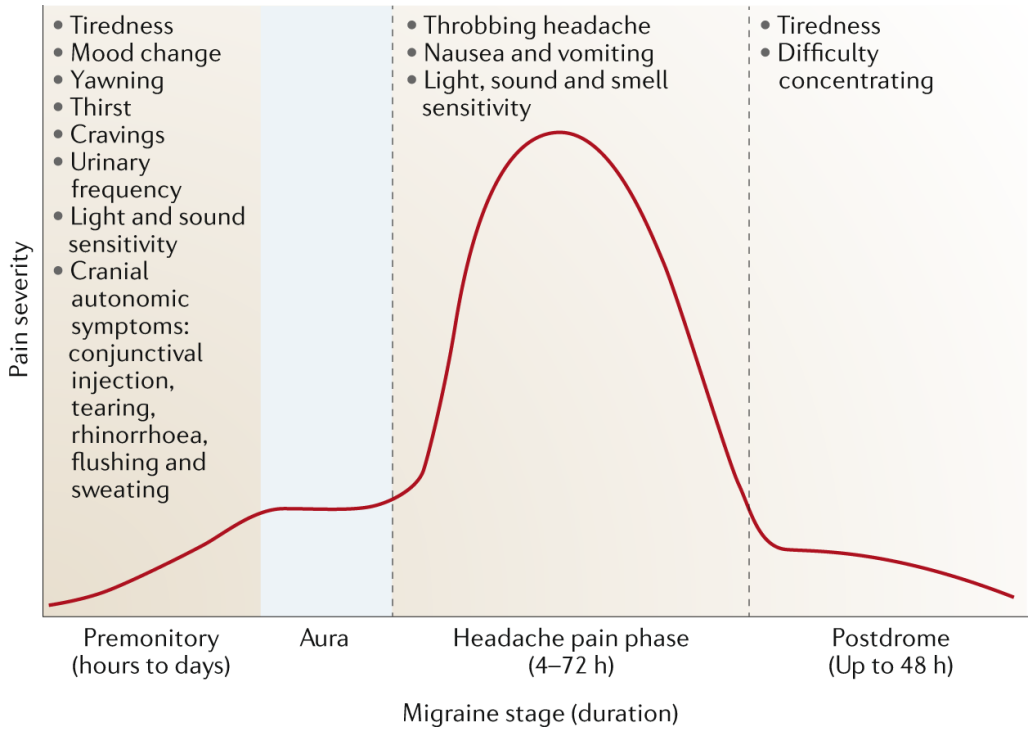

Figure 1.1: The different phases of a migraine attack. Premonitory symptoms including abnormal fatigue and alterations in homeostatic mechanisms can start hours or days before the headache pain phase. The headache pain phase can further coincide with or be preceded by aura in up to 30% of cases. Finally, following the cessation of the headache pain phase patients report postdromal symptoms including marked fatigue and difficulty concentrating (Karsan and Goadsby 2018).

A wider classification can also organize patients into those with ‘aura’, a set of more cortical-associated transient neurological symptoms. In comparison to the premonitory symptoms: these are manifested as visual, sensory and motor disturbances (2018, Headache Classification Committee of the International Headache Society (IHS)). The underlying mechanism of aura is strongly considered to be cortical spreading depression (CSD) (Charles and Brennan 2009, Charles and Baca 2013) which represents a spreading wave of depolarization across the cerebral cortex (Leao 1944, Leao 1947, Hadjikhani, Sanchez Del Rio et al. 2001). While the direct link between CSD and migraine remains contested, several preclinical studies have shown a link between CSD and activation of the trigeminovascular system (Zhang, Levy et al. 2011, Karatas, Erdener et al. 2013) at the level of the trigeminal nucleus caudalis (TNC). Alternatively, CSD has been shown to induce alterations in central pain modulating regions, suggesting no requirement for peripheral nociceptor activation to induce trigeminovascular activation (Lambert, Truong et al. 2011, Goadsby and Akerman 2012).

The phenomenon of CSD was initially identified in 1944 by Leao and was described as a wave of depolarization spreading across the cortex and consequential decrease in spontaneous activity (Leao, 1944). Despite the unclear origin of CSDs; a cascade release of amino acids and neurotransmitters such as Glutamate, are thought to trigger and maintain 30-60 second-long waves of neural and glial depolarisation through N-methyl-D-aspartate receptors (NMDARs)-activation (Hernández-Cáceres et al., 1987) (Marrannes, Willems at al. 1988) (Lauritzen & Hansen, 1992) (Nellgard and Wieloch, 1992). Downstream molecular events trigger increased extracellular potassium current, and intracellular sodium, chloride and calcium, causing ionic direct current (DC) shifts which can then be recorded extracellularly preclinically (Herreras & Somjen, 1993). Interestingly, animal genetic models of migraine such as Familial Hemiplegic migraine (FMH) which have shown increased susceptibility to trigger CSD events; involve mutations in neuronal Na+ and Ca+2 channels or glial Na+/K+ pump channels (Hansen, 2010). Preclinically recorded CSDs are immediately accompanied by an increase (1-2 minutes) and posterior significant decrease (1-2 hrs) in blood flow (Lauritzen, Dreier et al. 2011). Similarly; clinical BOLD fMRI studies have uncovered key temporal correlations between the aura symptoms and the decreased blood flow patterns observed as ischemic-like events (Lambert & Michalicek, 1994). BOLD hypoperfusion events in the visual cortex also appear strikingly temporally and spatially correlated with visual aura perturbances (Hadjikhani, Sanchez Del Rio et al. 2001). Abnormal increases in regional cerebral blood flow have also been associated with the resolution of the aura and posterior headache initiation (Olesen, Friberg et al., 1990).

The initiation of aura symptoms in patients can however vary throughout the migraine cycle; with the symptoms primarily emerging before the headache pain (36%) but also after it has resolved (9%) (Viana, Linde et al. 2016, Viana, Sances et al. 2017). Having said that; the relationship between the aura and the headache becomes more complex as observed in ‘acephalic migraine’; in which patients suffer from aura without an ensuing headache. Further; human provocation models that use nitroglycerin, CGRP and associated neuropeptides to induce an experimental migraine attack; are able to trigger the migraine headache but not the aura, in patients with migraine with aura (Christiansen, Thomsen et al., 1999). Despite the unknown mechanisms by which the aura is associated to the headache attack, several clinically used preventive treatments are known to decrease CSD frequency when administered chronically in rodents (Ayata, Jin

et al. 2006). As such, it is likely that aura and headache frequency share some common underlying risk factors and pathophysiological actions that can predispose individuals to repeated bouts of both aura and headache.

1.3. MIGRAINE HEADACHE AND THE TRIGEMINOVASCULAR SYSTEM

The relevance of the trigeminovascular system in migraine headache was initially observed by Ray and Wolff (Ray and Wolff 1940). Distention of the cerebral arteries and subsequent activation of the sensory afferents innervating them in conscious patients induced a characteristic referred pain that was localised to the periorbital area (around/behind the eye, **Figure 1.2**).

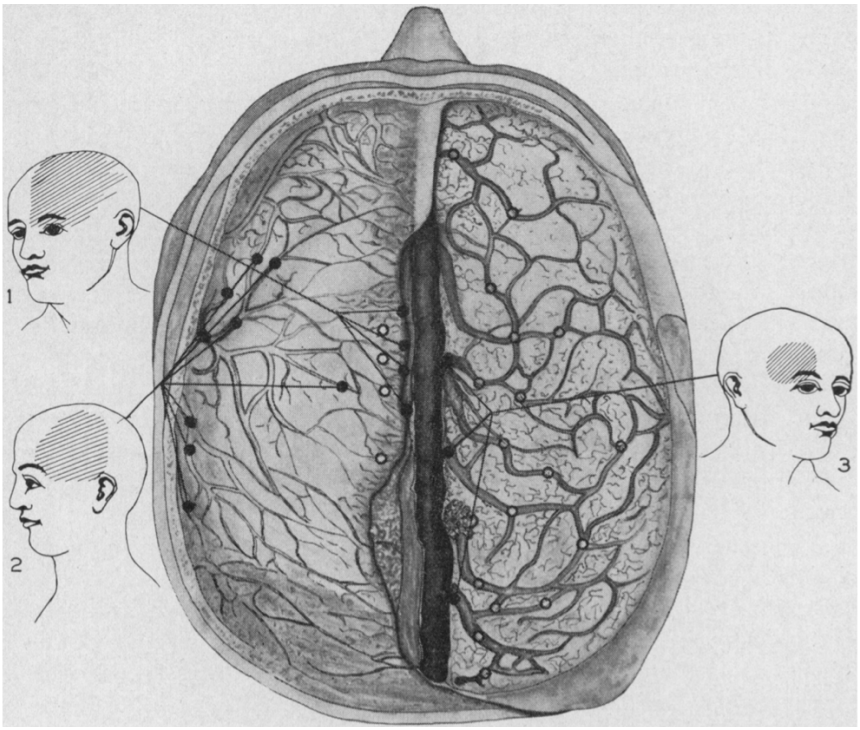

Figure 1.2. Experimental studies in awake conscious humans. They identified referred pain in the periorbital dermatome of the face following distention of cranial arteries and their innervation (Ray and Wolff 1940).

These sensory afferents represent the peripheral terminals of pseudo-unipolar neurons arising from the trigeminal ganglion (TG) whose central projections terminate in the dorsal horn of the trigeminal nucleus caudalis (TNC) and the first and second cervical levels (C1 and C2) (Penfield and McNAUGHTON 1940, Ray and Wolff 1940,

McNaughton and Feindel 1977). Together, the TNC, C1 and C2 regions are termed the trigeminocervical complex (TCC). Peripheral nociceptive afferents from the TG mainly consist of Aδ and C fibres forming three branches: the ophthalmic (V1), the maxillary (V2) and the mandibular (V3) territories that are distributed somatotopically across the face. The ophthalmic branch is considered the most pertinent for migraine-related pain given its innervation of the facial skin, eye, ethmoid and sphenoid sinuses, dura mater of the falx cerebri, tentorium cerebelli and the dura matter surrounding the middle meningeal artery (MMA) and superior sagittal sinus (SSS). The latter of which represent two common durovascular structures targeted experimentally to elicit activation of the trigeminal sensory innervation (Harriott, Strother et al. 2019, Vila-Pueyo, Strother et al. 2019, Holland, Sureda-Gibert et al. 2020, Vila-Pueyo, Page et al. 2021).

Primary afferents terminating in the TCC synapse on second order neurons that give rise to the trigeminothalamic tract (Burstein, Cliffer et al. 1987, Burstein, Cliffer et al. 1990), from which trigeminal sensory information is distributed widely to diverse cortical regions through key ascending pathways (Noseda, Jakubowski et al. 2011). In addition, trigeminal sensory information is conveyed to several key nuclei throughout the brainstem and diencephalon (**Figure 1.3**) (Matsushita, Ikeda et al. 1982, Shigenaga, Nakatani et al. 1983, Burstein, Cliffer et al. 1987, Burstein, Cliffer et al. 1990, Williams, Zahm et al. 1994, Malick and Burstein 1998, Malick, Strassman et al. 2000, Veinante, Jacquin et al. 2000, Malick, Jakubowski et al. 2001, Liu, Broman et al. 2008, Liu, Broman et al. 2009). While the primary thalamic target is the ventroposteromedial nuclei (VPM) (Zagami and Lambert 1990, Zagami and Lambert 1991, Burstein, Yamamura et al. 1998, Burstein, Jakubowski et al. 2010), trigeminal sensory information is also integrated and relayed via several thalamic sub nuclei, including the higher order posterior thalamic nuclei. Highlighting the complexity of trigeminal nociceptive processing, second order neurons from the TCC also target key brainstem nuclei, including the periaqueductal gray (PAG), locus coeruleus (LC), hypothalamic, including the lateral, anterior and posterior nuclei as well as several medullary nuclei, including the rostral ventromedial medulla (RVM) and parabrachial nucleus (PB). In agreement with this anatomical innervation of the TCC; animal studies have mapped this system by stimulating durovasculature nociceptive afferents that innervate the Middle Meningeal Artery (MMA) and/or Superior Sagittal Sinus (SSS). Chemical and electrical stimulation of these structures has enabled detailed mapping of neuronal activation patterns throughout the trigeminovascular system

(Kaube, Keay et al. 1993, Strassman, Mineta et al. 1994, Goadsby and Hoskin 1997, Sugimoto, He et al. 1998, Hoskin, Bulmer et al. 1999).

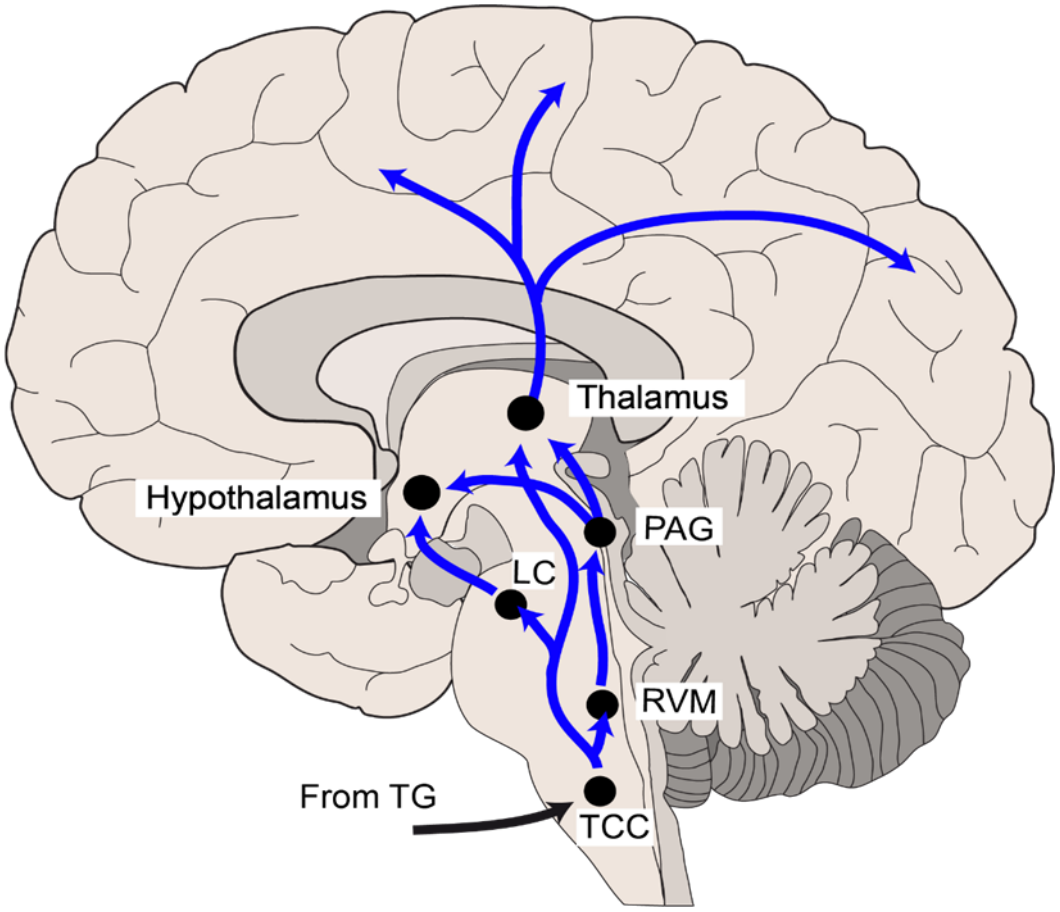

Figure 1.3. Ascending projections of the trigeminovascular system. Trigeminal incoming information is transmitted through second order neurons in the trigeminocervical complex (TCC) which project to diverse medullary, brainstem, diencephalic and cortical regions for the integration of trigeminal pain. The primary ascending projections from the TCC synapse on third order neurons in the ventroposteriomedial and posterior thalamic nuclei amongst others, en-route to diverse cortical regions including the somatosensory and visual cortices. Direct and indirect projections from the TCC additionally terminate in several discrete brain nuclei including the rostral ventromedial medulla (RVM), locus coeruleus (LC), periaqueductal grey (PAG) and the hypothalamus (blue arrows). (Adapted from Goadsby, Holland et al. 2017).

1.3.1. Ascending pathways from the TCC: functional importance.

The trigeminothalamic tract conveys trigeminal sensory information to several key nuclei involved in the integration and modulation of nociception (Goadsby, Holland et al. 2017). The integration of this information at a cortical level is of importance given the

range of cortical-associated symptoms observed during an attack: from cognitive imbalances, to anxiety-related responses and autonomic symptoms (Pareja-Angel and Campo-Arias 2004, Gelfand, Reider et al. 2013, Gil-Gouveia, Oliveira et al. 2016, Peres, Mercante et al. 2017, Pearl, Dumkrieger et al. 2020). These structures form a sensory processing and modulating network that functions in tandem to underpin the pain and associated symptomatology of migraine. The thalamus for instance, is key for integrating incoming nociceptive and other sensory-associated inputs. Clinical imaging studies have identified altered structural and functional connectivity in migraineurs (Magon, May et al. 2015, Coppola, Di Renzo et al. 2016), while thalamic activity is increased during the headache phase (Afridi, Giffin et al. 2005, Coppola, Di Renzo et al. 2016). The reported altered functional activity patterns represent the resulting activation from a stimulus; which is often a painful stimulus in the context of migraine (i.e. ammonia), in previously 'seeded' or established regions of interest (ROIs). The activation among established regions can then be time matched and thus phase-fixed to the specific stimulus to determine the functional relationship among different regions of interest. Interestingly, while these averaged connectivity patterns have been often compared to control non-migraine subjects; recent work has focused on exploring the changes in a migraine brain only throughout a 30-day time period (Schulte and May, 2016). Allowing us to understand the biological importance of such ROI-to-ROI relationship changes before, during and after an attack without subject variability. The outcome of such phase-locked changes appears to vary depending on the ROIs studied; with abnormal increases in connectivity between the hypothalamus and migraine-associated nuclei prior a migraine attack (Schulte and May, 2016), but decreases in connectivity between the thalamus and the visual cortex (Zou, Long et al., 2009). Dysregulation of thalamic sensory processing is considered to result in central sensitisation in migraine and underlie the occurrence of cephalic and extracephalic allodynia by transforming it into whole-body allodynia/hyperalgesia, during the headache attack (Burstein, Jakubowski et al. 2011). Indeed, altered functional connectivity patterns within the posterior thalamus, as well as with regions involved in the emotional component of pain; have been reported in patients with allodynia, compared to those without allodynia (Wang, Chen et al. 2015). This involved a reduced connectivity between the posterior thalamus and the ipsilateral limbic area and the dorsal medial prefrontal cortex (PFC), but increased connectivity between the thalamus and the contralateral ventral medial PFC, in patients with allodynia compared to those without. And interestingly, correlation analysis among these

connectivity patterns correlated well with the severity of allodynia. The thalamus is also considered to play a key role in the integration of emotional and cognitive aspects of migraine, with the thalamus and amygdala abnormally active in response to negative emotional stimuli (Wilcox, Veggeberg et al. 2016) in migraineurs. While altered functional connectivity between the thalamus and attention-associated networks in the interictal phase, has been associated with the commonly reported cognitive impairments (Coppola, Di Renzo et al. 2016, Wilcox, Veggeberg et al. 2016).

The mechanisms behind thalamic sensory functional integration have an added layer of complexity with known differential inter-thalamic processes. Sub-thalamic nuclei have differential roles in integrating multimodal information, with the VPM but not the dLGN responding to bimodal stimulation (light and touch) and enhancing its coupling with primary visual cortices (V1) (Herrera, Maysinger et al. 1993). Of particular importance to the current thesis, the VPM receives dense noradrenergic innervation from the brainstem LC (Westlund, Sorkin et al. 1990). As such, the LC is ideally placed to modulate trigeminal nociceptive processing across a wide array of regions, including the primary sensory integration at the level of the VPM (Simpson, Altman et al. 1997).

Clinical imaging studies have also identified the brainstem as a key region involved in the initiation of migraine. Largely focussing on the PAG, brainstem activation is observed during experimentally triggered and spontaneous migraine attacks (Weiller, May et al. 1995, Bahra, Matharu et al. 2001, Afridi, Matharu et al. 2005). While limited resolution limits the precise identification of brainstem nuclei, preclinical studies have highlighted increased c-Fos immunoreactivity in the PAG (Hoskin, Kaube et al. 1996) which supports its central role. The fine anatomical precision of c-Fos mapping following trigeminovascular activation has further highlighted trigeminal-evoked activation in the LC (Ter Horst, Meijler et al. 2001), rostral medulla and causal pons: trigeminal nucleus and superior salivatory nucleus (Knight, Classey et al. 2005). Indeed, a unilateral functional activation of the brainstem ipsilateral to the throbbing headache pain in patients, further supports the contribution of these structures in the pathogenesis of migraine-related pain (Afridi, Matharu et al. 2005).

Incoming ascending trigeminal nociceptive information is also directly processed directly by other relay nuclei such as the: Parabrachial nucleus (PB), the amygdala or the

hippocampus: which are thought to contribute to the high comorbidity of migraine with mood disorders such as anxiety and depression. Relevant direct functional connections have been observed along the trigemino-hypothalamic tract, with increased c-Fos expression in the supraoptic nucleus and posterior hypothalamus following trigeminovascular activation (Benjamin, Levy et al. 2004).

Interestingly; these altered hypothalamic and brainstem functional patterns exist during the interictal and premonitory phase of migraine (Maniyar, Sprenger et al. 2014, Schulte and May 2016). This persistent alteration in key hypothalamic and brainstem nuclei that is enhanced early prior to the headache phase suggests an already-existing central nervous system dysregulation as oppose to a simple response to ongoing pain. Such findings support alterations in key central neural networks as the primary mechanisms that sets the threshold for the initiation of an acute migraine attack (Goadsby, Holland et al. 2017). Great efforts have recently focused on understanding the role of these networks in the migraine disorder as a whole; and not simply the headache phase.

1.3.2. Descending pathways modulating the trigeminal nociception

The TCC represents the primary interface between the peripheral trigeminal sensory afferents and the central nervous system and as such represents a key region for the modulation of trigeminal nociception. However, the trigeminovascular system is subject to modulation at several levels. Arising in discrete cortical regions, these descending projections terminate in multiple diencephalic (thalamus and hypothalamus) and brainstem regions (PAG, pontine, RVM and LC) (Dimitriadou, Buzzi et al. 1991, Strassman, Raymond et al. 1996) (**Figure 1.4**).

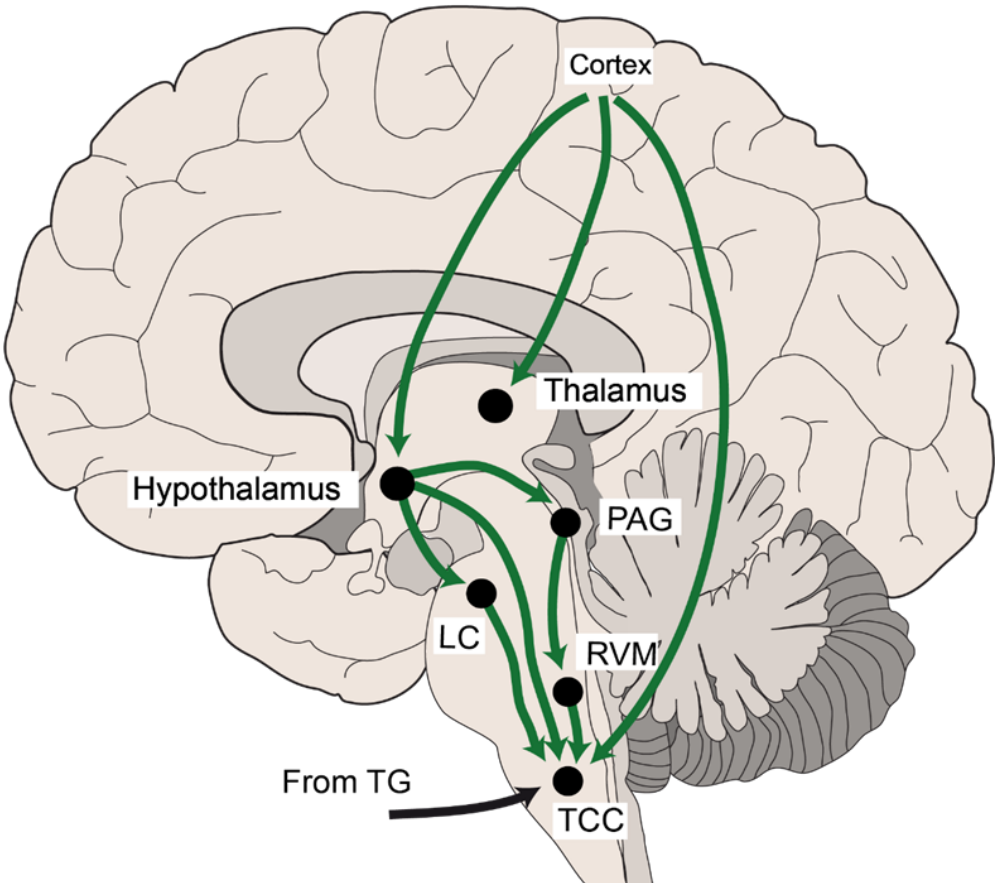

Figure 1.4. Descending direct and indirect cortical projections modulating trigeminal nociception. The trigeminocervical complex (TCC) is the primary relay for peripheral sensory information. It receives direct and indirect projections from several cortical regions. Indirect projections synapse in hypothalamic and brainstem nuclei that in turn can influence trigeminal sensory processing. Periaqueductal gray (PAG), Locus Coeruleus (LC), Rostral ventromedial medulla (RVM), Trigeminal ganglion (TG).

Key regions of these modulatory networks are abnormally active and show altered functional connectivity prior to pain and across the different migraine phases (Afridi, Giffin et al. 2005, Afridi, Matharu et al. 2005, Maniyar, Sprenger et al. 2014, Schulte and May 2016), suggesting a central role in attack initiation. Direct modulation of durovascular-evoked nociceptive responses can be achieved by stimulation of the vlPAG (Knight and Goadsby 2001) and the RVM (Edelmayer, Vanderah et al. 2009). Highlighting a role for the vlPAG-RVM network in modulating regular autonomic, sensory and motor processes. The TCC also receives direct descending noradrenergic projections from the LC (Sasa and Takaori 1973). Resting state functional imaging studies have identified abnormal increased hypothalamic functional connectivity with the LC during the interictal stages (between the attacks and outside the premonitory/preictal

phase); which suggest an already-existing network disruption under resting 'baseline' conditions (Moulton, Burstein et al. 2008).

The role of the LC in migraine is of particular interest to this thesis, given the reported α-2-adrenoreceptor-mediated analgesic action of Noradrenaline (NA) over both migraine-associated nociception (Vila-Pueyo, Strother et al. 2018) and chronic pain conditions. Besides NA; the LC is also known to also release key migraine-associated neuropeptides such as: CGRP, PACAP and substance P; all of which have been suggested to share a role in the pathophysiology of migraine.

The role of brainstem descending modulatory pathways becomes more complex with the co-existing pronociceptive and antinociceptive action of the PAG over the TCC (Knight and Goadsby, 2001) (Knight, Bartsch et al., 2002). The PAG partly projects to the spinal cord but densely innervates the RVM, its differential actions are thought to be mediated through the RVM which by expressing non-serotonergic 'ON', 'OFF' and 'Neutral' cells; can either facilitate or inhibit incoming ascending nociceptive information, through endogenous opioid signalling (Porreca, Ossipov and Gebhart, 2002) (Suzuki, Rygh and Dickenson, 2004) (Edelmayer, Vanderah et al., 2009) (Heinricher, Tavares et al. 2009). Similarly, the nucleus raphe magnus (NRM), which is the main source of serotonin in the brain and sits within the PAG, provides endogenous modulation over the spinal cord and trigeminal nociceptive processes (Fields, Basbaum et al., 1997). Serotonin-based treatments such as Naratriptan are able to decrease ON cell activity and enhance OFF cell activity in the NRM to achieve analgesic actions over the TCC (Ellrich, Messlinger et al., 2001).

The hypothalamus receives direct dural nociceptive information through the trigemino-hypothalamic tract (Malick, Strassman et al. 2000), and simultaneously modulates key homeostatic processes including appetite/energy regulation (Williams, Bing et al. 2001, Coll and Yeo 2013), pain (Siemian, Arenivar et al. 2021), fear (Soya and Sakurai 2020), sleep (Sakurai 2007) and migraine (Bartsch, Levy et al. 2004, Holland, Akerman et al. 2005, Holland, Akerman et al. 2006) through its reciprocal connections back to the spinal cord, brainstem and cortex. This diverse array of functions is regulated by a variety of hypothalamic nuclei (**Figure 1.5**) that sub serve specific functions. For example, the suprachiasmatic nuclei is the master clock, regulating biological rhythms

and entraining this circadian timing to the external environment via the light dark cycle (Hastings, Maywood et al. 2018). This has important implications for the timing of migraine, with migraineurs demonstrating more extreme chronotypes that can predict attack timing in humans (van Oosterhout, van Someren et al. 2018). Preclinically, the hypothalamus has been shown to potently regulate durovascular-evoked nociceptive processing in the TCC (Bartsch, Levy et al. 2004, Robert, Bourgeais et al. 2013), a mechanism that can be influenced by stress. Nociceptive processing in the TCC can be monitored by measuring *in vivo* neural activity from Aδ and C fibers in response to electrically stimulating the Middle Meningeal Artery (MMA); the afferents of which project to the TCC. Intracranial administration of orexinergic compounds directly into the hypothalamus has proven both analgesic and pronociceptive over nociceptive-responding neurons in the TCC; suggesting a descending modulatory control from hypothalamic projections (Bartsch, Levy et al. 2004). Further; retrograde tracing has mapped direct connectvitiy between the Paraventricular Hypothalamic Nucleus (PVN) to the spinal trigeminal nucleus (Sp5C). Indeed, intracranial administration of GABA-agonists into the PVN is able to inhibit spontaneous and dural-evoked activity in the TCC, but this inhibiiton is lost under stress-induced conditions (Robert, Bourgeais et al. 2013); suggesting again a state-dependent bidirectional hypothalamic descending modulatory network.

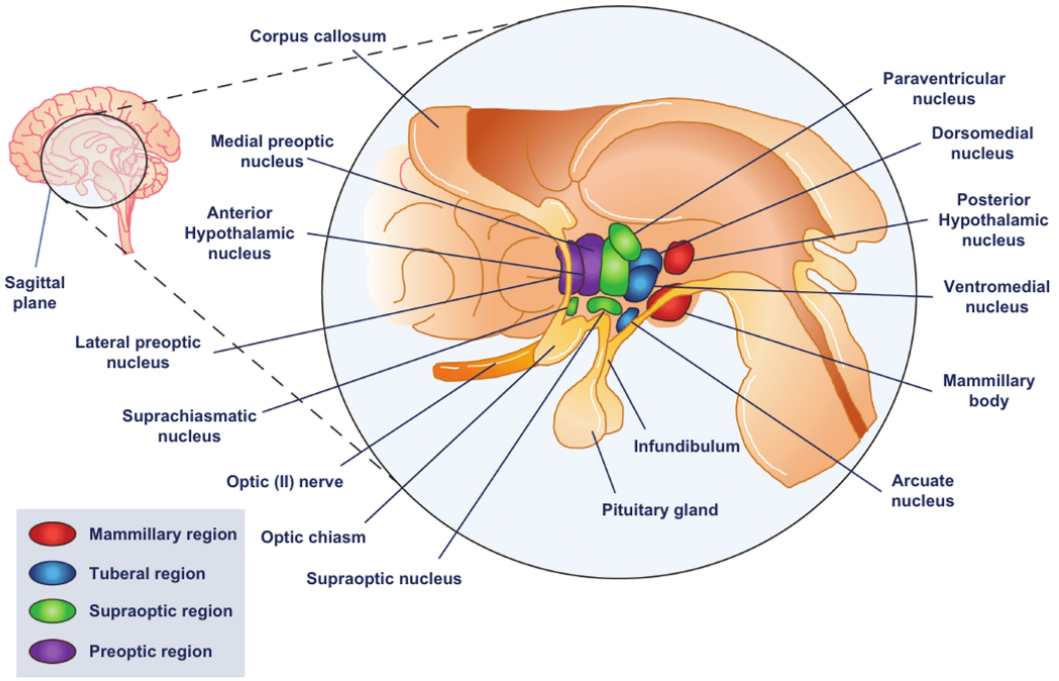

Figure 1.5. Hypothalamic structure. The hypothalamus consists of several discrete nuclei. Of particular interest to migraine the posterior, lateral, paraventricular and suprachiasmatic nuclei have been directly linked to trigeminal pain processing and the regulation of attack timing. https://ebrary.net/132029/health/hypothalamus_structure_functions.

The hypothalamus is thus considered a key structure involved in the pathophysiology of migraine and associated symptomatology due to the diversity of its functions. It is activated during the premonitory and headache phases (Maniyar, Sprenger et al. 2014) and preclinically expresses increased c-Fos in response to trigeminovascular activation (Benjamin, Levy et al. 2004). Interestingly, evidence suggests a direct link between this hypothalamic activation and the sleep-wake regulating orexinergic neurons in the lateral hypothalamus (Holland 2014). It is established that migraineurs have poorer sleep quality and sleep architecture (Stanyer, Creeney et al. 2021), while sleep disruption is a commonly reported attack trigger (Kelman 2007) and results increased susceptibility to cortical spreading depression (Negro, Seidel et al. 2020) and prolonged allodynia in response to capsaicin in rodents (Kim, Park et al. 2019). The importance of the hypothalamus in migraine is further highlighted by the link between neuroendocrine, appetite and hormonal alterations and trigeminal pain processing (Martins-Oliveira, Akerman et al. 2017, Li, Diao et al. 2018, Martins-Oliveira, Tavares et al. 2021).

The hypothalamus shares a variety of functions with the brainstem LC, playing key roles in the regulation of sleep/wake cycles (Takahashi, Kayama et al. 2010, Berridge, Schmeichel et al. 2012), homeostasis and the autonomic nervous system (Samuels and Szabadi 2008, Samuels and Szabadi 2008). Noradrenergic projections from the LC play a key role in the regulation of pain (Llorca-Torralba, Borges et al. 2016), with divergent responses likely due to the heterogeneous structure giving rise to discrete ascending (e.g. thalamus) and descending (spinal cord) projections. More recently, this divergent ascending and descending response has been demonstrated in a preclinical model of migraine. Lesioning of the LC, inhibited durovascular-evoked nociceptive transmission in the TCC via α-2-adrenoreceptor-dependent mechanisms and increased the susceptibility to cortical spreading depression (Vila-Pueyo, Strother et al. 2018). Notably, these divergent responses are reflective of an increasingly acknowledged differential modulation of the LC which is dependent on its output structures. While LC-cortical ascending modulation has shown to favour pronociceptive actions, LC-spinal cord descending modulation contrarily provide antinociceptive effects (Hirschberg, Li et al. 2016). CSD monitoring as a marker of a decreased thresholds for cortical excitable imbalances; in this instance, might be indicative of a mechanism by which altered LC ascending modulation over cortical processes lead to the migraine-associated events such as migraine aura. As such, and in accordance to the aims of this thesis, we hypothesised that a specific activation of LC NA projections would be inhibitory over migraine-associated nociception in the TCC.

As such, with migraine representing a pain state with associated multi-sensory integration it is likely that the above mentioned homeostatic/pain regulatory networks including the hypothalamus, PAG, LC and RVM play an important role in the underlying biology of migraine as well as influencing acute attack initiation.

1.4. THE PREMONITORY PHASE

The most common premonitory symptoms experienced prior to the onset of headache include: fatigue (72%), difficulty concentrating (51%), neck stiffness (50%), food cravings, repetitive yawning, photophobia, phonophobia, as well as changes in mood and activity (Giffin, Ruggiero et al. 2003, Maniyar, Sprenger et al. 2014). Several features of which remain during the postdromal phase (Bose, Karsan et al. 2018, Karsan, Perez-

Rodriguez et al. 2021). Pertinent to their potential utility as a modifiable disease process, up to three quarters of patients can accurately predict with an ensuing migraine based on their individual premonitory features (Giffin, Ruggiero et al. 2003). It is therefore not surprising, given this strong association that patients often mistake premonitory symptoms for attack triggers (Karsan, Bose et al. 2021). For example, it has been shown that patients who report bright light as a trigger are much more likely to experience photophobia during the premonitory phase (Schulte, Jurgens et al. 2015).

As previously detailed in **Figure 1.1.,** there are a diverse array of premonitory symptoms that can generally be classified into:

- **Cognitive or mood changes**
- **Homeostatic or hormonal changes**
- **Sensory sensitivities**
- **Cranial autonomic symptoms**

As such, the mechanisms and neural networks underlying common premonitory features represent an important gap in our knowledge and further offers an entirely novel approach to reduce attack susceptibility. The advantage of clinical imaging studies is that they are able to map brain network changes across the entirety of the migraine attack, including during resting state processes. When combined with human provocation models that use nitroglycerin, CGRP and associated neuropeptides to induce an experimental migraine attack; they have enabled the detailed studying of phenotypical and functional brain alterations during the premonitory phase. Importantly, in a subset of patients, these evoked premonitory symptoms can occur in the absence of an ensuing headache phase. Therefore, the premonitory phase is likely a threshold state in which alterations in CNS neural networks can predispose individuals to diverse symptomatology and an increased likelihood to migraine triggers (Schulte, Jurgens et al. 2015)**(Table 1.4.)**.

Table 1.4. Headache triggers and accompanying symptoms of headache (Schulte, Jurgens et al. 2015).

Headache Triggers	Food, stress, relieve from stress, weather/change in weather, decreased water intake, sleep abundance/deprivation, smells/odours, bright sunlight, flickering light, cold, physical exercise, sexual intercourse, irregular meals/skipping meals, holiday, alcohol, medication, hormonal changes, specific head movements, touch.
Accompanying symptoms of headache	Photophobia, phonophobia, osmophobia, need for rest, nausea, vomiting, skin allodynia, vertigo, facial rush, facial sweating, restlessness/agitation, swelling of lymph nodes, neck pain, tearing, blurred vision, difficulty speaking, nasal congestion.

As discussed, an early central representation of migraine (largely based around diencephalic and brainstem homeostatic networks) is indicative of disrupted CNS networks (Maniyar, Sprenger et al. 2014, Schulte and May 2016), independent of peripheral attack drivers (at least in the initial stages). Current treatments mainly act via peripheral mechanisms given that they have limited CNS penetrability (Edvinsson and Tfelt-Hansen 2008, Tso and Goadsby 2017), potentially acting to dampen the incoming sensory flow that is abnormally processed by perturbed higher order centres (Goadsby, Holland et al. 2017). This may explain why the triptans for example act preferentially when given early (Cady, Sheftell et al. 2000) and can result in significant rebound headache, acting to minimize sensory input, but failing to treat the central driver of the attack. The underlying biology of the premonitory phase of migraine thus represents a unique window of opportunity to target CNS neural networks that regulate the occurrence of acute attacks and represents the most viable approach to ultimately develop a cure for migraine.

1.5. BIOLOGY UNDERLYING THE PREMONITORY PHASE

Clinical imaging data has increasingly suggested a role for both the inter-ictal, pre-ictal and premonitory phases in determining an individual's attack susceptibility (Davies 2011). This supports the idea that the migraineous brain is characterized by a lack or inability to cope with filtering mechanisms responsible for preventing sensory overload. This physiological disturbance can be observed in the lead up to attacks, where activity in the visual, frontal and limbic cortices is altered (Evers, Quibeldey et al. 1999, Sand, Zhitniy et al. 2008), suggesting that these early changes in cortical function may underlie some of the visual, cognitive and emotional symptoms reported during the premonitory phase. However, these functional disturbances are not isolated to the cortex with evidence for alterations in key diencephalic and brainstem neural circuits (Porcaro, Di Lorenzo et al. 2017).

These early neurophysiological studies have gained substantial support from more recent neuroimaging approaches exploring brain changes during the different attack phases. One of the seminal studies identified early activation of the hypothalamic, pontine (i.e. Locus Coeruleus) and cortical regions during the premonitory phase (**Figure 1.6.)**; (Maniyar, Sprenger et al. 2014). Specifically, by use of a PET tracer (H215O) to measure changes in blood flow and as a marker of neural activity, they identified increased activity in these structures after inducing a migraine attack through NTG. Despite the unknown mechanisms behind NTG; it is proven as a reliable method to trigger attacks only in patients with a history of migraine, with the same features of a patient's routine attacks (Afridi, Giffin et al. 2005). Conversely, NTG triggers no migraine attack, but only a mild headache at the very initial stages when administered to non-migraine patients. In the latter study, only patients with a history of migraine without aura and commonly reported premonitory symptoms were included; allowing pre-NTG conditions to act as a control measure. This allowed a continuous within-subject analysis of functional changes at three different time points; baseline (pre-NTG) and post-NTG: during the premonitory phase and the headache phase (Afridi, Giffin et al. 2005).

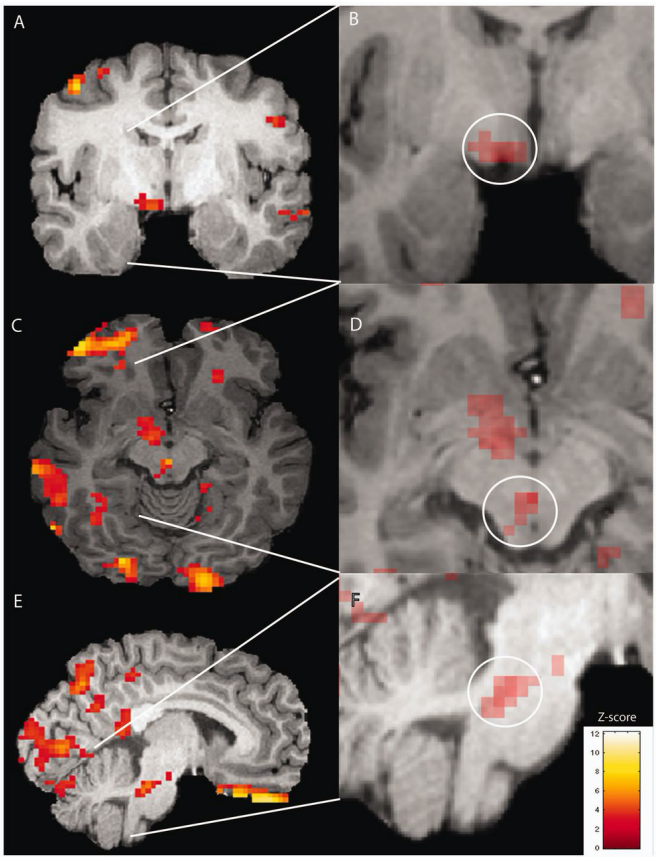

Figure 1.6. Brain regions activated during the premonitory phase of nitroglycerin-induced migraine attacks. Following nitroglycerin administration, but prior to the onset of headache during which time patients report premonitory symptoms activation is observed in the posterior hypothalamic region (**A-B**), periaqueductal gray (PAG; **C-D**) and dorsal pons such as the Locus Coeruleus (**E-F**) (Maniyar, Sprenger et al. 2014).

Importantly, these neural substrates were associated with specific symptomatology, e.g. patients reporting photophobia presented with increased activation in the visual cortex, those with mood/cognitive changes were associated with the anterior cingulate cortex and that yawning, fatigue, thirst etc. were associated with hypothalamic activation. At the level of the TCC, it is further demonstrated that the activity of the spinal trigeminal nucleus increases proportionally as the acute attack approaches (Stankewitz, Aderjan et al. 2011). Suggesting that premonitory-related CNS neural network dysfunction can alter trigeminal sensory gating at the spinal cord, leading to increased trigeminal nociceptive traffic. Building on this finding, Schulte and colleagues imaged the migraine cycle daily for one month (Schulte and May 2016), exploring altered CNS responses to intranasal ammonia. Comparison of inter-ictal (baseline) with pre-ictal (premonitory) phases

uncovered an increase in hypothalamic and visual cortex activity as the pre-ictal phase approached. Combined with altered activation of the hypothalamus, hypothalamic functional connectivity showed dynamic alterations across the cycle: with an increased coupling of the hypothalamus and the spinal trigeminal nucleus during the pre-ictal (premonitory) phase, and posterior increased connectivity to the dorsal rostral pons during the ictal phase (headache). This is in agreement with well-established increases in dorsal lateral pontine activation during the migraine pain phase (Afridi, Giffin et al. 2005) and supports the hypothesis that the hypothalamus and its associated neural networks may play a role in attack initiation but also the transition through the different phases and potentially the transition from episodic to chronic migraine (Schulte, Allers et al. 2017).

1.6. NEUROTRANSMITTER SYSTEMS INVOLVED IN MIGRAINE

As detailed, the combination of disease symptomatology, neuroimaging and functional network alterations have highlighted the potential involvement of several neurotransmitter systems in migraine.

1.6.1. Serotonin

A key neurotransmitter system known to modulate the trigeminovascular pathways is the serotoninergic system; as shown by a strong analgesic action of the specific 5-$HT_{1B/1D}$ (5-hydroxytryptamine; or serotonin) receptor agonist naratriptan over migraine pain but not over other pain types (Cumberbatch, Hill et al. 1998). Serotonin receptors are G-protein-coupled neurotransmitter receptors (GPCRs) which represent the largest family of GPCRs due to the wide range of genes (around 13) encoding for them. There is also once type of ligand-gated ion channel: 5-HT3 receptor. In the context of migraine; serotonin receptors have been identified in both the trigeminal nerve and cranial vessels, and have been postulated to act by promoting vasodilation, but also centrally; with 5HT3R modulating dopaminergic release. From the seven types of 5HT-receptors; three (5HT1, 5HT2 and 5HT3) have been largely associated with migraine (Aggarwal, Puri and Puri, 2021). The development of the triptan class of drugs was originally postulated following the observation that serotonin levels decreased in the plasma (Anthony, 1968) while its metabolites increased during attacks (Curran, Hinterberger and Lance, 1965) (Sicuteri, Periti et al. 1965).

The dorsal raphe nucleus, which is the main source of serotonin in the brain, is activated in response to dural-evoked responses (Knight, Classey et al. 2005) and is inhibited by naratriptan (Ellrich, Messlinger et al. 2001). Importantly, triptans have demonstrated similar inhibitory properties over the TCC and the vlPAG (Goadsby, Akerman et al. 2001, Bartsch, Knight et al. 2004). Building on the success of the triptans, lasmiditan a selective 5-HT_{1F} receptor agonist has received approval for migraine, highlighting the importance of serotonergic signalling in the modulation of trigeminal nociception (**see Table 1.1.;** (Vila-Pueyo, Page et al. 2021).

Despite the unique ability for triptans to abort migraine pain but no other somatic pain disorders, the exact mechanisms behind it remain unclear. The head-specific action of serotonin-based therapies is thought to be determined by the 5HT receptor expression; with high levels present in the trigeminal nerve and the cranial vessels (Rebeck, Maynardti et al., 1994, Berman, Puri et al., 2006), and consequential downstream decreases in the release and gene expression (Durham, Sharma et al., 1997) of CGRP as well as substance P from the trigeminal nerve endings, which have been shown to excite the trigeminovascular system.

1.6.2. Calcitonin Gene-Related Peptide (CGRP)

Activation of the trigeminovascular system either experimentally or during spontaneous migraine attacks results in the release of CGRP (Goadsby, Edvinsson et al. 1988, Goadsby, Edvinsson et al. 1990, Edvinsson and Goadsby 1995), which is a neuromodulator and vasodilator peptide. Following on from this, CGRP administration to humans induces migraine-like attacks (Hansen, Hauge et al. 2010) similar to the established experimental trigger nitroglycerin (Ashina, Hansen et al. 2017). The source of CGRP in migraine is considered to arise from the TG (**Figure 1.7.**) despite the widespread distribution of CGRP in the CNS (Russell, King et al. 2014). This has contributed to the continuous debate on the potential sites of action of CGRP; acting peripherally through its vasodilatory action and/or centrally (Doods et al., 2000). The specific mechanisms of the CGRP pathway remain unclear; but the peptide is known to act over its receptors, which require three components to be functional: calcitonin-receptor-like receptor (CLR), receptor component protein (RCP) and a receptor activity modifying protein 1 (RAMP1) (Olesen et al., 2004). CGRP binding to both RCP and CLR is crucial to successfully activate the CGRP receptor. Specifically; binding of CGRP will

activate the $G\alpha_S$ subunit of the CLR component, and consequentially activate adenylyl cyclase, and thus promote the release of cAMP; which will consequentially upregulate Protein Kinase A. This is of relevance given the role of PKA in for instance mediating neural excitability and plasticity in the amygdala during pain behaviors (Han, Li et al., 2005)

CGRP binding to its receptor will also lead to a phosphorylation of CLR and consequential internalization of the receptor. In the case of a constant exposure of a CGRP agonist to the receptor; this will continuously internalise the receptors and degrade them; whereas intermittent exposure of the CGRP agonist; will internalize the receptor and recycle it back onto the cell's surface (Manoukian, Sun et al., 2019).

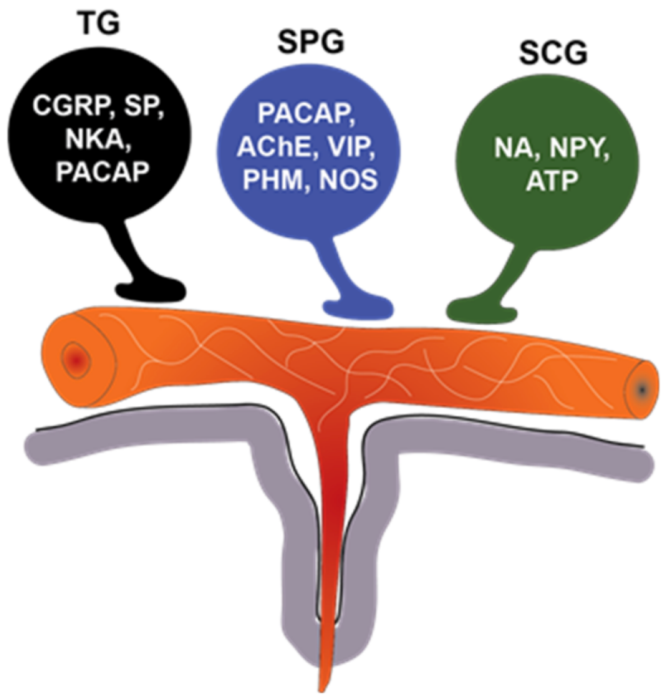

Figure 1.7. Neurotransmitter/peptide innervation of the dural vasculature. Trigeminal afferents arising in the trigeminal ganglion express calcitonin gene-related peptide (CGRP), neurokinin A (NKA), substance P (SP) and pituitary adenylate-cyclase activating polypeptide (PACAP). Alternate innervation of the dural vasculature arises in the sphenopalatine (SPG) which expresses PACAP, vasoactive intestinal peptide (VIP), acetylcholine (AChE), peptide histidine methionine (PHM) and nitric oxide (NOS) and the superior cervical ganglion, whose fibres express noradrenaline (NA), adenosine triphosphate (ATP) and neuropeptide Y (NPY).

The discovery of a key role for CGRP signalling in migraine pathogenesis has led to the development of several new therapies targeting CGRP itself or its receptor. To date three monoclonal antibodies targeting the CGRP receptor and one targeting CGRP have been approved for the preventative treatment of migraine (**see Table 1.2.;** (Diener, Charles et al. 2015, Tso and Goadsby 2017)). Additionally, three CGRP receptor

antagonists have been approved for the acute treatment of migraine and two of these have further been approved for preventative use (Holland and Goadsby 2018). CGRP-blocking therapies successfully increase pain freedom within 2 hrs from treatment, and importantly; also decrease to a lesser degree the presence of associated premonitory symptoms such as nausea, photophobia and phonophobia (Ho, Mannix et al., 2008) (Ho, Dahlof et al. 2012) (Voss, Lipton et al., 2016) (Diener et al., 2011). There is a tight relationship between CGRP and photophobia, with preclinical models with dysfunctional CGRP receptors showing increased light-sensitivity, but reversed through CGRP-receptor blockage (Recober and Kuburas et al., 2009). In comparison, the link between CGRP antagonism and migraine with aura is less clear, with only limited evidence reporting no effects on CSD, the preclinical correlate of aura (Filiz and Tepe et al., 2017).

1.6.3. Orexin

The current therapies targeting the 5-$HT_{1B/1D}$ receptors and CGRP signalling are largely considered to work outside the CNS due to their limited blood brain barrier penetrance (Diener, Charles et al. 2015). As discussed, migraine can be divided into migraine the disorder and migraine the acute attack. Hence novel CNS penetrant therapies that can target the underlying neural networks responsible for migraine initiation would represent a watershed moment in disease treatment. The hypothalamic orexinergic system has emerged as a key regulator of homeostasis and trigeminal sensory processing and therefore represents a potential disease modifying target (Holland 2017).

Orexinergic neurons are located exclusively in the hypothalamus and send projections across the majority of the CNS (Peyron, Tighe et al. 1998, Cutler, Morris et al. 1999, Horvath, Peyron et al. 1999, Mondal, Nakazato et al. 1999, van den Pol 1999, Blanco, Lopez et al. 2001, Johren, Neidert et al. 2001, Mintz, van den Pol et al. 2001, Randeva, Karteris et al. 2001, Zhang, Sampogna et al. 2001, Johren, Neidert et al. 2002, Zhang, Sampogna et al. 2002, Zhang, Sampogna et al. 2002, Zhang, Sampogna et al. 2004). The neurons express two forms of orexin, termed orexin-A and orexin-B cleaved from the same prepro-orexin (Lee, Bang et al. 1999). Orexin A and B act upon two G-protein coupled receptors termed the orexin 1 (OX_1) and 2 (OX_2) receptors (Foord, Bonner et al. 2005). The OX_1R is more selective for OxA than orexin B, while the OX_2R

has relatively equal affinity for both neuropeptides ((Sakurai, Amemiya et al. 1998, Lee, Bang et al. 1999); **Figure 1.8.**).

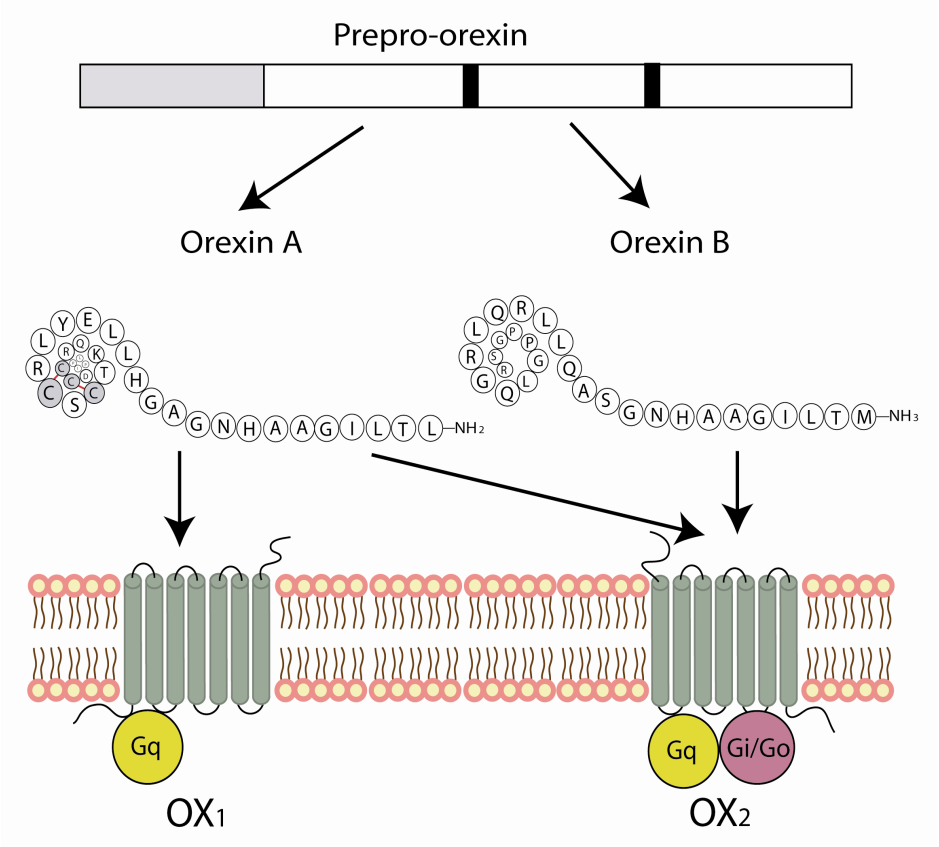

Figure 1.8. Orexin peptide and receptor signalling. Orexin A and B are cleaved from prepro-orexin and act on two G-protein coupled receptors termed OX_1 and OX_2. OX_1 couples exclusively to the G_q subclass of heterotrimeric G proteins, whereas OX_2 couples with $G_{i/o}$ and/or G_q. OX_1 is selective for orexin A, whereas OX_2 is non-selective for both orexin A and B (Sakurai, Amemiya et al. 1998, Lee, Bang et al. 1999).

While our knowledge of orexinergic functions is ever evolving, they were initially considered as regulators of feeding behaviour and subsequently sleep-wake regulation, due to the discovery that orexin deficiency results in narcolepsy. However, it is clear that orexins play a much wider role in several physiologies suggesting that they regulate multiple functions (**Figure 1.9.**). In general, they are considered to integrate internal and external cues essential for maintaining body homeostasis, ensuring the most appropriate physiological response in a state-dependent manner. Building on their initial association with feeding behaviour, it is now clear that they play a key role in energy homeostasis, linking metabolic state information and arousal regulation to ensure optimal feeding behaviours. Central administration of OxA and OxB induces acute feeding behaviour

(Sakurai, Amemiya et al. 1998) while blocking central orexinergic signalling reduces food intake (Haynes, Jackson et al. 2000). Therefore it appears that orexinergic neurons integrate several metabolic cues including glucose (Venner, Karnani et al. 2011), leptin and ghrelin (Yamanaka, Beuckmann et al. 2003) to influence eating and body-weight balance (Gonzalez, Jensen et al. 2016).

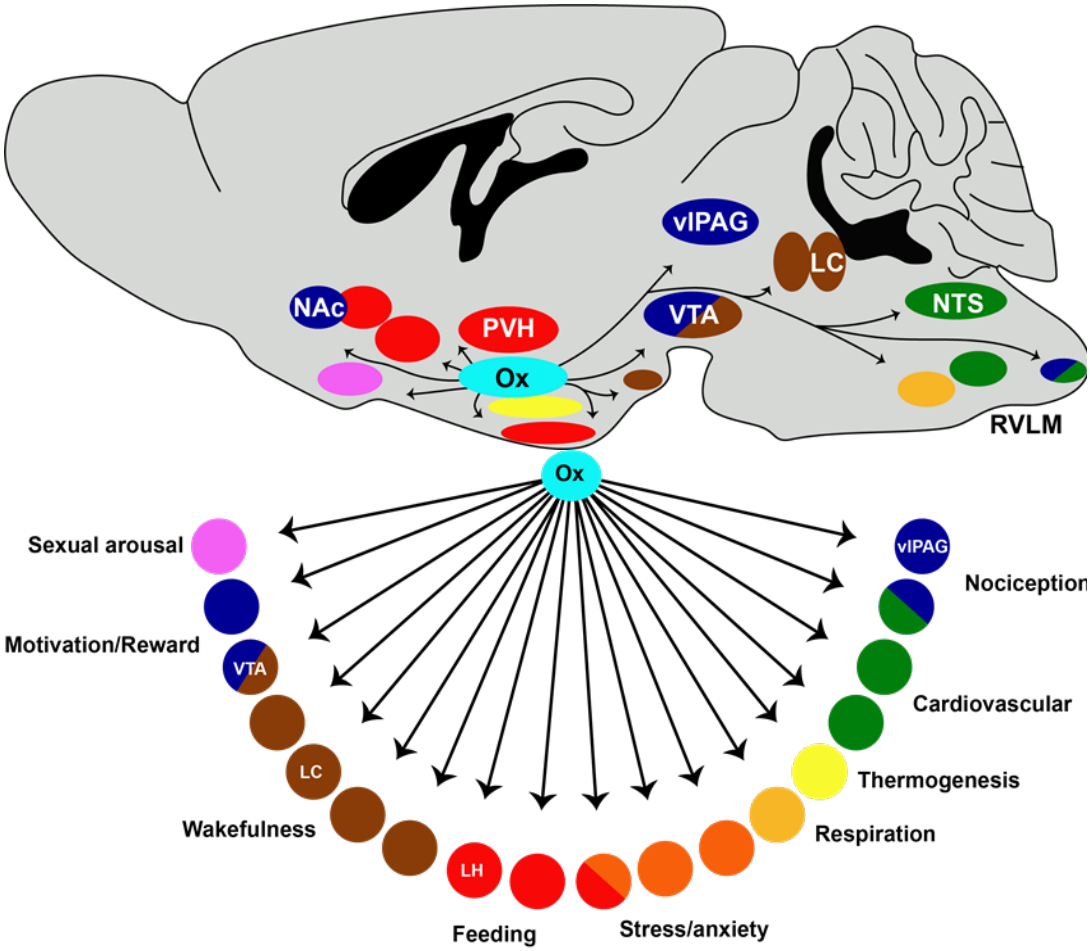

Figure 1.9. Example orexinergic projections and their proposed function. Orexinergic neurons (Ox) originating in the lateral hypothalamus send projections that terminate in several brain areas including the paraventricular hypothalamic (PVH), nucleus accumbens (NAc), ventrolateral periaqueductal gray (vlPAG), ventral tegmental area (VTA), locus coeruleus (LC) nucleus tractus solitaris (NTS) and the rostral ventrolateral medulla (RVLM). Via these projections, Ox neurons can regulate several physiological states including those relevant to migraine and its related symptomatology.

Of particular importance to migraine, orexinergic neurons have been associated with nociception, wakefulness, feeding, motivation/reward and stress. Increased levels of corticotrophin-releasing hormone result in increased orexinergic tone and vice-versa with orexin administration causing an increase in corticotrophin-releasing hormone and

hypothalamic-pituitary-adrenal axis activity (Makiko et al., 2000). Interestingly, stress or the release of stress represent one of the most commonly reported migraine triggers (Lipton, Buse et al. 2014). Often occurring during the premonitory phase of migraine: suggesting an underlying increased sensitivity to stress-associated responses during this period prior to an attack. Further, orexinergic neurons co-release dynorphin (Chou, Lee et al. 2001): a class of opioid peptides thought to modulate depressive-like negative emotional states (Tejeda and Bonci 2019). Given the common premonitory symptom of mood changes prior to an attack (Giffin, Ruggiero et al. 2003); altered dynorphin signalling may be a further target for migraine (Xie, De Felice et al. 2017). The association between orexinergic signalling and potential migraine triggers is not only limited to the stress axis, orexin-relevant environmental disruptions including sleep deprivation, changes in glucose intake or jet-lag are well-established triggers for migraine (Kelman 2007). The outputs from orexinergic neurons promoting food seeking behaviours, autonomic modulation, stress-related responses and fear-conditioned behaviours require an engagement of locomotor systems and wakefulness. While OX_2R signalling appears to be more directly associated to wakefulness, OX_1R modulation is largely involved in other functions such as: reward, appetite and autonomic regulation. Indeed; the wide range of orexinergic functions in homeostatic processing is thought to be associated to the receptor-type expression in the output regions to which orexin acts over. While OX_1R have higher coupling to G_q receptors, OX_2R couple through G_q or $G_{i/o}$ proteins (**see Figure 1.8.**).

1.6.3.1. The orexins and nociception

This differential impact of activating the OX_1R and OX_2R is also observed in the regulation of nociceptive processing and specifically trigeminal nociception. Centrally administered OxA is analgesic in thermal, inflammatory, visceral (Bingham, Davey et al. 2001, Yamamoto, Nozaki-Taguchi et al. 2002) and durovascular-evoked (Bartsch, Levy et al. 2004) pain. Underpinning these effects orexinergic neurons project several neuronal systems involved in nociceptive processing such as the Periaqueductal Grey (PAG), Locus Coeruleus (LC), Parabrachial Nucleus (PB), thalamus, among others (Peyron, Tighe et al. 1998, Trivedi, Yu et al. 1998, Cutler, Morris et al. 1999, van den Pol 1999, Marcus, Aschkenasi et al. 2001, Mintz, van den Pol et al. 2001, Zhang, Sampogna et al. 2001, Zhang, Sampogna et al. 2002, Zhang, Sampogna et al. 2002, Zhang, Sampogna et

al. 2004). Systemic administration of OxA demonstrates similar effects, inhibiting nociceptive responses in the rodent hotplate test and carrageenan-induced thermal hyperalgesia (Bingham, Davey et al. 2001). In addition to inhibiting durovascular-evoked trigeminal nociceptive responses and CGRP release from dural trigeminal afferents (Holland, Akerman et al. 2005, Holland, Akerman et al. 2006). This central and peripheral analgesic effects were both OX_1R-dependent (Bingham, Davey et al. 2001). In comparison to the OX_1R-dependent inhibitory actions of OxA, central administration of OxB facilitates trigeminal nociceptive responses (Bartsch, Levy et al. 2004), while peripheral administration has no impact over trigeminal sensory processing or CGRP-release (Holland, Akerman et al. 2005, Holland, Akerman et al. 2006). This preferential anti-nociceptive action for OxA is supported by a lack of action of OxB on heat-evoked hyperalgesia (Suyama, Kawamoto et al. 2004).

The distribution of the orexinergic projections (**see Figure 1.9.**) from the hypothalamus to the PAG, LC and spinal cord highlight the existence of both direct and indirect mechanisms of action over nociceptive processing (Bingham, Davey et al. 2001, Yamamoto, Nozaki-Taguchi et al. 2002, Cheng, Chou et al. 2003, Yamamoto, Saito et al. 2003, Yamamoto, Saito et al. 2003, Mobarakeh, Takahashi et al. 2005). The densest of all orexinergic projections is to the LC (Peyron, Tighe et al. 1998), which together with the hypothalamus; plays a key role in the regulation of wakefulness (Tsujino and Sakurai 2013) and has been linked to nociceptive processing (Inutsuka, Yamashita et al. 2016), including trigeminal nociceptive processing (Vila-Pueyo, Strother et al. 2018). Despite dense orexinergic innervation, retrograde labelling studies identified no reciprocal LC-derived monoaminergic innervation of orexinergic neurons. With only the noradrenergic A1 nuclei innervating orexin neurons (Sakurai 2005), likely involved in the regulation of food intake and energy homeostasis (Sofia Beas, Gu et al. 2020). The potential role of the LC in migraine, forming a functional network with the orexinergic hypothalamus will be discussed further in section 1.6.4. below.

1.6.3.2. The orexins and migraine: Proposed homeostatic mechanisms underlying migraine pathophysiology

The emergence of migraine attacks follows a circadian pattern (van Oosterhout, van Someren et al. 2018), mainly initiating in the morning, is precipitated by sleep

deprivation/elongation and conversely, sleep itself is one of the most common abortive strategies for an acute attack (Holland 2014). The association between sleep, orexin and migraine is noted in narcoleptic patients: where loss of orexinergic neurons leads to fragmented sleep-wake regulation and significantly increased migraine prevalence (Dahmen, Querings et al. 1999, Dahmen, Kasten et al. 2003). Further, insomnia is also often comorbid with migraine (Tiseo, Vacca et al. 2020) and can be treated by novel dual orexin receptor antagonists (Murphy, Moline et al. 2017, Waters 2021), although these have not proven effective for migraine alone (Chabi, Zhang et al. 2015), despite some preclinical evidence (Hoffmann, Supronsinchai et al. 2015). This is potentially due to the timing of treatment, as it was given at night-time when endogenous orexin levels are low; or perhaps more importantly; due to the lack of receptor specificity as existing evidence suggests that blocking the OX_1R alone holds the most promise for migraine (Bartsch, Levy et al. 2004, Holland, Akerman et al. 2005, Holland, Akerman et al. 2006). This association between sleep-wake regulation (Stanyer, Creeney et al. 2021) and migraine along with the prior demonstration of orexin's differential modulation of trigeminal sensory processing (Bartsch, Levy et al. 2004, Holland, Akerman et al. 2005, Holland, Akerman et al. 2006) has focused attention on the potential role of dysfunctional orexinergic signalling in migraine initiation. Clinical imaging in patients during spontaneous attacks has highlighted a switch in hypothalamic connectivity from the spinal trigeminal nucleus to the PAG as the premonitory phase approaches (Schulte & May, 2016) and both of these structures show abnormal activation during nitroglycerin triggered premonitory phase (Maniyar, Sprenger et al. 2014). Therefore, the hypothalamus may recruit divergent brainstem nuclei to help modulate increasing trigeminal excitation (Stankewitz, Aderjan et al. 2011), or a switch in hypothalamic-brainstem connectivity may predispose individuals to increasing excitability and attack initiation. As such, these brainstem and diencephalic structures become part of a neural network that is altered in the lead up to migraine-related headache attacks. Experimentally, several of these structures including the hypothalamus, PAG and TCC are activated (Hoskin, Kaube et al. 1996, Benjamin, Levy et al. 2004, Knight, Classey et al. 2005) following trigeminovascular activation, suggesting that they may form key hubs for the integration heightened trigeminal sensory activation. Conversely, these nuclei can all regulate trigeminal nociception (Knight and Goadsby 2001, Bartsch, Knight et al. 2004, Bartsch, Levy et al. 2004, Robert, Bourgeais et al. 2013), suggesting that as well as integrating trigeminal sensory activity they are ideally placed to act to regulate it.

The mechanisms to ensure a stable sleep-wake cycle rely on a feedback loop between orexin and monoaminergic neurons in the brainstem PAG, LC and Dorsal Raphe Nucleus (DRN) (**Figure 1.10**.). With the DRN being the main source of 5-HT in the brain: it has a key role in promoting wakefulness, potentially through thalamic-modulated processes. The action of adenosine over 5-HT during sleep is thought to contribute to the gating of sensory stimuli in order to facilitate sleep (Yang, Hu et al. 2015). Further, modulation of 5-HT signalling in the thalamus by the clinically approved triptan, naratriptan can reduce trigeminal sensory traffic (Shields and Goadsby 2006) highlighting the thalamus as a further hub for the integration and modulation of migraine and sleep-wake regulation.

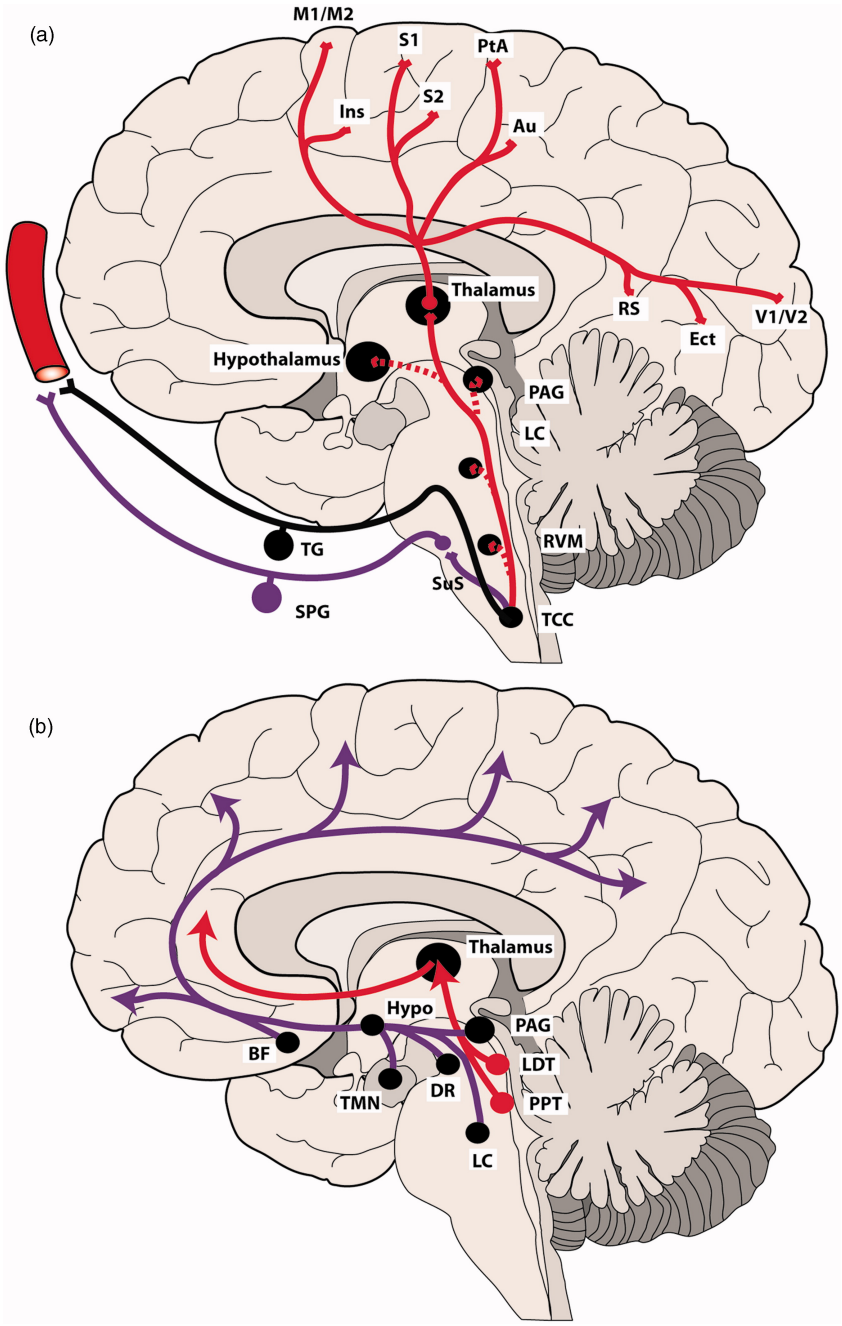

Figure 1.10. The underlying pathophysiology of headache (a) and arousal (b). (a) Sensory afferents arising in the trigeminal ganglion (TG) relay trigeminal sensory information into the dorsal horn of the trigeminocervical complex. This information is then relayed to the thalamus and onto multiple cortical regions. In addition trigeminal sensory information is relayed to the hypothalamus, periaqueductal gray (PAG), locus coeruleus (LC), rostral ventromedial medulla (RVM). A reflex connection from the TCC to the superior salivatory nucleus (SuS) exists which via the sphenopalatine ganglion (SPG) providing parasympathetic innervation to the head. The neural network underlying arousal shares several common pathways with migraine, including the LC, dorsal raphe (DR), PAG and tuberomammillary nucleus (TMN) that all project to the hypothalamus (orexin) and basal forebrain (BF). Together, they function to innervate the cortex and promote arousal and work in conjunction with the laterodorsal tegmental nuclei (LDT) and pedunculopontine (PPT) that project to the thalamus and control thalamic sensory gating. Ins: insula; PtA: parietal association; RS: retrosplenial; Au: auditory; Ect: ectorhinal; GABA: gamma-aminobutyric acid (Holland 2014).

Like sleep-wake regulation and as previously discussed, altered stress responses is a commonly reported migraine trigger that shows significant overlap with orexinergic signalling. Orexin neurons become active in response to stress, and consequentially inhibit pain transmission (Watanabe, Kuwaki et al. 2005); additionally; orexin knockout mice show reduced stress-induced analgesia (Waeber and Moskowitz 1995) as well as a reduced defence responses (Kayaba, Nakamura et al. 2003). In agreement with its role in nociception, discussed above, OxA-mediated inhibition of thermal-induced sensitivity is associated with an activation of OX_1R's, which is followed by an inhibition of GABAergic release (dis-inhibition) in the vlPAG (Ho, Lee et al. 2011). Administration of OX_1R-antagonists abolishes stress-induced (i.e. restraint stress and swim stress procedures) analgesia (Heidari-Oranjaghi, Azhdari-Zarmehri et al. 2012). With hypothalamic networks having a key role in modulating nociception in response to stress-associated environmental stimuli (Abdallah and Geha 2017); disrupted hypothalamic networks in migraine suggest an inability to cope or filter homeostatic changes. Consequentially, this may result in a lack of hypothalamic inhibition over trigeminal pain modulatory structures such as the vlPAG , the LC and thalamus. Given their key function in descending inhibition, this could result in their disinhibition and hyper-convergence of inputs such as: stress (Robert, Bourgeais et al. 2013), light (Noseda, Kainz et al. 2010), sound, touch, food or altered sleep (Blau 1990). Indeed, a polymorphism (G1222A) in the exon 7 of the OX_1R has been associated with a two-fold increased risk of migraine without aura. And despite the low power of male patients in this study; this association was only identified as significant in females (Rainero et al., 2011).

Finally, as discussed above, altered peripheral metabolic cues such as fasting or skipping meals, represent another commonly reported migraine trigger (Kelman 2007), and migraineurs demonstrate altered glucagon and insulin levels after fasting (De Silva, Ron et al. 1974) leading to higher insulin resistance in migraineurs (Bhoi, Kalita et al. 2012, Ozcan and Ozmen 2019). Importantly, neuroendocrine signalling can alter trigeminal nociception, with insulin, glucagon and leptin inhibiting durovascular-evoked nociceptive responses in the TCC, despite differential effects on blood glucose (Martins-Oliveira, Akerman et al. 2017). Orexinergic neurons are similarly highly modulated by metabolic cues such as glucose, ghrelin and leptin: with a decrease in these appetite modulators inducing orexinergic neuronal depolarization (Burdakov, Gerasimenko et al. 2005, Venner, Karnani et al. 2011).

As such, the orexinergic neurons may represent a key interface between internal and external stimuli (e.g. sleep-wake cycles, appetite regulation and exposure to stress/stress response) and trigeminal nociception, leading to migraine attack initiation and the association between migraine and altered body homeostasis. This may manifest as one of several commonly reported premonitory symptoms, including abnormal fatigue, sleep-wake disruption and appetite dysregulation (Giffin, Ruggiero et al. 2003), often mistaken for migraine triggers (Kelman 2007, Schulte, Jurgens et al. 2015).

1.6.4. Noradrenergic signalling

Given the role for orexin in the modulation of trigeminal nociceptive processing and its potential role in attack initiation an important question is how orexin may influence trigeminal sensory processing. As discussed, the LC receives the densest orexinergic projection from the hypothalamus (Peyron, Tighe et al. 1998), and is primarily modulated via an OX_1R-dependent mechanism. Given the observed anti-nociceptive effect of activating the OX_1R as compared to the OX_2R (Bartsch, Levy et al. 2004, Holland, Akerman et al. 2005) on trigeminal nociception, and the role of the OX_1R in the regulation of emotion, stress, arousal and autonomic function (Messina, Dalia et al. 2014, Bonaventure, Yun et al. 2015) the LC represents a key downstream nucleus through which orexinergic signalling could lead to the presence of premonitory symptoms and migraine initiation.

As noted, migraine is intrinsically linked with sleep-wake regulation and like the orexinergic neurons the LC shows clear alterations in diurnal activity (Jacobs 1986), with the greatest activation during arousal and the least during sleep. In terms of migraine, the LC is responsive to trigeminal nociceptive activation (Tassorelli and Joseph 1995, Ter Horst, Meijler et al. 2001) and disturbances in descending modulatory networks that include the LC is considered to play a role in the interictal and premonitory symptoms of migraine. Indeed, the LC resides within the dorsal rostral pons, an area that has been shown to be consistently abnormally activated during migraine (Afridi, Giffin et al. 2005, Maniyar, Sprenger et al. 2014, Schulte and May 2016), while specific functional alterations have been identified between the hypothalamus and LC (Moulton, Burstein et al. 2008, Moulton, Becerra et al. 2014). Despite this focus on the LC, central

noradrenergic projections emerge from seven brainstem nuclei: A1 to A7, of which the LC is termed A6 and forms the densest projections to the spinal cord (Nygren and Olson 1977). Functionally, the LC modulates a variety of neural networks via its expansive CNS projections. The functional outcome resulting from activation of these projections depends not only on the mode of neural activity, but also the receptor expression in the projected region. LC activity is characterized by two modes of activity: tonic and phasic. Phasic activity is triggered by task-related decision processes, and its activity is the highest both before a behavioural outcome and when learned tasks are performed well. Whereas, tonic activity is required for the disengagement of a current task and for the active searching of alternative behaviours (Poe, Foote et al. 2020).

1.6.4.1. Noradrenergic signalling and nociception

The noradrenergic system emerging from the LC is heterogeneous and can be divided into several functional regions each of which represents a different output channel with diverse functional implications ((Poe, Foote et al. 2020); **Figure 1.11.**). For example, specific subregions of LC neurons project to the prefrontal cortex where they modulate anxiety and aversion as compared to descending spinal projections that modulate nociception (Hirschberg, Li et al. 2016).

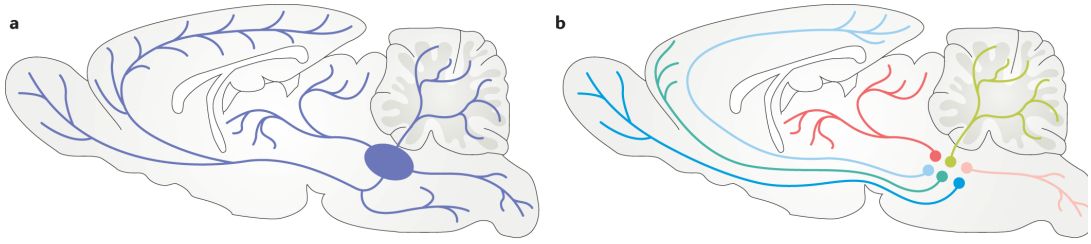

Figure 1.11. The evolving view of the locus coeruleus. The locus coeruleus sends noradrenergic projections throughout the brain (a); however, recent data is challenging the organisation of these projections with significant functional consequences. It is now considered that the LC projections are more restricted to functionally and anatomically defined target regions as highlighted by the colour coded projection pathways in (b) (Poe, Foote et al. 2020).

This functional and anatomical specificity is further characterised by the receptor localisation within the target region. Noradrenaline (NA) regulates its actions via adrenergic receptors, that can couple with either inhibitory or facilitatory G-proteins. The two main classes are the α and β adrenoreceptors. In term of spinal nociception, the α-

adrenoreceptor is expressed in the spinal cord and can be in the form of α1 or α2 adrenoreceptors. α1-adrenoreceptors have been mainly associated with excitatory activity (G_q-mediated), α2-adrenoreceptos have a prevalence for inhibitory responses (G_i-mediated) (**Figure 1.12.**). α2 adrenoreceptors can be located both post- and pre-synaptically: as 'auto-receptors' – to detect any excess NA in the synaptic cleft and inhibit further release from the pre-synaptic terminal. An excess of NA can then either be degraded or recycled back into the pre-synaptic terminal.

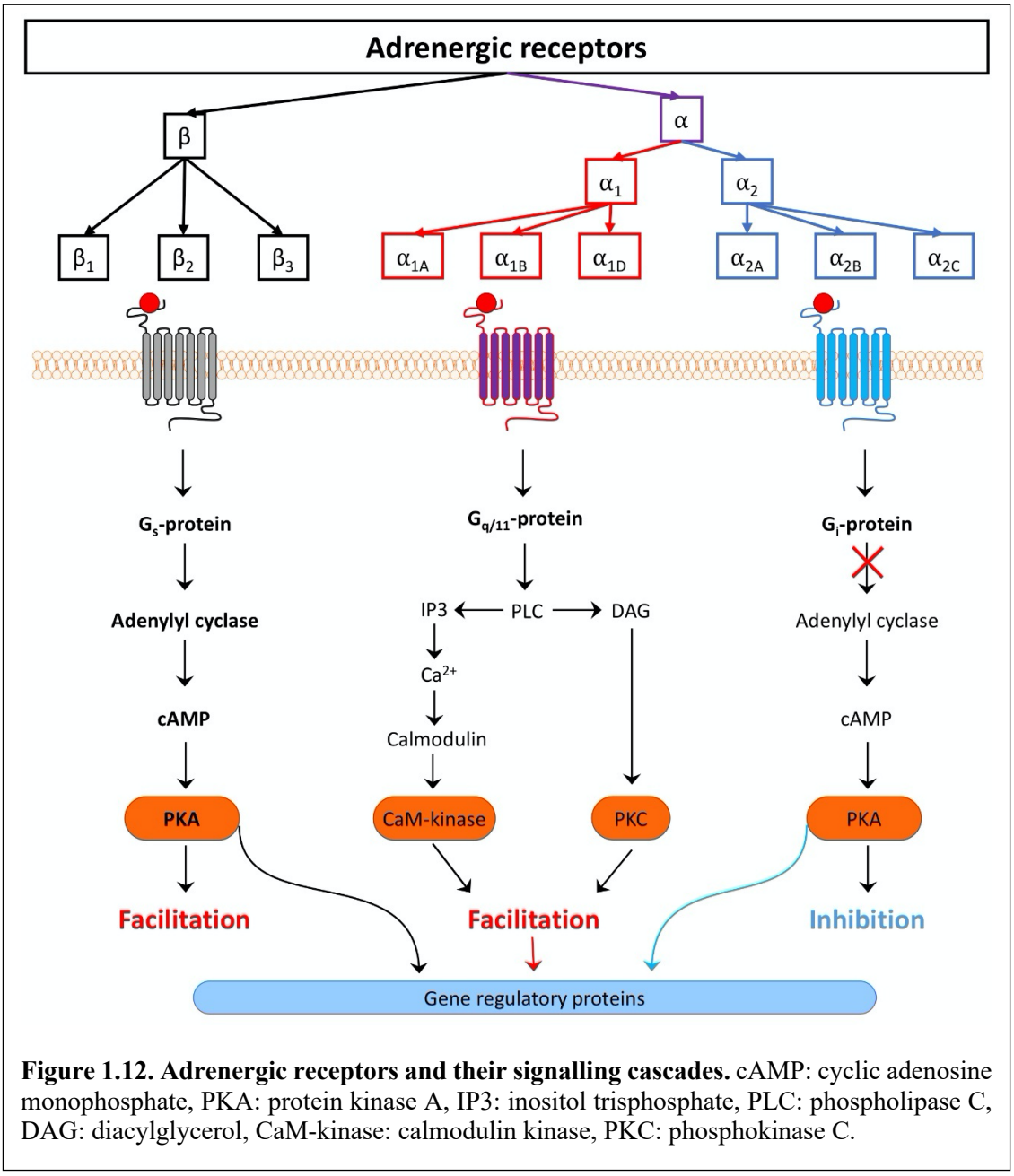

Figure 1.12. Adrenergic receptors and their signalling cascades. cAMP: cyclic adenosine monophosphate, PKA: protein kinase A, IP3: inositol trisphosphate, PLC: phospholipase C, DAG: diacylglycerol, CaM-kinase: calmodulin kinase, PKC: phosphokinase C.

Descending noradrenergic inhibition is considered to be most active in response to prolonged noxious stimuli (Azami et al., 2001), and play a minimal role in tonic control of nociceptive responses (Hylden et al., 1991; Jasmin et al., 2003), as ablation or blockade of α-adrenoreceptors did not impact acute pain responses. The descending noradrenergic system appears therefore to have a key modulatory role over pain-associated nuclei, as shown in models of neuropathic sensitization. The general consensus is that a reduction in noradrenergic descending inhibition is involved in the sensitization of first-order neurons at the level of the spinal cord. α2receptor antagonists have shown to facilitate sensitization post-nerve injury, and this is partially reversible with a NA-reuptake inhibitor. In addition, α2-mediated inhibition acts to spatially restrict the effects of sensitization: with contralateral sensitization observed only when intrathecally administering yohimbine (α2 adrenoreceptor antagonist) after a nerve injury (Hwang, D'Souza et al. 2001). Nevertheless, inhibitor treatments applied just after injury, appear to lose their analgesic effects over time (i.e. post-injury recovery) (Llorca-Torralba, Borges et al. 2016), which might be explained by the 'auto-receptor' action of α2 adrenoreceptors in the pre-synaptic terminal (Wei and Pertovaara 2006). While intact neuropathic models appear to describe a switch from an initial inhibition to a facilitation of pain; LC descending noradrenergic pathways in models of acute nociception describe a predominant inhibitory role (Llorca-Torralba, Borges et al. 2016). Both electrical and optogenetic activation of the LC has demonstrated antinociceptive effects over thermal stimulation and tail-flick responses (Janss and Gebhart 1988, Hickey, Li et al. 2014).

LC noradrenergic networks are also known to have a key role in generating 'diffuse noxious inhibitory control (DNIC)' in the spinal cord, which is a type of descending inhibitory control. DNIC is defined as the inhibition of nociceptive responses as a response of another conditioning nociceptive stimulus (Le Bars, Dickenson and Besson, 1979). Specifically; a continuous excitatory/inhibitory balance among noradrenergic and serotonergic networks, together with parallel opioid and GABAergic processes, are thought to control spinal nociceptive transmission. In neuropathic pain models however, this balance seems to shift towards enhancing excitatory pathways modulated by 5HT2 and 3 receptors, and decreasing NA α2-adrenoreceptors-mediated inhibitory pathways (Bannister and Dickenson, 2016). Indeed, preclinical nerve injury models have described a complete loss of NA descending inhibitory control over the SC and identified α2-adrenoreceptors to have a key role in the progression from acute to chronic pain (Xu;

Kontinen and Kalso, 1999) (Hughes, Hickey et al., 2013). Having said that, serotonergic modulation can also exert inhibitory actions through 5HT-7R activation in both SNL (Bannister and Dickenson, 2016) and Osteoarthritis chronic pain models (Lockwood et al., 2018).

The mechanism behind DNIC can be measured in patients through a Conditioned Pain Modulation (CPM) paradigm, which is defined as the decreased painful response to a noxious stimulus during or after the application of another noxious stimulus. With CPM levels being predictive of developing chronic pain post-surgical intervention (Arendt-Nielsen, Nie et al. 2010), and a blockage of α2-adrenoreceprors capable of blocking DNIC (Peters, Hayashida et al., 2015); recent efforts have focused on developing monoaminergic therapies which can increase DNIC and potentially reduce chronic pain.

In the context of nociceptive processing; the anatomical projections from the LC to the dorsal horn spinal cord descending pathway have recently clearly mapped through NA-specific retrograde viruses. Injection of NA-specific retrograde Adeno-associated viruses (AAVs; (Howorth, Thornton et al. 2009)) and retrograde Canine-adenosine Viruses (CAVs) into the spinal cord: have shown transduction in cell bodies within: the A7, A5 and, and primarily to the A6 (LC) (80% of these projecting to the LC). Interestingly, inhibition of noradrenergic projections from the LC to the lumbar dorsal horn through an AVV-PRS-hKir2.1, induced thermal hyperalgesia and higher sensitization in response to complete Freund's adjuvant and formalin but no mechanical hyperalgesia (Howorth, Thornton et al. 2009). Newly developed viral approaches based on CAV vectors: which are suggested to have higher transduction efficacy at high titters (Hirschberg, Li et al. 2016) and safer profiles clinically (Kremer, Boutin et al. 2000), have also reported a LC-spinal cord noradrenergic-modulated analgesic action over thermal-induced sensitivity. That agrees with the previously suggested modular organization within the LC (**Figure 1.13.;** (Hirschberg, Li et al. 2016).

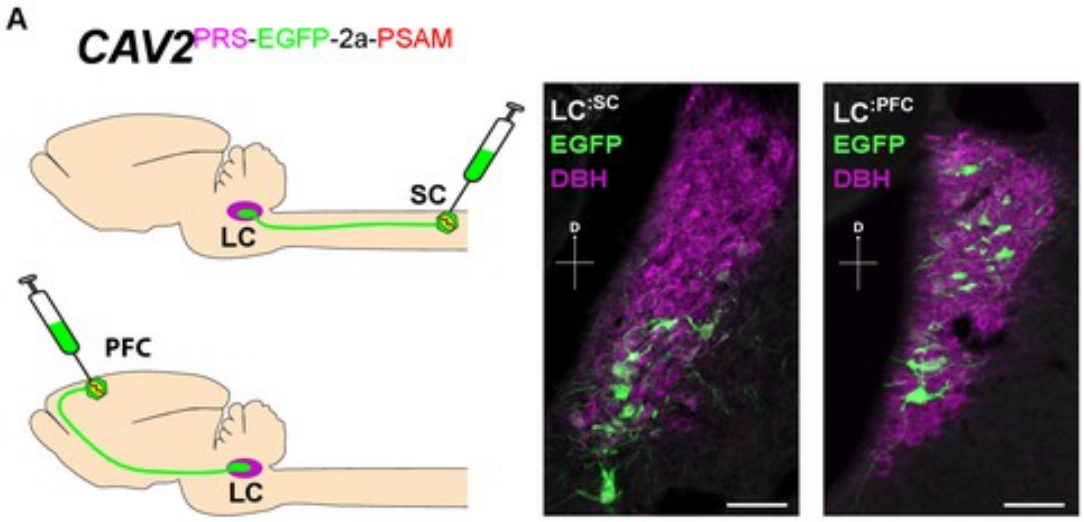

Figure 1.13. Differential location of noradrenergic projections in the locus coeruleus (LC) terminating in the spinal cord (SC) and prefrontal cortex (PFC) (Hirschberg, Li et al. 2017).

In comparison, recent research exploring the role of the noradrenergic LC in preclinical models of migraine identified a potent inhibitory action of LC lesioning over durovascular-evoked nociceptive responses (Vila-Pueyo, Strother et al. 2018). Further, activation of α2-adrenoreceptors in the LC recapitulated this inhibitory effect, while activation of α1-adrenoreceptors produced a phasic response. Demonstrating an initial acute inhibition that transitioned to a facilitatory response over time. In agreement with the heterogenous subpopulations of LC noradrenergic projections, ablation of the noradrenergic fibres produced a state of hyperexcitability within the cortex that manifest as an increased susceptibility to cortical spreading depression, the electrophysiological correlate of migraine aura (Vila-Pueyo, Strother et al. 2018).

1.6.4.2. The noradrenergic locus coeruleus and migraine: Proposed homeostatic mechanisms underlying migraine pathophysiology

Orexin A-mediated activation of the LC is required to modulate arousal and locomotor activity (Hagan, Leslie et al. 1999, Ivanov and Aston-Jones 2000), which involves an OX_2R-mediated regulation of wakefulness/NREM transitions as observed through OX_2R-KO models of narcolepsy (Willie, Chemelli et al. 2003). In comparison, OX_1R-mediated modulation has been associated with REM sleep suppression (Bourgin, Huitron-Resendiz et al. 2000); suggested to act primarily through noradrenergic neurons

in the LC (Mieda, Tsujino et al. 2013). The role of the LC in modulating transitions from sleep and awake states is crucial to the extent that orexin stimulation with simultaneous LC noradrenergic inhibition: inhibits orexin-mediated sleep-wake transitions. Whereas simultaneous orexin and noradrenergic stimulation acts only as an enhancer, increasing the frequency of sleep-wake transitions (Carter, de Lecea et al. 2013). The lateral hypothalamic orexinergic system becomes active in response to food, fasting, reward, fear conditioning (Sakurai, 2014) among others, and through primarily OX_1R-mediated pathways generates the most appropriate motivated behaviours. For instance; OxA modulation through the ventral tegmental area is involved in generating reward-learning and memory through OxA (Harris, Wimmer et al. 2005), whereas OX_1R-mediated effects through the LC are responsible for consolidating fear-conditioned memory (Soya, Takahashi et al. 2017) and extinction of fear memory (Flores, Valls-Comamala et al. 2014).

Based on this; a downstream network arising from the lateral hypothalamic orexinergic neurons over the LC noradrenergic signalling exists that can act over the amygdala to modulate fear expression; with activation of both orexin and the LC noradrenergic neurons able to induce freezing behaviours (Soya, Takahashi et al. 2017), and knockout of the OX_1R in the LC impairs this response (Soya, Shoji et al. 2013). Retrograde chemogenetic approaches combined with tract-tracing approaches have identified orexin neurons to have monosynaptic connectivity with LC noradrenergic cell bodies, located in the most posterior region of the LC that project to the amygdala (Soya et al., 2017). An altered orexinergic signalling pathway of this network is clear in narcoleptic patients who have impaired fear responses (Khatami, Birkmann et al. 2007), as well as in patients with anxiety or PTSD who are often treated with B-adrenergic antagonists (Vaiva, Ducrocq et al. 2003), and importantly; B-blockers (i.e. Propanolol) have been for a long time the first line of treatment for preventive migraine (Sprenger, Viana et al. 2018). This is important in terms of drug targets but also to understand the mechanisms underlying it, as there is a clear association with migraine being highly comorbid with anxiety and depression (Pearl, Dumkrieger et al. 2020, Welander, Mwinyi et al. 2021).

Importantly, the role of the LC in attention-focused processes is robust in cognitive processes. *In vivo* optogenetic LC silencing impairs learning and loss of cognitive

flexibility in response to attentional set shifting tasks (Janitzky, Lippert et al. 2015), and LC activation; promotes memory enhancement in response to novel tasks (Takeuchi, Duszkiewicz et al. 2016). This is again extremely relevant for migraine with cognitive and concentration impairments being increasingly reported throughout the phases of a migraine attack, including the premonitory phase, and largely contributing to its overall disability (Santangelo, Russo et al. 2016).

1.7. AAV-MEDIATED CHEMOGENETIC MODULATION OF OREXINERGIC NETWORKS

The development of induced gene targeting strategies have allowed the engineering of specific gene mutations in rodents in order to understand their functions *in vivo.* A common method to engineer their genome relies on the bacteriophage P1 Cre/loxP system; by which the enzyme Cre recombinase recognizes a loxP site in the P1 genome and catalyses the recombination of the DNA sequence between two loxP sites. The orientation of the loxP sites will determine the type of Cre excision; with Cre inducing an excision of the DNA sequence when the loxP sites are facing the same direction, but an inversion of the DNA sequence when the loxP sites are facing opposite directions (Sauer 1998). This system has been extensively applied for gene targeting in rodent models to create knock-out or gain-of-function models of specific genes in the CNS. One of the challenges of this method however, is the induction of the knockout or inducible genes since development, which does not allow for a representative analysis of the acute function of that network. An alternative method to targeting Cre-labelled specific cells in a time-controlled manner is through the stereotaxic administration of Cre-dependent Adeno-associated viruses (AAVs). These are Cre-dependent meaning that their construct contains the loxP sequences and therefore will only be expressed in Cre-containing neurons.

In agreement with the Cre/loxP system previously described; these constructs have been built accordingly so that the Cre will flip the direction of the sequence within the loxP sites to be able to expressed. In this case, the floxed sequence can contain either: a diphtheria toxin A fragment (**dtA**) or a Designer Receptor Exclusively Activated by Designer Drugs (DREADDs); which consists of G-protein coupled receptors (**hM3Dq/hM4Di**) that can only become active through the action of an exogenous synthetic ligand (Clozapine-N-oxide, CNO) ((Campbell and Marchant 2018); **Figure**

1.14.). The change in orientation will allow the expression of either the diphtheria toxin A (**dtA**) or these receptors (**hM3Dq/hM4Di**) in a cell-specific manner; depending on the promoter where Cre is coupled in the mouse line.

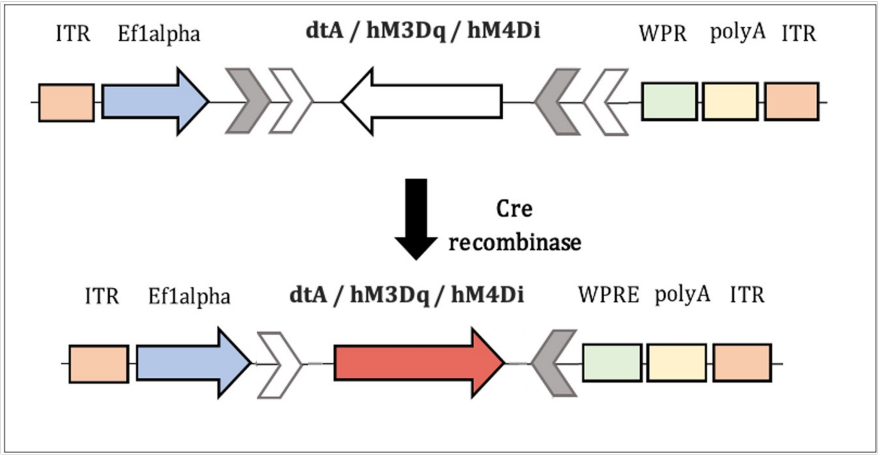

Figure 1.14. Action of the enzyme Cre-recombinase over the loxp sites allows the transcription and expression of the sequence: the gene of interest. Adapted from (Campbell and Marchant 2018)

In the case of expression of a toxin such as diphtheria toxin A; this will cause cell death of the transduced neurons by catalysing the ADP-rybolisation of an intracellular protein (eukaryotic elongation factor 2) and thus inhibiting protein synthesis (Oppenheimer and Bodley 1981). The type of coupled GPCRs will determine the outcome on the transduced neurons; with hM3Dq inducing depolarization and neuronal activation (Alexander, Rogan et al. 2009), and hM4Di silencing neurons through inwardly rectifying potassium channel activation (Zhu and Roth 2014). Importantly, GPCRs are insensitive to endogenous Acetylcholine and have been genetically modified to only become active in response to a synthetically generated ligand: Clozapine-N-Oxide (CNO). The systemic administration of CNO makes this a non-invasive system capable of temporally modulating a network *in vivo* and for a time window long enough for behavioural exploration (Alexander, Rogan et al. 2009). CNO plasma levels peak within 30 minutes from a single acute intraperitoneal dose and behavioural effects can last up to six hours, however continuous CNO administration is also available through food/water for long-term modulation (Sternson and Roth 2014).

A commonly reported limitation of CNO is its partial metabolic conversion into clozapine, which commonly acts as an antipsychotic and might have effects over startle

responses and in amphetamine-induced hyperlocomotion in rats (MacLaren, Browne et al. 2016). An accumulation of clozapine over time (< 2 hours) might in fact have stronger effects over the DREADDs than CNO itself; the levels of which might be high enough to non-specifically act over endogenous receptors (Gomez, Bonaventura et al. 2017). The use of low doses of clozapine rather than CNO has been suggested to avoid downstream non-specific effects and act within a shorter window of action, however given the purpose of the DREADDs approach to offer a long-time window for behavioural exploration, this might not be entirely plausible (Mahler and Aston-Jones 2018). Further, low doses of clozapine alone have indeed reported DREADD-independent and dose-dependent effects on locomotion and anxiety-related responses (Ilg, Enkel et al. 2018), whereas doses up to 10 mg/kg of CNO have reported no behavioural side effects within the 150 minutes from intraperitoneal administration (Mahler and Aston-Jones 2018). Recent efforts have developed alternative exogenous ligands, including compound 21 (Goutaudier, Coizet et al. 2020); however, these to have substantial limitations. A novel compound: deschloroclozapine, which was yet not available throughout this thesis' experiments, instead requires very low doses has recently shown high-affinity and selectivity for DREADDs G-protein coupled receptors, as well as high brain permeability and rapid receptor activation within 10 minutes from systemic administration (Nagai, Miyakawa et al. 2020).

With this; the overall aim of this thesis is to identify the role of the hypothalamic orexinergic networks in migraine susceptibility. In order to characterize previously exposed phenotypes and functional changes, we aim to modulate orexinergic networks *in vivo* through Cre-dependent AAV approaches; primarily AAV-dtA-mediated ablation, in consciously freely behaving animals, and overcome any effects of anaesthesia, as the orexinergic system itself seems to be greatly attenuated by anaesthesia (Inutsuka, Yamashita et al. 2016). For this purpose, we will use an in-house bred Orexin-Cre^{+} mouse line which expresses Cre specifically in orexin cell bodies in the lateral hypothalamus (a kind gift from Prof de Lecea, Stanford) allowing us to target them through these Cre-dependent AAV chemogenetic approaches (further details of which can be found in the methods).

1.8. CANINE ADENOVIRUS (CAV)-MEDIATED CHEMOGENETIC MODULATION OF NORADRENERGIC NETWORKS

The Canine adenovirus-2 (CAV-2) is a retrograde virus that was initially developed for vaccines against canine-adenovirus in dogs (Kremer, Boutin et al. 2000). It has high effective retrograde properties which makes is an extremely helpful tool to delineate and manipulate functional pathways in rodents. Its ability to retrogradely propagate from the axon's terminals back to the soma and successfully drive gene expression is mediated through a CAR receptor present in neuronal presynaptic sites (Chillon and Kremer 2001). CAV-2 is also characterised for its preferential transduction to neurons (Soudais, Laplace-Builhe et al. 2001) as well as long-term, stable and high-level expression and lack of cytotoxicity making it an ideal candidate to target networks *in vivo*. Another advantage of CAV vectors is their large size; allowing them to replicate sequences up to 36 kbp. This also allows for insertion of a wide range of promoters and genes to be able to express for instance; recombinases simultaneously with fluorophores and LoxP/Flp sequences, among others (Lavoie and Liu 2020).

The nature of the CAV-2 approach however does not allow targeting a single pathway given its non-specificity retrogradely projecting from the dendrites and axons in the injected region of interest (ROI). One approach to overcome this is to inject a CAV-2 vector containing Cre recombinase in the output region, and simultaneously inject an AAV containing a gene flanked by loxP sites into the input region. Having retrogradely transduced all projections from the output region, and with the Cre enzyme being able to target only loxP sequence sites; the CAV-2 will only express that gene in the input region. The combination of both CAV2 and AAV-mediated chemogenetic approaches makes single-pathway and neuron-specific modelling *in vivo* possible (Lavoie, 2020).

As previously mentioned, CAV2-mediated labelling has uncovered differential modules of noradrenergic cells within the LC; the location of which varies depending on the output region to which these connect to: with cell bodies projecting to the spinal cord appearing in the central LC, and those projecting to the prefrontal cortex localized ventrally (Hirschberg, Li et al. 2016). The advantage of having a singular input nucleus with noradrenergic cell bodies projecting all throughout the brain; allowed the differential modulation of these pathways *in vivo* by injecting the CAV2 into either the spinal cord or

the mPFC. The CAV2 vector was built to contain a NA-specific promoter: PRS, a fluorophore: EGFP and an excitatory receptor: PSAM. PSAM can only be activated by a synthetically generated ligand: PSEM308, which is administered intraperitoneally prior to the behavioural readouts. Extended details on this vector are described in the 'General Methods' chapter of this thesis. Activation of the LC-SPC pathway uncovered an analgesic action over mechanical and thermal-induced nociceptive stimuli, whereas the LC-PFC network showed a preferential modulation of anxiogenic behaviours (Hirschberg, Li et al. 2016). Disynaptic connectivity of the noradrenergic system has also been mapped by combining CAV vectors with Rabies viruses (RVdG). With Rabies having the ability to move from postsynaptic to presynaptic neurons transynaptically; they are able to identify differential inputs into LC noradrenergic neurons based on their output projections (Schwarz, 2015). Rigorous labelling of these projections uncovered key functional properties by which inputs into the LC could determine a modular LC organization based on the output of the LC projections (Hirschberg, Li et al. 2016).

1.9. AIMS AND OBJECTIVES:

1. Orexinergic networks emerging from the lateral hypothalamus have demonstrated a differential modulatory action over migraine-associated nuclei such as the trigeminocervical complex in *in vivo* anaesthetised animal models. In this project we aim to further investigate the role of the orexinergic system in the regulation of trigeminal nociception and migraine-related symptoms using cre-dependent AAV- ablation approaches in freely behaving rodents.

2. Downstream from the hypothalamus; orexinergic projections are known to densely innervate the locus coeruleus, which is the main source of noradrenaline in the central nervous system. We thus then aim to determine the potential mechanism of action of orexin A via orexin 1 receptors in the locus coeruleus.

3. Given the known role of the locus coeruleus to modulate trigeminal nociception through noradrenaline, we will then optimise a novel retrograde canine-adenovirus 2 (CAV2) vector to permit chemogenetic activation of locus coeruleus noradrenergic neurons in freely behaving rats. Through clozapine-N-oxide-mediated activation of these noradrenergic neurons, we seek to determine its role over trigeminal nociception as well as migraine-associated allodynia by measuring periorbital mechanical sensitivity.

2. Chapter 2 – General Materials and Methods

2.1. ANIMALS

The animals used for all experiments in this thesis were male and female mice (n = 17 orexin-cre^{+} and 60 wild type on a C57Bl6/J background, 20-30g, Charles River, UK), and male and female Sprague Dawley rats (n = 80, 100-300g). All animals were housed in groups of 4-5 unless stated otherwise in 21ºC and humidity-controlled rooms with a normal 12-h light/dark cycle and had free access to food and water. All experiments were conducted under a project and personal license approved by the UK Home Office under the Animals (Scientific Procedures) Act 1986 and in agreement with the ARRIVE guidelines (Percie du Sert, Hurst et al. 2020) and the International Association for the Study of Pain guidelines for the use of animals in research. Given the nature of the animal models used (i.e. transgenic mouse lines); the number of Female and Male animals was not large enough to further analyse any sex differences, although no gross differences were observed between males and females.

2.2. MICE

2.2.1. Stereotaxic surgery (Chapters 4 & 5)

Eight-week old orexin-cre^{+} and wild type littermate mice were initially anaesthetised under oxygen-enriched isoflurane (5%) and maintained at 2% throughout the surgery. The scalp of the mice was initially shaved to facilitate wound care and decrease any post-operative risk of infection, and mice were then placed in a stereotaxic frame (Kopf Instruments). Tear drop eye gel was applied to the eyes to keep them moist throughout the surgery. Once successfully fixed in the frame, a skin incision (following a straight line from Bregma to Lambda) was performed and the skin separated, followed by careful cleaning of the surface of the skull with phosphate buffer solution (PBS).

Having set a straight orientation between Bregma and Lambda, the coordinates for the corresponding region of interest (ROI) were then marked on the skull. Holes were carefully drilled into the skull with a hypodermic needle (Terumo, 25G x 1 1⁄2”), and a glass capillary (G-1 Borosilicate, Narishige) lowered into the ROI (see specific chapters,

Patxinos And Franklin's mouse atlas). A Narishige Injector (IM-11-2 pneumatic injector, Narishige) was used to unilaterally or bilaterally inject at 2 nL/sec the corresponding viral/control solutions. Following injection: the capillary was left to rest for seven minutes and then removed at intervals of 0.5 mm/minute. Mice were then injected intraperitoneally (i.p.) with saline (1 mg/kg) to facilitate their recovery post-surgery. The skin was closed with vet-bond super glue, and mice were placed in a warmed recovery chamber until fully awake. They were allowed to recover for four to five weeks to ensure full viral transduction, prior to being subjected to the correspondent behavioural assays or tissue collection procedures.

2.2.2. Adeno-associated viruses (AAVs)

Cre-dependent AAV approaches were used to label specific neural populations and modulate their activity in a time-controlled manner in freely behaving mice. By use of a transgenic orexin-cre^{+} mouse line (gift from Prof De Lecea, Stanford), in which a knock-IN allele is obtained after a knock-in IRES-Cre cassette replaces the TGA stop codon of the mHCRT (orexin) gene (Giardino, Eban-Rothschild et al. 2018), in conjunction with cre-dependent Adeno-associated viruses (AAVs), we could specifically transduce hypothalamic orexinergic neurons (full description in section 1.7., page 52). For labelling studies, we made use of cre-dependent AAV tagged to an eGFP marker: AAV1-EF1a-DIO-membraneGFP (Gifted by Dr. Delogu: Matsuda and Cepko, 2007) which under a EF1a promoter specifically transduces orexinergic neurons, labelling the cell membrane of cre-expressing neurons. Mice were allowed to recover for three to four weeks to ensure full viral transfection.

In order to induce a progressive ablation of these orexinergic pathways *in vivo*, the following cre-dependent construct was used: rAAV5-EF1a-Lox-Cherry-lox(dtA)-lox2 (UNC, Vector core, **Table 2.1**). This is a cre-dependent double-floxed coupled AAV with the mCherry fluorescent tag under the control of the EF1a promoter. The diphtheria toxin (dtA) will only be expressed in cre-expressing orexinergic neurons and induce a progressive cell death (Brockschnieder, Lappe-Siefke et al. 2004), and all infected cells in the region (non-Cre) will be visualised through mCherry. This progressive cell death is generated through catalysing the ADP-rybolisation of an intracellular protein

(eukaryotic elongation factor 2) and thus inhibiting protein synthesis (Oppenheimer and Bodley 1981). In a preliminary labelling study only included in the discussion section of chapter 3, we also made use of cre-dependent retrograde AAV2s: pAAV2-hSyn-DIO-hM3D(G_q)-mCherry, (Addgene plasmid: # 44361-AAVrg), which through its retrograde properties is taken up by the axon terminals and transported back to the cell bodies. This vector is coupled to DREADDs (Designer Receptors Exclusively Activated by Designer Drugs), it specifically transduces neurons (hSyn), is cre-dependent (double-floxed: DOI), and contains a fluorophore to visualise the AAV (mCherry), as well as a modified muscarinic receptor (hM3D(G_q)). The hM3D (G_q) receptor has been modified to no longer respond to endogenous acetylcholine, but only to a synthetic exogenous ligand: Clozapine-N-Oxide (CNO). CNO binds specifically to the synthetic receptor and, in this case, given the nature of the receptor being excitatory, activates the transduced neuron. Administration of CNO allows for temporally controlled activation *in vivo* in the presence of suitable controls, to account for potential effects of viral transduction or off target effects of CNO metabolites (Gomez, Bonaventura et al. 2017) (**Figure 2.1.**).

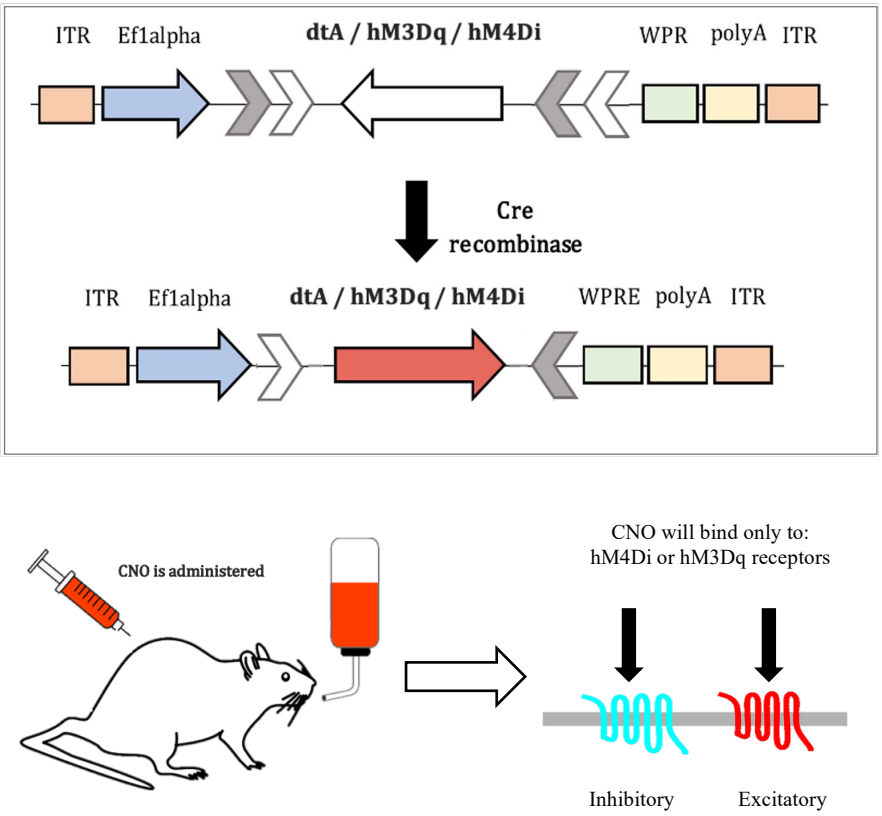

Figure 2.1. Representative diagram of the application of the DREADD approach. Given our in-house bred transgenic mouse line: orexin-Cre^{+}; the Cre-dependent AAV which contains a double floxed inverted DREADD: will only target those cell bodies (orexins) containing Cre-specific drivers. Cre enzyme is specific to binding to these lox sites; meaning that it will flip the direction of the DREADDs sequence to allow the recombination of the sequence. For the purpose of our studies; this sequence will mainly involve a dtA (toxin), but can also include either a hM4Di or hM3Dq receptor. CNO, which can be administered intraperitoneally or through food/water intake: is an exogenous compound which will bind only to the DREADD sequence and activate the corresponding receptor: hM4Di, which is inhibitory or hM3Dq which is excitatory (Zhu and Roth 2014).

Table 2.1. List of Adeno-associated viruses used in this thesis to label and target orexinergic neurons and their projections *in vivo*.

Construct	Source and catalogue nº	Applications
AAV1-EF1a-DIO-membraneGFP	Gift from Dr. Delogu's laboratory. (Matsuda and Cepko, 2007)	Labelling of orexin-cre^{+} cell bodies in the lateral hypothalamus
rAAV5-EF1a-Lox-Cherry-lox(dtA)-lox2	UNC Vector code but the same vector is currently available at: Addgene, #58536-AAV	Progressive ablation of orexin-cre^{+} cell bodies in the lateral hypothalamus
pAAV2-hSyn-DIO-hM3D(G_q)-mCherry	Addgene, #44361-AAVrg	Activation of orexin-cre^{+} projections from the lateral hypothalamus to the locus coeruleus

2.2.3. Behavioural assays (Chapters 3, 4 and 6)

2.2.3.1. Periorbital mechanical withdrawal threshold

Measuring orofacial sensory threhsolds to mechanical stimuli has been largely applied in preclinical migraine models (Harriott, Strother et al. 2019, Holton, Strother et al. 2020, Saengjaroentham, Strother et al. 2020, Bertels, Singh et al. 2021) to uncover the presence of a migraine-related alterations in trigeminal sensory processing. Measuring the sensitivity around the periobrital region (**Figure 2.2. and 2.3.**) is thus reflective of the cephalic cutaneous sensitivity (allodynia) to touch and pain, that around 70-80% of migraine patients suffer before or during the migraine attack (Burstein, Cutrer et al. 2000, Burstein, Yarnitsky et al. 2000, Burstein, Collins et al. 2004, Burstein, Jakubowski et al. 2010). Alterations in mechanical withdrawal thresholds can be measured by the use of calibrated von Frey filaments, by determining the 50% mechanical withdrawal threshold by an established up-down mechanism (Chaplan, Bach et al. 1994).

For this behavioural assay, animals were positioned over a wire mesh base, and individually placed in clear-walled individually compartmentalised plexiglass 6 x 6 cm boxes, with restricted vision between animals (Ugo Basile, UK). The mice are placed in this apparatus with a small 6oz espresso cup to facilitate access to the periorbital dermatome. Importantly, this behavioural assay follows the same protocol when used in

rats; only that these are placed in larger boxes (20(d) x 62(w) x 14(cm)) also with restricted vision between animals, and on top of the wire mesh base.

1. **Pre-test preparation:** Prior to the experimental day, mice were left to rest in the espresso cups for one hour to habituate to the apparatus. Mice were then handled and taught to calmly sit in the small 6oz espresso cups. If by the end of the session, animals had not learn to sit in the cups or appeared to be agitated, an additional habituation session would be performed on a separate day. Rats were instead left to rest in the boxes and handled for habitation to the experimenter. Other factors which were considered to avoid stress-related responses and high variability were:

    a. Habituating and testing the animals at the same time of day, between 9 a.m. to 2 p.m. to avoid any pain threshold variability due to circadian cycles.

    b. Keeping the room quiet and at low light conditions (30 - 50 Lux) with regular cleaning it after every behavioural session.

    c. Keeping one cup (or box) per animal consistently (cup would be replaced when it was too soiled) and positioning each animal in the same position throughout the behavioural study.

2. **Baseline periorbital sensitivity:** Once mice/rats were successfully habituated to the rack and cups, a first measure of their baseline mechanical withdrawal threshold was performed using the UP-DOWN method of analysis (Chaplan, Bach et al. 1994). Periorbital mechanical withdrawal thresholds were measured by applying a set of von Frey graded filaments over the periorbital region. The pressure (g) of these filaments include: 0.02, 0.04, 0.07, 0.16, 0.4, 1 and 1.4g. the pressure (g) used for rats instead include: 0.4, 0.60, 1.0, 2.0, 4.0, 6.0, 8.0 g, and were applied through the following method:

    a. Filaments were applied perpendicular to the orofacial region, ensuring the filament would bend and not slip along the skin surface, and were held for a few seconds, with the aim to elicit a reflex- positive response.

b. For mice; the sequence always started with the 0.4g filament and the proceeding filaments' used varied depending on the animal's sensitivity; if the animal responded to 0.4g, the next filament in the sequence with less pressure would be applied (0.16g), and if no response was observed: the next filament with higher pressure would be used (1g). the same sequence procedure was applied for rats but with the first filament applied being 1g, and the highest pressure being 8g. Negative responses are recorded as O and positive as X.

c. A positive response was defined by moving of the head downwards, shaking the head, bowing/burrowing the head, or brushing the head repeatedly with the paw.

d. This was performed until a total of five recordings from the first positive response are measured (including the first positive response).

A. **B.**

Figure 2.2. Periorbital threshold testing in mice. A. Periorbital region (white dotted line) in which the filament is perpendicularly placed to elicit a reflex-based response. Mice are often sitting within the espresso cups to facilitate their stillness and accurate recording, whereas rats learn to stay calm in their boxes. B. Set of filaments used: periorbital recordings in mice start at 0.4g and usually have baseline sensitivity of around 0.6g, whereas in rats start at 1g with baselines of around 1g.

3. Data collection and analysis: The 50% mechanical withdrawal threshold was then calculated by the up-down mechanism (Chaplan, Bach et al. 1994): an algorithm that is able to translate the observed sensitivity in a quantitative manner to represent the underlying biological mechanisms. The UP-DOWN algorithm (as per below) consisted of an 'interval value, δ' which is the mean difference in log units between the filaments applied. Considering that the filaments and step size between them were different for mice and rats, the interval value used for mice was: 0.224, and rats: 0.354.

The second variable of the equation: 'k' was provided by the Dixon statistics table, and is a negative log likelihood constant generated from the XO series/pattern from each animal. The third variable inserted into the equation was the 'X_f value' (in log units) of the last Von Frey filament in the XO series. Having gathered all the previous variables; the UP-DOWN equation then calculated the grams in which the mouse responded 50% of the times (50% mechanical withdrawal threshold)(Chaplan, Bach et al. 1994).

$$\textbf{50\% threshold, g} = (10^{[X_f + k\delta]}) / 10{,}000$$

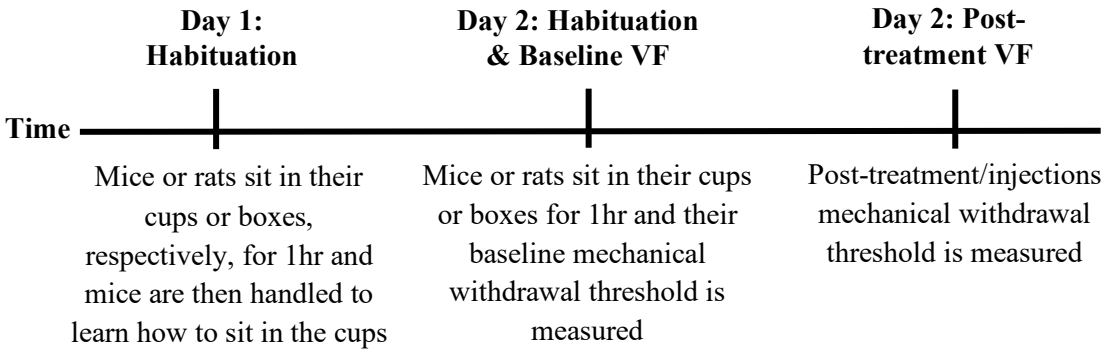

Figure 2.3. Representative timeline of the von Frey behavioural assessment. This might vary among cohorts depending on the average sensitivity and other confounders. Whenever one habituation session is not enough for mice to remain calm in the cups or rats in their boxes; average, a second or third habituation session will be added. The same applied for stable baseline mechanical periorbital thresholds; whenever these were not stable enough, they might be replicated on a consecutive day.

2.2.3.2. Open field

The open field is a 72 (length) x 72 (width) x 33 (height) cm square wall-enclosed arena (**Figure 2.4.**), which is used to measure anxiety-related behaviours and general locomotor activity in mice (Seibenhener and Wooten 2015). For our purpose, we used the open field assay to monitor general locomotor activity in a natural (spontaneous) and non-reinforced environment, as a surrogate readout of fatigue. During the recording, a camera was set-up on top of the arena in order to record the rodents' movement and behaviour for ten minutes through the Ethovision software. The following procedure was used to perform the recordings:

1. **Pre-test preparation:** The light intensity in the arena was set to be no higher than 20 Lux to avoid any bright light stress-induced responses. The camera was set-up to accurately set the signal to noise ratio and identify the mouse and allow tracking through the Ethovision software. In order to be able to also measure anxiety-associated responses; an 'inner 'zone measuring 36 x 36 cm was drawn in the centre of the arena, leaving the remaining surrounding region: the 'outer' zone. Before and after each test the box was cleaned carefully with 1% Anistel® to remove potential odour cues.
2. **Testing:** Mice home cages were always kept in a quiet room, separate from the testing room to avoid any confounding effects with other mice in the testing room during the assay. Immediately before testing; each corresponding cage was brought to the testing room and the mouse was then placed in the open field facing an outer wall to begin the test (placing the mouse in the middle of the arena might induce stress). The Ethovision trial was then initiated and the experimenter left the room for the duration of the trial (10 minutes).

3. **Data collection and analysis:** The Ethovision software tracks a wide range of parameters: the distance and speed travelled, as well as the time spent in various regions (i.e. centre vs outer area). Alongside their locomotion, any anxiety-associated behaviours were also measured to account for any stress-induced effects. Given the tendency for mice to avoid the central zone of a novel environment, we would then measure their anxiety from their avoidance of the central zone. This is measured through their time, distance and speed spent in each zone**.**

A. **B.**

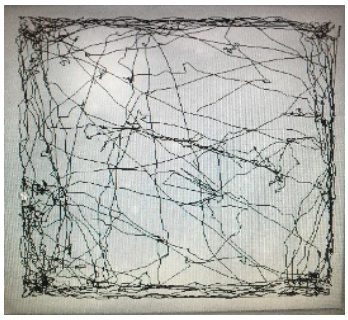

Figure 2.4. A. Open field arena: 72 (length) x 72 (width) x 33 (height) cm squared arena. B. Representative image of a wild type non-ablated locomotor activity tracking for 10 minutes.

2.2.4. Immunohistochemistry/Immunofluorescence

2.2.4.1. Tissue collection and perfusion

Mice were anaesthetized with Euthatal (10 mg/kg intraperitoneally, I.P.) and transcardially perfused by insertion of a butterfly needle into the left ventricle, and then snipping the right atrium. Twenty millilitres of 1% Heparinised PBS were then infused (Harvard infusion pump at 2 ml/min) into the left ventricle, followed by 20 ml of 4% paraformaldehyde (PFA) (Sigma-Aldrich, UK), at 2ml/min. Brains were dissected out, post-fixed overnight (4% PFA) and then cryoprotected in 30% sucrose (SLR, Fisher, UK) for at least 48 hours, until they sank. The samples were then snap frozen on Cryo-m-bed embedding compound (53581-1, Bright Instruments) and cryostat (Bright cryostat, details) cut coronally at 30 µm (free floating in antifreeze) and stored at -80°C until use.

2.2.4.2. Orexin A, B & Melanin-Concentrating Hormone

Coronal sections of interest: lateral hypothalamus, locus coeruleus (LC) and trigeminocervical complex (TCC; spinal trigeminal nucleus and the 1st and 2nd cervical levels (C1 and C2) were selected and submerged in PBS in 6 x 6 plate wells. The sections were initially blocked for 15 minutes in 3% hydrogen peroxide solution at room temperature, then blocked with horse serum (10% horse serum, and 0.25% Triton-X in PBS, Vector labs, CA) for orexin A and B (OxA/B), and goat serum (10% goat serum, and 0.25% Triton-X in PBS, Vector labs, CA) for melanin-concentrating hormone (MCH), for one hour. Endogenous avidin and biotin was then further blocked with avidin and biotin (1:100 Vector Laboratories, CA) independently, for 15 minutes each. The sections were then incubated overnight with the primary antibodies at 4ºC goat anti- OxA and goat anti-OxB (sc-8070; Santa Cruz Biotechnology) at 1:500 (in 5% horse serum, and 0.25% Triton-X in PBS) and rabbit anti-MCH at 1:500.

The secondary antibody solution: biotinylated anti-goat (BA-9500, Vector labs, CA) in horse, or biotinylated anti-rabbit in goat (BA-1000, Vector labs, CA) was diluted in the blocking buffer (5% Horse serum or 5% Goat serum, 0.25% Triton-X in PBS) and incubated for 90 minutes at room temperature. The ABC reagent (Vector labs, CA) was

then applied for 30 minutes. For the immunofluorescence staining, either Fluorescein Avidin D (green) or Texas Red avidin D (red) was incubated for one hour at room temperature. Samples were then washed for three times 15 minutes, and mounted, air dried in the dark and cover-slipped with Silver Prolong Mounting medium.

To visualize orexinergic fibre density, the samples were stained with diaminobenzidine (DAB) and ammonium nickel sulphate (DAB Substrate Kit, Vector SK-4100) (brown) instead of the previously described Avidin D fluorophores. Each slice was left in DAB for the same fixed time and moved into ice cold PBS to terminate the reaction. These samples were then mounted on microscope slides and air dried at room temperature, dehydrated (50, 75, 95 and 100% ethanol) and mounted using DPX mounting medium.

2.2.4.3. c-Fos, Tyrosine-Hydroxylase and Green Fluorescent Protein – independent or combined protocols

The sections were initially washed for three times 5 minutes with PBS and then be blocked for 2 hours with 7% Goat Serum with 0.3% Tx PBS. These were then incubated for 48 hours with the primary antibodies at 4°C: anti c-Fos (9F6) raised in rabbit (1:6000) mAb for c-Fos, and anti-tyrosine hydroxylase (TH) raised in mouse (1:500) for TH, anti-green fluorescent protein (GFP) raised in chicken (1:10.000) for GFP. On the 3rd day, samples were washed for four times 10 minutes with PBS, and then incubated with the secondary antibodies for two hours at room temperature with: goat anti-rabbit Alexa 488, goat anti-mouse Alexa 488 or goat anti-chicken Alexa 488. Finally, they were washed for four times 5 minutes in PBS, air dried and mounted and coverslipped with Silver Prolong Mounting medium. TH & c-Fos was on occasion also co-localised by use of a goat anti-rabbit Alexa 647 for c-Fos.

2.2.4.4. mCherry

Similar to the previous protocol, the sections were initially washed for three times 5 minutes with PBS and blocked for 2 hours with 7% donkey serum with 0.3% Tx PBS. These were then incubated for 24 hours with the primary antibodies at 4ºC: anti c-mCherry in rabbit for mCherry. On the 2nd day, samples were washed for four times 10

minutes with PBS, and then incubated with the secondary antibodies for two hours at room temperature with: donkey anti-rabbit Alexa 568. To finalise, they were washed for four times 5 minutes with PBS, then air dried, mounted and coverslipped with silver prolong mounting medium.

Table 2.2. Antibodies used to label the different markers in all studies of this thesis; with their corresponding source, catalogue number and dilution.

Antigen	Primary antibody (Source, Dilution)	Secondary antibody (Source, Dilution)	Secondary antibody
Orexin A (OxA)	Anti-orexin A Ab (Santa Cruz Biotechnology, #sc-8070, 1:500)	Biotinylated anti-goat raised in horse (Vector Labs, #BA-9500, 1:500) **OR** anti-goat AF 488 (Thermo Fisher, 1:500)	Fluorescein Avidin D (Vector Laboratories, A-2001-5) or DAB
Orexin B (OxB)	Anti-orexin B Ab (Santa Cruz Biotechnology, #sc-8070, 1:500)	Biotinylated anti-goat raised in horse, BA-9500 **OR** anti-goat AF 488 (Thermo Fisher, 1:500)	Fluorescein Avidin D (Vector Laboratories, A-2001-5) or DAB
Melanin-Concentrating Hormone (MCH)	Anti-MCH Ab (Phoenix, #H-070-47, 1:500)	Biotinylated anti-rabbit raised in goat (Vector Labs, #BA-1000, 1:500)	Fluorescein Avidin D (Vector Laboratories, A-2001-5)
cFos	Anti c-Fos raised in rabbit mAb (Cell Signalling technology, #9F6, 1:6000)	Goat anti-rabbit, Alexa 488 (Thermo Fisher, 1:500)	
Tyrosine Hydroxylase (TH)	Anti-TH raised in mouse (1:500)	Goat anti-mouse, Alexa 488 (Thermo Fisher, 1:500)	
Green Fluorescent Protein (GFP)	Anti-GFP raised in chicken (ThermoFisher, #A10262 1:10.000)	Goat anti-chicken, Alexa 488 (Thermo Fisher, 1:500)	
mCherry	Anti- mCherry in rabbit (Biovision, #5883, 1:2000)	Donkey anti-rabbit, Alexa 568 (Thermo Fisher, 1:500	

2.2.5. Immunocytochemical acquisition and analysis

Images of the stained sections were acquired through an AxioPlan microscope (Zeiss Axioimager) or A1R Confocal microscope and saved as .zvi. files to retain all their information. For quantitative analysis of co-localisation and cell counts, these were then transferred into ImageJ and manually counted, blindly using the multi-point tool in Fiji, which allows you to record the total number of points and the double-positive somas. Quantitative counting of cell bodies within the lateral hypothalamus and LC were performed by selecting 6-7 sections in total (every second section, with a slice thickness of 30 μm) covering the entire nuclei, and averaging the counts. Lack of normal distribution of the raw data was firstly analysed in SPSS through a normality test (Shapiro Wilk test).

For fibre density analysis of DAB-stained fibres; a common threshold was initially established by selection of random sections. The files were initially converted into 8-bit format to a white-grey scale. A fixed ROI of 6 x 6 mm was applied equally over all samples in the LC, PAG and TCC: with around 4-6 ROIs required at the C1, C2 and TNC level. The % of area surpassing the previously set threshold was measured on ImageJ (Fiji) and the sum of the % area for each hemi-section was calculated. All the sections in each level; C1, C2 and TNC level were then averaged for statistical analysis.

2.2.6. Drug administration and compounds

We utilised an intranasal administration protocol to administer OxA intranasally, using a minimally-invasive approach in freely behaving mice (Hanson, Fine et al. 2013). We initially determined the optimal method of administration, as well as compound dose before testing its effects acutely and then chronically (twice per day for 5 days). Mice were habituated to handling, specific scruffing (**Figure 2.5.**), and saline intranasal administration for one month, before providing the compound.

Intranasal delivery allows direct access to the central nervous system, bypassing the blood brain barrier, resulting in greater bioavailability, lowed concentrations required and reduced off-target side effects. Particularly for our study aims: the intranasal delivery of OxA has shown to have a preferential distribution in migraine-relevant nuclei (ie.

trigeminal nerve and hypothalamus) (Dhuria, Hanson et al. 2009) and has proven to have a more profound impact on sleep deprivation-induced metabolic activity and cognitive performance than a significantly higher intravenous dose (Deadwyler, Porrino et al. 2007).

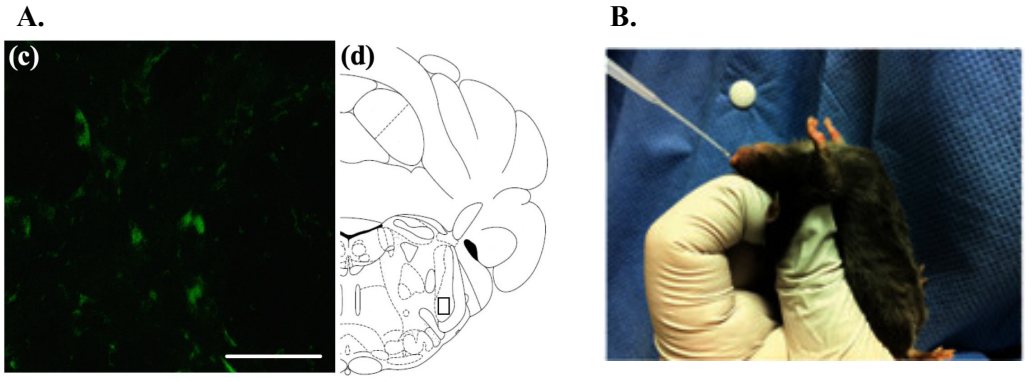

Figure 2.5. Intranasal administration protocol. A. Intranasal administration of labelled OxA shows a high fluorescently-labelled distribution of OxA in the spinal trigeminal nucleus (Dhuria, Hanson et al. 2009). B. Scruffing and intranasl administration technique in mice (Hanson, Fine et al. 2013).

An initial optimisation of this approach allowed us to determine the optimal dose for future studies. Dose-dependent effects were determined by measuring their locomotor activity for the following 30 minutes after OxA administration in individually housed cages with an overhead passive infrared sensor to detect movement. Our pilot study highlighted that a dose of 10 ng/µl resulted in optimal increased activity when compared to saline treated mice. This is in agreement with the central nervous system arousal promoting actions of OxA (Tsujino and Sakurai 2013). As nocturnal animals, mice would usually start decreasing their locomotor activity at 7 a.m. (lights ON); however intranasal OxA resulted in increased activity from 7 to 10 am compared to the saline-treated mice (**Figure 2.6.**).

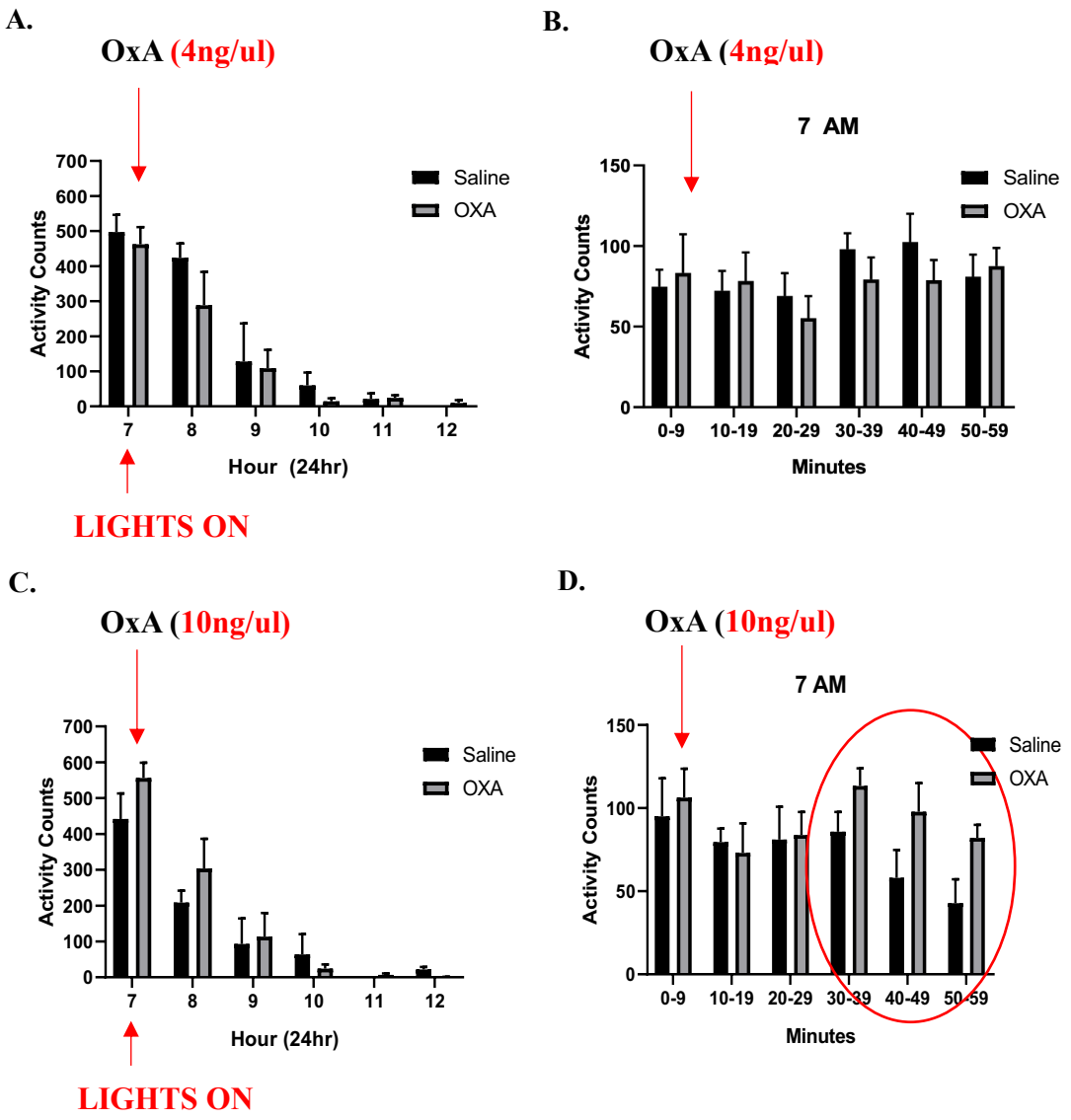

Figure 1.6. Optimisation of orexin A (OxA) administration dose. Intranasal OxA 4 ng/µl at lights on showed no changes in activity counts (7 a.m. to 12 p.m.) (A), or acute responses over the first hour (B). The graphs show the time unit (hours or minutes) in the x-axis, whreas Y-axis presents the average activity counts (n = 5 per group). A higher dose of OxA (10 ng /µl) resulted in a distinctive increase in activity counts from 7am to 9am (C), specially from 30 to 60 minutes post OxA administration (D), compared to the saline. This was a preliminary exploratory study with low group sizes, which aimed to qualitatively identify the optimal concentration of OxA, therefore no statistical anlaysis was performed.

2.3. RATS

2.3.1. Stereotaxic surgery

Similar to the mice protocol, rat surgeries were performed under oxygen-enriched Isoflurane anaesthesia (2%; following 5% for induction) in a stereotaxic frame (Kopf Instruments). Four week old Sprague-Dawley rats were injected unilaterally or bilaterally with the corresponding PRS-mediated canine-associated virus (CAV2) by use of a Nanolitre Injector (Drummond Scientific). The glass capillary needle attached to the injector was initially back-filled with mineral oil to then be front-filled with the virus. The rodent's head was then set accordingly to have Bregma and Lambda linearly oriented to each other. Holes were drilled into the skull with a saline cooled dental drill, and the glass capillary was lowered into the LC. The coordinates used were: Lambda -2.30mm, mediolateral +- 1.30mm dorsoventral: -6.00, -5.50, -5.00 and -4.50mm (Paxinos and Watson 1986). These were initially optimised by stereotaxically injecting both ink and a cholera-B-toxin fluorophore into the LC. Following injection of the compound at a rate of 2 nL/sec, the capillary was left to rest for 5 minutes at each depth and then removed at intervals of 0.50 mm/minute to prevent viral back propagation up the injection track. The skin incision was stitched with absorbable sutures, the rats were administered saline to aid recovery and the animals were allowed to recover for 3-4 weeks to allow full viral transduction, to then be subjected to the correspondent electrophysiological measures, behavioural assays or tissue collection procedures (age: 7-8 weeks old, weight; 300-400g).

2.3.2. Canine Associated Viruses (CAVs) and Adeno-associated Viruses (AAVs)

Noradrenergic networks provide essential modulation over arousal promoting pathways (Berridge, Schmeichel et al. 2012) and also modulate trigeminal nociception (Vila-Pueyo, Strother et al. 2018). To assess this, we applied a novel PRS-viral promoter to selectively target noradrenergic projections between the LC and migraine-associated nuclei such as the trigeminocervical complex, the hypothalamus or LC. This PRS promoter is coupled to a Canine Associated Virus (CAV2), which is characterized by its high transduction and retrograde properties (Li, Hickey et al. 2016). With this we aimed

to map noradrenergic descending projections known to innervate the spinal cord, trigeminocervical complex or other higher order nuclei.

Dopamine beta-hydroxylase (DBH) is the enzyme responsible for converting dopamine into noradrenaline, and its promoter has been extensively used to target catecholaminergic neurons (adrenergic and non-adrenergic) (Kim, Seo et al. 1998). A prevailing challenge is to identify a promoter that enhances transgene expression specifically to noradrenergic neurons, and thus differentiate its role from adrenergic neurons. Yang and Ishiguro however identified a specific sequence: upstream of the 5' end of the DBH promoter, which is required for DBH transcription, but more importantly it is unique to noradrenergic neurons (Ishiguro, Kim et al. 1995, Yang, Kim et al. 1998).

This sequence contains various elements that are critical for noradrenergic specific transcription, known as: Homeodomain (HD) transcription factors (TFs): PHOX2A/Arix and PHOX2B/NBPhox. These TFs will bind to three binding sites found in the 5' upstream sequence: PRS 1-3 (cis-regulatory elements) **(Figure 2.7.).** The binding of these elements will then allow the transcription of the DBH promoter, which has proven to be critical for the development of NA neurons (Boulaire, Balani et al. 2009).

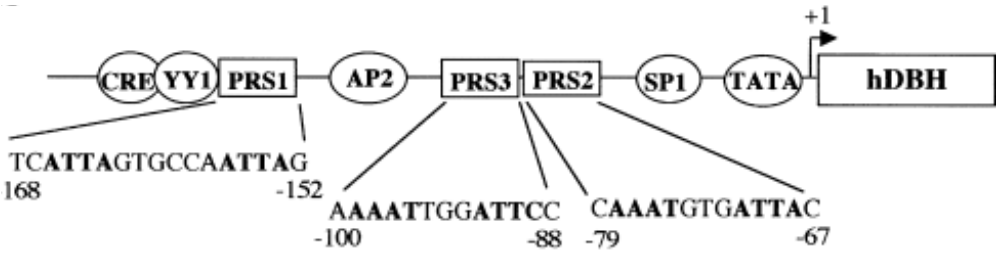

Figure 2.7. 5' upstream sequence of the hDBH gene. Homeodomain TFs: PHOX2A/Arix and PHOX2B/NBPhox, will bind to three cis-regulatory elements: PRS1, PRS2 and PRS3, found 5' upstream of the hDBH gene to regulate its expression. These homeodomains can be found in the form of PHOX2A or PHOX2B proteins; each of which have different affinities to the cis-regulatory elemetns, with PRS2 having shown higher affiniity to PHOX2A compared to PRS3 (Hwang, D'Souza et al. 2001).

A common limitation when generating constructs is that some promoters are too weak to produce strong transgene expression, thus promoter engineering techniques are used to boost the expression. To generate the synthetic PRSx8 promoter, Hwang and colleagues

modified this 5' upstream sequence to the DBH promoter by multimerizing (8-12 copies) one of the cis-acting elements: PRS2. Compared to intact DBH promoter construct often used in the literature: this has shown higher promoter activity, the same ability to target transgene expression in NA neurons, and higher specificity to NA neurons with less non-NA expression (adrenergic) (Hwang, D'Souza et al. 2001). This newly synthesized promoter has thus been coupled to a CAV2 vector in order to transduce NA-specific projections in the central nervous system.

For the current work, a 'Dual Viral approach' was firstly adopted by combining a CAV2 construct: CAV2-Cre-PRS-V5, with an anterograde AVV-DREADD: pAAV-hSyn-DIO-hM3D(G_q)-mCherry (#44361, Addgene). The CAV2 is coupled to the described noradrenergic-specific synthetic promoter: PRSx8 (PRS), as well as to a tag: V5 used to visualize the virus. For our purposes, we will only be visualizing the transduced cells through mCherry provided by the cre-dependent AAV, rather than the V5 tag. Compared to the previous approaches with the use of transgenic lines containing cre, the advantage of this construct is that it provides cre itself, allowing us to use this construct in wild-type rats (**Figure 2.8. (A)**).

A second construct was used as a 'single viral approach': CAV2-PRS-hM3D(G_q)-mCherry, which does not require an additional AAV to modulate noradrenergic neurons *in vivo* (**Figure 2.8. (B)**). The CAV2, NA-specific construct contains both the hm3D(G_q) receptor, specifically responding to CNO, as well the fluorophore marker: mCherry. Both constructs were provided by a collaborator: Professor Tony Pickering, University of Bristol. While the first vector has been extensively used *in vivo* in the form of PSAM and CHR2-based optogenetic approaches (Li, Hickey et al. 2016), the second was recently developed. The initial applications of this CAV vector in this project thus involved the optimisation of this vector for *in vivo* purposes, alongside its characterization *in vitro* by the collaborating laboratory.

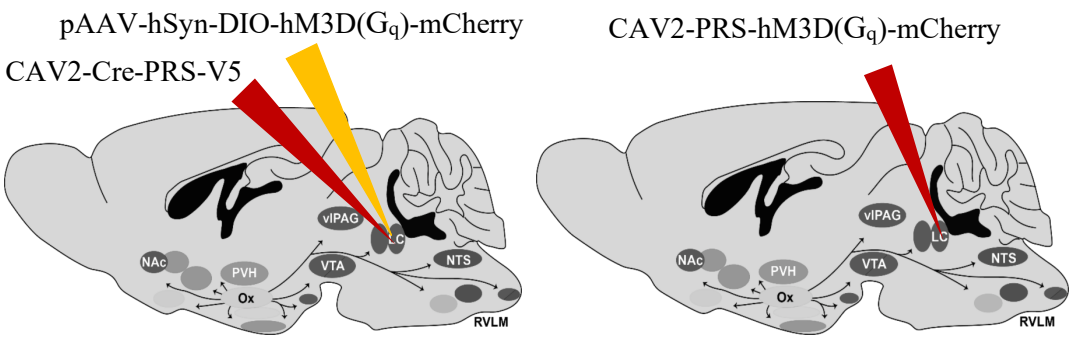

Figure 2.8. Representative diagrams of the two CAV2-mediated vector approaches that will be used in our studies. While the dual viral approach requires a cocktail of two vectors: CAV2-Cre-PRS-V5 and pAAV-hSyn-DIO-hM3D(G_q)-mCherry, the single viral approach will only involve a single vector: CAV2-PRS-hM3D(G_q)-mCherry.

2.3.3. Anaesthesia and maintenance

Animals were initially anaesthetised under oxygen-enriched Isoflurane anaesthesia (5%) then be maintained with intravenous injection of Propofol (33 – 50 mg/kg/hr) through the cannulated femoral vein. The cardiovascular and respiratory constants, as well as hind-paw withdrawal reflex, were continuously checked to monitor the depth of the anaesthesia. The left femoral artery was cannulated to monitor the blood pressure, and the vein to administer the anaesthetic. For this, the skin was incised and muscle opened through blunt cutting to expose both. These were cannulated with a polythene cannula (external diameter, 0.96 mm, Portex Ltd., UK) and connected to either Profopol (vein) or the blood pressure monitor (artery). A tracheotomy was then performed to ventilate with oxygen-enriched air and monitor the end-tidal CO2 (3.5%-4.5%), through a connected ventilator (Harvard Apparatus, small animal ventilator) and end-tidal CO_2 monitor (Kent Scientific), respectively. The body temperature was constantly measured (36. 5-37ºC) by use of a rectal probe attached to a heating pad (Harvard apparatus, UK). The blood pressure was constantly monitored to remain within suitable physiological values (80-120 mmHg). At the end of the experiments, animals were euthanised by an overdose of intraperitoneal euthatal. They were then perfused with 300 ml of 0.01M heparanised (1:10) PBS, followed by 300 ml of 4% PFA in 0.01M PBS through a peristaltic pump (Watson Marlow) at 14 revolutions per minute (2-4 ml/min). After removal of the brain

and spinal cord, these were post-fixed overnight with 4% PFA and then cryoprotected in 30% sucrose for at least 48 hours, snapped frozen and stored at -80°C until used.

2.3.4. Electrophysiological recordings

2.3.4.1. Locus Coeruleus exposure and *in vivo* recordings:

For LC *in vivo* recordings, the orientation of Bregma-Lambda was firstly measured to be set in the same angle of orientation, ensuring there was no difference higher than 0.01mm. A burr hole was drilled via a saline-cooled dental drill into the skull, and the dura was then carefully retracted to allow the electrode to be lowered into the brain. The electrode was placed at the optimised coordinates: Anterior-posterior (from Lambda): -2.30 mm, Medio-lateral: 1.25 mm, Dorso-Ventral: -5.60mm from the surface of the brain (Paxinos and Watson 1986). It was initially placed at -4 mm from the brain level and lowered at 50 μm increments until LC neurons were identified. A syringe attached to a cannula was also positioned intraperitoneally at the start of the surgery, to allow for intraperitoneal administration of compounds at any time point during the experiment.

Extracellular recordings from LC neurons were performed using a tungsten microelectrode (1 MΩ), referenced against a silver chloride pellet (Word Precision Instruments, UK) located on the neck. The signal was initially processed via an AC preamplifier (Neurolog NL104, gain ×1000), and then band-pass-filtered (NL125, bandwidth 300 Hz - 6 KHz) (Li, Hickey et al. 2016). Data was initially collected at a sampling rate of 52KHz, converted through an ADC system and stored on a PC to be analysed within Spike2 software. It should be noted that while these recordings would measure group-cell activity; noradrenergic neurons in the LC were later identified in post-hoc cell sorting based on the following criteria:

1. An action potential of >1ms and a characteristic large amplitude waveform.

2. Spontaneous activity with a frequency of firing of 0.5-7Hz.

3. Biphasic responses to contralateral hind-paw pinch (lasting 1 second): an immediate activation followed by an inhibition period (Cedarbaum and Aghajanian 1978).

Once neurons were identified, a total of five contralateral hind-paw pinches were performed every 5 minutes. The baseline firing rate was measured for 15 minutes prior to providing the compound: Clozapine-N-Oxide (CNO) intravenously. Given that it takes 30 minutes for CNO to enter the CNS when given intraperitoneally, for the initial optimization of the vectors; we administered it intravenously to confirm a successful activation of TH neurons in the LC *in vivo* **Figure 2.9.**).

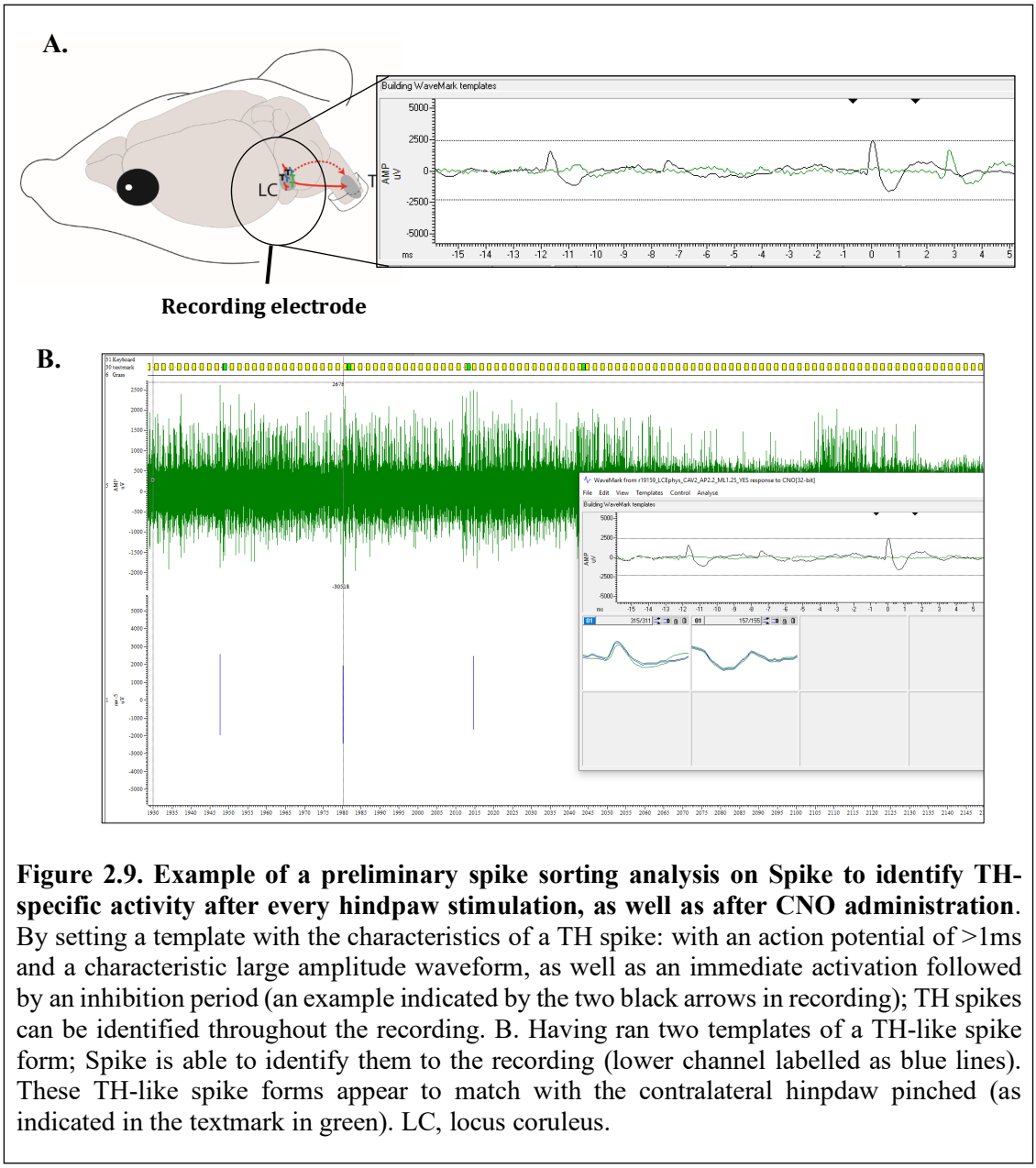

Figure 2.9. Example of a preliminary spike sorting analysis on Spike to identify TH-specific activity after every hindpaw stimulation, as well as after CNO administration. By setting a template with the characteristics of a TH spike: with an action potential of >1ms and a characteristic large amplitude waveform, as well as an immediate activation followed by an inhibition period (an example indicated by the two black arrows in recording); TH spikes can be identified throughout the recording. B. Having ran two templates of a TH-like spike form; Spike is able to identify them to the recording (lower channel labelled as blue lines). These TH-like spike forms appear to match with the contralateral hinpdaw pinched (as indicated in the textmark in green). LC, locus coruleus.

2.3.4.2. Trigeminocervical complex exposure and in vivo recordings:

Trigeminal nociceptive neurons are facial-receptive neurons with convergent nociceptive inputs from the middle meningeal artery (MMA), terminating within the trigeminocervical complex. *In vivo* recordings of these neurons involved: an initial laminectomy to expose the cervico-medullary junction and position an electrode into the area receiving sensory afferents from the ophthalmic dermatome, followed by the exposure of MMA and placement of a bipolar stimulating electrode (F.H.C. Inc.) across the MMA to activate durovascular nociceptive afferents.

In order to expose the trigeminocervical complex, the skin and muscles in the dorsal neck were firstly separated with the use of scissors and forceps (**Figure 2.10.**). Once identified the first bone of the C1 vertebrae, the ipsilateral side to both: the LC CAV2 transduction injection and the MMA stimulation, was drilled away. The dura on top of the brainstem C1 level was then pinched and carefully removed to allow the electrode to be placed at the surface of the brainstem. At this point, and prior to placing the electrode in the spinal cord, the MMA was exposed (as detailed in section 2.3.4.3.).

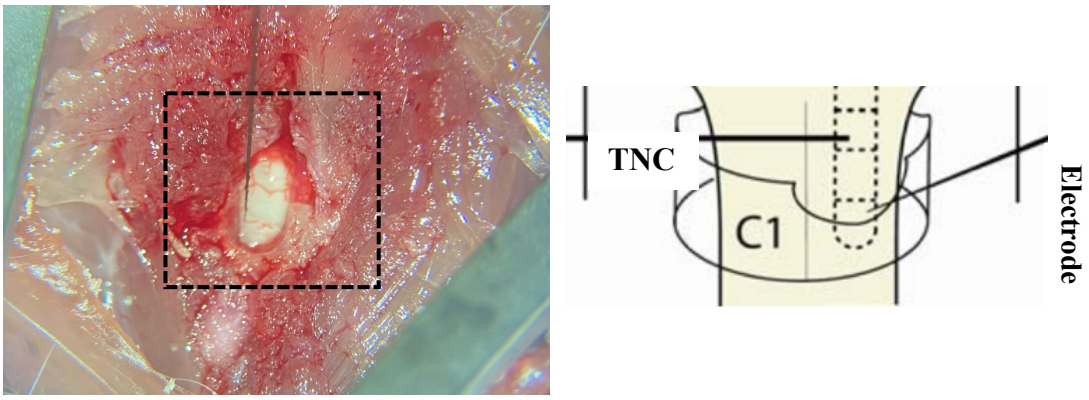

Figure 2.10. Representative image of the laminectomy performed over the C1 spinal cord level. The muscles have been pulled apart enough to allow access but not to the extent to cause excessive bleeding. The bone was carefully drilled in a curvature shape to allow access to carefully pinch the dura. The electrode (seen in black) was then positioned slightly lateral in order to gather the largest V1 area accoridng to the V1, V2 and V3 distribution (see Figure 2.11. below). TNC = Trigeminal Nucleus Caudalis.

Once the MMA was exposed a tungsten microelectrode was then lowered at 5 µm increments into the trigeminocervical complex. As the electrode is lowered into the

trigeminocervical complex the orofacial dermatomes are brushed gently until a sufficient depth is reached whereby the electrode is within he termination zone of the ophthalmic (V1) dermatome, based on the somatotopic organisation in the spinal cord (**Figure 2.11.**). Specifically, V1-specific responding neurons were spatially constricted to the region around the eye (**Figure 2.11**.): corresponding to the referred pain often reported behind the eye in patients (2018, Headache Classification Committee of the International Headache Society (IHS)). Once V1-responding neurons were encountered, the electrode was left for 30 minutes to rest.

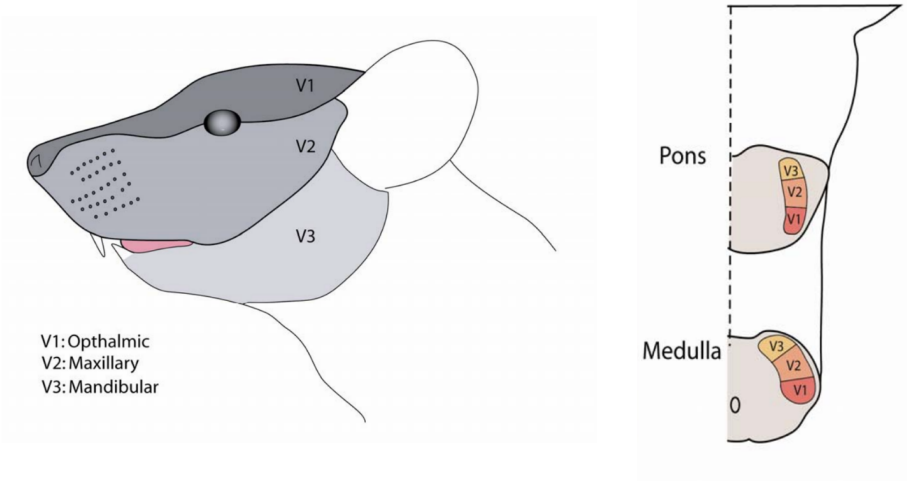

Figure 2.11. The somatotopic organisation of trigeminal afferents innervating the face and their terminations in the spinal cord. V3, mandibular; V2, maxillary and V1, ophthalmic region of the trigeminal nerve.

2.3.4.3. Middle Meningeal Artery (MMA) exposure and stimulation

As mentioned, the MMA is stimulated in order to identify durovascular-evoked nociceptive responses within the trigeminocervical complex. Following the laminectomy, the MMA was exposed by an initial incision of the skin covering the dorsal skull and retracting the surrounding muscles. The craniotomy was performed by carefully drilling a window of 5 x 5 mm over the MMA and ensuring the dura remained untouched with a saline cooled drill. The bone covering the dura was carefully peeled off with fine forceps to avoid any damage. After this, as previously described, the tungsten electrode was then placed into the spinal cord V1 region and 30 minutes were allowed for both the laminectomy and MMA craniotomy to rest. During this period, heavy mineral oil was

placed over the MMA to avoid dehydration. Finally, a bipolar stimulating electrode (F.H.C. Inc.) was placed over the dura mater covering the MMA. This electrode was attached to a stimulus isolation unit (Grass S1) connected to a Grass S88 stimulator (voltage system): allowing us to manually control the frequency, duration, and rate of stimulation using a constant voltage. (**Figure 2.12**.).

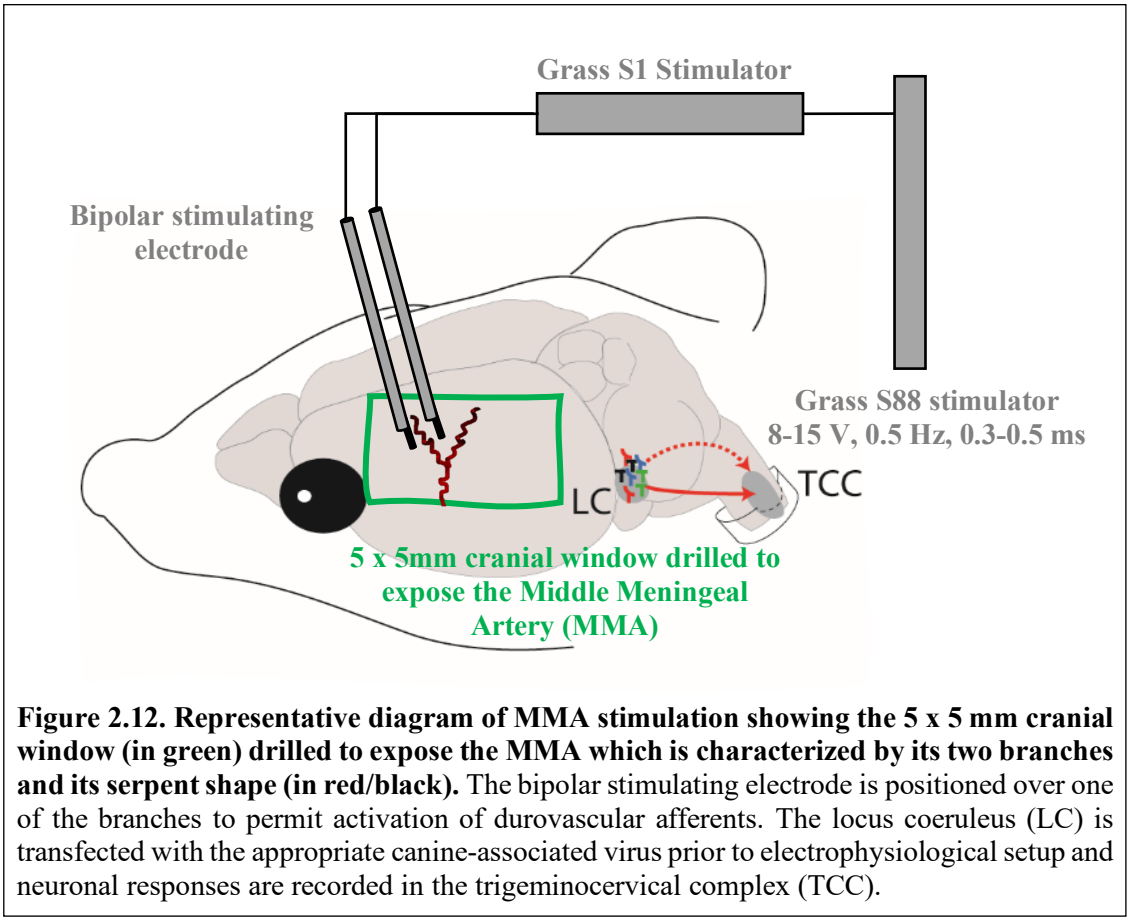

Figure 2.12. Representative diagram of MMA stimulation showing the 5 x 5 mm cranial window (in green) drilled to expose the MMA which is characterized by its two branches and its serpent shape (in red/black). The bipolar stimulating electrode is positioned over one of the branches to permit activation of durovascular afferents. The locus coeruleus (LC) is transfected with the appropriate canine-associated virus prior to electrophysiological setup and neuronal responses are recorded in the trigeminocervical complex (TCC).

Having confirmed facial-receptive neurons in V1 ophthalmic region (through gentle brushing), specific dural nociceptive neurons are then identified in the trigeminocervical complex by stimulating the MMA with pulses of: 8 - 15 V, 0.5 Hz, 0.3 - 0.5 ms. Single pulses with these range of features were applied until a neural population with consistent responses was identified. Once established the region (V1) and presence of dural Aδ nociceptive neurons (responding to MMA stimulation within 5 - 20 ms to ensure Aδ-fibres were distinguished from C-fibres), three sets of 20 stimuli each, were applied every 5 minutes, the average of which was used as the baseline response. Measurement of the distance between the MMA stimulating site and the cervicomedullary recording site (25–30 mm), including 1 ms for the central synaptic delay, allowed the calculation of neuronal

conduction velocities. Neurons were then classified as receiving input from Aδ-fibres, latency of 4–20 ms or C-fibres, latency of greater than 20 ms. The data collected from Aδ-fibre units represents the total number of cells fired over a 10 ms time period in the region of 4–20 ms post stimulation over the 20 collections (**marked in red; Figure 2.13., A).**

Post-stimulus histograms (PSTHs) across 20 sweeps were then generated at regular intervals. PSTH values represent the number of spikes that surpass an established threshold over a defined 200 μs bin. Each PSTH value thus represents the total number of spikes fired over 20 sweeps, within the temporal window of 5-20ms post stimulation (**marked in red; Figure 2.13., A).** An average of these three PSTH baselines was recorded ensuring that the total PSTH was within a range of 85-100 (total number of units responding to durovascular stimulation), and that there was no more than 10% difference between the three baseline responses. The number of units that fire above a predefined threshold is represented in the PSTH histogram (**marked in red; Figure 2.13., B).**

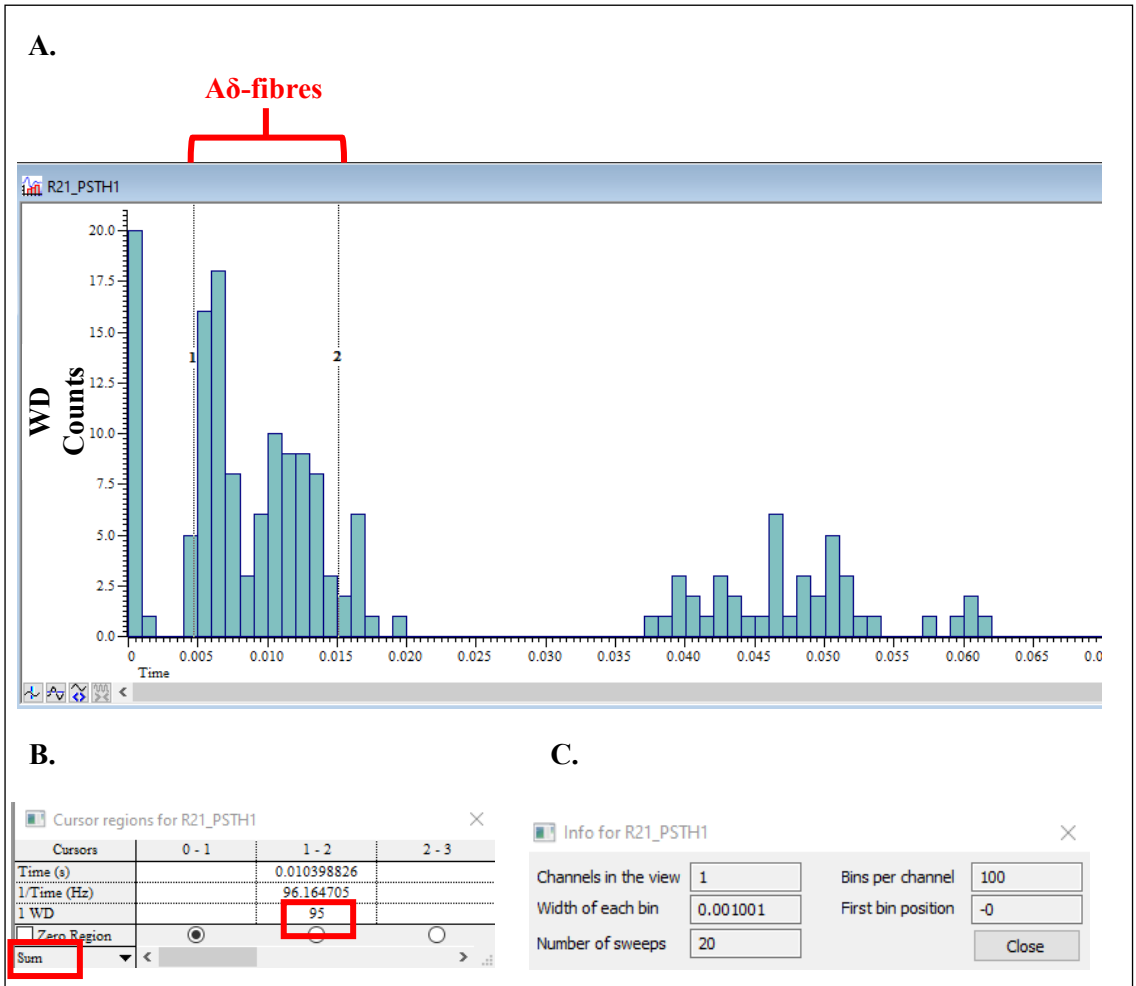

Figure 2.13. A. Representative diagram of a PSTH resulting from electrically stimulating the MMA. The PSTH is the total spike count (Y-axis) which surpassed the established threshold (20.6) within a 10 msec (0.01sec) time window (X-axis) **B.** Cursor regions are set to determine the time window post-MMA stimulation: from 0.005 to 0.015 seconds to selectively identify Aδ-fibres. Notice that at later time points (0.040 sec) there is another active cluster of cells responding to the dural-evoked stimulation: potentially C-fibres. **C.** Indicative of the number of stimulations: Number of sweeps, being 20, and the width of each bin: 0.001.

1. For Chapter 6, section 6.3.4.2., in order to activate the LC-noradrenergic populations *in vivo*: at this point of the experiment; the syringe connected to the i.p. cannula was then switched to deliver CNO, and CNO was slowly administered ensuring no leakage from the cannula. Whereas, in section 6.3.3.; CNO was administered intravenously.

2. For Chapter 5, in order to activate the LC through orexinergic compounds; at this point the orexinergic compound (OxA, OX_1R antagonist or saline (NaCl 0.9%))

were microinjected into the LC through a multi-barrel pipette attached to a pressurized syringe system.

For all studies; changes in spontaneous (Hz) and durovascular-evoked (number of units) nociceptive responses were then recorded for the subsequent one to three hours. Durovascular-evoked responses (MMA stimulation) were performed at different time points depending on the study design, and the values annotated accordingly. Spontaneous activity was measured through Peri-stimulus histograms. These are measured as the constant firing rate throughout the whole recording, which represent the spikes over time (in Hz: frequency per second). In order to gather the changes in spontaneous firing; a time window was manually set 10 ms prior to the dural-evoked stimulation; and the mean of the spikes was measured in that period. Non-nociceptive and nociceptive facial stimulation was also measured throughout the experiment, which involved a brush (non-nociceptive) and a pinch (nociceptive) over the ophthalmic dermatome. Importantly, facial stimulation would be only performed after the according MMA stimulation at that time point, to allow enough time for neural activity to normalize before the next dural-evoked response (MMA stimulation).

1. For Chapter 6, section: 6.3.4.2.; two baseline brush and pinch responses were measured pre-CNO: after the first and third baselines and averaged for the posterior analysis. These were then measured at the following time points (minutes) post-CNO: 10, 45, 75, 105, 135, 165 and 195, making a total of eight data points per animal (**Figure 2.14.**).

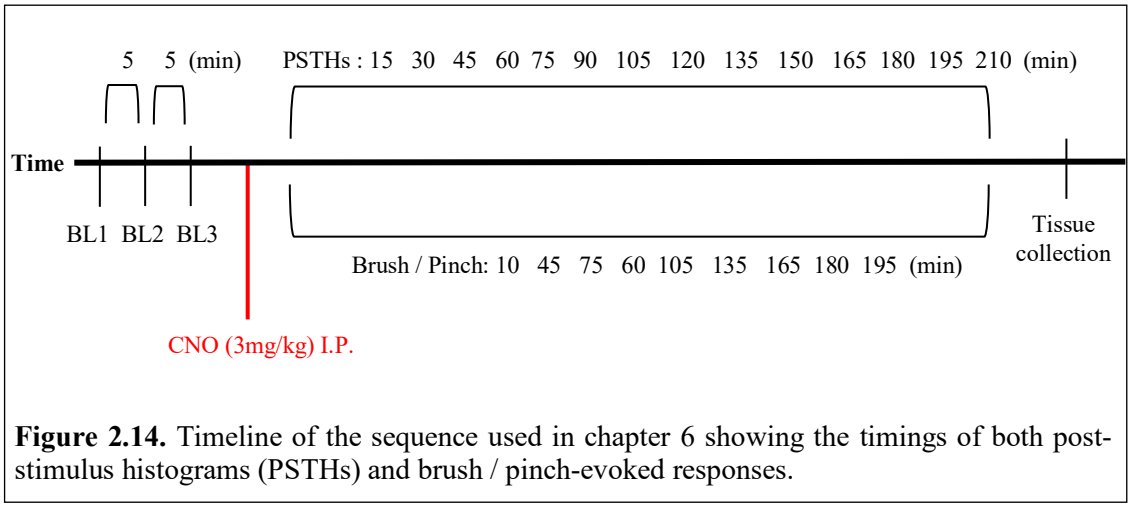

Figure 2.14. Timeline of the sequence used in chapter 6 showing the timings of both post-stimulus histograms (PSTHs) and brush / pinch-evoked responses.

2. For Chapter 5, study 5.3.; two baseline brush and pinch responses were also measured pre-compound administration: after the first and third baselines and averaged for the posterior analysis. And these continued to be measured at time points (minutes) post-compound microinjection: 15, 35 and 65, making a total of four data points per animal (**Figure 2.15.**).

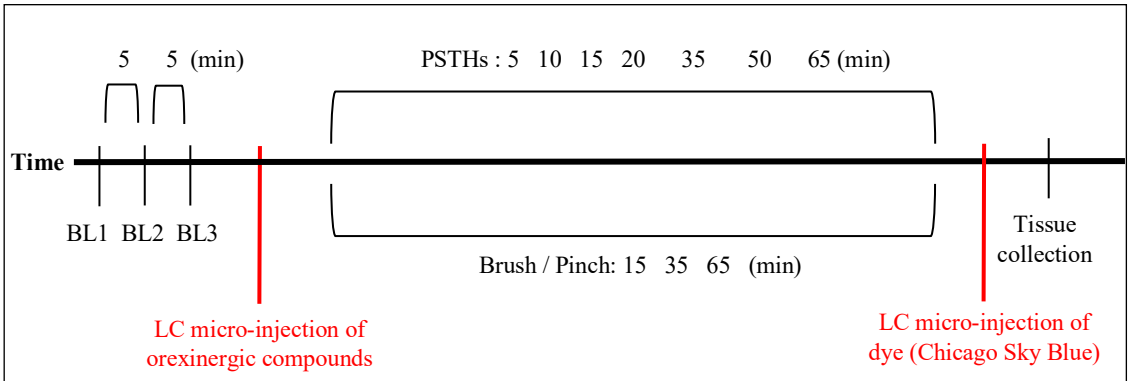

Figure 2.15. Timeline of the sequence used in Chapter 5 showing the timings of both post-stimulus histograms (PSTHs) and brush / pinch-evoked responses.

2.3.5. Immunohistochemistry/Immunofluorescence

2.3.5.1. Tissue collection and perfusion

For Chapter 6, at the conclusion of the recordings, rats were anesthetized with Euthatal (i.p.) and transcardially perfused by insertion of a butterfly needle into the left ventricle, and then snipping the right atrium to allow the expel of blood. Two hundred ml of 1% heparinised PBS was then pumped into the left ventricle, followed by 200 ml of 4% paraformaldehyde (PFA) (Sigma-Aldrich, UK). Brains were dissected out, post-fixed overnight (4% PFA) and then cryoprotected in 30% sucrose (SLR, Fisher, UK) for at least 48 hours, until they sink. The samples were then snap frozen and cryostat (Bright Instruments) cut coronally at 30 µm (free floating in antifreeze) and stored at -80°C until use. For chapter 5, upon injecting Chicago sky blue (Biotechne, Tocris, #0846) into the LC, the brains were cryosectioned at 50 µm to confirm the injection site. The slices were mounted directly onto slides, air dried and coverslipped.

2.3.5.2. c-Fos, Tyrosine-Hydroxylase (TH)

The immunohistochemical protocol used to stain for cFos and TH was identical to that detailed in **section: 2.2.4.3**.

2.3.6. Drug compounds

Animals were intraperitoneally administered with CNO (Sigma-Aldrich, C0832) at 3 mg/kg based on literature reporting this as the minimal effective dose (Jendryka, Palchaudhuri et al. 2019). CNO is a pharmacologically inert compound designed to specifically target and activate hM3Dq receptors, which are in this case bound to the CAV2 vector. CNO was initially dissolved in one ml of saline (NaCl 0.9%) (5 mg/ml) and aliquoted at -20ºC until further use. On the day of the experiment, the aliquot was defrosted and diluted to a final concentration of 3 mg/kg in saline (room temperature for i.p. administration).

In chapter 5; OxA (Tocris, Cat No: 1455) and the OX_1R-antagonists, SB-334867 (Tocris, UK) were microinjected into the LC at a concentration of 0.01 mM; at which they were previously established to have a biologically effect (Bartsch, Levy et al. 2004, Holland, Akerman et al. 2006). Stock OxA was initially diluted in saline whereas SB334867 was diluted in DMSO and both were kept frozen at -20ºC. On the day of the experiment, both compounds were defrosted and diluted accordingly to 0.01 mM. The control group was treated with saline diluted at the same concentration of DMSO as SB334867.

2.3.7. Drug administration

2.3.7.1. Intraperitoneal

Once the rat was placed in the frame, and prior to starting any further surgical procedure, a short cannula (external diameter, 0.96 mm, Portex Ltd., UK) was attached to a needle and syringe (1 ml) and placed into the i.p. space. In order to administer the active compound: the empty syringe was then switched to that with the compound and slowly injected ensuring no leakage (the cannula initially contained saline to avoid any

air bubbles when switching the syringe). The cannula remained untouched for the whole duration of the surgery to ensure that the animal did not move and thus displacement of the electrode in the spinal cord.

2.3.7.2. Intravenous

Venous cannulation was performed at the beginning of the experiment to allow continuous infusion of propofol (30 – 50 mg/kg/hr) to maintain anaesthesia. The rate of infusion would slightly vary depending on the animal's size and age, but would typically start at 1.4 - 1.5 ml/hour. This was progressively decreased by constant monitoring of the blood pressure and CO_2 throughout the surgery, typically ending with a rate of 0.8 -0.9 ml/hour after the 5-6 hours of surgical procedure.

2.3.7.3. Intracranial

Intracranial microinjections into the LC (Chapter 5) were carried out with multi-barrel glass capillary pipettes (USP-4, MicroData Instruments). These were initially pulled (MicroData Instruments) to generate a tip long enough (6 - 7 mm) to reach the LC, with a tip diameter of around 150 µm. The corresponding drugs and compounds were back-filled into the pipette's capillaries, and each was attached to a plastic/rubber connected to a 50 ml syringe. Once within the LC, the drugs and compounds were then independently released through a pressurized system manually regulated by the syringe. This consisted of a 50ml syringe attached to a manual pressurized system with five port entries; each of which was positioned around each pipette's capillary. Volumes of 200 – 250 nL were microinjected over a period of 60 seconds through manual pressure. At the end of the experiment, Chicago Sky blue was also injected to ensure a successful injection site.

3. Chapter 3 – Effects of Cre-mediated ablation of orexins in the LH on periorbital mechanical allodynia

3.1. Introduction:

As detailed in Chapter 1 (section 1.4, page 31), migraine is defined by a complex range of highly disabling symptoms that can occur up to three days prior to the headache attack (2018, Headache Classification Committee of the International Headache Society (IHS)), including abnormal fatigue, photophobia (light aversion) (Schulte, Jurgens et al. 2015), loss of appetite and difficulty concentrating (Giffin, Ruggiero et al. 2003). These symptoms have been linked to a disruption of body homeostatic mechanisms largely orchestrated by the hypothalamus (Goadsby, Holland et al. 2017) that result in abnormal sensory processing.

In agreement with this hypothesis, recent clinical PET and fMRI studies have uncovered abnormally active hypothalamic and brainstem nuclei during this symptomatic phase (Afridi, Giffin et al. 2005, Afridi, Matharu et al. 2005, Maniyar, Sprenger et al. 2014), as well as changes in functional connectivity among these nuclei as the patient progresses towards the next acute attack (Stankewitz, Aderjan et al. 2011, Schulte and May 2016). We thus hypothesized that altered arousal/homeostatic-related networks that include key hypothalamic and brainstem (LC, vlPAG) nuclei may play a prominent role in migraine attack initiation (Holland 2014). As such, we aimed to determine the impact of modulating migraine-relevant neurotransmitter pathways on migraine pain and associated phenotypes *in vivo* through chemogenetic and AAV based ablation approaches.

Focusing on hypothalamic function and the association between migraine and the potential dysregulation of sleep (Holland 2014, Stanyer, Creeney et al. 2021), marked fatigue (Giffin, Ruggiero et al. 2003, Peres, Stiles et al. 2005) and appetite regulating neural networks (Martins-Oliveira, Akerman et al. 2017, Martins-Oliveira, Tavares et al. 2021, Rivera-Mancilla, Al-Hassany et al. 2021); the hypothalamic orexinergic system emerged as a potential key system. The orexins (OxA and OxB; (Sakurai, Amemiya et al. 1998, Sakurai 2005)) are two neuropeptides co-expressed with dynorphin (Chou, Lee et al. 2001) mainly in a population of neurons that reside in the lateral hypothalamic nuclei,

making them an attractive neuronal population to study due to the discrete anatomical distribution. From the hypothalamus orexinergic neurons project throughout the majority of the brain and spinal cord (Peyron, Tighe et al. 1998, Cutler, Morris et al. 1999, Horvath, Peyron et al. 1999, Mondal, Nakazato et al. 1999, van den Pol 1999, Blanco, Lopez et al. 2001, Johren, Neidert et al. 2001, Mintz, van den Pol et al. 2001, Randeva, Karteris et al. 2001, Zhang, Sampogna et al. 2001, Johren, Neidert et al. 2002, Zhang, Sampogna et al. 2002, Zhang, Sampogna et al. 2002, Zhang, Sampogna et al. 2004). This includes several areas considered to play important roles in migraine; the cortex, thalamus, PAG, raphe nuclei, LC and trigeminal nuclei. At the level of the spinal cord, orexin neurons innervate the deeper laminae of the dorsal horn, suggesting an impact over ascending nociceptive transmission, with innervation considered highest in the cervical levels (Date, Mondal et al. 2000).

This pattern of innervation, and the co-release of dynorphin (Podvin, Yaksh et al. 2016) highlights the potential involvement of orexinergic modulation of pain processing (Bingham, Davey et al. 2001, Inutsuka, Yamashita et al. 2016). In terms of trigeminal pain processing, several studies have identified differential responses to OxA and OxB. Direct injection of OxA into the posterior hypothalamic nuclei is anti-nociceptive in a preclinical model of migraine, namely durovascular evoked TCC neuronal responses, while OxB is pro-nociceptive (Bartsch, Levy et al. 2004). Similarly, systemic administration of OxA is also antinociceptive, while systemic OxB has no effect (Holland, Akerman et al. 2006) and finally OxA and not OxB inhibits CGRP release from the trigeminal nerve in a dose-dependent manner (Holland, Akerman et al. 2005). The ability to inhibit CGRP release is considered a key therapeutic mechanism for the acute and preventive treatment of migraine (Tso and Goadsby 2017, Holland and Goadsby 2018).

Several studies have targeted the orexinergic system and explored the impact of its ablation/manipulation on diverse functions. Genetic ablation of these neurons results in a narcoleptic phenotype, reduced calorific intake and conversely late onset obesity (Hara, Beuckmann et al. 2001). However, partial ablation does not recapitulate the narcoleptic phenotype, suggesting that it may be a more relevant strategy to maintain relatively normal sleep-wake patterns and study alternate functions (Black, Sun et al. 2018). Others have used lentivirus approaches (Roh, Jiang et al. 2014) using the hypocretin gene

promoter (Sanchez-Garcia, Cabral-Pacheco et al. 2018) to ablate orexinergic cells in a specific manner; however, specific lentiviruses were not commercially available, therefore we sought to use standard AAV-based toxin approaches combined with a transgenic orexin-cre^{+} mouse line. mHCRT (hypocretin/orexin)-IRES-cre mice under the HCRT (orexin) promoter (Giardino, Eban-Rothschild et al. 2018) were a kind gift from Professor de Lecea, Stanford.

3.2. METHODS:

3.2.1. Animals

Fourteen male and female mice: 8 Orexin-Cre+ and 6 WT-littermates (20-35g), were used in this study. All animals were housed in groups of 4-5 in 21ºC and humidity-controlled rooms with a normal 12-h light/dark cycle and had free access to food and water.

3.2.2. Stereotaxic surgery

Eight-week old Orexin-Cre^{+} (n = 6) and wild type littermate mice (n = 6) were injected bilaterally with 1 µl of the Cre-dependent rAAV5-EF1a-Lox-Cherry-lox(dtA)-lox2 (UNC, Vector core) or saline (NaCl 0.9%), respectively, via a Narishige microinjector (IM-11-2, Pneumatic Microinjector, Narishige, Japan). Four small holes (two injection sites along the Anterior-Posterior axis per hemisphere, i.e. 2 per side) were created in the skull using a hypodermic needle (Terumo, 25G x 1 1⁄2") that was carefully rotated until it penetrated the skull, leaving the underlying meninges intact. A glass capillary needle filled with the AAV or control substance was slowly lowered into the lateral hypothalamus. The coordinates used were: Bregma -1.40 mm and -1.80 mm, dorsoventral -5.10 and -5.30mm and mediolateral +- 0.9 mm (Paxinos and Franklin 2014). These were initially optimised by stereotaxically injecting an AAV-Cre-GFP, and co-localised with antibodies raised against OxA and OxB (Santa Cruz Biotechnology, USA) to ensure successful targeting and coverage of the orexinergic population **(Figure 3.1.)**. Following injection of 250 nL per depth (x2) per site at a rate of 2 nL/sec, the capillary was left to rest for 7 minutes and then removed at intervals of 0.50 mm/minute to ensure no back spread of virus along the injection tract. Mice were injected intraperitoneally with saline (1 mg/kg) to facilitate their recovery post-surgery, initially in a warmed recovery chamber and closely monitored for the first week post-surgery. Mice were then recovered for at least 4 weeks to ensure successful orexinergic ablation and transcardially perfused under terminal anaesthesia 8 weeks post-surgery at the completion of the experimental protocol **(Figure 3.1.)**.

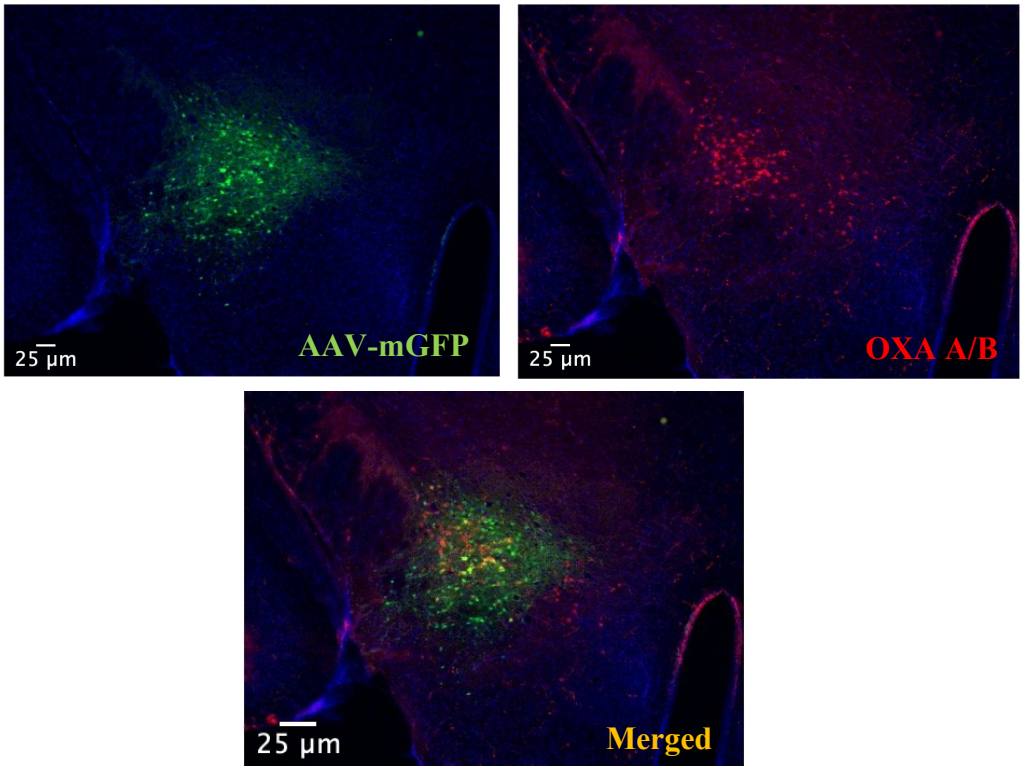

Figure 3.1. Representative images of AAV-Cre-mGFP stereotaxic injection into the lateral hypothalamus. Endogenous fluorescence of the cell bodies and fibres transduced with the mGFP (green) in the lateral hypothalamus: indicative of a successful location and spread of the injection. Staining for cell bodies and fibres of the lateral hypothalamic orexinergic population (red). Co-localisaiton of mGFP-Cre-transduced cell bodies (green) and OxAB (red) observed in orange: indicative of a successful trandcution of Cre-labelled OxA cell bodies. x10 magnification.

3.2.3. Immunohistochemistry

At the conclusion of the experiment mice were either transcardially perfused with heparinised phosphate buffered saline, followed by 4% paraformaldehyde in phosphate buffered saline. Their brains and spinal cords were dissected and cryoprotected in 30% sucrose for at least 48 hours, prior to being sectioned at 30 µm in a freezing cryostat (Bright Instruments, UK).

Immunohistochemical staining was then performed according to the antigen of interest. For the preliminary characterisation of an OX-specific transduction in the LH; GFP was not stained due to its strong endogenous fluorescence, but OxA and B were stained as described in section: 2.2.4., page 64, General Methods. Below are the details of the antibodies used **(Table 3.1).** The tissue obtained from the behavioural cohort was

then stained for either: OxAB cell bodies in the LH (chromagen: Fluorescein Avidin D), MCH cell bodies in the LH chromagen: Fluorescein Avidin D), or OxAB fibres in the LC, PAG and TCC (using the same protocol as the former OxAB fluorescence staining but with DAB as a chromagen). Once stained; sections were mounted and cover-slipped with Silver Prolong Mounting medium to then be imaged at an Axiovision fluorescence microscope.

Table 3.1. List of antibodies used in this study.

Antigen	Primary antibody (Source, Dilution)	Secondary antibody (Source, Dilution)	Chromagen
OxA	Anti-orexin A Ab (Santa Cruz Biotechnology, #sc-8070, 1:500)	Biotinylated anti-goat in horse (Vector Labs, #BA-9500, 1:500)	Fluorescein Avidin D (Vector Laboratories, A-2001-5) or DAB
OxB	Anti-orexin B Ab (Santa Cruz Biotechnology, #sc-8070, 1:500)	Biotinylated anti-goat in horse, BA-9500	Fluorescein Avidin D (Vector Laboratories, A-2001-5) or DAB
MCH	Anti-MCH Ab (Phoenix, #H-070-47, 1:500)	Biotinylated anti-rabbit in goat (Vector Labs, #BA-1000, 1:500)	Fluorescein Avidin D (Vector Laboratories, A-2001-5)

With the orexinergic population extending from Bregma -1 mm to -2 mm, the number of cell bodies was counted every fourth section, with a total of four-five sections per sample (sections being cut at 30um).

As mentioned; to determine whether the Cre-dependent AAV had successfully ablated the orexinergic population, we examined the total cell number of orexinergic neurons in the LH in both groups 8 weeks post-surgery; after finalizing the behavioural assays. Importantly, n=1 animal within the orexin-Cre^{+} ablated group showed no successful ablation of its orexinergic population (with an average of 119.5 orexinergic cell bodies), and as such it was excluded from all further analysis.

3.2.4. Behavioural assays

To validate the potential impact of ablation of a proportion of orexinergic neurons in orexin-cre^{+} mice, we assessed periorbital mechanical withdrawal thresholds using von

Frey filaments and locomotor function in the open field test. Full details are included in the general methods section: 2.2.3, pages 60-64.

Mice were transported to the testing room and allowed to acclimatise for one hour prior to testing. In brief, the mice were placed in an enclosed arena (72 x 72 x 33 cm high). To avoid potential photophobic responses, light intensity was regulated to 20 lux and the inner zone was set as 36 x 36 cm square in the centre of the arena. Activity was tracked via an overhead camera system connected to Ethovision software. The mouse was placed in the arena facing the outer wall the recording (10 minutes) commenced and the blinded investigator left the room to minimise any confounding factors. The total distance travelled and time in the inner and outer zones was recorded and used to analyse total locomotor activity and potential stress responses, respectively. This data was collected at baseline and at six weeks post injection and the arena was carefully cleaned between mice to prevent any odour transfer.

Mice were subsequently processed to assess their periorbital mechanical withdrawal thresholds as a surrogate readout of orofacial allodynia (Navratilova, Behravesh et al. 2020). Following habituation to the small espresso cups that permit access to the periorbital region, mice were moved to the testing room and again allowed to acclimatise for at least one hour. Lighting levels were maintained at approximately 30-50 lux and mice were then placed in the testing apparatus that consisted an acrylic chamber upon a mesh rack (Ugo Basile, UK), including an individual espresso cup assigned to that animal. Following 30 minutes habituation mice were gently picked up in the espresso cups and their periorbital mechanical withdrawal thresholds assessed by calibrated von Frey filaments placed perpendicularly on the surface of the periorbital dermatome above and between the eyes. Sensory responses to the filaments were then converted into a 50% mechanical withdrawal threshold using the standard up-down procedure and measured at baseline and then both five and seven weeks post-dtA/vehicle injection. The week seven readout was conducted to further assess if any observed orofacial sensitivity could be exacerbated by the clinical migraine trigger nitroglycerin (Demartini, Greco et al. 2019) **(Figure 3.2.)**

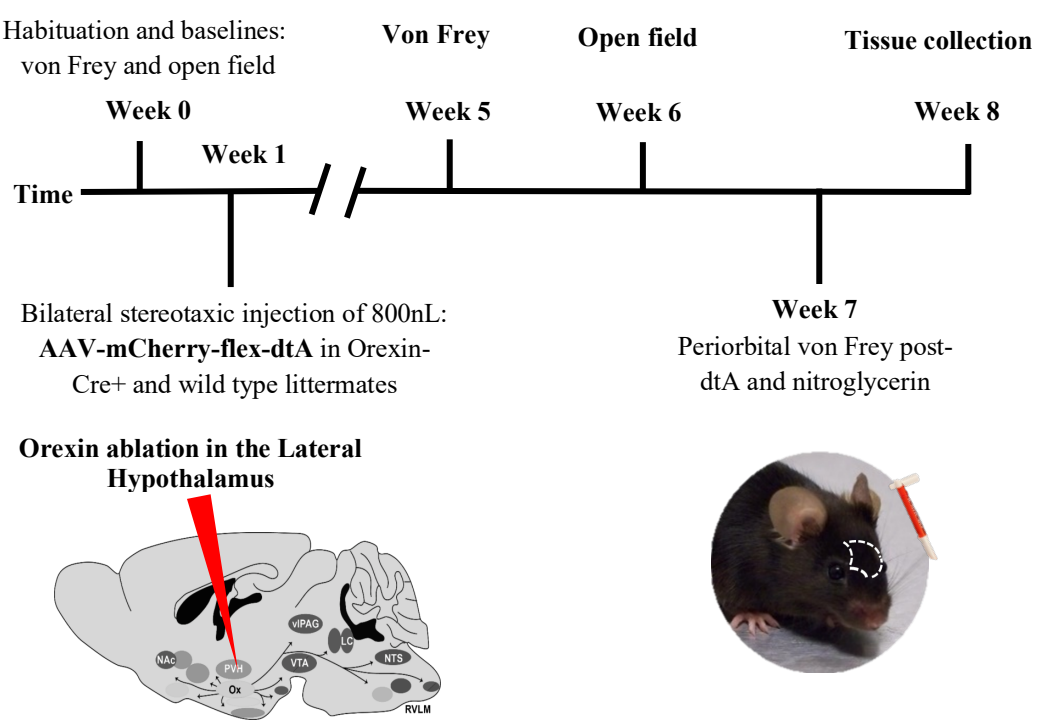

Figure 3.2. Timeline of the experimental protocol. Stereotaxic injections of AAV-mCherry-flex-dtA or saline (NaCl 0.9%) were performed on week 1 and mice were allowed to recover for four weeks to ensure successful ablation. The time-points of von Frey testing being: weeks 0, 5 and 7, and locomotor testing: weeks 0 and 7. Tissue was collected on week 8.

3.2.5. Statistical analysis and data presentation

The inclusion criteria for the behavioural analysis required a successful transduction of the AAV-dtA vector into orexinergic neurons and subsequently successful ablation of orexinergic neurons. In order to establish this; lateral hypothalamic orexinergic cell counts were compared between wild type and orexin-ablated mice. Given the nature of cell count quantification data; which is associated to a nominal rather than interval scale, as well as the small group size of this study, and lack of normal distribution (Shapiro-Wilk test); the data was considered non-parametric and group wise comparisons were conducted via the Mann Whitney U test. The 50% mechanical withdrawal threshold was calculated using the established up-down method (Chaplan, Bach et al. 1994) in response to the presence or absence of an evoked response to the application of calibrated force to the periorbital region. Changes in mechanical withdrawal threshold were recorded as a readout of periorbital allodynia and the difference between the groups (wild type and

orexin-ablated) was compared using an unpaired *t*-test. We also further explored the effects of low dose nitroglycerin (5 mg/kg) on both groups, compared to their baseline conditions (pre-nitroglycerin), to uncover any further sensitivity, by use of a two-way repeated measures ANOVA, with familywise error rates corrected for using Sidak's correction. Changes in locomotor activity at baseline and following six weeks post injection were compared between groups using a two-way repeated measures ANOVA, with familywise error rates corrected for using Sidak's correction. While normal distribution and sphericity were analysed in SPPS (IBM SPSS Statistics), the remaining analysis was performed in GraphPad Prism 7.01 software (La Jolla, CA), and a p-value < 0.05 was considered significant.

3.3. RESULTS

3.3.1. Cre-mediated orexinergic ablation

In accordance with similar AAV-based ablation approaches we established four to five weeks as an appropriate time point post-surgery to initiate the behavioural assays to ensure successful ablation. Upon the completion of behavioural analysis (8 weeks) we identified a significant reduction in orexinergic cell bodies in the orexin-Cre^{+} group compared to the wild-type littermates, ($U = 0$, $p < 0.01$). The number of cell bodies was decreased from 125.30 [IQR: 94.50 – 135.60] in wild type mice to 0 [IQR: 0 – 1.75] in orexin-cre^{+} expressing mice **(Figure 3.3.).** A total of four to five sections were selected per animal, to ensure a full coverage of the entire LH. Sections were selected from every fourth section from Bregma -1mm to -2mm (sections being cut at 30 µm).

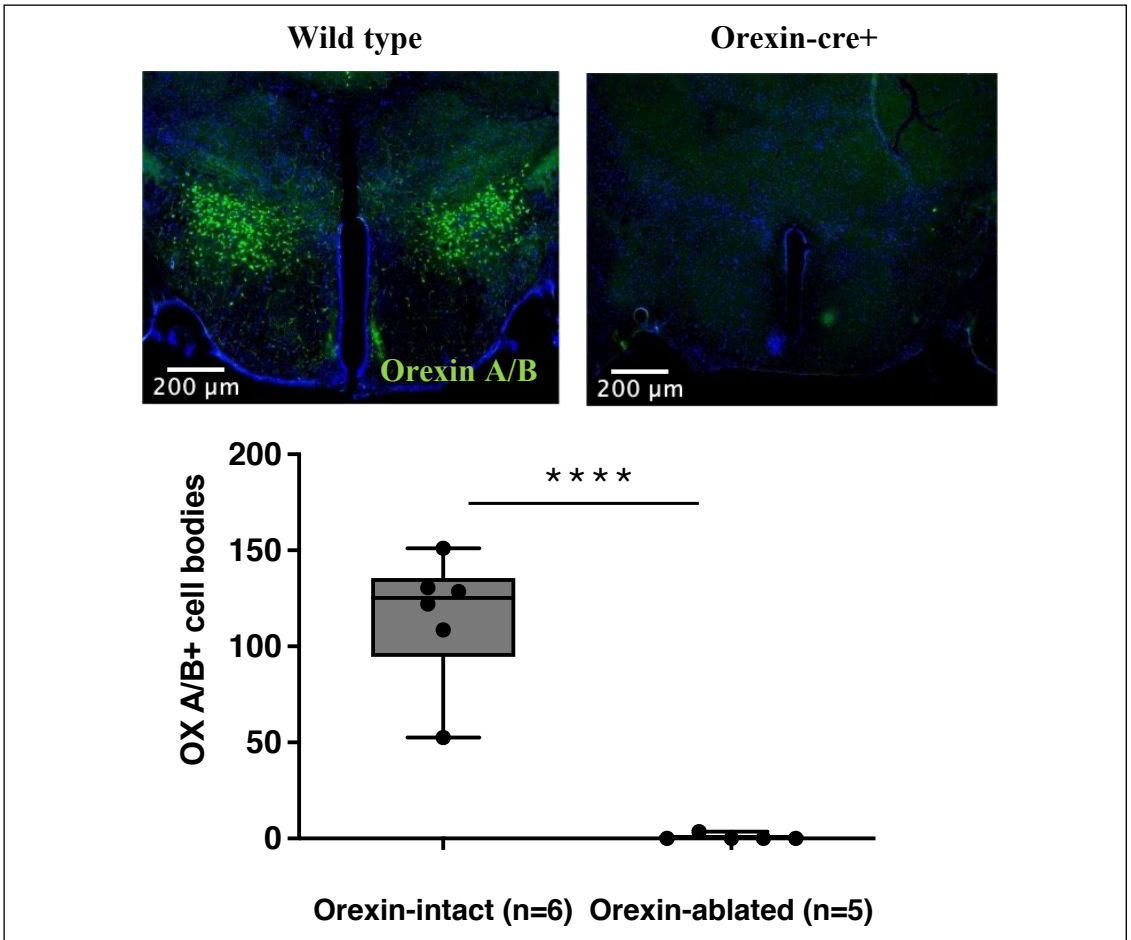

Figure 3.3. Cre-dependent ablation of orexinergic neurons in the lateral hypothalamus. Eight weeks post dtA injection there was a significant reduction in orexinergic positive neuronal cell bodies (green) in the lateral hypothalamus ($U = 0$, $p < 0.01$; 125.30 [IQR: 94.50 – 135.60] to 0 [IQR: 0 – 1.75] of wild type and orexin-Cre+ mice respectively. x10 magnification. *$p \leq 0.05$. Group wise comparisons were conducted via the Mann Whitney U test.

Given the widespread orexinergic projections from the lateral hypothalamus (Peyron, Tighe et al. 1998), we further quantified the level of orexinergic fibre terminals innervating key migraine-associated nuclei. The % area which surpassed the established threshold of fibre density (shown as OXAB-ir fibre density in **(Figure 3.4.)**) was used for analysis. There was a significant reduction in % area stained with orexin fibres projecting to the LC ($U = 0$, $p < 0.01$) with a reduction from 43141 [IQR: 37373-58439] in the wild type mice to 3603 [IQR: 1406 - 6292] in the orexin-cre^{+} expressing mice. In agreement, there was also a reduction in the % area stained for orexinergic expressing fibres in the PAG ($U = 2$, $p < 0.01$) from 125660 [IQR: 45305 - 180355] to 9310 [IQR: 2907 - 46479], respectively. As well as a significant reduction in % area stained for orexin fibres projecting to the TCC ($U = 0$, $p < 0.01$), from 24.24 [IQR=20.09-32.68] in the wild type mice to 1.036 [IQR: 0.765-8.433] in the orexin-cre^{+} expressing mice **(Figure 3.4.).**

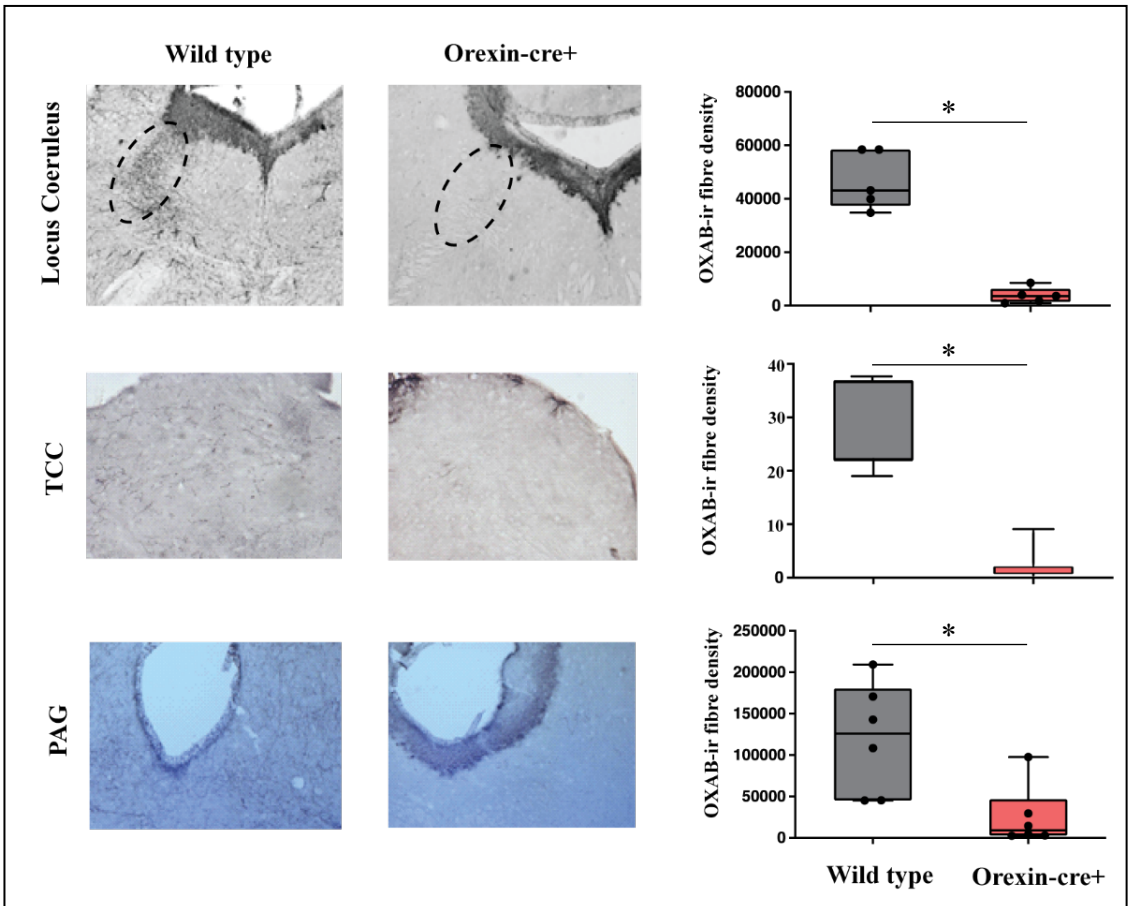

Figure 3.4. Cre-dependent ablation of orexinergic fibres projecting from the lateral hypothalamus to the locus coeruleus (LC, top), trigeminocervical complex (TCC, middle) and periaqueductal gray (PAG, bottom). Eight weeks post dtA injection there was a significant reduction in orexinergic fibres in the LC ($U = 0$, $p < 0.01$); 43141 [IQR: 37373-58439] to 3603 [IQR: 1406 - 6292], TCC ($U = 0$, $p < 0.01$); 24.24 [IQR=20.09-32.68] to 1.036 [IQR: 0.765-8.433] and PAG ($U = 2$, $p < 0.01$); 125660 [IQR: 45305 - 180355] to 9310 [IQR: 2907 - 46479], in wild type and orexin-Cre+ mice respectively. x10 magnification. *$p \leq 0.05$. Group wise comparisons were conducted via the Mann Whitney U test.

In order to confirm the relative specificity of the transgenic mouse line (Giardino, Eban-Rothschild et al. 2018) we further sought to analyse the expression of lateral hypothalamic melanin-concentrating hormone (MCH) neuronal cell bodies that are interspersed with orexinergic neurons (Concetti and Burdakov 2021). Overall there was no significant reduction in MCH expressing neurons in the lateral hypothalamus ($U = 10$, $p = 0.2143$) of wild type 111.3 [IQR: 75.13 – 157.9] and orexin-cre^{+} 148.0 [IQR: 111.3 – 159.3] mice **(Figure 3.5.)**.

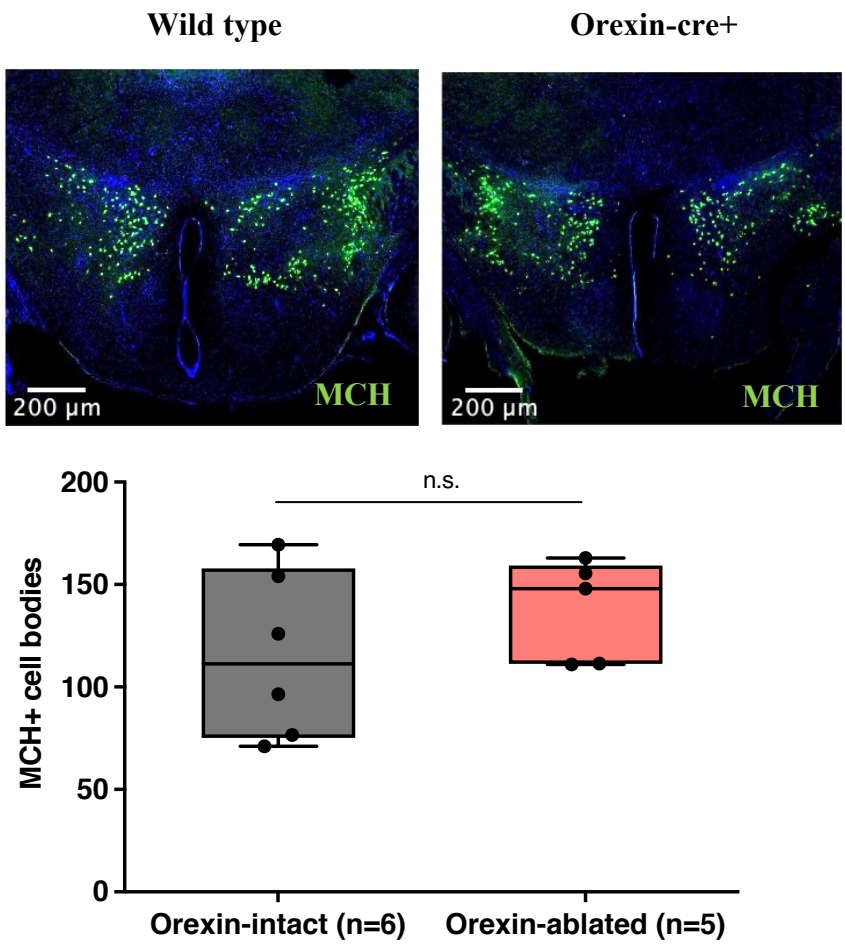

Figure 3.5. No Cre-dependent ablation of melanin-concentrating hormone (MCH) neurons in the lateral hypothalamus. Eight weeks post dtA injection there no significant reduction in MCH positive neuronal cell bodies (green) in the lateral hypothalamus ($U = 10$, $p = 0.2143$; 111.3 [IQR: 75.13 – 157.9] and 148.0 [IQR: 111.3 – 159.3]of wild type and orexin-Cre+ mice respectively. x10 magnification. n.s, non-significant. group wise comparisons were conducted via the Mann Whitney U test.

3.3.2. Altered Periorbital Mechanical sensitivity with an ablated orexinergic population

Having confirmed the succesfull ablation of orexinergic but not MCH-expressing lateral hypothalamic neurons we proceeded to determine if orexinergic ablation would impact locomotion. At baseline, prior to the stereotaxic injection there was no significant difference in periorbital mechanical withdrawal thresholds between orexin-cre^{+} and wild type littermate mice ($t_{(9)} = 0.217$, $p = 0.833$; n = 5, 6, respectively). Periorbital mechanical withdrawal thresholds were 0.734 (± 0.107) and 0.7641 (± 0.093) g, respectively **(Figure 3.6.)**.

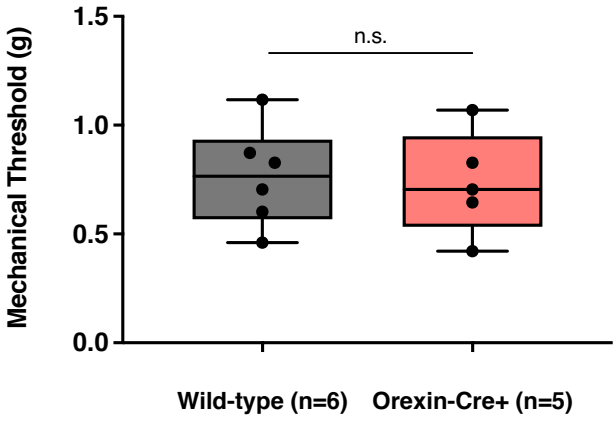

Figure 3.6. Periorbital mechanical withdrawal thresholds in orexin-Cre+ and wild type mice prior to ablation. There was no significant difference in baseline mechanical withdrawal thresholds prior to stereotaxic injection of dtA ($t_{(9)} = 0.2167$, $p = 0.8332$; n = 6 (WT) and n=5 (orexin-Cre^{+}) per group). Unpaired *t*-test.

Allowing five weeks post dtA injection for optimal viral transduction and orexinergic ablation, orexin-ablated mice and their wild type littermates were habituated to the testing apparatus. One orexin-cre^{+} expressing mouse was excluded due to no orexinergic ablation, likely due to a lack of anatomical precision when injecting. In comparison to baseline withdrawal thresholds, dtA-mediated ablation of orexinergic neurons resulted in a significant decrease in periorbital mechanical withdrawal thresholds ($t_{(9)} = 0.308$, $p < 0.013$) from 1.196 (± 0.1509) in wild type mice to 0.526 (± 0.154) g in orexin-ablated mice **(Figure 3.7.)**.

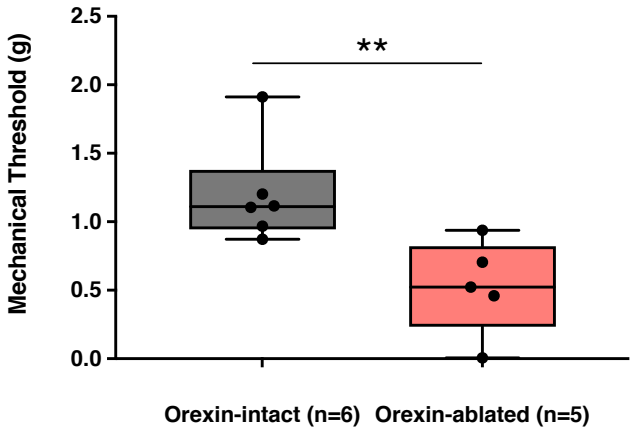

Figure 3.7. Periorbital mechanical withdrawal thresholds in orexin-Cre+ and wild type mice following orexinergic ablation. There was a significant decrease in mechanical withdrawal thresholds following orexinergic ablation ($t_{(9)}$ = 0.308, p = 0.013; n = 6 (WT) and n=5 (orexin-Cre^{+}) per group). * p < 0.05. Unpaired *t*-test.

Nitroglycerin is a common human experimental migraine trigger which is also used preclinically (Maniyar, Sprenger et al. 2014, Demartini, Greco et al. 2019) to induce migraine-like symptoms including periorbital allodynia. It is further known that mice harbouring mutations for migraine-related genes (Brennan, Bates et al. 2013) show a hypersensitivity to nitroglycerin, responding to a dose of 5 mg/kg that is half that required in wild type mice. To determine if orexinergic ablation impacted nitroglycerin sensitivity in mice, both the orexin-Cre^{+} (orexin-ablated) and wild type littermate mice used above were subsequently given 5 mg/kg nitroglycerin intraperitoneally two hours before periorbital mechanical thresholds were retested. In agreement with our prior identification of reduced sensory thresholds in orexin-ablated mice **(Figure 3.7.)**, there was a significant difference in periorbital mechanical withdrawal thresholds prior to nitroglycerin administration ($F_{(1,9)}$ = 14.01, p = 0.005) and this sensitivity in orexin-ablated mice was not further enhanced in the presence of nitroglycerin. Further post-hoc comparisons (Sidak's) among groups also uncovered a significant difference between orexin-Cre^{+} (orexin-ablated) and wild type littermate mice 2hrs post-NTG ($t_{(18)}$ = 3.125, p = 0.012). This was similar to the previously observed significant difference between orexin-Cre^{+} (orexin-ablated) and wild type littermate mice post-dtA baseline (pre-NTG) ($t_{(18)}$ = 2.857, p = 0.021) **(Figure 3.8.)**.

Despite the lack of insight into mechanisms behind NTG-induced mechanical periorbital sensitivity, evidence suggests it is mediated by an initial vasodilatory effect

followed by a conversion of NTG into Nitric Oxide within the CNS (Bates, Nikai et al., 2010). Having observed a lack of further sensitisation in the absence of orexins in this study; this might suggest a 'requirement' for orexins to facilitate the cascade of events from NO which induce migraine-like behaviours.

Our data highlight that specific ablation of orexinergic expressing neurons in the LH leads to altered mechanical sensitivity in mice. Specifically, orexin-ablated mice show reduced mechanical withdrawal thresholds which is akin to the cephalic allodynia observed in people with migraine during their spontaneous migraine attacks. Previous data (Bartsch, Levy et al. 2004) has highlighted a potential divergent role for orexin signalling over trigeminal nociception; however, our data suggests that the net role of orexin signalling from the LH is anti-nociceptive. Further it has been shown that transgenic mice carrying a familial advanced sleep mutation in casein kinase 1 delta that is comorbid in humans with migraine with aura respond to significantly lower doses of the experimental human migraine trigger NTG when compared to their WT littermates (Brennan, Bates et al., 2013). We did not observe an increased sensitivity to NTG in orexin-ablated mice, suggesting no or limited interaction.

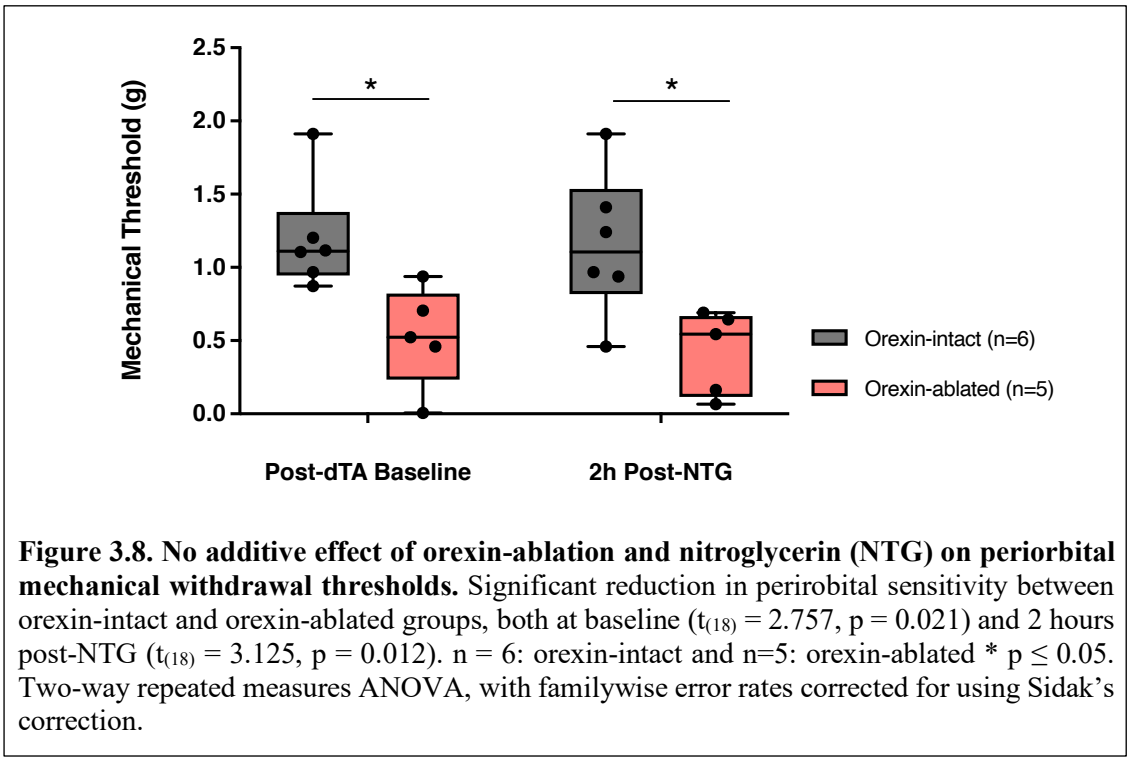

Figure 3.8. No additive effect of orexin-ablation and nitroglycerin (NTG) on periorbital mechanical withdrawal thresholds. Significant reduction in perirobital sensitivity between orexin-intact and orexin-ablated groups, both at baseline ($t_{(18)} = 2.757$, $p = 0.021$) and 2 hours post-NTG ($t_{(18)} = 3.125$, $p = 0.012$). n = 6: orexin-intact and n=5: orexin-ablated * $p \leq 0.05$. Two-way repeated measures ANOVA, with familywise error rates corrected for using Sidak's correction.

3.3.3. No altered hindpaw mechanical and thermal sensitivity with an ablated orexinergic population

Given our identification of altered periorbital mechanical withdrawal thresholds in orexin-ablated mice and the previous identification of reduced non-trigeminal pain behaviours in total orexin-ablated mice (Inutsuka, Yamashita et al. 2016) we next sought to determine if orexin ablation impacted non-trigeminal pain processing in our cohort. Comparing orexin-ablated mice to orexin-intact mice we identified no significant alteration in hindpaw mechanical withdrawal thresholds ($t_{(9)}$ = 1.714, p = 0.121; **Figure 3.9. (A)**) with mean values of: 0.619g (± 0.108) and 1.077g (± 0.2251), respectively. Following this, we next sought to test hindpaw thermal withdrawal thresholds using the hotplate test, measured across three different sessions. There were no significant changes in hindpaw thermal sensitivity between the orexin-ablated and the orexin-intact group ($t_{(9)}$ = 1.787, p= 0.108; **Figure 3.9. (B)**), with mean values of: 10.02s (± 0.876) and 11.95s (± 0.663), respectively. Contrary to previously reported significant reductions in hind paw sensitivity in orexin-ablated models (Inutsuka, Yamashita et al. 2016); a reduced trend in hind paw sensitivity in this preliminary study might be suggestive of a small sample size and slightly different ablation strategy.

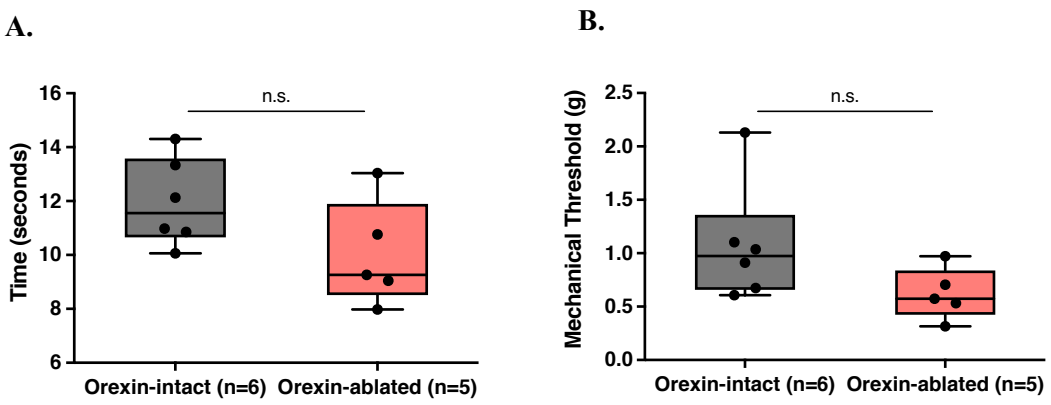

Figure 3.9. No alteration in hindpaw mechanical or thermal withdrawal thresholds in orexin-ablated mice. A. No significant changes in hindpaw mechanical sensitivity (VF test) between the orexin-ablated and the orexin-intact groups ($t_{(9)}$ = 1.714, p = 0.108) with mean values of: 0.619 (± 0.108) and 1.077 (± 0.225), respectively. B. No significant changes in hindpaw thermal sensitivity (Hotplate test) as measured in seconds ($t_{(9)}$ = 1.787, p = 0.108; with mean values of: 10.02 (± 0.876) and 11.95 (± 0.663), for the orexin-ablated and orexin-intact mice, respectively. n = 6: orexin-intact and n=5: orexin-ablated. n.s., non-significant. Unpaired *t*-tests.

3.3.4. Cre-mediated orexinergic ablation: significant reduction in locomotor activity but no changes in body weight

The orexinergic system is known to have a prevalent role in nociception (Bartsch, Levy et al. 2004, Holland, Akerman et al. 2006, Inutsuka, Yamashita et al. 2016) but also in arousal (Yamanaka, Beuckmann et al. 2003, Tsujino and Sakurai 2013). As noted, migraine patients often report abnormal fatigue as a common premonitory symptom (Giffin, Ruggiero et al. 2003), which can be measured preclinically as a reduction in locomotor activity, commonly assessed via home-cage video monitoring, telemetry and open field assays (Wolff, Raheem et al. 2018). As rotarod assessment can be impacted by gross motor abnormalities, muscle weakness and require reward mechanisms to engage with the task, we sought an alternate readout. Given the reliance on mouse spontaneous behaviour, we opted to assess locomotor function in the open field arena.

In this initial assessment, orexin-ablated mice demonstrated a significant reduction in total distance travelled ($F_{(1,9)} = 9.715$, $p = 0.012$) at week 6 post-treatment, which was not present at baseline ($p = 0.051$; **Figure 3.10**.).

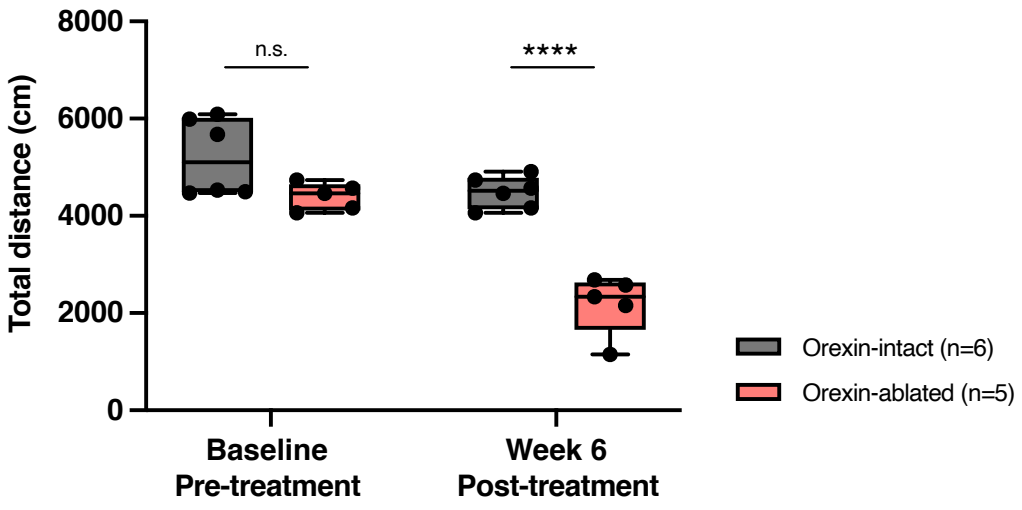

Figure 3.10. Reduced locomotion as a potential readout of fatigue in orexin-ablated mice. Locomotor activity was measures through the open field assay at both baseline (pre-treatment) and at week 6 post-treatment. There was a significant decrease in locomotor activity in the orexin-ablated group compared to the orexin-intact at week 6 post-treatment ($F_{(1,9)} = 9.715$, $p = 0.012$), whereas there were no significant changes between the groups at baseline ($p = 0.0508$). Two-way repeated measures ANOVA, with familywise error rates corrected for using Sidak's correction. n.s., non-significant. *$p \leq 0.05$.

In agreement with orexins role in appetite and obesity (Nixon, Mavanji et al. 2015), we monitored the weight of the animals for six weeks post-treatment. There were no significant changes between orexin-ablated and orexin intact groups across the three time points ($F_{(2,8)} = 1.582$, $p = 0.233$, **Figure 3.11.**), suggesting no alteration in feeding/energy expenditure.

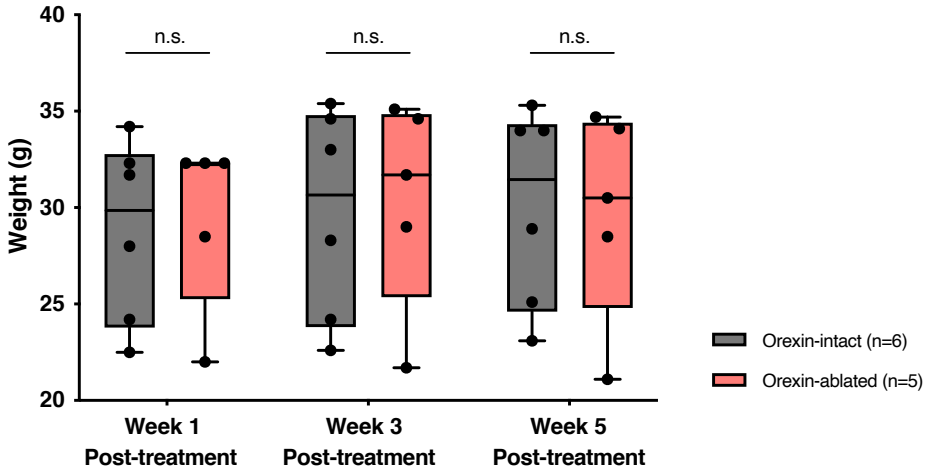

Figure 3.11. No overt change in body weight for up to 6 weeks post orexinergic neuronal-ablation ($F_{(2,8)} = 1.582$, $p = 0.233$). n.s., non-significant. Two-way repeated measures ANOVA, with familywise error rates corrected for using Sidak's correction. n.s., non-significant. *$p \leq 0.05$.

3.4. DISCUSSION

3.4.1. Cre-specific ablation

In this study, we aimed to ablate orexinergic neurons in the lateral hypothalamus using a newly produced orexin-Cre^{+} mouse line (Giardino, Eban-Rothschild et al. 2018). We decided to use this mouse following our and others failure to replicate orexinergic transfection and specific ablation using a lentivirus approach under the hypocretin (orexin) promoter (Roh, Jiang et al. 2014, Sanchez-Garcia, Cabral-Pacheco et al. 2018). The overall aim of which is to permit the study of the behavioural consequences of orexinergic-ablation in awake freely behaving mice that would enable us to study the underlying biology of premonitory symptoms (Giffin, Ruggiero et al. 2003, Karsan and Goadsby 2018). In agreement with our approach, previous research has identified altered pain behaviours following genetic-based ablation of orexinergic neurons in adult mice (Inutsuka, Yamashita et al. 2016). However, it is likely that our viral-based approach relying on targeted injection of a dtA-AAV into the lateral hypothalamus may less efficiently ablate orexin neurons compared to a genetic approach. Similar to other dtA-based models (Inutsuka, Inui et al. 2014), and having not established the ablation at different time-points, the experimental design allowed four to eight weeks for progressive orexinergic neuronal ablation. We observed a significant ablation of orexinergic cell bodies in the lateral hypothalamus in the orexin-Cre^{+} group compared to the wild type group; which was injected with saline, at 8 weeks post-treatment. The degree of orexinergic ablation also caused a significant reduction in orexinergic efferent fibres projecting to densely innervated migraine-associated nuclei, such as the LC, the PAG and the TCC **(Figure 3.4.).**

Descending projections from the lateral hypothalamus send direct and indirect fibres that terminate in several brainstem regulatory nuclei, including the LC, PAG and TCC (Peyron, Tighe et al. 1998, Cutler, Morris et al. 1999, Horvath, Peyron et al. 1999, Mondal, Nakazato et al. 1999, van den Pol 1999, Blanco, Lopez et al. 2001, Johren, Neidert et al. 2001, Mintz, van den Pol et al. 2001, Randeva, Karteris et al. 2001, Zhang, Sampogna et al. 2001, Johren, Neidert et al. 2002, Zhang, Sampogna et al. 2002, Zhang, Sampogna et al. 2002, Zhang, Sampogna et al. 2004), resulting in altered trigeminal nociceptive processing (Bartsch, Levy et al. 2004, Robert, Bourgeais et al. 2013). Altered

functional connectivity between these pain-modulatory structures has been reported as early as the interictal preictal phases (Stankewitz, Aderjan et al. 2011, Maniyar, Sprenger et al. 2014, Schulte and May 2016). Importantly, these changes are often accompanied by premonitory symptoms such as: photophobia, fatigue and food cravings (Maniyar, Sprenger et al. 2014); all of which have been functionally linked to the hypothalamic orexinergic system (Stankewitz, Aderjan et al. 2011). A significant ablation of orexinergic fibres in these downstream nuclei in our model is reaffirming to understand through which potential migraine-associated nuclei the altered nociceptive responses are being generated.

In accordance with previous work using the same IRES-Cre transgenic mouse line (Giardino, Eban-Rothschild et al. 2018), by stereotaxic injection of a Cre-dependent AAV-mGFP we observed a relatively specific targeting of the orexinergic population with 70-80% specificity (data not shown). This is still slightly less than the previous reports from the producer of the mouse line (de Lecea) which have reported > 90% specificity. Given the common concern of Cre-lines losing their specificity throughout the generations, we aim to continue to characterize this mouse line accordingly to ensure there is no further loss in specificity. With this in mind, positive controls for ablation were also performed in these studies to ensure no other lateral hypothalamic-populations, such as MCH (Concetti and Burdakov 2021) had been affected during the ablation. This specificity was confirmed after observing equal numbers of MCH somas in the lateral hypothalamus in both the orexin-intact and orexin-ablated groups **(Figure 3.5.)**. This is in agreement to previous orexin ablation models (Hara, Beuckmann et al. 2001, Inutsuka, Yamashita et al. 2016). What remains unclear is which other peptides co-released from orexinergic neurons or expressed in the lateral hypothalamus might contribute to the overall effects induced by this model. Dynorphin for example, is a peptide co-released from orexinergic neurons (Chou, Lee et al. 2001, Muschamp, Hollander et al. 2014) which has also demonstrated a role in the modulation of nociception (Podvin, Yaksh et al. 2016). Future work using this ablation model would benefit from quantifying the expression of dynorphin post ablation; as this would be expected to be also significantly ablated (Inutsuka, Yamashita et al. 2016).

Other neurotransmitters and neuropeptides which are co-released from orexinergic neurons and should be explored in terms of their ability to modulate nociceptive-

associated pathways are; Neurotensin (Furutani, Hondo et al. 2013), Nociceptin/orphanin FQ (N/OFQ) (Maolood and Meister 2010) and Glutamate (Schone, Apergis-Schoute et al. 2014). Indeed, glutamate is suggested to have a role in pain processing, migraine and central sensitization (Hoffmann and Charles 2018), as well as being involved in the underlying mechanisms of cortical spreading depression (Enger, Tang et al. 2015), the electrophysiological correlate of migraine aura (Charles and Baca 2013). Clinically, reported increases in glutamate in the blood, CSF and saliva of migraine patients: before and during an attack, motivated the development of preventive treatments to inhibit glutamate release (Charles and Baca 2013). Interestingly, the amyloid polypeptide (Iapp), which is a precursor to amylin, might also be co-expressed with orexin neurons to modulate food intake (Li, Kelly et al. 2015). This is a relevant shared mechanism in migraine (Ghanizada, Al-Karagholi et al. 2021) given that amylin is a member of the CGRP peptide family that can induce migraine attacks in patients, while inhibiting amylin signalling has emerged as a potential novel therapeutic target for migraine. With this in mind, further rigorous quantification of these peptides could be explored in this mouse line to understand potential confounding neuropeptide systems (**Figure 3.12**).

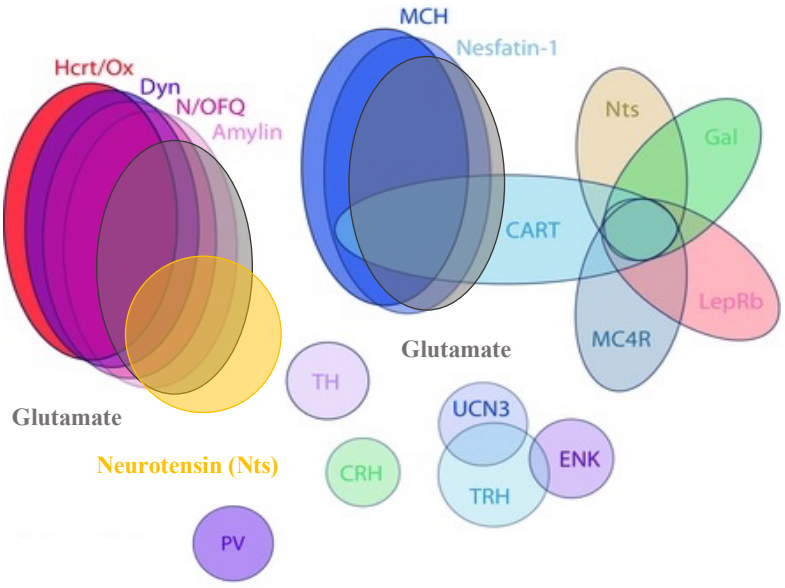

Figure 3.12. Representative image of the various clusters of cell bodies in the lateral hypothalamus. As indicated in the left side of the image: studies have shown a co-localisation of orexins with dynorphin, N/OFQ, amylin and glutamate (added in grey in both rexin and melanin-concentrating hormone (MCH) co-release), and partial co-localisation with neurotensin (Nts, added in yellow). Other peptides include: MCH which was used as positive control in our studies to ensure an orexin-spceific ablation, as well as nesfatin-1 (Adapted from (Bonnavion, Mickelsen et al. 2016)). TH, tyrosine hydroxylase; Gal, galanin; CART, cocaine- and amphetamine regulated transcript; LepRb, long-form of the leptin receptor; MC4R, melanocortin receptor 4; UCN3, urocortin-3; TRH, thryotropin-releasing hormone; ENK, enkephalin; CRH, corticotropin-releasing hormone.

3.4.2. Periorbital mechanical sensitivity

Cre-dependent ablation through an AAV-dtA approach of the lateral hypothalamic orexinergic population in orexin-Cre^{+} mice induced a significant decrease in periorbital mechanical sensitivity, compared to non-ablated wild type littermate mice. A decrease in periorbital mechanical threshold suggests an increased sensitivity in the periorbital region, which is widely considered a preclinical readout of allodynia (Xie, De Felice et al. 2017, Saengjaroentham, Strother et al. 2020), a common feature of migraine and chronic migraine (Lipton, Bigal et al. 2008, Mathew, Cutrer et al. 2016). These results suggest that loss of orexinergic regulation from the lateral hypothalamus dysregulates descending pain modulation, potentially via other migraine-associated pain nuclei: suggesting a potential disinhibition of trigeminal-associated nociceptive pathways in this model. This is in agreement with orexinergic ablation through a similar dtA-induced ablation, causing increased hindpaw sensitivity to mechanical thermal and cold stimuli (Inutsuka, Yamashita et al. 2016). Chemogenetic activation of orexinergic neurons in comparison decreases hindpaw sensitivity to both thermal and chemically-induced stimuli (Zhou, Cheung et al. 2018). Interestingly, evidence suggests a differential role for OxA and OxB in modulating trigeminal nociception. Direct injection of OxA into the posterior hypothalamus inhibits trigeminal nociception at the level of the TCC, while OxB induces a pro-nociceptive response (Bartsch, Levy et al. 2004). In agreement, systemically administered OxA but not OxB inhibits TCC nociceptive responses and CGRP release from the peripheral terminals of the trigeminal nerve (Holland, Akerman et al. 2005, Holland, Akerman et al. 2006). Our findings fit with the general consensus that a robust and non-differential modulation the lateral hypothalamic orexinergic neurons appears to have a primary antinociceptive action. The importance of the current study is that it now allows the translation of these findings to conscious awake animals. The orexinergic system is impacted by anaesthesia, whereby normal orexinergic activation in response to noxious thermal stimulation is completely abolished by anaesthesia (Inutsuka, Yamashita et al. 2016) and as such future studies should consider exploring orexinergic function in conscious awake mice, potentially using freely behaving or head-fixed approaches. The current study represents a first step in optimizing such studies with respect to migraine.

3.4.3. Locomotor deficits post OxA ablation

Separate from nociceptive modulation; the orexinergic system is involved in modulating a range of homeostatic processes, involving arousal, stress and appetite (Sakurai, Amemiya et al. 1998, Mondal, Nakazato et al. 1999, Sakurai 2005, Venner, Karnani et al. 2011, Nixon, Mavanji et al. 2015, Inutsuka, Yamashita et al. 2016, Soya and Sakurai 2020); all of which appear associated with many premonitory symptoms/triggers such as increased fatigue, as well as sensitivity to: stress, and to certain foods (Giffin, Ruggiero et al. 2003, Kelman 2007, Schulte, Jurgens et al. 2015).

For this initial characterisation of orexin ablation, we aimed to apply a natural (spontaneous) and non-reinforced environment, to measure the impact of orexin ablation on locomotion rather than reward-motivated locomotion; such as in the rotarod. To ensure there were no reward-motivated pathways involved that may be impacted by orexinergic ablation (Muschamp, Hollander et al. 2014); the open field arena was thus used as a surrogate marker of fatigue. We thus recorded the general locomotor activity in the open field arena; pre and post ablation in orexin-Cre^{+} or wild type littermate mice. Our findings identified a reduction in total locomotion six weeks post ablation that is in agreement with extensive literature supporting a role for orexins in arousal and locomotion (Yamanaka, Beuckmann et al. 2003, Tsujino and Sakurai 2013, Concetti and Burdakov 2021). As such, the reduced locomotion may be considered a surrogate readout of the marked fatigue that emerges during the migraine premonitory phase (Giffin, Ruggiero et al. 2003). However, fatigue is a complex phenotype that is difficult to measure in rodents (Wolff, Raheem et al. 2018). Of interest, migraine patients often report that their pain in exacerbated by movement and several preclinical models including those for migraine-related photophobia use lack of movement in the dark-zone as a preclinical readout of photophobia (Wang, Mason et al. 2021), therefore the relationship between migraine, movement is complex and requires further attention. Especially when it is considered that a hallmark of cluster headache, a related primary headache condition is exacerbated movement (2018, Headache Classification Committee of the International Headache Society (IHS)), suggesting that altered motor control may be linked to headache disorders as observed with the link between migraine and restless leg syndrome (Ghasemi, Khaledi-Paveh et al. 2020).

3.4.4. Orexin ablation strategies: Implications for pain research

The previously mentioned models of orexinergic ablation (e.g. (Inutsuka, Yamashita et al. 2016)) have largely explored the contribution of the orexinergic system in non-trigeminal pain, demonstrating decreases in mechanical and thermal thresholds in the hindpaw post-orexin ablation. While our pilot data did not identify a significant decrease, we did observe a trend towards reduced hindpaw mechanical and thermal withdrawal thresholds, which may be due to our relatively small sample size and ablation strategy. While the bulk of data suggests that orexins may regulate pain more generally, there is evidence to suggest a potential trigeminal-focused effect. For example, orexinergic fibres innervating the spinal cord preferentially terminate in the cervical level that receives facial sensory afferents (Date, Mondal et al. 2000), and their density reduces along the rostro-caudal axis. Experimental differences might however also be attributed to the ablation approach used and its level of efficacy. Some of the previous models of orexinergic ablation have applied Cre-dependent approaches based on Orexin-tTA; TetO dtA mice, in which the orexin-tTA line exclusively expresses tTA in orexinergic neurons, and by crossing it with: TetO dtA mice, dtA will then expressed in orexinergic neurons in the absence of DOX. DOX-containing chow is then constantly administered since birth to be removed for a period of 4-5 weeks to induce orexin ablation (Inutsuka, Yamashita et al. 2016). This approach will ablate the entire hypothalamic orexinergic population due to its global action compared to our more targeted approach. AAV-mediated targeting relies on local injection of the vector and its efficiency is highly dependent on successful coverage of the whole nucleus, as well as high transduction of the AAV.

With these approaches however, one should also consider establishing higher regional specificity due to the topographical and functional organization of orexin subtypes in the hypothalamus. Previous studies have suggested a divergent projection pattern in which orexinergic projections from the dorsomedial and perifornical hypothalamus are associated with arousal (Estabrooke, McCarthy et al. 2001), whereas projections from the lateral hypothalamus are preferentially involved in feeding (Sakurai, Amemiya et al. 1998) and reward-associated behaviours (Harris, Wimmer et al. 2005, Aston-Jones, Smith et al. 2010). It now seems that this strict topographical representation is sparser than expected; with orexin cells projecting to brainstem structures such as: the LC or ventral tegmental area (Gonzalez, Jensen et al. 2012), or dorsal raphe,

pedunculopontine or laterodorsal tegmental nuclei (Arima, Yokota et al. 2019) appearing to be equally distributed throughout four hypothalamic subdivisions: the perifornical area, lateral hypothalamus, dorsomedial hypothalamus and zona incerta. Only a modest topographical distribution is evident when these efferent fibres are organized between the lateral and medial hypothalamus. Lateral cell bodies are more likely to project to the LC, and medial cell bodies to the VTA; suggesting that a convergence of distinct orexin 'populations' might functionally facilitate the temporal merging of arousal and reward inputs into the hypothalamus (Harris and Aston-Jones 2006). Indeed, a mechanism by which orexin activity becomes rapidly amplified and acts locally to integrate diverse information is through OXR2 on hypothalamic orexin neurons. Orexin-to-orexin communication within the hypothalamus is suggested to create a positive-feedback loop for local orexinergic action to maintain arousal and vigilant states and provide fast responses to inputs such as noradrenaline or serotonin, from a wide range of nuclei (Yamanaka, Beuckmann et al. 2003).

Future studies should further consider targeting pathway specific orexinergic structures based on available retrograde AAV's to overcome the potential heterogeneous orexinergic population. Chemogenetic approaches offer the potential to target specific networks through these retrograde AAV approaches (Pantazis, James et al. 2021). Recent improvements in AAV production have developed constructs coupled to a specifically retrograde AAV serotype: 2, allowing its injection into an output nucleus, to be taken up by the axon terminals and retrogradely transported back to the somas. While regional specificity allows us to understand the contribution of a specific region, migraine is more often understood as a network disorder (Goadsby, Holland et al. 2017, Brennan and Pietrobon 2018). The high heterogeneity in symptoms and complex interaction with other regions between the hypothalamus throughout the various phases of migraine (Maniyar, Sprenger et al. 2014, Schulte and May 2016), is indicative of alterations in functional connectivity. Which is why; as part of ongoing work in the laboratory; we aimed to apply this approach in this orexin-Cre^{+} line with the aim to modulate specific orexin projections to downstream migraine-associated nuclei, such as the LC and PAG **(Figure 3.13. preliminary data not included in results).**

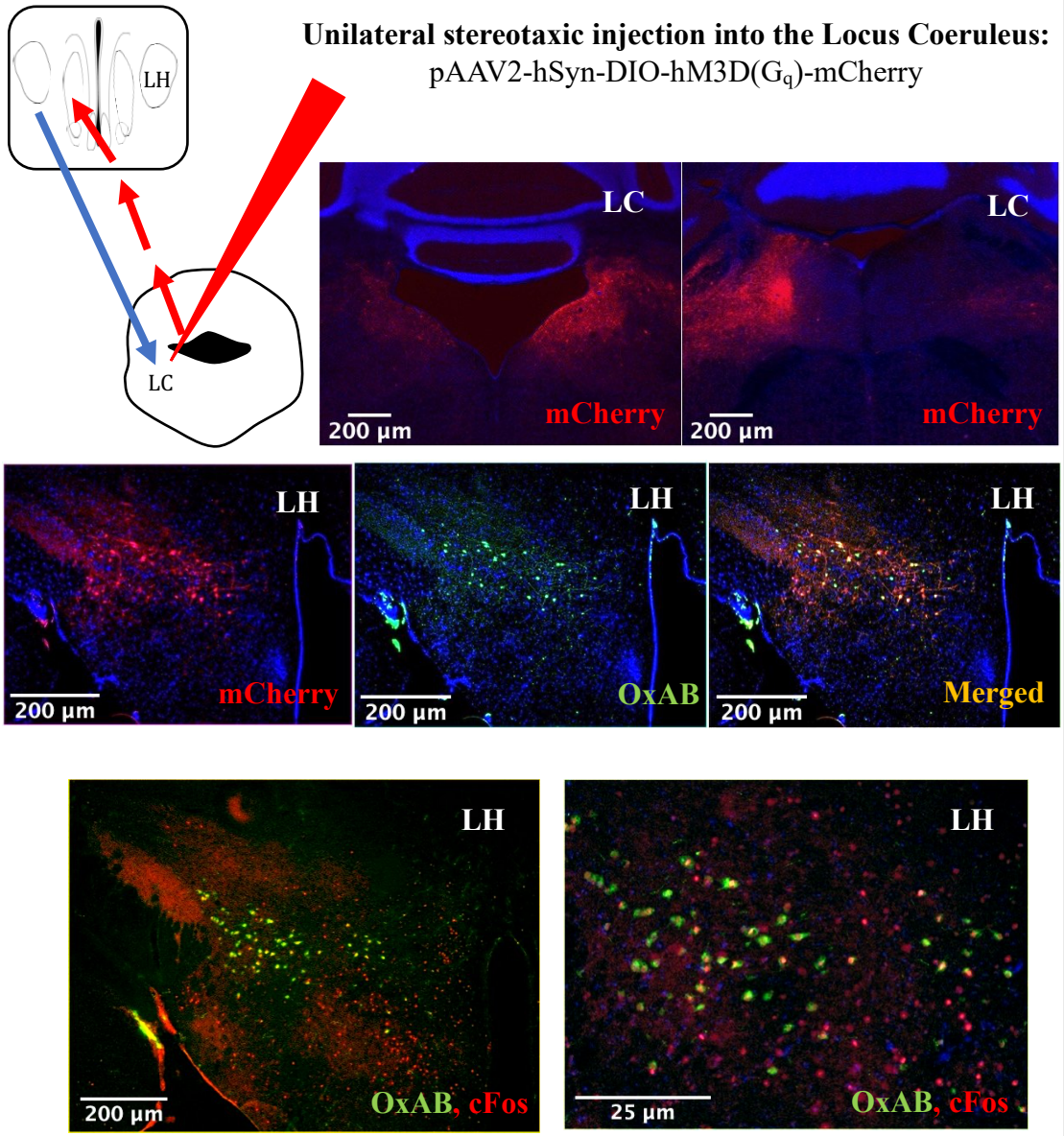

Figure 3.13. Stereotaxic injection of retrograde AAV's into the locus coeruleus (LC) to target specific orexinergic projections. Following stereotaxic injection of the retrograde AAV, pAAV2-hSyn-DIO-hM3D(G_q)-mCherry into the LC, the virus enters the orexinergic expressing fibres and is retrogradely transported back to the orexinergic neurons in the lateral hypothalamus (LH) that send projections to the LC. As this virus contains an excitatory DREADD's construct, these orexinergic neurons can then be selectively activated to establish their specific function. This is a representative example of an ongoing preliminary study.

3.4.5. Functional relevance of orexin A and B in migraine

One limitation of the above approaches to consider when investigating the effects of such robust ablation is the over-generalization of a more complex underlying orexinergic

network. As previously mentioned, the orexinergic system consists of two peptides: OxA and OxA which can act over two receptors: OX_1R and OX_2R, with differential affinity, and in some cases: opposing effects. Previous studies combining electrophysiological approaches with administration of pharmacological compounds has allowed us to dissect the specific neuropeptides underlying the observed responses. With this, it has been shown that a differential orexinergic modulation exists over the TCC: with OxA being anti-nociceptive when injected direct into the posterior hypothalamus or systemically (Bartsch, Levy et al. 2004, Holland, Akerman et al. 2006) and reducing CGRP release from the trigeminal nerve (Holland, Akerman et al. 2005), via an OX_1R-dependent mechanism. In contrast OxB is pronociceptive when injected into the posterior hypothalamus (Bartsch, Levy et al. 2004), while having little impact when given systemically (Holland, Akerman et al. 2005, Holland, Akerman et al. 2006). Having observed a pronociceptive response from ablating both peptides, one could argue for a primary role for OxA as analgesic, over orexin B as pronociceptive in our and other's (Inutsuka, Yamashita et al. 2016) behavioural models. This is in agreement with the failure of dual orexin receptor antagonists (DORAs) for the treatment of migraine (Chabi, Zhang et al. 2015), as the burden of evidence would suggest that activation of the OX_1R is most likely to herald antinociceptive therapeutic success. A hypothesis that we have tested in future chapters of this thesis.

3.4.6. Clinical/overall relevance/impact of these findings

Having discussed the main challenges and implications of the current ablation approach, which will be considered for the following studies; an overarching observation which might itself be extremely biologically relevant is the difference on the impact of the orexinergic system over whole body versus trigeminal pain. In further support of a potential orexinergic role in trigeminal pain, the orexinergic system has been linked to the pathophysiology of cluster headache (Rainero, Gallone et al. 2008, Holland and Goadsby 2009, Barloese, Jennum et al. 2015). The trigeminal afferents arising in the trigeminal ganglion have further been observed to send direct projections to key pain regulatory areas, bypassing the classic spinal integration. Rodriguez and colleagues uncovered direct excitatory projections from the trigeminal ganglion to the lateral parabrachial nucleus (Rodriguez, Sakurai et al. 2017). An area that innervates orexinergic neurons involved in the regulation of arousal (Arima, Yokota et al. 2019). As such,

trigeminal nociception may specifically activate networks involved in the regulation of pain and arousal, including indirectly via orexinergic neurons.

Further, relevant direct functional connections have been observed along the trigemino-hypothalamic tract, with increased c-Fos expression in the supraoptic nucleus and posterior hypothalamus following trigeminovascular activation (Benjamin, Levy et al. 2004). Clinically, functional imaging has provided crucial translational data which has identified the hypothalamus to be abnormally active throughout all the phases of a migraine attack; with an increased coupling of the hypothalamus and the spinal trigeminal nucleus during the pre-ictal (premonitory) phase, and posterior increased connectivity to the dorsal rostral pons during the ictal phase (headache). Clinical evidence has also suggested its abnormal activity during the premonitory and headache phases (Maniyar, Sprenger et al. 2014) might be linked to the neuroendocrine, appetite and hormonal alterations and trigeminal pain processing (Martins-Oliveira, Akerman et al. 2017, Li, Diao et al. 2018, Martins-Oliveira, Tavares et al. 2021).

Based on clinical functional activity and associated symptomatology and its limited insight into the potential neurotransmitter systems which might be underlying it; preclinical findings have identified hypothalamic orexins to modulate migraine-associated processes. Overall, evidence suggests that hypothalamus and its associated neural networks may play a role in attack initiation but also the transition through the different phases and potentially the transition from episodic to chronic migraine (Schulte, Allers et al. 2017).

4. Chapter 4. Effects of chronic intranasal Orexin A treatment on periorbital mechanical allodynia in a Cre-mediated orexin ablation model

4.1. Introduction:

As discussed, migraine patients commonly report a set of highly disabling symptoms prior to an attack, some of which include: marked fatigue, lack of concentration and photophobia (Giffin, Ruggiero et al. 2003, Schulte, Jurgens et al. 2015). Clinical imaging studies have identified changes in hypothalamic connectivity in each of the phases of the migraine cycle, with increased hypothalamic connectivity with the LC during the interictal period, and increased connectivity with the spinal trigeminal nucleus during the premonitory phase (Maniyar, Sprenger et al. 2014, Schulte, Jurgens et al. 2015).

Given this emerging importance of the hypothalamus we and others have begun to explore the potential hypothalamic-mediated modulation of trigeminal nociceptive processing in migraine (Bartsch, Levy et al. 2004, Robert, Bourgeais et al. 2013, Schulte, Allers et al. 2017). Focusing on hypothalamic orexinergic signalling, it has previously been shown that OxA is antinociceptive (Bartsch, Levy et al. 2004, Holland, Akerman et al. 2005, Holland, Akerman et al. 2006), while orexin B shows a differential pro-nociceptive response when administered centrally (Bartsch, Levy et al. 2004). Building on this, we demonstrated in chapter 3 that dtA-mediated ablation of orexinergic neurons in the lateral hypothalamus reduces periorbital withdrawal thresholds in mice, suggesting the emergence of an allodynia-like phenotype in mice. This is in agreement with a net pro-nociceptive effect of diminished orexinergic signalling (Inutsuka, Yamashita et al. 2016). Orexins act via two G-protein coupled receptors, termed the OX_1R and the OX_2R, with OxA showing equal affinity for both and OxB preferentially acting via the OX_2R (Sakurai, Amemiya et al. 1998). Evidence suggests that OxA is likely acting via the OX_1R to produce its antinociceptive effects (Bingham, Davey et al. 2001, Holland, Akerman et al. 2005, Holland, Akerman et al. 2006) in both trigeminal and non-trigeminal pain models. Supported by the failure of a dual orexin receptor antagonist for the treatment of migraine (Chabi, Zhang et al. 2015), despite preclinical evidence on their analgesic properties over the dural-evoked responses in the TCC (Hoffmann, Supronsinchai et al.

2015) and their successful approval for insomnia (Murphy, Moline et al. 2017, Gamble, Katsuki et al. 2020) which is commonly comorbid with migraine (Buse, Reed et al. 2020).

To further assess the antinociceptive potential of OxA, we sought to determine if intranasal OxA could reverse the periorbital mechanical hypersensitivity observed in orexin-ablated mice. Intranasal delivery has emerged as a novel approach for migraine therapy (Rapoport, Bigal et al. 2004), with intranasal dihydroergotamine recently being approved as novel therapeutic option (Shrewsbury, Jeleva et al. 2019). Compared to traditional oral approaches, intranasal drug delivery holds several advantageous features. Several drugs show low bioavailability and limited brain exposure when given orally, limiting their potential CNS actions. For example, and of relevance to the current research OxA but not OxB rapidly crosses the blood brain barrier (Kastin and Akerstrom 1999), potentially explain the lack of effect of OxB when administered intravenously in preclinical models of migraine (Holland, Akerman et al. 2005, Holland, Akerman et al. 2006). In comparison. intranasal delivery allows direct access to the central nervous system, bypassing the blood brain barrier, resulting in greater bioavailability, lowed concentrations required and reduced off-target side effects.

In terms of orexinergic signalling, the intranasal delivery of OxA has been shown to have a more profound impact on sleep deprivation-induced metabolic activity and cognitive performance than a significantly higher intravenous dose (Deadwyler, Porrino et al. 2007). Focussing on migraine intranasal delivery shows a preferential distribution in migraine-relevant nuclei. For example, intranasal delivery of OxA in an anaesthetised rat shows highest tissue to blood concentration ratios in the trigeminal nerve ((Dhuria, Hanson et al. 2009)**, Figure 4.1.**) with further focused binding in the hypothalamus. Importantly, OxA has been administered to patients and shown to be beneficial with respect to narcolepsy (Weinhold, Seeck-Hirschner et al. 2014), further enhancing the potential translational potential of intranasal OxA for migraine.

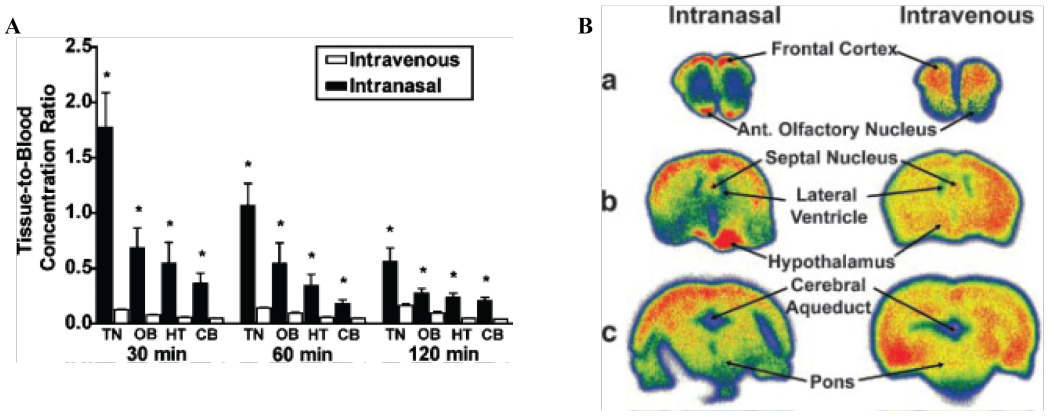

Figure 4.1. Intravenous delivery of orexin A. As compared to the intravenous route, intranasal orexin A shows a significantly higher tissue to blood concentration ration in the trigeminal nerve (TN), olfactory bulb (OB), hypothalamus (HT) and cerebellum for up to 2 hours post-delivery **(A)**. Autoradiographic measurement of labelled orexin A distribution in the rodent brain following intranasal and intravenous delivery **(B).** (Dhuria, Hanson et al. 2009).

4.2. METHODS:

4.2.1. Animals

Eighteen male and female mice: 9 Orexin-Cre^{+} and 9 wild type-littermates (20-30g) were used in this study. All animals were housed in groups of four-five in 21ºC and humidity controlled rooms with a normal 12-h light/dark cycle and had free access to food and water, as detailed in the general methods section: 2.1. The number of Female and Male animals was not large enough to run a split analysis on any gender-effects.

4.2.2. Adeno-associated viruses (AAV) and Stereotaxic surgery

In keeping with our optimisation of dtA-mediated orexinergic ablation in orexin-Cre^{+} mice (chapter 3) orexin-Cre^{+} and wild type mice were stereotaxically injected into the lateral hypothalamus with rAAV-EF1a-Lox-Cherry-lox(dtA)-lox2 (UNC, Vector core). In this case, the presence of Cre will permit the induction of the dtA sequence, while the lack of Cre in wild type mice will permit the expression of mCherry only for confirmation of successful targeting of the lateral hypothalamus. Orexin-Cre^{+} (n = 9) and wild type littermates (n = 9) were injected bilaterally with 1 ul of the Cre-dependent rAAV-EF1a-Lox-Cherry-lox(dtA)-lox2, by use of a Narishige Injector (IM-11-2 Pneumatic injector, Narishige). Following incision and retraction of the skin, the skull was carefully cleaned of all connective tissue. Four holes (two per hemisphere, along the anteroposterior axis) were drilled into the skull with a hypodermic needle (Terumo, 25G x 1 1⁄2"), and a glass capillary needle (Microinjection Capillaries Borosilicate Glass 3.5 inch length) was lowered into the stereotaxic coordinates of the lateral hypothalamus. The coordinates were: caudal from Bregma: -1.40 mm and -1.80 mm, dorsoventral -5.10 and -5.30 mm and mediolateral ± 0.9mm (**Figure 4.2. (A),** (Paxinos and Franklin 2014).

Following injection of 250 nL per depth per site at a rate of 2 nL/sec, the capillary was left to rest for seven minutes and then removed at intervals of 0.50 mm/minute. Mice were injected subcutaneously with 0.9% isotonic saline to facilitate their recovery post-surgery and closely monitored for the first week post-surgery. Allowing at least four weeks for full viral transfection, and successful orexinergic neuronal ablation, mice were subjected to the correspondent behavioural assays **(Figure 4.3.)**.

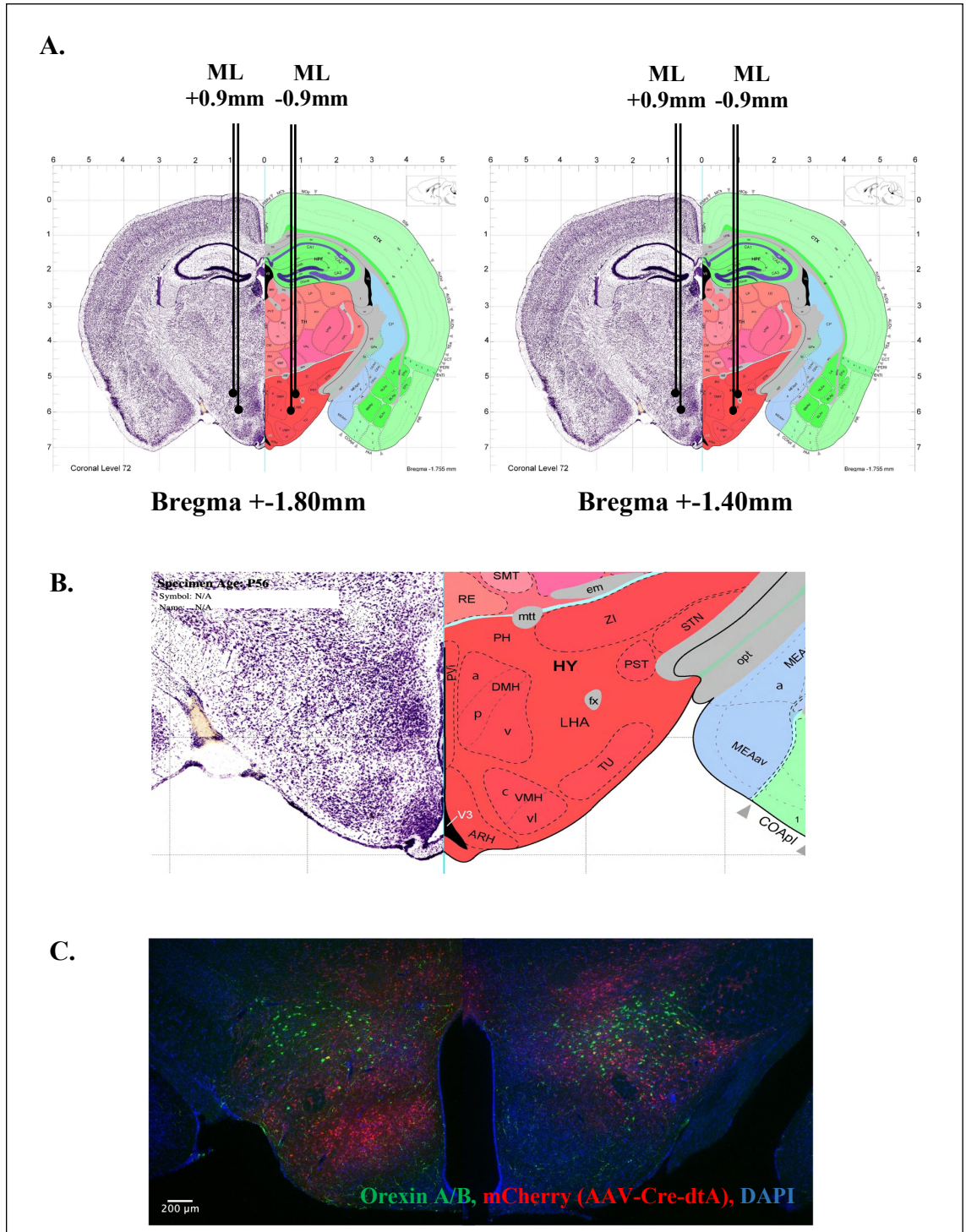

Figure 4.2. Targeted ablation of orexinergic neurons in the lateral hypothalamus. A. Coronal sections (adapted images from the Allen brain atlas) showing the stereotaxic injection sites. Given the large dimensions of the lateral hypothalamus, mice were injected at two anterior-posterior (A-P) coordinates: Bregma -1.80 mm (left image) and -1.40 mm (right image), mediolateral (M-L): ±0.90 mm and at a depth of: X and Y. **B.** Coronal map of the lateral hypothalamic region (Allen brain altas). **C.** Representative section of an orexin-intact animal with the cre-dependent AAV-dtA (red) injected into the lateral hypothalamus: expressing mCherry in the injected region and with no ablation of the orexinergic population (green) due to the absence of cre.

To successfully ablate orexinergic neurons in the lateral hypothalamus, we again made use of a transgenic orexin-cre^{+} mouse line (Giardino, Eban-Rothschild et al. 2018). As suggested by the previous preliminary study (chapter 3) and previous literature (Inutsuka, Yamashita et al. 2016), we allowed five weeks post-dtA to ensure a high ablation of the orexinergic population. At this time point we performed the corresponding read-outs to measure any changes in periorbital sensitivity and locomotor activity. Animals were continuously handled all throughout this period to habituate them to the intranasal handling and administration (Hanson, Fine et al. 2013). To confirm ablation tissue was collected as previously described on week 8.

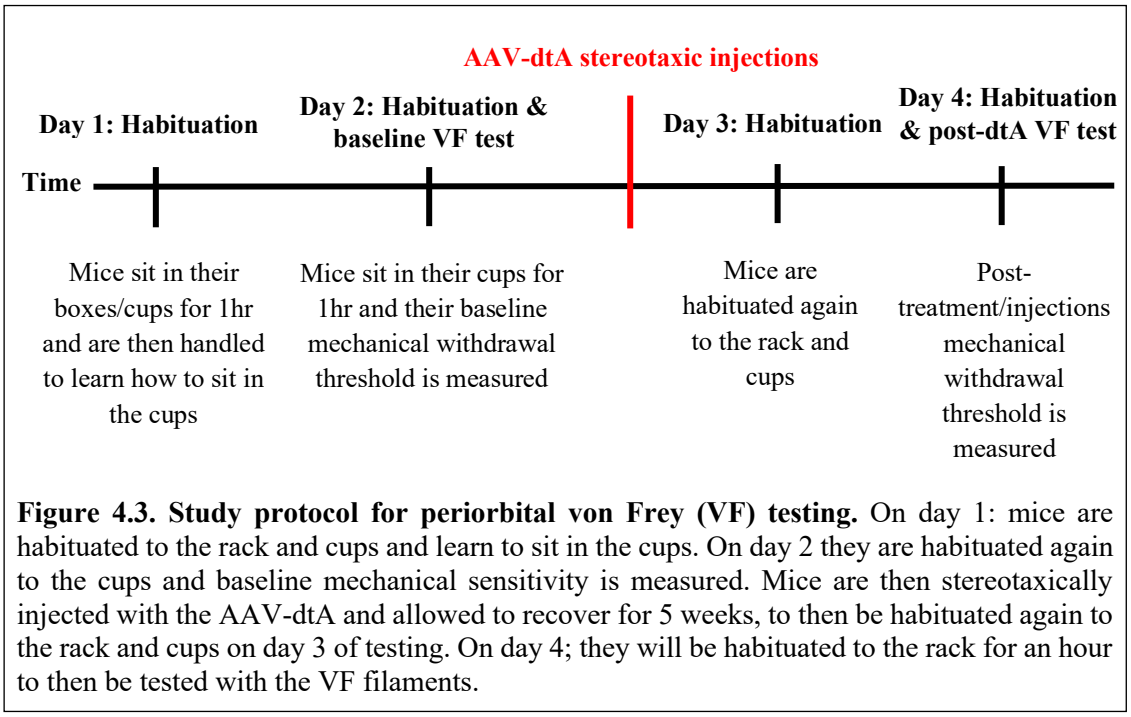

Figure 4.3. Study protocol for periorbital von Frey (VF) testing. On day 1: mice are habituated to the rack and cups and learn to sit in the cups. On day 2 they are habituated again to the cups and baseline mechanical sensitivity is measured. Mice are then stereotaxically injected with the AAV-dtA and allowed to recover for 5 weeks, to then be habituated again to the rack and cups on day 3 of testing. On day 4; they will be habituated to the rack for an hour to then be tested with the VF filaments.

4.2.3. Behavioural assays

As detailed in the main 'General Methods' chapter: the locomotor activity of these animals was measured at predefined time points through the open field assay: in which the total distance travelled (in cm) was recorded for ten minutes in a 72 (length) x 72 (width) x 33 (height) cm square wall-enclosed arena.

As previously described; patients often report extrecephalic cutaneous sensitivity to touch and pain before or during the migraine attack (Burstein, Cutrer et al. 2000, Burstein, Yarnitsky et al. 2000, Burstein, Jakubowski et al. 2010), and periorbital mechanical

sensitivity is used as a proxy of trigeminal sensitivity in preclinical models (Holton, Strother et al. 2020, Saengjaroentham, Strother et al. 2020, Bertels, Singh et al. 2021). Calibrated von Frey filaments are used to measure periorbital mechanical withdrawal thresholds. The pressure of the filaments ranges from 0.02 - 1.4 g and are applied perpendicular to the periorbital region, above and between the eyes, ensuring the filament bends slightly, with the aim to elicit a reflex response. The sequence starts with the 0.4 g filament and the proceeding filaments' varies depending on the animal's sensitivity; if the animal responds to 0.4 g, the next filament in the sequence with less pressure would be applied (0.16 g), and if there is no response the next filament with higher pressure is used (1 g). This is repeated until a total of five filaments from the first positive response were measured and the 50% mechanical withdrawal threshold calculated using the up-down method (Chaplan, Bach et al. 1994).

On week six, we proceeded to give an acute intranasal (Hanson, Fine et al. 2013) dose of saline on day one and an acute dose of OxA on day two. Allowing six days of wash-out, on week seven we administered OxA intranasal chronically for five consecutive days, twice per day.

Following habituation to the testing apparatus, mice were subsequently habituated to the intranasal application (Hanson, Fine et al. 2013) that consisted of scruffing the mice in a prone position and carefully placing drops of 2 ul per nostril (alternating nostril), throughout a period of two minutes, to avoid any solution being sniffed out and to avoid causing any further stress in the animal**.** To exclude any stress-induced effects by the INA procedure over the behavioural readout: a positive control was performed the day before by administration of Saline to both groups. We initially conducted a small pilot study to explore the optimal dosing (data summarised in the General Methods) and decided upon 30 µl at 10 ng/µl as this demonstrated increased arousal when administered acutely to mice during the early light phase. The acute treatment protocol consisted of a single dose of OxA (ToCris, 1455) followed by the corresponding behavioural testing. OxA was administered intranasally at a concentration of 10 ng/ul; which we previously established to have a biologically effect ('General Methods' section). Stock OxA was initially diluted in saline and kept frozen at -20ºC. On the day of the experiment, it was defrosted and diluted accordingly to 10 ng/ul.

Following the acute administration, we then switched mice to a more chronic administration paradigm **(Figure 4.4.)**, in which OxA was administered for five consecutive days: two doses (10 ng/ul) per day (08:00 and 17:00) from day one to four, plus an additional dose on day five immediately prior to testing. The effects on periorbital sensitivity were measured twice on day five: at basal conditions, prior to the final OxA administration and thirty minutes after the last dose.

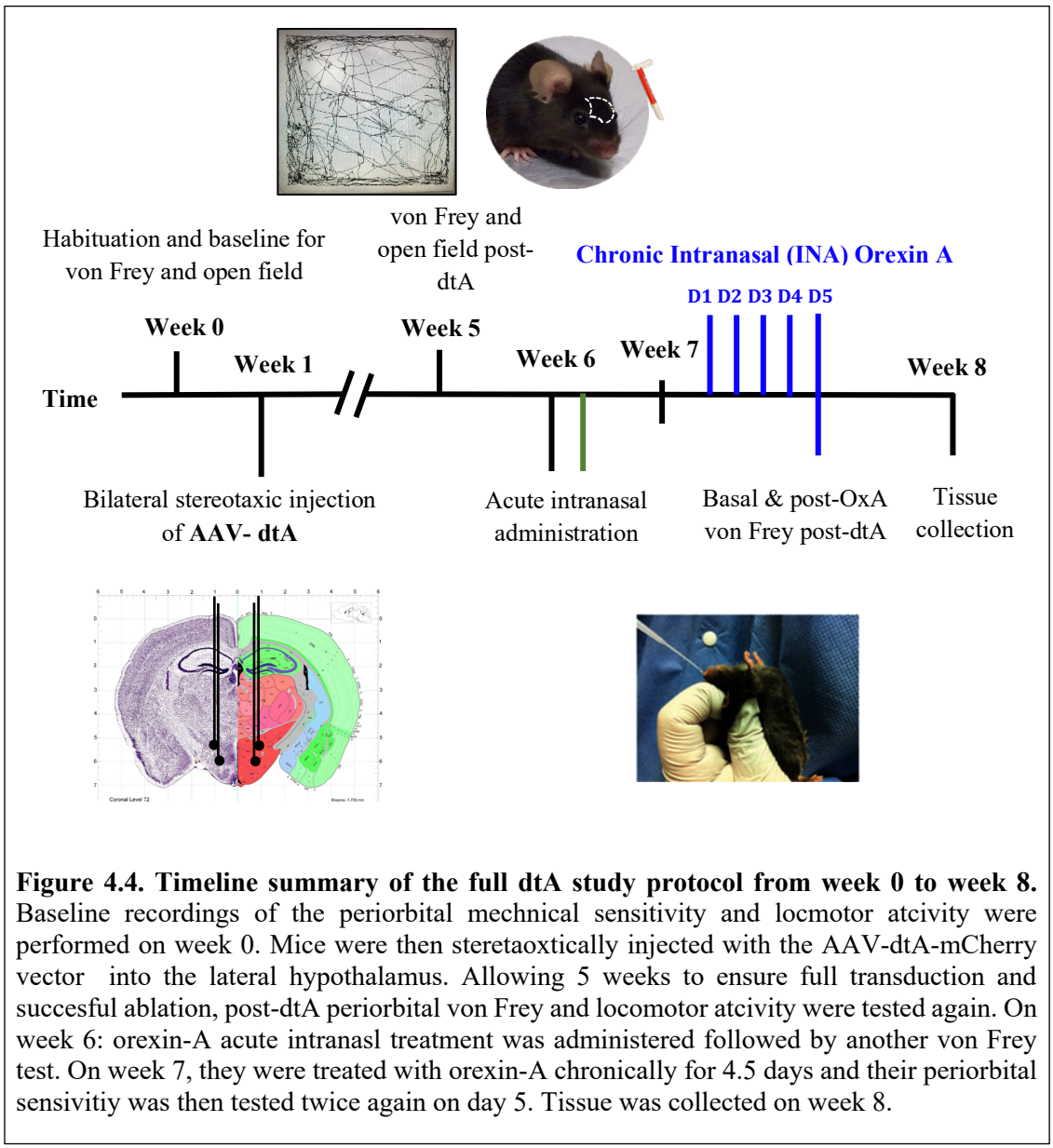

Figure 4.4. Timeline summary of the full dtA study protocol from week 0 to week 8. Baseline recordings of the periorbital mechnical sensitivity and locmotor atcivity were performed on week 0. Mice were then steretaoxtically injected with the AAV-dtA-mCherry vector into the lateral hypothalamus. Allowing 5 weeks to ensure full transduction and succesful ablation, post-dtA periorbital von Frey and locomotor atcivity were tested again. On week 6: orexin-A acute intranasl treatment was administered followed by another von Frey test. On week 7, they were treated with orexin-A chronically for 4.5 days and their periorbital sensivitiy was then tested twice again on day 5. Tissue was collected on week 8.

Having allowed one week of wash-out following chronic OxA administration, the last aim was to determine the specific receptor-mediated mechanisms through which OxA acts. For this, we administered an OX_1R-antagonist (SB-334867) together with OxA, with

one dose of the antagonist and the same two doses of OxA per day. We administered the antagonist at a concentration of 20 and 10 mg/kg given the previously reported locomotor deficits at high doses of 30 mg/kg (Sharf et al., 2010).

4.2.4. Statistical analysis

Quantitative counting of cell bodies within the lateral hypothalamus was performed by calculating the average of a total of four to five sections: with each slice being the sum of cell bodies from both hemispheres. Slices were selected every fourth level from Bregma -1mm to -2mm, and the same amount of sections among groups were included. The distribution in the raw data was initially analysed in SPSS through a normality test. And given the lack of normalised data, the unpaired non-parametric Mann Whitney U test was performed to explore group wise differences in the number of neuronal cell bodies expressing OxA/B and MCH. Von Frey mechanical withdrawal thresholds (presented as Mean ± SEM) and locomotor activity were initially compared between wild type and orexin-Cre^{+} groups via an unpaired *t*-test. The impact of chronic intranasal OxA after dtA-mediated ablation was analysed via a one-way repeated measures ANOVA by comparing: the post-dtA von frey sensitivity after saline treatment, to the post-dtA with basal chronic OxA and post-dtA with chronic OxA. Locomotor activity between orexin-intact and orexin-ablated mice: before and after administration of the AAV-dtA compound was analysed via a two-way repeated measures ANOVA.

4.3. RESULTS:

4.3.1. Cre-mediated AAV-dtA selectively ablates orexinergic neurons in the Lateral Hypothalamus

As described in the experimental design, we made use of a transgenic orexin-Cre$^+$ mouse line to ablate lateral hypothalamic orexinergic neurons via the stereotaxic injection of a Cre-dependent AAV coupled to a diphtheria toxin (dtA). Based on previous work on ablation using a DOX-method (Inutsuka, Yamashita et al. 2016), and our preliminary data (chapter 3), we decided to start our behavioural assessments on week five post-ablation. At the end of the experimental design: on week eight, the tissue was collected and analysed to assess the degree of ablation. Post-histological analysis was performed in n = 8 wild type and n = 7 orexin-Cre$^+$ mice as one sample could not be processed. While there were orexin-immunoreactive cell bodies in the lateral hypothalamus of wild type mice (104.80 [IQR: 77.81 – 125.90]), the number of orexin$^+$ neuronal cell bodies in the orexin-Cre$^+$ mice were significantly reduced (U = 0, p = 0.000; 22.50 [IQR: 1.50 – 41.75]; **Figure 4.5 & 4.6.**). In agreement with our pilot data (chapter 3) there was no significant change in MCH expression (U = 21, p = 0.4634) between wild type mice 92.21 [IQR: 83.06 – 110.40]) and orexin-Cre$^+$ mice 105.30 [IQR: 91.00 – 115.30]), **Figure 4.7.**) highlighting the specificity of the orexinergic ablation.

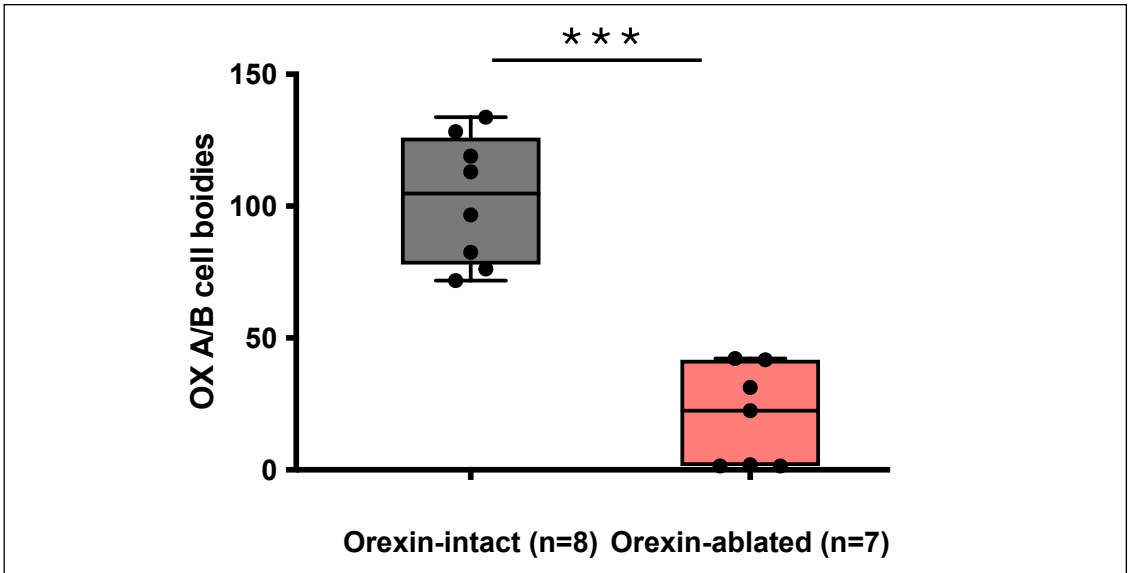

Figure 4.5. Cre-dependent ablation of orexinergic neurons in the lateral hypothalamus. Eight weeks post dtA injection there was a significant reduction in orexinergic positive neuronal cell bodies in the lateral hypothalamus (U = 0, p = 0.000; 104.80 [IQR: 77.81 – 125.90]), 22.50 [IQR: 1.50 – 41.75] of wild type (orexin-intact) and orexin-cre+ (orexin-ablated) mice respectively. *p ≤ 0.05. Group wise comparisons were conducted via the Mann Whitney U test.

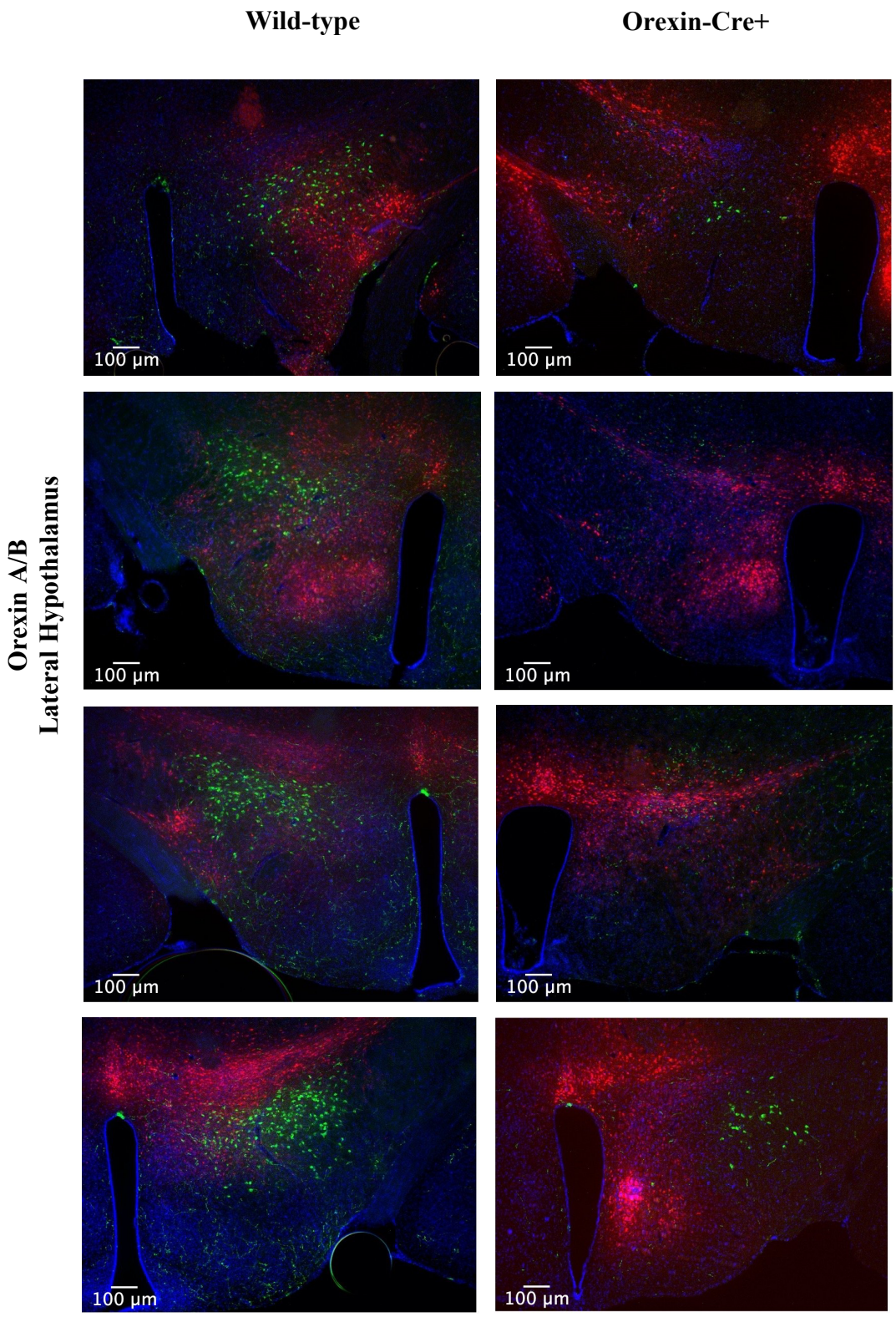

Figure 4.6. Representative images of orexinergic cell bodies in the lateral hypothalamus in the orexin-intact (left column) and orexin-ablated groups (right column). Orexin A/B cell bodies (green), and mCherry (AAV-dtA, red). As observed, the distribution and quantity of orexinergic cell bodies has a similar pattern in orexin-intact mice, whereas this is significantly reduced in orexin-ablated mice. Each row represents a different pair of animals. x5 magnification.

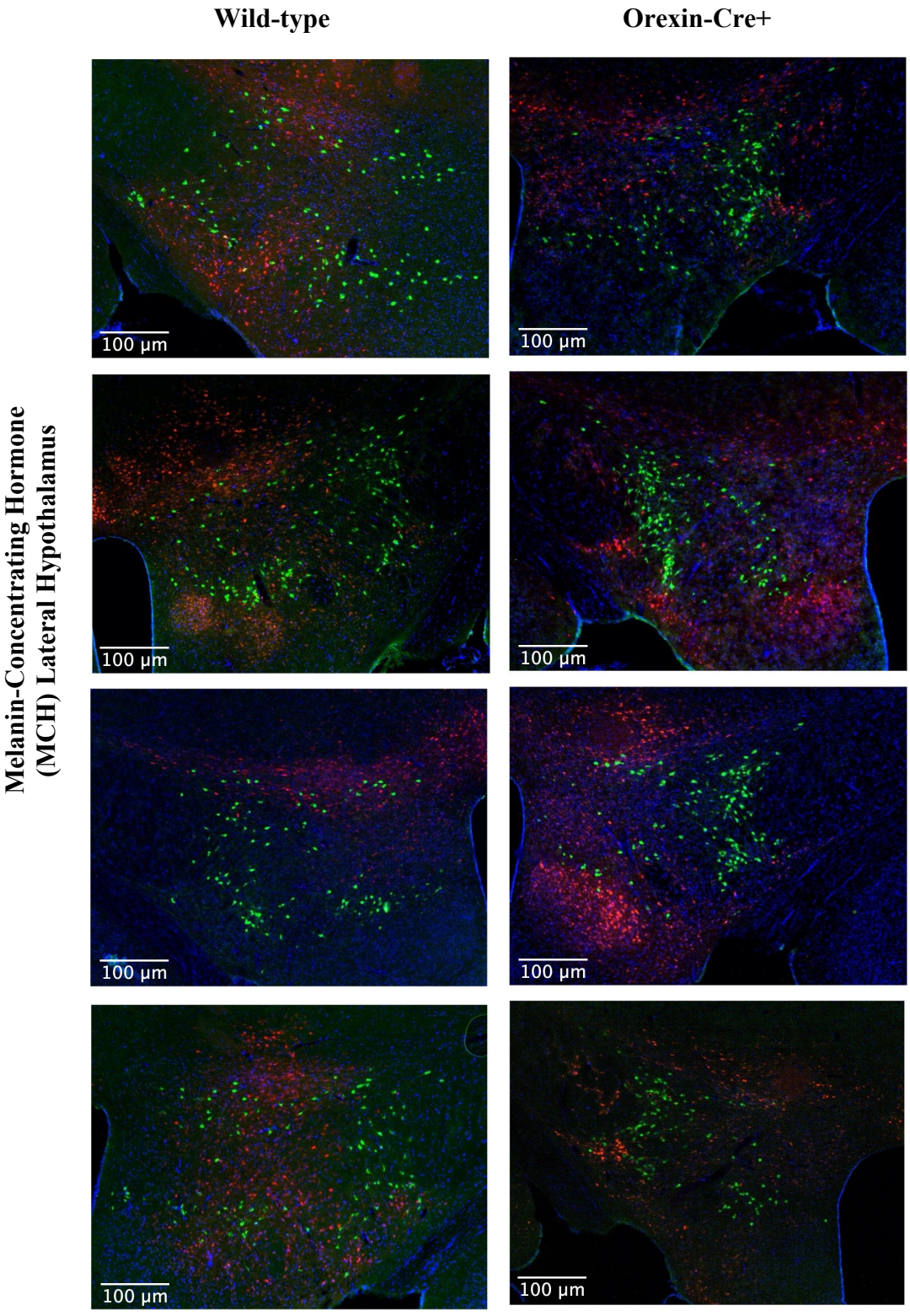

Figure 4.7. Representative images of melanin-concentrating hormone (MCH) cell bodies in the lateral hypothalamus of orexin-intact (left column) and orexin-ablated mice (right column). MCH cell bodies (green), and mCherry (AAV-dtA, red). As observed, the distribution of MCH has this characteristic difusse pattern throughout the lateral hypothalamus that does not differ between groups. x10 magnification.

4.3.2. Ablation of lateral hypothalamic orexinergic neurons decreases periorbital mechanical withdrawal thresholds

On Week 0, prior to stereotaxically injecting the AAV-dtA, both groups were acclimatised to the von Frey assay, and baseline measures conducted. Baseline measures in the periorbital von Frey test were used to compare responses in wild type littermates (n = 9) and orexin-Cre^{+} (n = 7) mice, due to the exclusion of two orexin-Cre^{+} mice who presented with chronically low mechanical withdrawal thresholds. Mechanical withdrawal thresholds were overall significantly lower (approximately 24%) in orexin-Cre+ mice compared to their wild type littermates ($t_{(16)} = 2.616$, p= 0.020; **Figure 4.8.**), with thresholds of 0.851g ± 0.050 and 0.645g ± 0.062 (Mean ± SEM), respectively. It is not uncommon to observe such group differences and under normal conditions we counterbalance the mice to groups after basal measurement (Holton, Strother et al. 2020); however, the use of transgenic mice here prevented this. As such, all future analysis of sensory thresholds post dtA are conducted with respect to the individual groups baseline measurement.

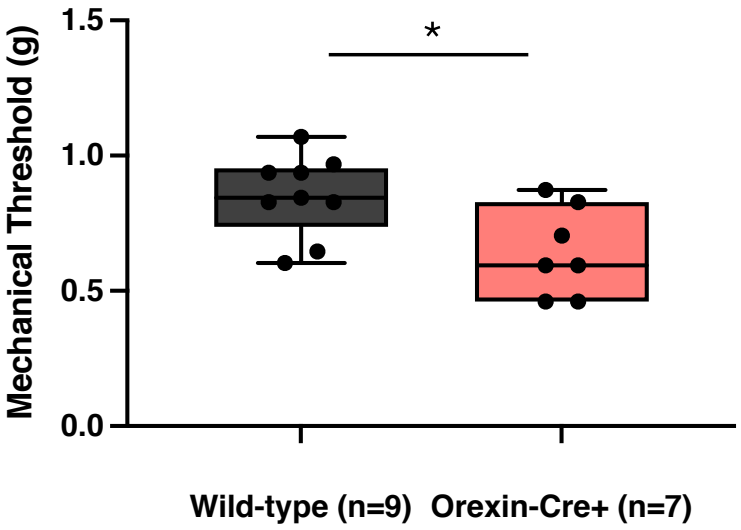

Figure 4.8. Baseline mechanical withdrawal thresholds. Wild type and orexin-cre+ mice differ in their baseline mechanical withdrawal thresholds prior to orexinergic-ablation ($t_{(16)} = 2.616$, p= 0.020). * $p \leq 0.05$. Unpaired t-test.

Allowing five weeks for full viral transduction and orexinergic ablation post stereotaxic injection of the AAV-dtA, both groups: orexin-ablated (orexin-Cre^{+}) and orexin-intact mice (wild type littermates) were habituated again to the von Frey apparatus

and tested to measure their periorbital mechanical withdrawal thresholds. As noted, comparisons were conducted in relation to the baseline reading in each genotype due to a modest but significant reduction in periorbital sensitivity in orexin-Cre^{+} mice. There were no significant difference in periorbital mechanical thresholds within the orexin-intact group, pre and post-dtA treatment ($t_{(7)}$ = 1.784, p=0.117**; Figure 4.9. (A)**), at 0.877 ± 0.049g and 0.774g ± 0.069 (Mean ± SEM), respectively. In comparison, there was a significant decrease in periorbital mechanical thresholds in the orexin-ablated mice ($t_{(6)}$ = 10.09, p < 0.000; **Figure 4.9.(B)**), with thresholds decreased from 0.645g ± 0.062 to 0.036g ± 0.017 (Mean ± SEM) respectively, representing a greater than 90% reduction in periorbital mechanical thresholds as compared to their pre-ablation levels.

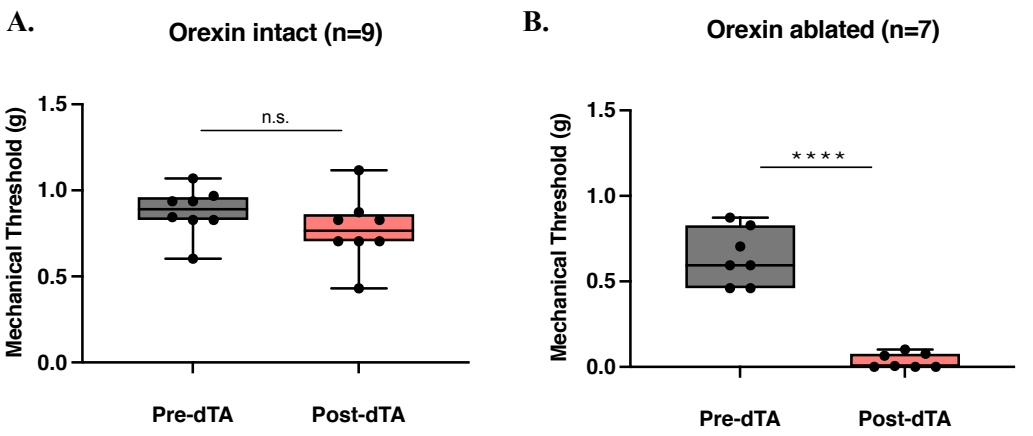

Figure 4.9. Mechanical withdrawal thresholds before and after orexinergic-ablation. A. No significant reduction in periorbital mechanical sensitivity in the Orexin-intact group pre-dta compared to post-dtA ($t_{(7)}$ = 1.784, p=0.117 at 0.877 ± 0.049 and 0.774 ± 0.069, respectively **B**. A significant reduction in periorbital mechanical threshold in orexin-cre^{+} ablated mice at pre-dta compared to post-dtA ($t_{(6)}$ = 10.09, p < 0.001) 0.645 ± 0.062 to 0.036 ± 0.017g, respectively. *p ≤ 0.05. Paired t-tests.

4.3.3. Ablation of lateral hypothalamic orexinergic neurons has no effect on locomotor activity

Having previously observed changes in locomotor activity post-orexinergic ablation **(see Figure 3.10.)**, the locomotor activity of both groups was measured in the open field assay at two different time-points: pre-dtA and post-dtA at week five, to attempt to replicate our previous findings. Prior to the dtA stereotaxic procedure, the average locomotor activity during 10 minutes (total distance covered, in cm) was compared

among wild type littermates and orexin-Cre^{+} mice, demonstrating no significant differences (U = 26, p = 0.222**; Figure 4.10**.)**,** at 4381cm [IQR: 3858 – 4784] and 4817cm [IQR: 4498 – 5007], respectively.

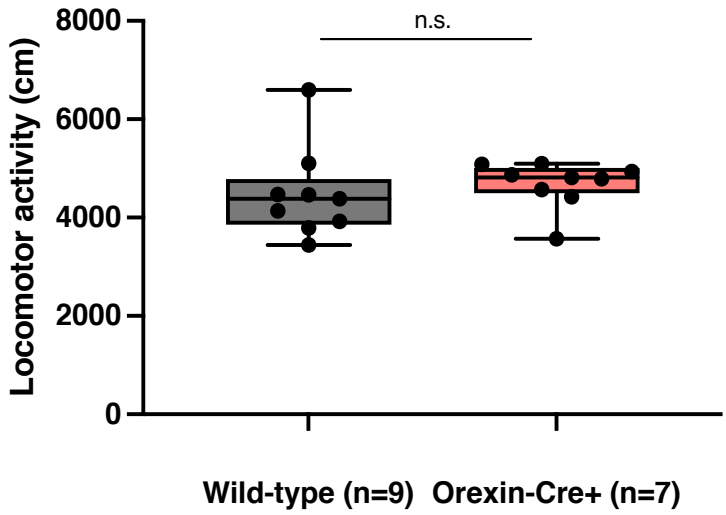

Figure 4.10. Baseline locomotor activity (in cm). No significant differences in locomotor activity at baseline between wild type and orexin-cre+ mice (U = 26, p = 0.222) at 4381 [IQR: 3858 – 4784] and 4817 [IQR: 4498 – 5007], respectively. n.s., non-significant. Group wise comparisons were conducted via the Mann Whitney U test.

Having observed no significant changes in baseline locomotor activity, we proceeded to compare the pre-dtA and post-dtA activity in both orexin-intact and orexin-ablated groups. In contrast to our previous findings, there was no significant changes in locomotion between orexin-intact and orexin-ablated mice pre and post-dtA, with no significant treatment effect ($F_{(1,16)} = 0.28$, p = 0.607; **Figure 4.11**). Having observed an additional decrease in locomotor activity in the orexin-intact group might suggest an anxiety-induced reduction in movement due to this cohort having been single-housed.

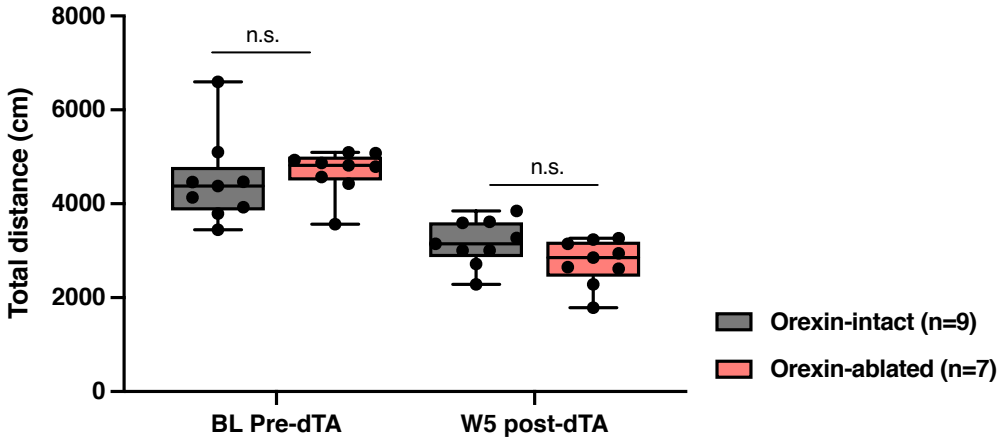

Figure 4.11. Locomotor activity before and after ablation. No change in locomotion between orexin-intact and orexin-ablated mice pre or post ablation ($F_{(1,16)} = 0.28$, $p = 0.607$). There was an overall reduction in locomotion at 5 weeks post stereotaxic injection; however, this did not differ between groups. Two-way repeated measures ANOVA, with familywise error rates corrected for using Sidak's correction.

In addition to the open field assay; three weeks post-dtA, the whole cohort was placed in individually-home-cages in which passive infrared detectors measured their total home cage activity. Surprisingly, this more natural and long-term assay of locomotor activity uncovered a significant decrease (U=2, p=0.000) in average total activity (per day) in the orexin-ablated mice (2509 [IQR: 2134 – 2813]) compared to the orexin-intact group (4684 [IQR: 4213 – 5302]) (**Figure 4.12).** Suggesting long-term recordings such as home-caged infrared monitoring might be more representative of their overall locomotor profiles, compared to 10-minute recordings in the open field arena.

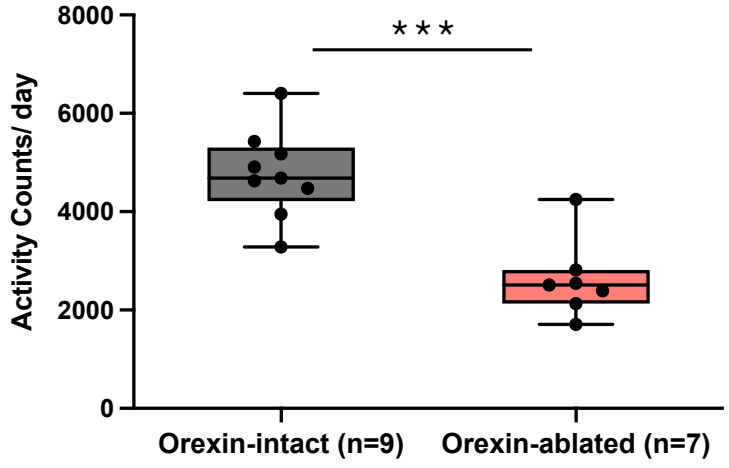

Figure 4.12. Average activity counts per day after dtA. Significant difference in locomotor activity between orexin-intact and orexin-ablated mice post ablation (U=2, p=0.000). Group wise comparisons were conducted via the Mann Whitney U test.

4.3.4. Acute administration of intranasal orexin A does not reverse orexin ablation-mediated reductions in mechanical withdrawal thresholds

Six weeks post-dtA-mediated ablation of orexinergic neurons: orexin-ablated and orexin-intact mice were habituated again to the testing apparatus for one hour. On day one, mice were administered a single dose of intranasal saline (30 ul total volume) and returned to the testing apparatus for another hour prior to reassessing their periorbital mechanical sensitivity. On day two, the same protocol was applied: by administering a single acute dose of OxA and their periorbital sensitivity reassessed one hour later. There was no significant difference in mechanical withdrawal thresholds in orexin-intact wild type mice in response to saline or OxA administration ($t_{(8)}$ = 1.411, p = 0.196,; **Figure 4.13**.) with thresholds of 0.481 ± 0.072 and 0.552 ± 0.057, respectively. Suggesting that acute OxA has no effects over periorbital thresholds under normal conditions.

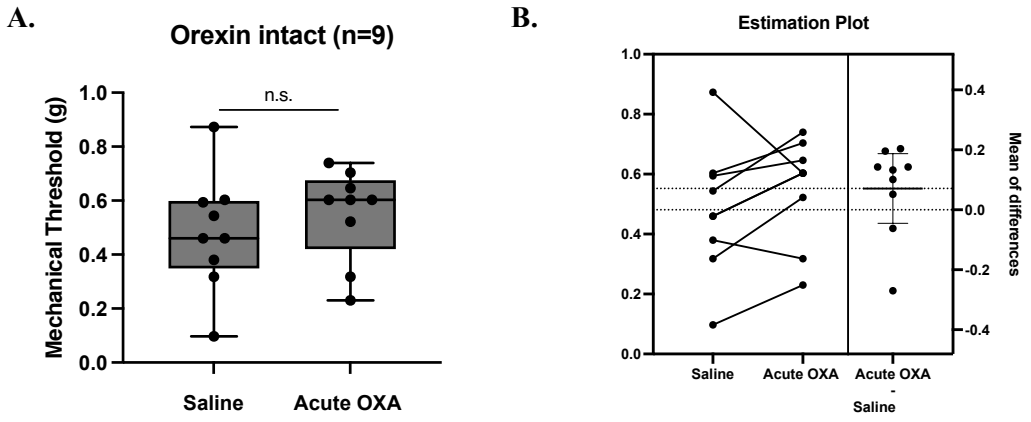

Figure 4.13. No change in mechanical withdrawal thresholds in orexin-intact mice in response to acute intranasal orexin A (OxA). A. An acute dose of intranasal OxA had no effect on periorbital mehcnical withdrawal thresholds in orexin-intact mice, when compared to the intranasal administration of saline ($t_{(8)}$ = 1.411, p = 0.196) with thresholds of 0.552 ± 0.057, and 0.481 ± 0.072, respectively. Paired t-test B. Estimation plot represents the distribution of the data: with the left column showing the raw data, and the right column the 95% confidence intervals for the mean differences displayed.

To understand whether the same single dose of OxA could have any antinociceptive effects in orexin-ablated mice, we next assessed the orexin-Cre^{+} mice. There were no significant differences in periorbital mechanical withdrawal thresholds in response to saline or acute OxA ($t_{(6)}$ = 0.734, p = 0.490; **Figure 4.14**.), with thresholds of 0.016 ± 0.006 and 0.028 ± 0.014, respectively. Again suggesting that a single dose of intranasal OxA is inefficient to recover orexin ablation-mediated reductions in sensory thresholds.

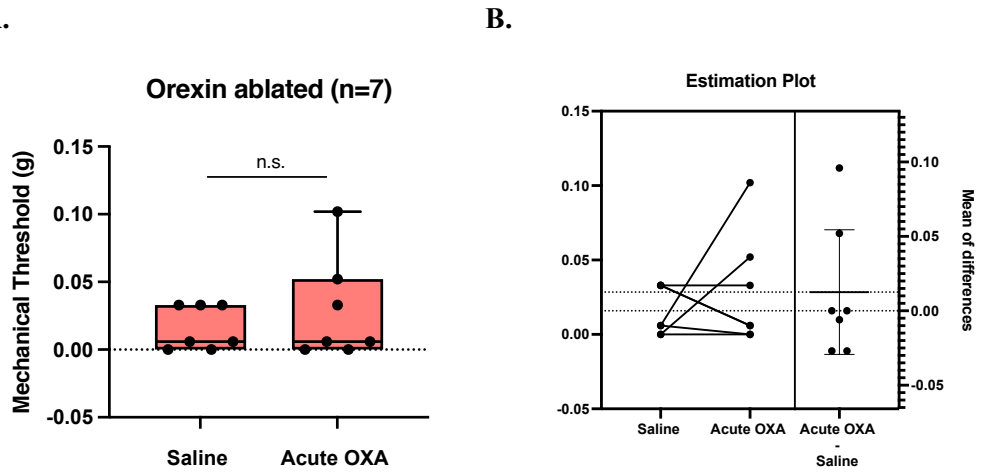

Figure 4.14. No change in mechanical withdrawal thresholds in orexin-ablated mice in response to acute intranasal orexin A (OxA). A. An acute dose of intranasal OxA had no effect on periorbital mechanical withdrawal thresholds in orexin-ablated mice, when compared to the intranasal administration of saline ($t(6) = 0.734$, $p = 0.490$) with thresholds of 0.028 ± 0.014 and 0.016 ± 0.006, respectively, Paired t-test B. Estimation plot represents the distribution of the data: with the left column showing the raw data, and the right column the 95% confidence intervals for the mean differences displayed.

4.3.5. Chronic intranasal administration of orexin A partially recovers orexin ablation-mediated reductions in mechanical withdrawal thresholds

Having observed no effect from a single dose of intranasal OxA and with OxA having previously shown peak expression in the CNS after 30 minutes of intranasal administration (Dhuria, Hanson et al. 2009), we next sought to test if daily administration of OxA, twice per day would show beneficial effects. Mice received a total of 9 doses of OxA, the last of which was administered 30 minutes before behavioural assessment on day 5. Periorbital mechanical withdrawal thresholds were compared within each group at two different time points on day 5. prior to (basal chronic) and 30 minutes post OxA. There was no significant change in thresholds between pre and post-orexin responses in orexin-intact mice ($F_{(1.5, 12.1)} = 0.873$, $p = 0.414$; **Figure 4.15. (A)**). In comparison, the orexin-ablated mice demonstrated a significant difference in periorbital mechanical withdrawal thresholds across the groups following chronic OxA ($F_{(1.9, 11.4)} = 8.611$, $p = 0.006$; **Figure 4.15. (B)**). Specifically, there was a significant difference in periorbital sensitivity between the control treatment day (saline) and the final dose of chronic OxA

administration (q(6) = 5.755, p = 0.016), with a mean of 0.016 ± 0.006 and 0.400 ± 0.092, respectively, reflecting a 96% increase in mechanical thresholds. Suggesting that chronic exposure to intranasal OxA may represent a novel anti-nociceptive therapeutic option for migraine.

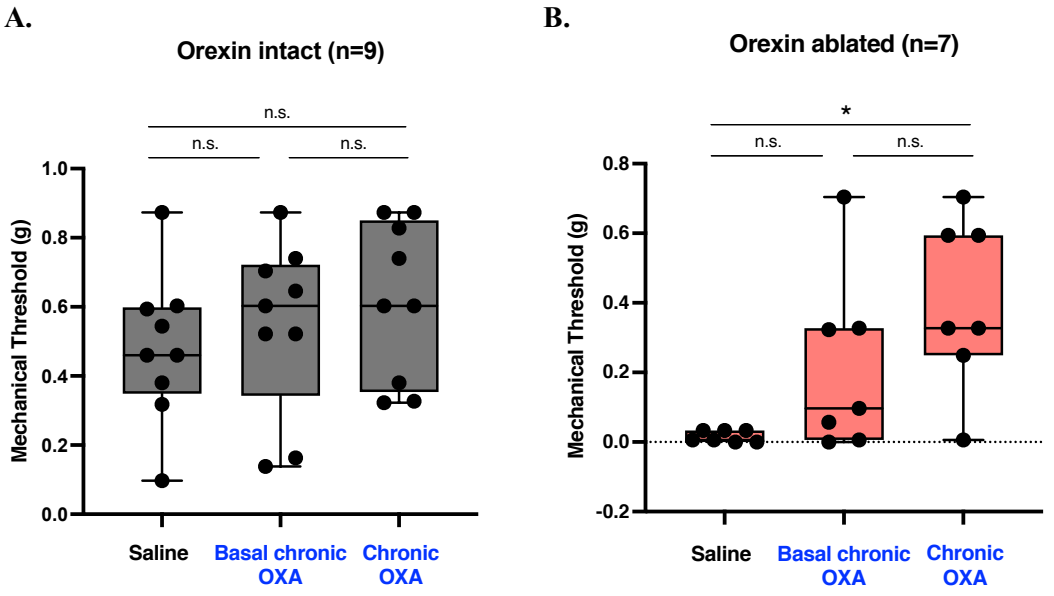

Figure 4.15. Chronic intranasal orexin A (OxA) recovers orexin ablation-mediated decreases in periorbital mechanical withdrawal thresholds. A. There were no significant changes in periorbital mechanical sensitivity when comparing: baseline saline-treated, basal chronic OxA and chronic OxA groups in the orexin-intact group ($F_{(1.5, 12.1)} = 0.873$, $p = 0.414$). B. Whereas, the orexin-ablated group demonstrated a significant increase in periorbital mechanical withdrawal thresholds between saline and chronic OxA treatment ($F_{(1.9, 11.4)} = 8.611$, $p = 0.006$). One-way ANOVA.

4.3.6. Loss of lateral hypothalamic orexinergic neurons correlates with the degree of periorbital mechanical sensitivity

To assess for potential relationships between orexinergic cell loss and periorbital mechanical thresholds we conducted a simple regression correlation analysis. We observed a significant linear correlation between the number of orexinergic cell bodies in the lateral hypothalamus and the degree of periorbital mechanical sensitivity, with an R squared value closer to 1., R = 0.5442 (p = 0.002), (**Figure 4.16).**

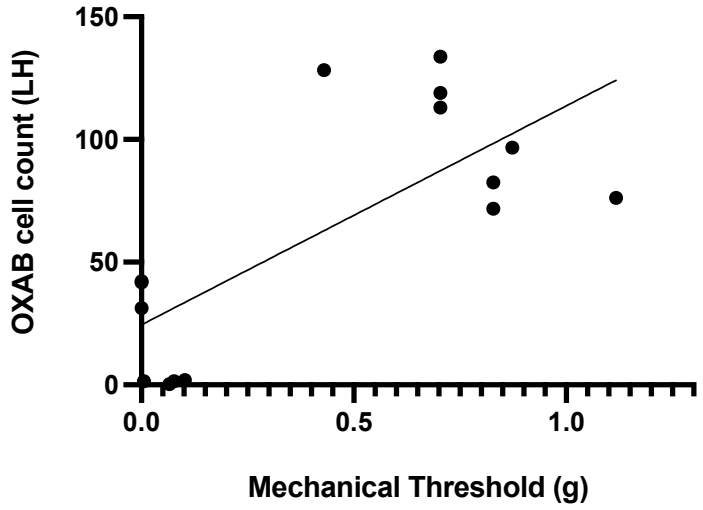

Figure 4.16. An exploratory analysis of the number of orexinergic neurons in the lateral hypothalamus (LH) correlates with periorbital mechanical withdrawal thresholds at week six post-dtA (corresponding to the post-dtA values in Fig 4.9 from both groups) in mice. The number of orexinergic neurons represents the average cell body count of four to five sections covering the entire LH; having left four sections in between (to avoid double counting). A simple regression correlation analysis observed a significant linear correlation between the number of orexinergic cell bodies in the lateral hypothalumus and the degree of periorbital mechanical sensitivity ($R = 0.5442$ ($p = 0.002$)).

4.4. DISCUSSION

4.4.1. Cre-mediated ablation

As previously mentioned; complete ablation of the hypothalamic orexinergic population cannot differentiate the role of each orexinergic neuropeptide: OxA and OxB; which have previously shown to differentially modulate trigeminal nociception (Bartsch, Levy et al. 2004, Holland, Akerman et al. 2005, Holland, Akerman et al. 2006). Hence in this study we sought to determine if modulation of orexinergic signalling could reverse orexin ablation-mediated reductions in periorbital mechanical withdrawal thresholds. In agreement with the preliminary study (chapter 3); we observed a significant reduction (79%) in orexinergic cell bodies in the lateral hypothalamus in the orexin-ablated group compared to the orexin-intact group, confirming the successful ablation of the orexinergic population. In this study both groups were injected with the same AAV-dtA vector to account for any potential effects caused by the AAV alone. The amount of MCH was also analysed to ensure no off-target ablation, and no significant changes in MCH neurons were observed between the groups.

4.4.2. Periorbital mechanical sensitivity

Orexin-Cre+ mice and wild-type littermates were injected with the AAV-dtA stereotaxically into the lateral hypothalamus and allowed to recover for at least four weeks. As previously observed in Chapter 3; orexin-ablated mice displayed a decrease in periorbital mechanical withdrawal thresholds, compared to the orexin-intact mice (wild type littermates). Confirming that a net loss of orexinergic signalling produces a pronociceptive effect over trigeminal pain processing. Previous research has highlighted an antinociceptive effect of OxA (Bartsch, Levy et al. 2004, Holland, Akerman et al. 2005, Holland, Akerman et al. 2006) and a pronociceptive effect of OxB (Bartsch, Levy et al. 2004) under different experimental conditions. Our findings suggest that normal orexinergic signalling inhibits trigeminal nociceptive processing, potentially via direct (Date, Mondal et al. 2000) or indirect projections pathways. Sensory fibres from the trigeminal nerve synapse on second order neurons in the trigeminocervical complex, and it has been shown that higher order centres such as the hypothalamus are able to modulate the incoming nociceptive information from the TCC (Bartsch, Levy et al. 2004, Robert,

Bourgeais et al. 2013) directly or indirectly through the PAG, LC or rostral ventromedial medulla (Millan 2002). As such, it is likely that a loss of orexinergic tone impacts several nuclei that themselves modulate trigeminal pain processing. For example, the densest orexinergic projections in the brain terminate in the LC (Horvath, Peyron et al. 1999) a structure that itself regulates trigeminal nociception (Vila-Pueyo, Strother et al. 2018).

Clinically, a loss of orexinergic neurons leads to narcolepsy (Mahoney, Cogswell et al. 2019) a condition that infers a 2-fold increased prevalence of migraine (Dahmen, Kasten et al. 2003), while migraine itself has been reported to be a risk factor for narcolepsy (Yang, Hsieh et al. 2017). Although not substantiated, the hypocretin (orexin) 1 gene has been proposed as genetic susceptibility loci for migraine (Rainero, Rubino et al. 2011), all of which when taken together suggests a potential shared pathophysiological pathway relevant to both disorders. It was this phenotypic overlap, including the role of orexins in arousal (Harris and Aston-Jones 2006) and the marked fatigue present during the migraine premonitory phase (Giffin, Ruggiero et al. 2003) that initially led our intention to study the role of orexinergic mechanisms in migraine. In contrast to our previous results (chapter 3), we did not observe any reduced locomotion in orexin-ablated mice compared to their wild type littermates; however, locomotion did decrease across both groups, perhaps suggesting a lack of novelty-based exploration behaviour. In an alternate analysis we explored total home cage activity counts as measured by passive infrared detectors in orexin intact and orexin-ablated mice. In this more natural environment, we observed a significant decrease in activity counts in orexin-ablated mice across both the light and dark phase across an extended monitoring period out to 8 weeks post ablation. This reduced locomotor function is in agreement with our initial pilot studies and published literature (Inutsuka, Yamashita et al. 2016, Karnani, Schone et al. 2020). Overall the burden of evidence suggests that loss of orexinergic tone impacts locomotion; however, our data does not support that locomotor activity in the open field is a reliable surrogate readout of fatigue. Fatigue is a complex behaviour (Wolff, Raheem et al. 2018), the underlying mechanism of which remain poorly understood and as such, significantly more research is required to validate an appropriate fatigue based readout that can be used to model migraine-related fatigue in rodents.

4.4.3. Associated symptomatology: fatigue

The orexinergic system is of great interest given its roles in both long term modulation of homeostatic changes (Chieffi, Carotenuto et al. 2017), as well as tonic rapid responses to sensory cues (Inutsuka, Yamashita et al. 2016). Despite ablation studies being challenged by potential compensatory mechanisms occurring throughout the time window of progressive ablation; the main purpose of our studies was to investigate the effects of rather long term altered orexinergic modulation. A chronic loss of orexinergic tone is unlikely in migraine given the episodic nature of the disease; however, an underlying dysfunctional homeostatic regulator would explain the myriad of extrinsic and intrinsic triggers reported by patients and the cyclic nature of migraine. Often underappreciated, premonitory symptoms represent the earliest identifiable symptoms of migraine, and marked fatigue ranks highly as one of the most bothersome premonitory symptoms. As such, arousal-associated symptomatology offers a novel insight into the underlying mechanisms of migraine. This marked fatigue is however, not solely present during the premonitory phase, with patients reporting feeling washed out during the postdromal phase, after the headache cessation (Bose, Karsan et al. 2018). While we have been unable to demonstrate a reliable fatigue-like phenotype in our orexin-ablated mice, it remains likely that a dysfunctional orexinergic system in part underlies the alteration in trigeminal nociception and arousal-based phenotypes in migraine. Thus targeted modulation of orexinergic signalling should be considered as a novel therapeutic target. Importantly, such approaches, targeting central nervous system neural networks involved in migraine biology may herald an entirely novel treatment approach, treating the disorder as oppose to the most salient symptom, migraine-related pain.

4.4.4. Orexin A and the orexin 1 receptor as potential therapeutic targets

The orexins have been linked with the regulation of trigeminal and non-trigeminal pain, and the majority of studies have highlighted the potential antinociceptive effects of OxA (Bingham, Davey et al. 2001, Bartsch, Levy et al. 2004, Holland, Akerman et al. 2005, Holland, Akerman et al. 2006). Several of which have highlighted that OxA's antinociceptive effects are OX_1R-dependent (Holland, Akerman et al. 2005, Holland, Akerman et al. 2006). In the current study we determined if intranasal OxA could recover the trigeminal sensory hypersensitivity induced by orexin ablation. The intranasal route

is of particular interest as it offers a more direct entry route into the central nervous system (Rapoport, Bigal et al. 2004, Dhuria, Hanson et al. 2009, Hanson, Fine et al. 2013, Weinhold, Seeck-Hirschner et al. 2014, Shrewsbury, Jeleva et al. 2019), while the anatomical localisation of the trigeminal nerve results in it demonstrating some of the highest tissue to blood distribution ratios. This includes for orexin, where intranasal administration produced a more focused drug distribution in the trigeminal nerve and hypothalamus compared to the intravenous route (Dhuria, Hanson et al. 2009).

Acute administration of a single dose of OxA intranasally in mice failed to recover orexin ablation-mediated reductions in trigeminal sensory thresholds; however, a more chronic paradigm proved effective. This is likely due to the short half-life of OxA (Ehrstrom, Naslund et al. 2004) meaning that a more chronic delivery method is required to exert a functional effect on trigeminal pain processing. The chronic administration protocol did not alter trigeminal sensory thresholds in orexin-intact mice suggesting that the actions of OxA may be nociceptive specific. This is in keeping with studies highlighting that OX_1R's mediate antinociceptive actions in a rodent of diabetic neuropathic pain with no impact on sham animals (Kajiyama, Kawamoto et al. 2005). Therefore, the orexinergic system may represent a state-dependent neural network that when perturbed can alter descending pain modulatory circuits to increase trigeminal nociceptive traffic. Our findings are in contrast to previous work studying narcolepsy whereby acute (Mieda, Willie et al. 2004) and chronic (Kaushik, Aritake et al. 2018) orexin administration showed significant effects. During dose optimisation we did observe increased activity following a single acute dose, suggesting that these systems may be regulated via different downstream mechanisms that share a similar orexinergic drive.

Irrespective of the dosing regimen, the ability of OxA to reverse the phenotype in orexin-ablated mice suggest that OxA, likely acting via the OX_1R (Holland, Akerman et al. 2005, Holland, Akerman et al. 2006) results in an antinociceptive response when administered intranasally. This response is independent of physiological activation of orexin projection neurons that would co-release other neurotransmitters including dynorphin (Chou, Lee et al. 2001, Muschamp, Hollander et al. 2014, Podvin, Yaksh et al. 2016). As such, our findings support the targeted delivery of OxA or OX_1R agonists/positive allosteric modulators for migraine and when combined with the novel

intranasal route offer the potential to treat not only migraine-related pain but also to boost arousal in patients who commonly report marked fatigue as a hallmark of the disease.

5. Chapter 5: Effects of intracranial LC orexinergic modulation on TCC electrophysiological responses

5.1. Introduction

Considering that modulation of orexinergic signalling alters trigeminal nociceptive processing ((Bartsch, Levy et al. 2004, Holland, Akerman et al. 2006) and chapter 3 – 4) we next considered through which downstream pathways orexin may be acting. The brainstem LC receives one of the densest orexinergic projections (Horvath, Peyron et al. 1999, Gonzalez, Jensen et al. 2012) and like the hypothalamus plays a key role in body homeostasis, regulating arousal networks and promoting wakefulness (Takahashi, Kayama et al. 2010, Breton-Provencher and Sur 2019, Poe, Foote et al. 2020). The LC is activated in response to activation of the trigeminovascular system (Tassorelli and Joseph 1995, Ter Horst, Meijler et al. 2001), suggesting that it is ideally placed to monitor and respond to altered trigeminal pain processing. For this reason, previous research from our group explored the ability of the LC to regulate trigeminal nociception. Electrolytic and chemical ablation of the LC decreased trigeminal nociceptive-evoked responses, suggesting a tonic facilitatory role of LC noradrenergic projections (Vila-Pueyo, Strother et al. 2018). Importantly, the LC is primarily modulated via an OX_1R-dependent mechanism that based on our demonstration of OxA-mediated antinociceptive effects and prior studies showing that this effect was OX_1R-dependent (Holland, Akerman et al. 2005, Holland, Akerman et al. 2006), highlight it as a potential target for therapeutic intervention. The modulation of which has implications for emotional, stress, arousal and autonomic function (Messina, Dalia et al. 2014, Bonaventure, Yun et al. 2015).

Migraine is intrinsically linked with sleep-wake regulation and like the orexinergic neurons the LC shows clear alterations in diurnal activity (Jacobs 1986), with the greatest activation during arousal and the least during sleep. Clinically, the dorsal rostral pons which includes the LC is abnormally activated during migraine (Afridi, Giffin et al. 2005, Maniyar, Sprenger et al. 2014, Schulte and May 2016), while specific functional alterations have been identified between the hypothalamus and LC (Moulton, Burstein et al. 2008, Moulton, Becerra et al. 2014).

The noradrenergic LC is a heterogeneous structure with several functional regions each of which represents a different output channel with diverse functional implications (Poe, Foote et al. 2020). For example, specific subregions of LC neurons project to the prefrontal cortex where they modulate anxiety and aversion as compared to descending spinal projections that modulate nociception (Hirschberg, Li et al. 2016). These descending spinal cord projections are considered to regulate prolonged noxious stimuli (Azami et al., 2001), having a key modulatory role over ascending nociceptive transmission. They have also proven crucial in determining the progression from acute to chronic pain (Hughes et al., 2013), as observed through a significant decrease/loss in DNIC in pain models with intact descending modulatory networks (Dickenson and Le Bars, 1983). Some of the neurotransmitter constituents of these networks include opioid and GABAergic signalling. SNL-induced-losses in DNIC responses were shown to be recovered by local blocking of Kappa opioid signalling in the central Amygdala; suggestive a potential role of opioid signalling in inhibiting DNIC in these conditions (Phelps et al., 2019). Interestingly, orexins are known to co-release the inhibitory opioid peptide: dynorphin; the action of which through Kappa opioid receptors is known to contribute to mediate both reward seeking behaviours (Baimel et al., 2015) and depressive-like states (Knoll and Carlezon, 2009). The relationship among these now neurotransmitter systems is highly translatable to many allodynic and phenotypic (i.e. food cravings and mood changes) features we observe in migraine patients. Which is why, here we sought to determine if direct excitation of LC noradrenergic neurons by OxA would impact trigeminal nociceptive processing and further to test if any responses were OX_1R-dependent.

5.2. METHODS

For this study, the spontaneous and dural nociceptive-evoked neural activity in the trigeminocervical complex was measured in 6-week-old rats (n = 23 total) before and after stereotaxic administration of the experimental compounds into the LC. The study comprised three groups: those stereotaxically injected with OxA (n = 7), those with a OX_1R-antagonist (SB 334867, ToCris Biotechne) followed by OxA (n = 6), and those injected with vehicle control (saline mixed with DMSO) group (n = 6). Animals were initially anesthetised (5% followed by 2% isoflurane) and maintained with a continuous intravenous administration of propofol as detailed in the general methods section 2.23, page 72.

5.2.1. Microinjection

In brief, to permit access to the LC a craniotomy was performed above the stereotaxic coordinates (caudal from Lamda: -2.40mm, Medio-Lateral: +/- 1.30mm, DV: 6.00mm) and a multibarrel glass capillary (USP-4, MicroData Instruments) was carefully lowered into the LC, unilaterally. The different barrels contained the experimental compounds and were connected to a manual pressure ejection system. OxA (Tocris, Cat No: 1455) and the OX_1R-antagonists, SB-334867 (Tocris, UK) were microinjected into the LC at a concentration of 0.01 mM; at which they were previously established to have a biologically effect (Bartsch, Levy et al. 2004, Holland, Akerman et al. 2006). Stock OxA was initially diluted in saline whereas SB334867 was diluted in DMSO and both were kept frozen at -20ºC. On the day of the experiment, both compounds were defrosted and diluted accordingly to 0.01 mM. The control group was treated with saline diluted at the same concentration of DMSO as SB334867.

Once in the LC the appropriate volume (200 – 250 nl) of a specific drug was then carefully pressure ejected over a period of 60 seconds to minimise tissue distortion and injection sites confirmed via the deposition of Chicago sky blue dye at the conclusion of the experiment.

5.2.2. Electrophysiology

The middle meningeal artery (MMA) was exposed via a craniotomy to allow the placement of a bipolar stimulating electrode (FHC Inc.) to drive durovascular

nociceptive-evoked responses in the TCC. Subsequently, the skin and muscle above the first cervical vertebrae were retracted to gain access and a small hemi laminectomy performed to expose the underlying cervicomedullary junction. A tungsten microelectrode (1 MΩ) was then carefully lowered into the TCC, ipsilateral to the MMA and the relative position mapped against the facial dermatome using gentle brushing. Once periorbital receptive fields were present the animal was left to rest for 30 minutes and subsequently the durovascular responses were evoked via electrical stimulation (Grass S88, Grass Instruments; 8 – 15 V, 0.5 Hz, 0.3 – 0.5 ms). Once a stable baseline response to durovascular stimulation was determined (responding to MMA stimulation within 5-20ms), three sets of 20 stimuli each, were applied every 5 minutes and used as the baselines. Durovascular nociceptive-evoked, and spontaneous TCC neuronal activity were then recorded at 5, 10, 15, 20, 35, 50 and 65 minutes post injection of experimental or control drugs into the LC, and facial noxious (pinch) and non-noxious (brush) responses were measured at time points: 15, 35 and 65 minutes post injection.

All animals included for the analysis of electrophysiological data in this study, had to fit the following criteria:

1. Three stable dural-evoked responses in trigeminocervical neurons that also responded to stimulation of the ophthalmic (V1) dermatome. Three baseline measures were taken at 5 minute intervals, prior to commencing any acute interventions.

2. A recorded time window of a minimum of 60 minutes post-LC compound administration

3. A successful injection of the compound into the LC, as observed through Chicago Sky Blue (CSB) staining for both control and active cohorts (post-hoc tissue analysis).

5.3. RESULTS

5.3.1. Locus coeruleus orexin A-induced inhibition of dural-evoked responses in the trigeminocervical complex is mediated through orexin 1 receptors

Dural-evoked cell firing is representative of the number of units responding to durovascular stimulation. By use of low impedance (1Ω) tungsten microelectrodes we are able to record group cell activity, rather than individual unit responses.

There was a significant reduction in durovascular-evoked nociceptive responses in the TCC ($F_{(3.05, 18.27)}$ =.151, p = 0.021, n = 7), following microinjection of OxA (0.01mM) into the LC as compared to baseline responses (**Figure 5.1. (A-B)).** This reduction was significant at 15 (77.86 ± 6.285, $q_{(6)}$ = 3.658, p = 0.045), 50 (72.71 ± 6.855, $q_{(6)}$ = 4.527, p = 0.018) and 65 minutes (80.71 ± 7.263, $q_{(6)}$ = 4.121, p = 0.027) post OxA administration. There was no significant difference in rats receiving vehicle control into the LC ($F_{(3.34, 20.04)}$ = 0.8436, p = 0.497, n = 6, **Figure 5.1. C**).

Given the demonstration of an antinociceptive action of OxA, we next sought to determine if this response was OX_1R -dependent. Administration of the OX_1R antagonist SB-334867 into the LC, followed 5 minutes later by OxA (0.01mM) completely abolished the antinociceptive effects of OxA ($F_{(2.76, 13.36)}$ = 0.484, p = 0.679, n = 7, **Figure 5.1D**). Comparison of dural-evoked responses at different time points within each group were analysed through a one-way ANOVA (mixed-effects analysis).

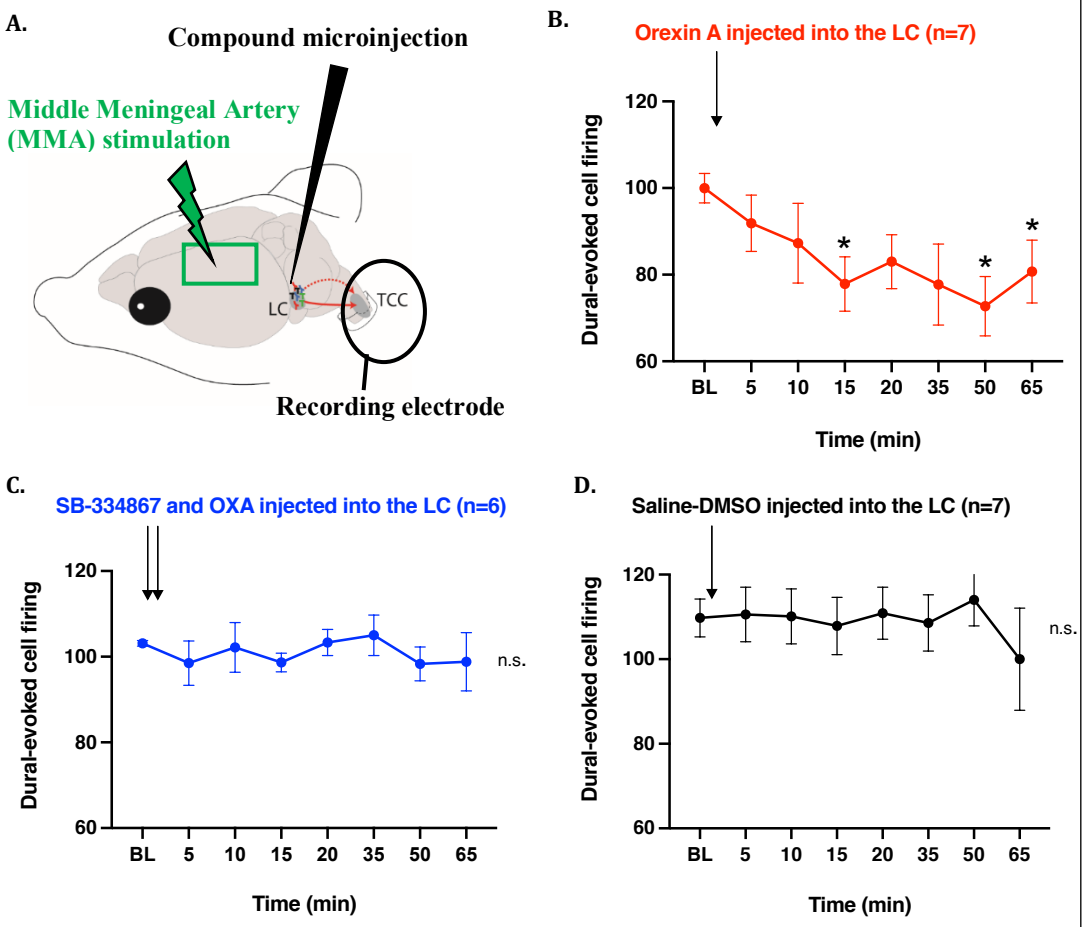

Figure 5.1. Significant reduction in durovascular-evoked nociceptive responses in the TCC. A. Experimental setup. B. There was a significant reduction in durovascular-evoked responses pre and post-OxA (0.01mM) microinjection in to the locus coeruleus (LC; $F_{(3.05, 18.27)} = 4.151$, $p = 0.021$), $n = 7$). C. There were no significant changes following saline-DMSO injection or when the OX_1R antagonist SB-334867 was pre-treated by OxA (D). *$p \leq 0.05$. n.s. non-significant. Arrows represent injection times.

5.3.2. Orexin A-mediated activation of the locus coeruleus has no impact on spontaneous neuronal activity in the TCC

In comparison to durovascular-evoked nociceptive responses, microinjection of OxA into the LC had no impact on ongoing spontaneous neuronal activity (in Hz: frequency per second) ($F_{(1.93, 11.55)} = 1.507$, $F_{(DFn, DFd)}$, $p = 0.262$), **Figure 5.2. (A)**). Similarly, spontaneous activity is not impacted following pre-treatment with the OX_1R antagonist SB-334867 prior to OxA ($F_{(1.41, 7.05)} = 0.8840$, $F_{(DFn, DFd)}$, $p = 0.417$, **Figure 5.2. (B)**). However, there was a modest significant reduction in vehicle-treated rats ($F_{(4.12, 24.7)} =$

3.634, p = 0.018, **Figure 5.2. (C)**), following 65 minutes only which was the final time point measured (10 ± 0.756, $q_{(6)}$= 4.291, p = 0.023).

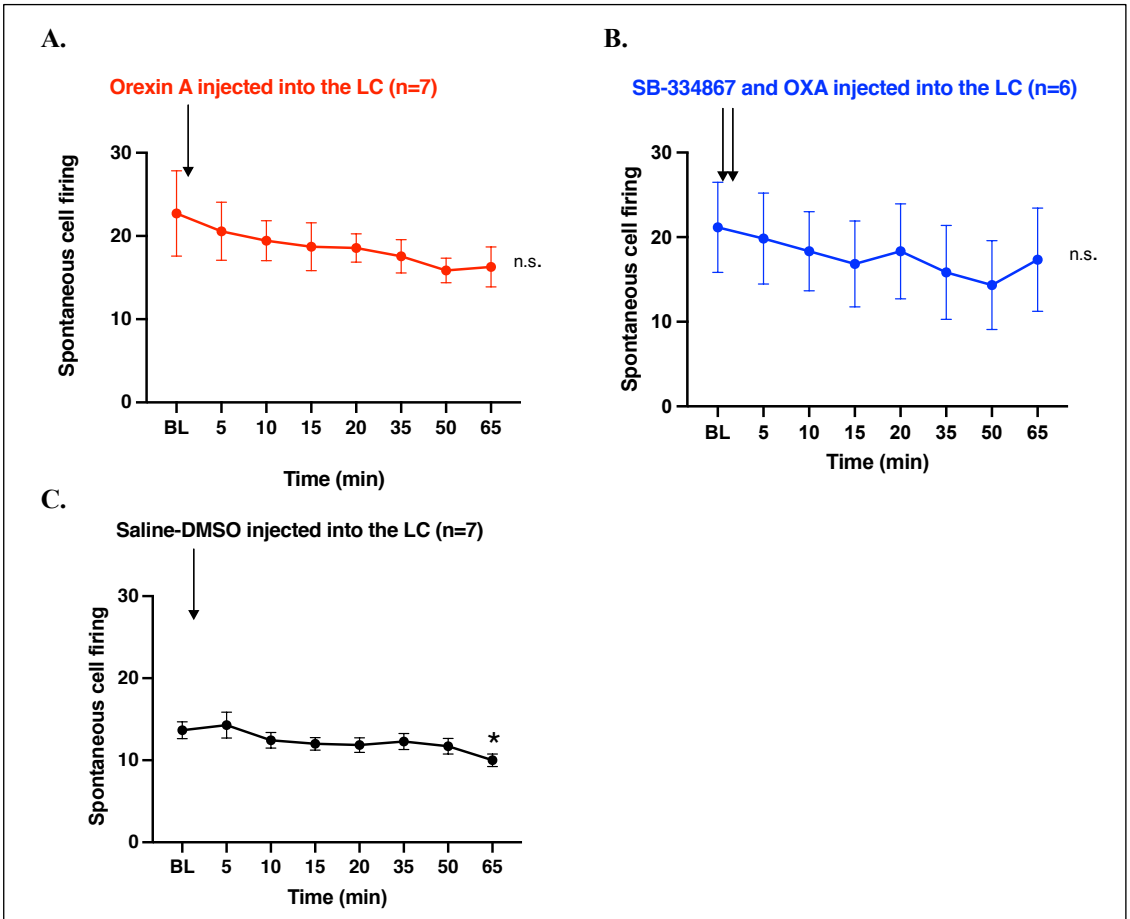

Figure 5.2. No significant impact of orexin A on spontaneous neuronal activity (Hz) in the TCC. No change in spontaneous activity to orexin A (OxA, $F_{(1.93, 11.55)}$ = 1.507, p = 0.262, A), OxA and the OX_1R antagonist SB-334867 ($F_{(1.41, 7.05)}$ = 0.8840, p = 0.417, B). There was a significant reduction in spontaneous activity in vehicle treated rats ($F_{(4.12, 24.7)}$) = 3.634, p = 0.018, C). * p ≤ 0.05 compared to baseline. n.s. non-significant. One way ANOVA on the changes in spontaneous cell firing pre and post-OxA microinjection into the LC however showed no significant changes (p = 0.2615), and no changes in the group injected with SB-334867 & OxA either (p = 0.4171). There was a significant decrease however in the saline-DMSO group at time point 65 min post-injection (p = 0.0227).

5.3.3. No alteration in noxious pinch or non-noxious brush-evoked responses in the TCC

To account for changes in spontaneous activity in the vehicle-treated rats (**Figure 5.2. (C)**; the analysed data corresponds to the ratio of the brush or pinch-evoked response over the baseline spontaneous activity previous to that time point. Brush and pinch-evoked stimuli were applied around the V1 dermatome in the periorbital area. Orexin-A

microinjection into the LC resulted in no significant changes in brush-evoked responses ($F_{(1.42,\ 8.5)}$ = 0.2451, $F_{(DFn,\ DFd),}$ p = 0.714, **Figure 5.3. (A)**). Similarly, pinch-evoked responses were unchanged following OxA injection ($F_{(1.42,\ 8.5)}$ = 0.4451, p = 0.59), **Figure 5.3. (B)**). There was additionally no alteration in responses following pre-treatment with the OX_1R antagonist SB-334867 prior to OxA for brush ($F_{(1.31,\ 5.65)}$ = 0.4133, p = 0.598, **Figure 5.4. (A)**) or pinch-evoked ($F_{(1.33,\ 5.77)}$ = 0.5012, p = 0.558, **Figure 5.4. (B)**) responses. Similarly, there was no changes following pre-treatment of saline-DMSO as control, for either brush ($F_{(1.43,\ 8.62)}$ = 0.5798, p = 0.527, **Figure 5.5. (A)**) or pinch ($F_{(1.43,\ 8.55)}$ = 1.442, p = 0.277, **Figure 5.5. (B)**).

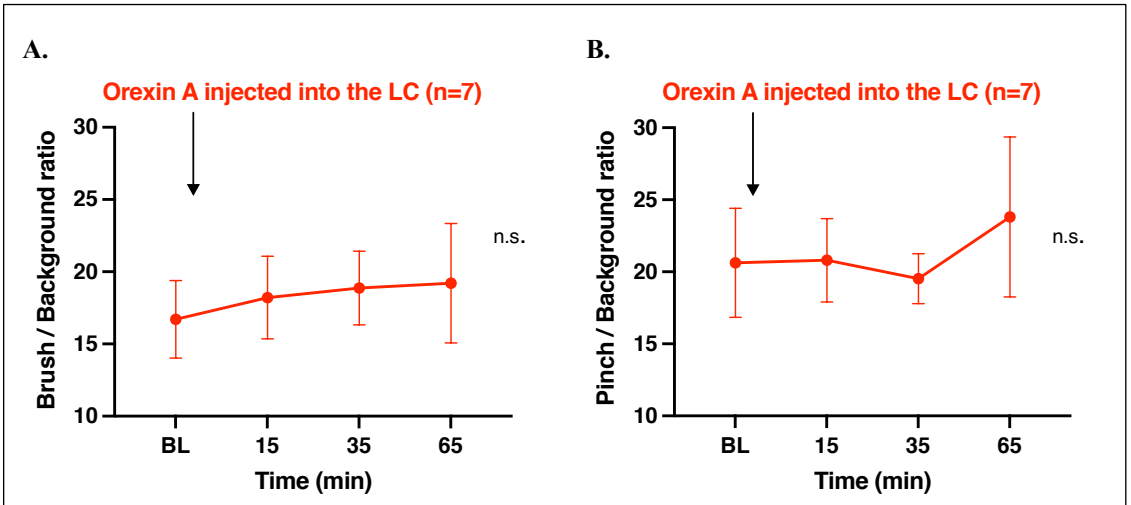

Figure 5.3. Brush and Pinch-evoked responses following orexin A. No change in non-noxious (brush, A, $F_{(1.42,\ 8.5)}$ = 0.2451, p = 0.714) and noxious (pinch, B, $F_{(1.42,\ 8.5)}$ = 0.4451, p = 0.59) responses following orexin A (OxA) injection into the locus coeruleus. n.s. non-significant.

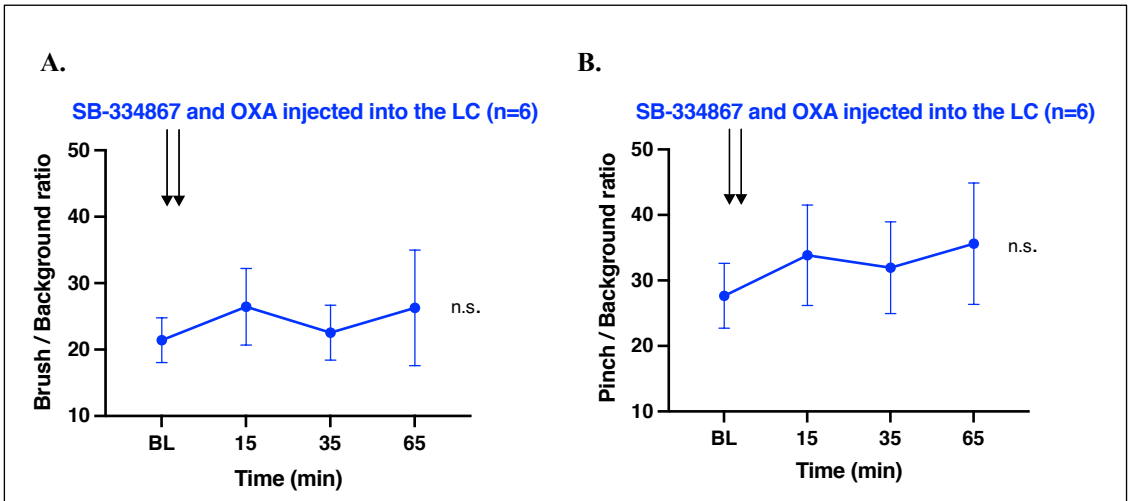

Figure 5.4. Brush and Pinch-evoked responses following SB-334867 and orexin A. No change in non-noxious (brush, A, $F_{(1.31,\ 5.65)}$ = 0.4133, p = 0.598) and noxious (pinch, B, $F_{(1.33,\ 5.77)}$ = 0.5012, p = 0.558) responses following injection of the OX_1R antagonist SB-334867 and orexin A (OxA) into the locus coeruleus. n.s. non-significant.

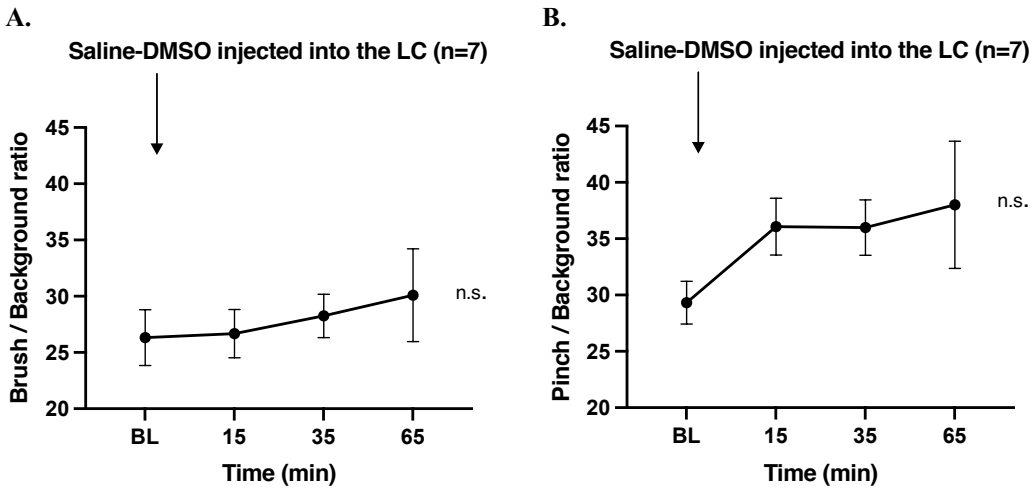

Figure 5.5. Brush and Pinch-evoked responses following saline. No change in non-noxious (brush, A, $F(1.43, 8.62) = 0.5798$, $p = 0.527$) and noxious (pinch, B, $F(1.43, 8.55) = 1.442$, $p = 0.277$) responses following injection of the OX_1R antagonist SB-334867 and orexin A (OxA) into the locus coeruleus. n.s. non-significant.

5.4. DISCUSSION

Our data demonstrate that OxA acting via OX_1R's in the LC has the potential to inhibit trigeminal nociceptive processing, with no impact on non-nociceptive neuronal activity. These findings are in agreement with published literature where OxA injected into the posterior hypothalamus evoked an antinociceptive response in the TCC (Bartsch, Levy et al. 2004). Similarly, systemic OxA is able to inhibit CGRP release from the peripheral terminals of the trigeminal sensory afferents and inhibit durovascular-evoked TCC neuronal responses, both of which were shown to be OX_1R -dependent (Holland, Akerman et al. 2005, Holland, Akerman et al. 2006). When taken in conjunction with our previous studies (chapter 3 and 4), whereby orexinergic ablation in the hypothalamus produced a pronociceptive effect on periorbital mechanical withdrawal thresholds, the body of evidence suggests a prominent regulation of trigeminal nociceptive processing by the orexinergic system. The hypothalamic orexinergic system has been linked to several pain states and OxA and subsequently the OX_1R has emerged as a potential novel therapeutic target (Bingham, Davey et al. 2001). However, the mechanisms and potential sites of action of OxA remain to be fully explained.

Herein, we identify the brainstem LC as a key target for orexinergic regulation of trigeminal nociception. The LC receives one of the densest orexinergic projections in the brain (Bingham, Davey et al. 2001), largely via activation of the OX_1R, having key functions in the regulation of emotion, stress, arousal and autonomic function (Messina, Dalia et al. 2014, Bonaventure, Yun et al. 2015). Considering migraine as a disorder of sensory processing, it is likely that multiple neural networks (Burstein, Noseda et al. 2015), expressing a variety of neurotransmitters across several key nuclei play an important role in the underlying pathophysiology of the disorder, the perturbation of which, as evidenced through the array of premonitory symptoms present in patients, likely precedes and potentially underlies the induction of an acute attack **(Figure 5.6.)**. Our data and that of others, places the hypothalamic orexinergic system as an important hub in this design. Focusing on nociception, the LC sends noradrenergic projections to the spinal cord to modulate incoming nociceptive signals (Hirschberg, Li et al. 2016). This descending inhibition is considered to respond most strongly to prolonged noxious stimuli (Azami et al., 2001) which is in keeping with our data whereby OX_1R-mediated activation of the LC preferentially inhibits intense durovascular-evoked activation over spontaneous

neuronal activity and acute noxious or non-noxious responses. It must be noted however, that our pharmacological approach, relying on local injection of OxA into the LC does not take account of the heterogeneous nature of the LC, considered to consist of several distinct functional units that demonstrate differential terminal projections and functional effects (Hirschberg, Li et al. 2016). This compartmental approach to LC function is an important one to consider in future targeted studies, with previous work from our group demonstrating that global ablation across these functional units has a differential impact on migraine-related symptoms (Vila-Pueyo, Strother et al. 2018). Namely, trigeminal nociceptive processing following electrolytic lesioning or DSP-4 (which is a toxin specific to LC NA neurons (Ross & Stenfors, 2014)), toxin-mediated ablation of the LC noradrenergic neurons inhibited trigeminal nociceptive responses in the TCC; however, DSP-4-abated rats presented with a concurrent increased susceptibility to CSD, the underlying electrophysiological correlate of migraine aura.

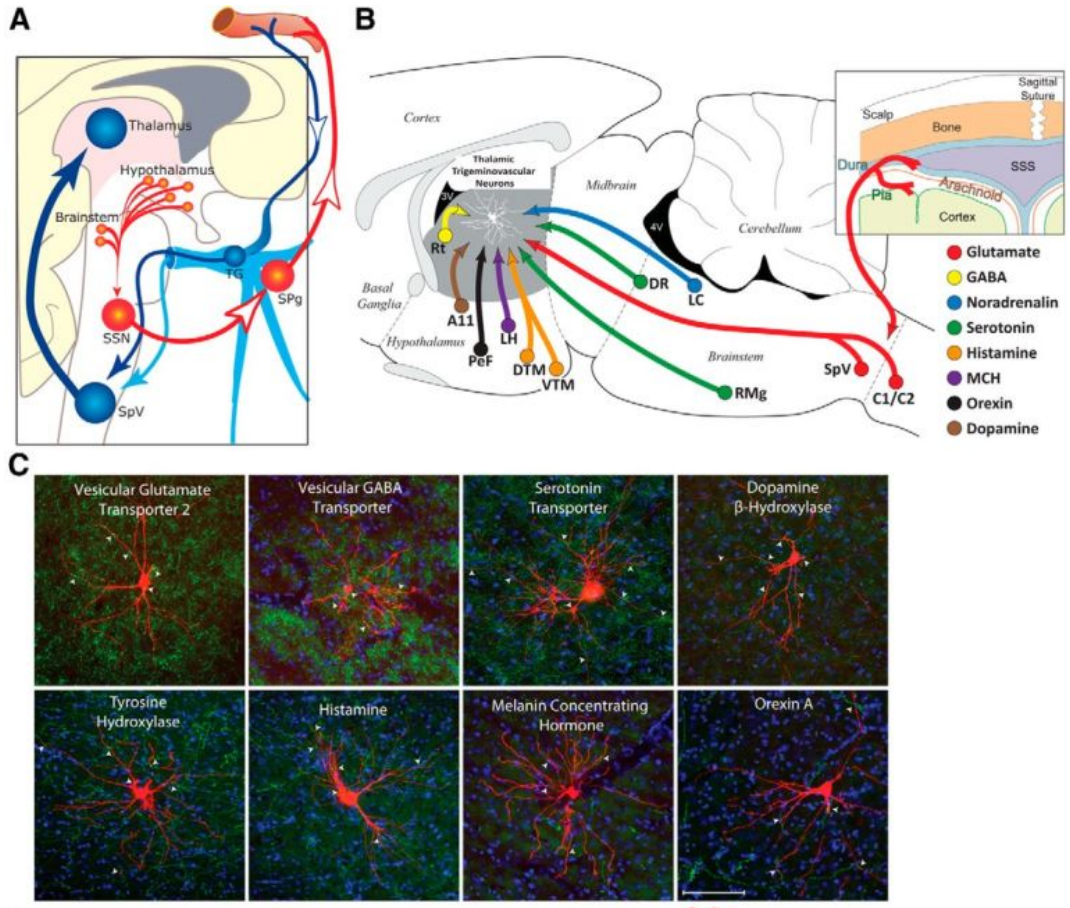

Figure 5.6. Ascending neurotransmitter systems integrated into the thalamus; linking migraine premonitory symptoms and altered trigeminal nociception. A. Hypothalamic circuits regulating trigeminal and parasympathetic neural networks regulating migraine. **B and C**. Multiple neurotransmitter pathways converging on thalamic relay neurons are able to monitor and respond to alterations in key homeostatic mechanisms (sleep-wake, food intake and emotion) as well as gate trigeminal sensory processing. The orexinergic pathway is shown, with noradrenergic projections from the locus coeruleus (LC) also known to modulate thalamic processing. SSN, superior salivatory nucleus; SpV, spinal trigeminal nuclei; SPG, sphenopalatine ganglion; TG, trigeminal ganglion. A11, hypothalamic dopaminergic nucleus; DR, dorsal raphe nucleus; DTM, dorsal tuberomammary hypothalamic nucleus; C1/C2, cervical spinal cord levels; ; LH, lateral hypothalamus; PeF, perifornical area; RMg, nucleus raphe magnus (Burstein, Noseda et al. 2015).

The LC represents a key relay nucleus through which orexinergic and other descending modulatory structures can influence spinal nociception. While anatomical precision is lacking, the dorsal rostral pons that included the LC is abnormally active (Afridi, Giffin et al. 2005, Maniyar, Sprenger et al. 2014, Schulte and May 2016) during migraine. Its connectivity to the lateral hypothalamus is also altered across the migraine cycle LC (Moulton, Burstein et al. 2008, Moulton, Becerra et al. 2014) and it is activated

in response to trigeminovascular activation (Tassorelli and Joseph 1995, Ter Horst, Meijler et al. 2001). Orexin 1 receptor-dependent activation of the LC modulates arousal and locomotion (Hagan, Leslie et al. 1999, Ivanov and Aston-Jones 2000), rapid eye movement sleep suppression (Mieda, Tsujino et al. 2013). Thus, in terms of arousal, inhibition of the LC prevents orexin-mediated sleep-wake transitions, while co-activation enhances them (Carter, de Lecea et al. 2013). It is therefore reasonable to speculate that an indirect action through the LC may be a key mechanism by which OxA modulates trigeminal nociception, linking this hypothalamic-LC homeostatic network to the regulation of migraine-related pain. This hypothesis proposes that hypothalamic and brainstem nuclei, including the LC, that regulate physiological homeostatic responses to external and internal triggers can permit increased nociceptive traffic in the trigeminovascular system, a key mechanism in the onset of migraine-related pain. This modulation can occur at several levels including the spinal cord (trigeminocervical complex) and thalamus, ultimately increasing the trigeminal sensory information that is transmitted to the cortex. These cortical areas also receive robust innervation from these hypothalamic and brainstem structures, including the orexinergic circuits that act to increase arousal (Bayer, Serafin et al. 2004, Concetti and Burdakov 2021) and noradrenergic projections from the LC that regulate cerebral blood flow (Goadsby and Duckworth 1989) and attention (Vazey, Moorman et al. 2018), with the potential to link altered arousal (marked fatigue) and cognitive difficulties observed prior to and during migraine to altered migraine-related pain.

6. Chapter 6: *In vivo* Noradrenergic modulation through a novel CAV2 vector

6.1. Introduction

We have identified the brainstem LC as a key output partner for the LH orexinergic neurons and their modulation of trigeminal nociception as well as arousal and wakefulness. Similar to the orexinergic neurons; the LC shows clear alterations in diurnal activity (Jacobs 1986), with the greatest activation during arousal and the least during sleep. This is of key relevance to migraine given its intrinsic links to sleep-wake regulation; with sleep deprivation being a key trigger to migraine and sleep itself being a common abortive measure for the headache. This makes the LC a potential downstream nucleus through which orexinergic signaling could lead to the presence of premonitory symptoms and migraine initiation. Further, the LC is known to modulate DNIC responses at the level of the spinal cord; which interestingly; also appear to be disrupted in both: tension-type headache (Pielsticker, Haag et al., 2005) (Buchgreitz, Egsgaard et al., 2008) (Cathcart, Winefield et al., 2010), and migraine (Sandrini, Rossi et al., 2006) (Nahman-Averbuch et al., 2013) (clinically measured as CPM responses).

Orexinergic projections activate the brainstem LC (Hagan, Leslie et al. 1999), with key roles in arousal, and in chapter 5, we further identified that OxA, acting via the OX_1R within the LC preferentially inhibits trigeminal nociceptive processing. Further, previous work from our group has demonstrated that α-2-adrenoreceptor activation of the LC inhibits trigeminal nociceptive processes. Interestingly, the same study also observed an inhibition of these nociceptive processes after ablation of LC noradrenergic cell bodies (Vila-Pueyo, Strother et al. 2018). As such, both LC disruption and activation appear to inhibit trigeminal nociception, suggesting a complex interplay between the LC and migraine-related pain. This is likely due to the heterogeneous nature of the LC (Poe, Foote et al. 2020), whereby total ablation using a noradrenergic-specific toxin DSP-4 ablates the majority of LC noradrenergic neurons impacting both ascending and descending circuits. In agreement with this scenario, it was shown that while descending spinal projections produced antinociception, at the level of the cortex there was an increased excitability that manifest as a decreased threshold for cortical spreading depression, the electrophysiological correlate of migraine aura (Charles and Brennan 2009, Charles and

Baca 2013). In comparison, our microinjection study, likely lacked the widespread effects of DSP-4, instead exciting restricted regions of noradrenergic neurons.

Based on this; we sought to explore if an *in vivo* chemogenetic and NA-specific modulation of the LC would directly impact trigeminal nociception and if orexins could be acting via this pathway. We thus applied a novel PRS-viral promoter to selectively target noradrenergic neurons in the LC. This PRS promoter is coupled to a Canine Associated Virus (CAV2), which is characterized by its high transduction and retrograde properties (Li, Hickey et al. 2016). The primary advantage of this approach being that it allows noradrenergic control in conscious freely behaving rodents. Given the desire to explore migraine-related premonitory symptoms, the transition to circuit level manipulation in freely behaving rodents represents a key step in achieving this. Following confirmation of the successful transfection and activation of LC noradrenergic neurons via this novel CAV2 approach, we next sough to determine its impact on trigeminal nociception. This was conducted initially *in vivo* using the same electrophysiological procedure used in chapter 5 and finally via a small pilot study that assessed periorbital mechanical withdrawal thresholds in rats and their alteration by LC noradrenergic chemogenetic activation.

6.2. METHODS

6.2.1. Animals

Both male and female Sprague Dawley wild-type rats (4-weeks old, Charles River, UK), were used in this study. All animals were housed in groups of three to four in 21°C and humidity controlled rooms with a normal 12-hour light/dark cycle and had free access to food and water.

6.2.2. Stereotaxic surgery

To confirm the transfection and successful activation of LC noradrenergic neurons four-week old rats were injected unilaterally into the LC with one of the following combinations:

1. Cholera-Toxin B (stock undiluted CTB-Alexa Fluor 488 (Thermo Fisher, #C34775), n = 4).

2. CAV-PRS-Cre-V5 (1:10 dilution from stock, supplied by Prof. Pickering, University of Bristol combined with the pAAV-hSyn-DIO-hM3D(G_q)-mCherry (#44361, Addgene), n = 4)

3. CAV-PRS-hM3Dq-mCherry (1:10 and 1:20 dilution from stock, supplied by Prof. Pickering, University of Bristol, n = 10)

In order to study the effect of noradrenergic activation in the LC and after confirming successful chemogenetic approaches, 4 week old rats were injected bilaterally with either:

1. Single-viral approach CAV vector: CAV2-PRS-hM3D(G_q)-mCherry, n = 11).

2. Control CAV (CAV-CMV-mCherry), n =11.

In both cases a burr hole was carefully drilled above the coordinates of the unilateral or bilateral LC coordinates (AP: 2.30mm, ML: -1.30mm, DV: -6.00, -5.50, -5.00 and -4.50mm) and the dura mater carefully removed to prevent damage. A glass capillary

needle was lowered into the LC. Following injection of 250 nL per depth per site at a rate of 2 nL/sec, the capillary was left to rest for 7 minutes and then removed at intervals of 0.50 mm/minute to prevent back propagation of the virus along the capillary track. Rats were injected i.p. with saline (NaCl 0.9%) (1 mg/kg) to facilitate their recovery post-surgery and closely monitored. Allowing three to four weeks for full viral transfection the rats were then used for one of the following purposes:

1. Rats were treated with CNO (Intraperitonially, acute single dose (3mg/kg)) and subsequently perfused and the tissue was then cut and processed for immunohistochemical analysis to confirm successful transfection and activation. CNO (# C0832, Merck) was initially diluted at 5mg/ml and aliquoted at -20º until the experimental day which was defrosted and further diluted to the corresponding concentration with Saline (NaCl 0.9%)
2. Rats were used for electrophysiological recordings from the LC (**Figure 6.1.**) to confirm CAV-mediated activation.
3. Rats were used for electrophysiological recording in the trigeminocervical complex (**Figure 6.2.**) to assess durovascular-evoked responses to CAV2-mediated LC activation.
4. Rats were used to assess alterations in periorbital mechanical withdrawal thresholds (**Figure 6.3.**) in response to CAV2-mediated LC activation.

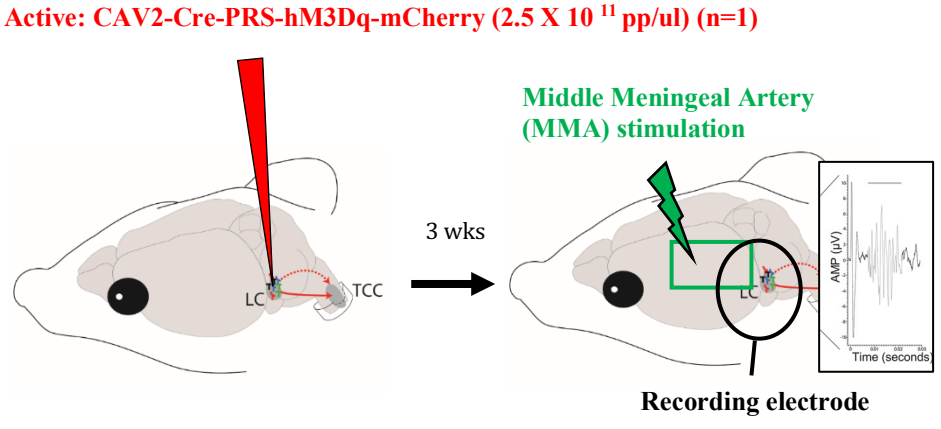

Figure 6.1. Optimisation of a novel CAV2 approach to target locus coeruleus (LC) neurons. Rats were stereotaxically injected with the vector: CAV2-Cre-PRS-hM3Dq-mCherry (2.5 X 10 ^{11} pp/ul) into the LC and allowed to recover for up to three weeks to ensure a full viral transduction. After that, LC *in vivo* electrophysiological recordings were measured as a response to the hM3Dq-specific compound: CNO.

Tissues were processed in agreement with the methods detailed in general methods, section 2.3.5, page 83-84 and electrophysiological recording was in agreement with the methods detailed in chapter 5 (**Figure 6.2.**), with the exception that instead of direct microinjection into the LC, LC noradrenergic neurons were activated via the appropriate CAV2-mediated approach and in agreement with the following criteria:

1. Three stable dural-evoked responses for V1 specific trigeminal neurons. Three baseline measures were taken with 5 minutes in between, prior to administering any CNO.
2. A recorded time window of a minimum of 165 minutes post-CNO administration.

3. A successful transduction of the virus in the LC, as observed through mCherry expression, for both control and active cohorts (post-hoc tissue analysis.

4. For the active cohort, those animals who demonstrated successful activation of the LC NA neurons (c-Fos).

5. An absence of any injection and/or vector-related toxicity and/or cell death in the LC.

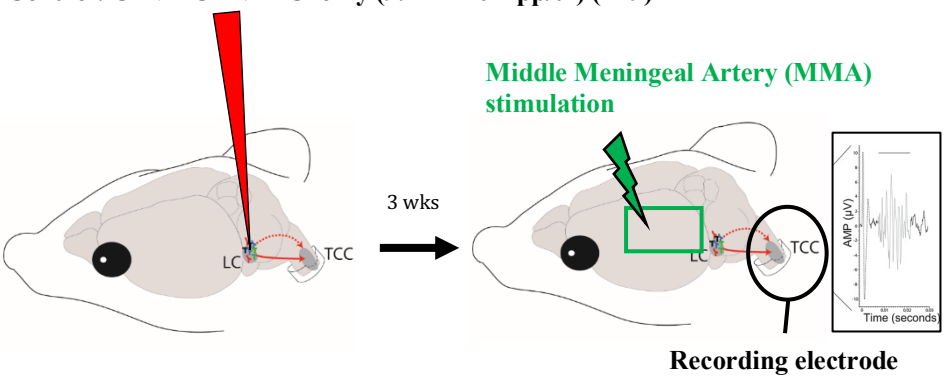

Figure 6.2. Electrophysiological determination of noradrenergic regulation of trigeminal nociception using chemogenetics. In order to understand the NA modulatory role of the locus coeruleus (LC) over the trigeminocervical complex (TCC): rats were stereotaxically injected with either the active the vector: CAV2-Cre-PRS-hM3Dq-mCherry or the control: CAV2-CMV-mCherry into the LC and allowed to recover for up to three weeks to ensure a full viral transduction. After that, TCC *in vivo* electrophysiological recordings were taken before and after administering CNO (3mg/kg) i.p.

6.2.3. Periorbital mechanical withdrawal thresholds

For this study, 4-week-old rats (n = 14 total) underwent targeted unilateral stereotaxic administration of either the single-viral approach CAV vector: CAV2-PRS-hM3D(G_q)-mCherry) (n = 7) or a control CAV (CAV-CMV-mCherry) into the LC (n = 7; **Figure 6.3.**). Rats were allowed to recover for two to three weeks to allow for successful viral transduction and the corresponding behavioural test for periorbital mechanical sensitivity was then performed. For that, on day 1: rats were habituated to the von Frey apparatus by leaving them undisrupted for one hour. On day 2: they were left for another hour to habituate to the rack and boxes, and a first baseline recording was performed. Allowing two days in between to avoid any induced periorbital sensitivity, on day 5: their baseline periorbital mechanical sensitivity was tested again in the morning (9 a.m.). Both groups were then administered CNO i.p. (3 mg/kg) and the von Frey measurements repeated 90 minutes post-CNO (in accordance to the electrophysiological data showing the highest significant decrease at this time-point). In order to ensure successful transfection and activation the tissue was collected immediately after the final behavioural test.

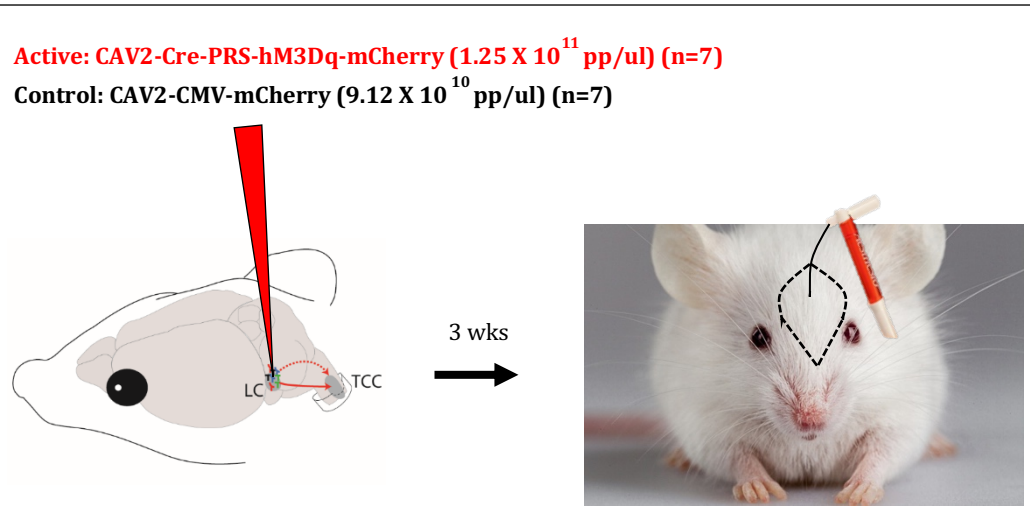

Figure 6.3. Behavioural determination of noradrenergic regulation of trigeminal nociception using chemogenetics. Having established an locus coruleus (LC) noradrenergic -mediated inhibition of durovascular-evoked responses in the trigeminocerical complex (TCC): we now wanted to understand if this is also translated into the migraine-associated phenotype of periorbital allodynia. For this, rats were stereotaxically injected with either the active the vector: CAV2-Cre-PRS-hM3Dq-mCherry or the control: CAV2-CMV-mCherry into the LC and allowed to recover for up to three weeks to ensure a full viral transduction. After that, baseline von frey measurements of their periorbital mechanical sensitivity were taken to then be re-tested 2 hours post-CNO administration.

6.3. RESULTS

6.3.1. Locus Coeruleus (LC) coordinate optimisation

Having optimised the preliminary coordinates for the LC through stereotaxic injections with Chicago Sky blue; these were fully established by injection of a Cholera Toxin B (CTB) (n = 3) (Thermo Fisher, #C34775) vector to account for any further viral spread. CTB is a probe with retrograde properties often used for tracing purposes in neural tissue, and its conjugated with Alexa 488, which allows for fluorescent labelling in the injected region. Allowing three to four days for fluorophore labelling, animals were perfused with 300 ml of 0.01M of heparinised (1:10) PBS, followed by 300 ml of 4% PFA in 0.01 M PBS then cryoprotected in 30% sucrose solution. Brain sections were then cut at 40 μm thickness and stained for DAPI. mounted, air dried and cover slipped before being imaged through an Axioplan fluorescence microscope. With this, we stablished the coordinates for a four-week old rat: caudal from Lamda:- 2.30 mm, ML: ± 1.30 mm, DV: 6.00mm (**Figure 6.4.).**

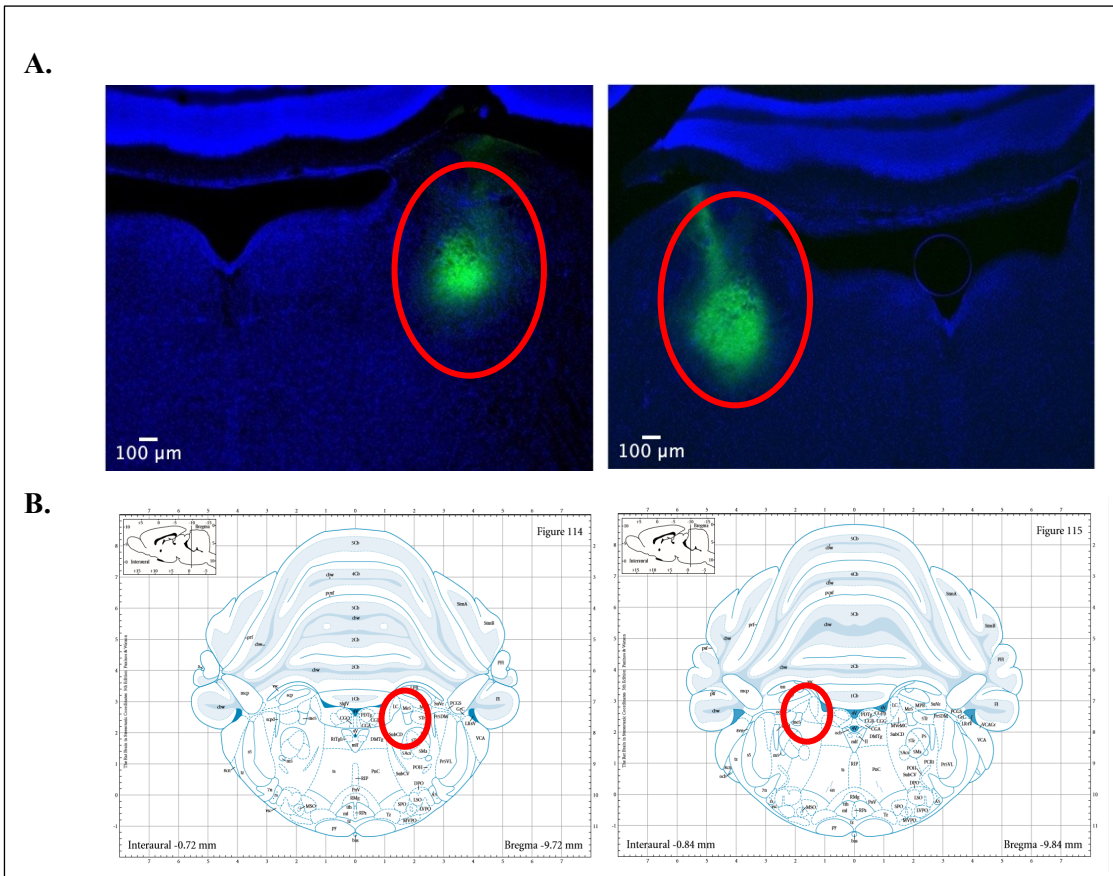

Figure 6.4. Locus coeruleus (LC) coordinates were initially established by stereotaxic injection of a fluorescent-tagged Cholera Toxin B (CTB) vector. Rats were injected with CTB and allowed to recover for three to four days. The tissue was then collected and perfused to localise the region of injection. A. Representative images of the LC coordinates with CTB (in green) and DAPI-stained nuclei. B. Representative images taken from the Patxinos rat brain atlas correponding to the A. CTB-tagged image above them (coresponding LC region marked as red circles). From left to right: anterior to posterior coronal sections, including Bregma -9.72 and -9.84mm (Paxinos and Watson 1986).

Coordinates were then adapted by injecting at fourth depths to account for the spread of the CAV2 vector and ensure a coverage of the entire LC in four-week old rats (n = 3). Given the previously published work using the dual viral approach: CAV-Cre-PRS-V5, initial optimization was performed with only this vector. A cocktail of: CAV-Cre-PRS-V5 with pAAV-hSyn-DIO-hM3D(G_q)-mCherry (#44361, Addgene) was injected at: AP: 2.30mm, ML: -1.30mm, DV: -6.00 (200 nL), -5.50 (200 nL), -5.00 (200 nL), -4.50 (200 nL). Allowing two-three weeks for viral transduction, animals were injected i.p. with CNO (# C0832, Merck), and two hours later perfused to collect the tissue. Samples were stained for tyrosine hydroxylase (TH) and mCherry, or c-Fos and mCherry, to characterise the viral spread, level of specificity and degree of activation. The results showed a successful spread of the virus throughout the LC nucleus (**Figure 6.5**.), as well

as high specificity for TH^+ neurons and successful c-Fos activation (tissue was collected 2hrs post-CNO administration to allow c-Fos expression and posterior analysis) (**Figure 6.6.**). For initial optimization, the LC was injected unilaterally with the corresponding CAV vector, allowing us to use the non-injected contralateral LC as an internal control for each animal, representative of a lack of viral transduction and thus c-Fos activation. These qualitative observations are in agreement with previous work from Prof. Pickering, and were used as a basis to optimize the novel single viral approach: CAV-PRS-Cre-hM3Dq-mCherry.

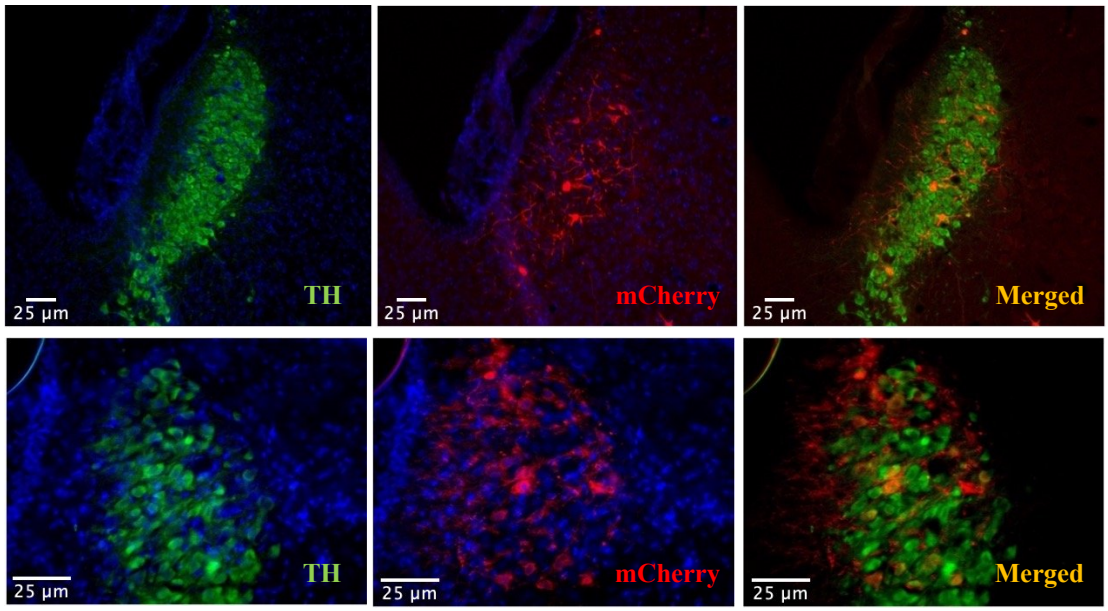

Figure 6.5. Representative images of the spread and TH-specificity of the CAV-Cre-PRS-V5 with pAAV-hSyn-DIO-hM3D(G_q)-mCherry into the locus coeruleus. The superior row of images (10X) shows the correspondent images of tyrosine hydroxylase (TH)-staining (left), and mCherry staining (with anti-mCherry antibody) from the vector (centre); with the co-localisation of both (right image). The same is observed in the inferior row of images but at 20X magnification.

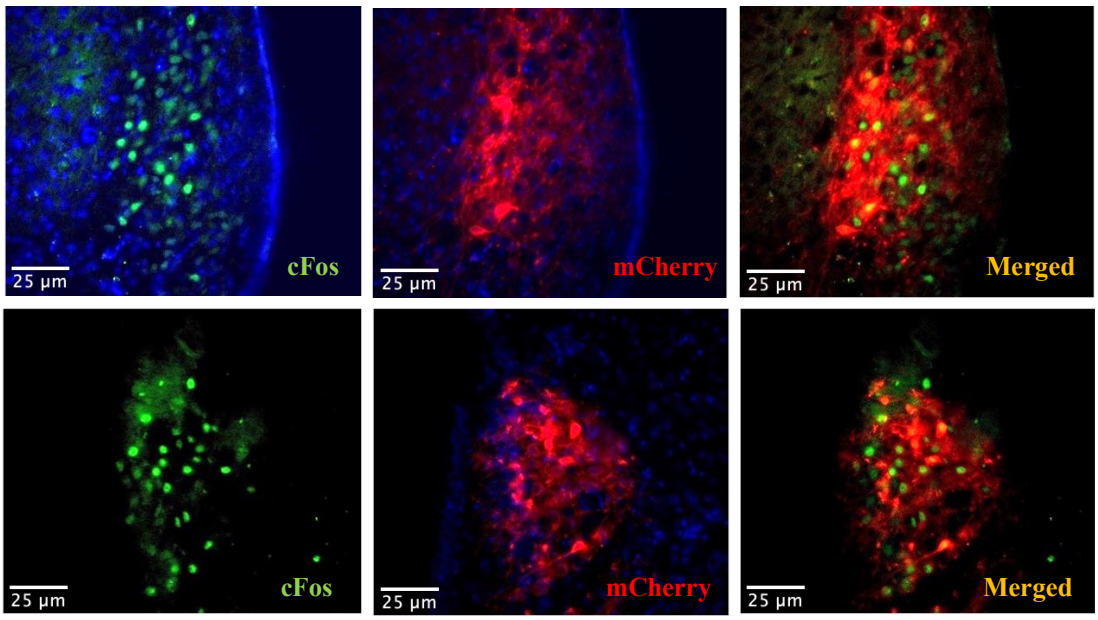

Figure 6.6. Representative images of the spread and TH-specificity of the CAV-Cre-PRS-V5 with pAAV-hSyn-DIO-hM3D(G_q)-mCherry (endogenous mCherry) into the locus coeruleus. The superior row of images shows the correspondent 20X images of cFos +ve (left), and mCherry +ve from the vector (centre); with the co-localisation of both (right image). The same is observed in the inferior row of images.

6.3.2. Viral titre optimisation and PRS-TH specificity: single viral approach

Recent work has emphasised the need to rigorously optimise the titre used with CAV2 vectors due to the reported presence of toxicity in rat neural tissue at high concentrations (Stevens, Larsen et al. 2021). As described in the methods; rats were stereotaxically injected into the LC with the novel single viral approach: CAV-PRS-Cre-hM3Dq-mCherry (original concentration: 2.5 x 1012 pp/ml) (n = 3) at 2X dilution (diluted in NaCl 0.9%) into the previously established coordinates (Section 6.3.1.) and allowed to recover for two-three weeks to ensure full viral transduction. The tissue was then collected and perfused accordingly to be cut and stained for TH, mCherry and DAPI. Qualitative analysis of these sections showed robust signs of toxicity in the ipsilateral LC, compared to the contralateral side. There was a loss of cells in the injected region as observed through a loss of DAPI-stained nuclei (white circle, **Figure 6.7.**), together with a reduced LC size, and signs of microglial inflammation as shown through the clusters of DAPI-stained nuclei alongside the few transduced cell bodies (white dashed line, **Figure 6.7.**).

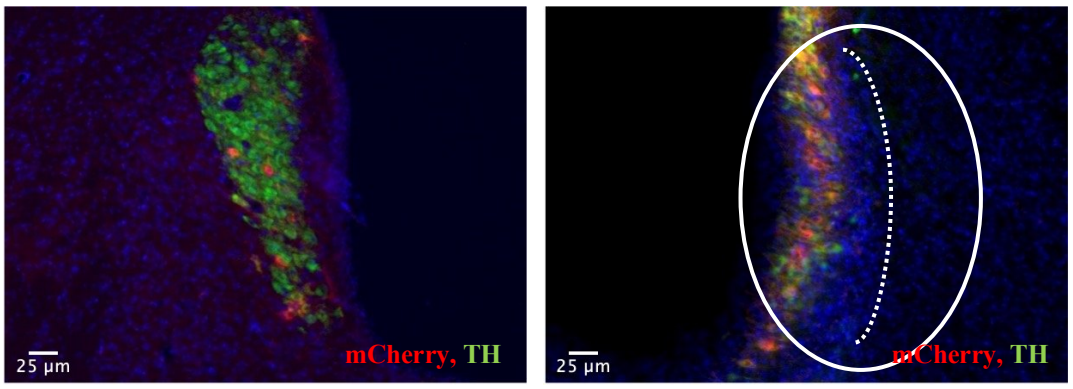

Figure 6.7. Representative images (10X) of the contralateral locus coeruleus (LC) (A.) to the ipsilateral LC (B.) which was stereotaxically injected with: the CAV-PRS-Cre-hM3Dq-mCherry (2X). Viral transduction shown in red (mCherry), tyrosine hydroxylase $(TH)^+$ neurons in green (AF488), and Merged cells in orange A. Contralateral LC side from the injection shows no signs of cell death or inflammation, with a clear presence of TH^+ neurons (green), as well as bilateral transduction of the virus due to its retrograde properties. B. Ipsilateral LC shows clear signs of inflammation with a cluster of DAPI-stained nuclei (dotted white line), as well as cell loss in the injection site (circular white label); identified as both a loss of TH^+ and DAPI-stained cell bodies, alongside the few surviving TH and $mCherry^+$ (Merged: orange) cell bodies.

The following concentrations of vector were tested: 2.25 X 10^{11} pp/ul (10X dilution) (**Figure 6.8. (A)**) (n = 4) and 1.25 X 10^{11} pp/ul (20X dilution) (n = 4). Each vector was injected unilaterally in the LC at the four established depths, with 200 nl volume per depth. Allowing two-three weeks for full viral transduction, the tissue was collected and processed accordingly to visualize mCherry transduction as well as TH. Qualitative analysis showed no signs of toxicity in any of the two titters, with the same degree of TH-specificity and transduction efficacy. To ensure the lowest risk of developing toxic effects, we decided to progress with the remaining studies with the second concentration: 1.25 X 10^{11} pp/µl. Quantitative analysis showed this to have around 91% of TH-specificity (number of TH^+ cell bodies over the total number of transduced mCherry cells) (**Figure 6.8. (B and C)**), and an 86% effectivity of activation of those transduced cell bodies (number of active cell bodies over total transduced) (n = 12 slices from n = 4 animals) (**Figure 6.8. (D)**).

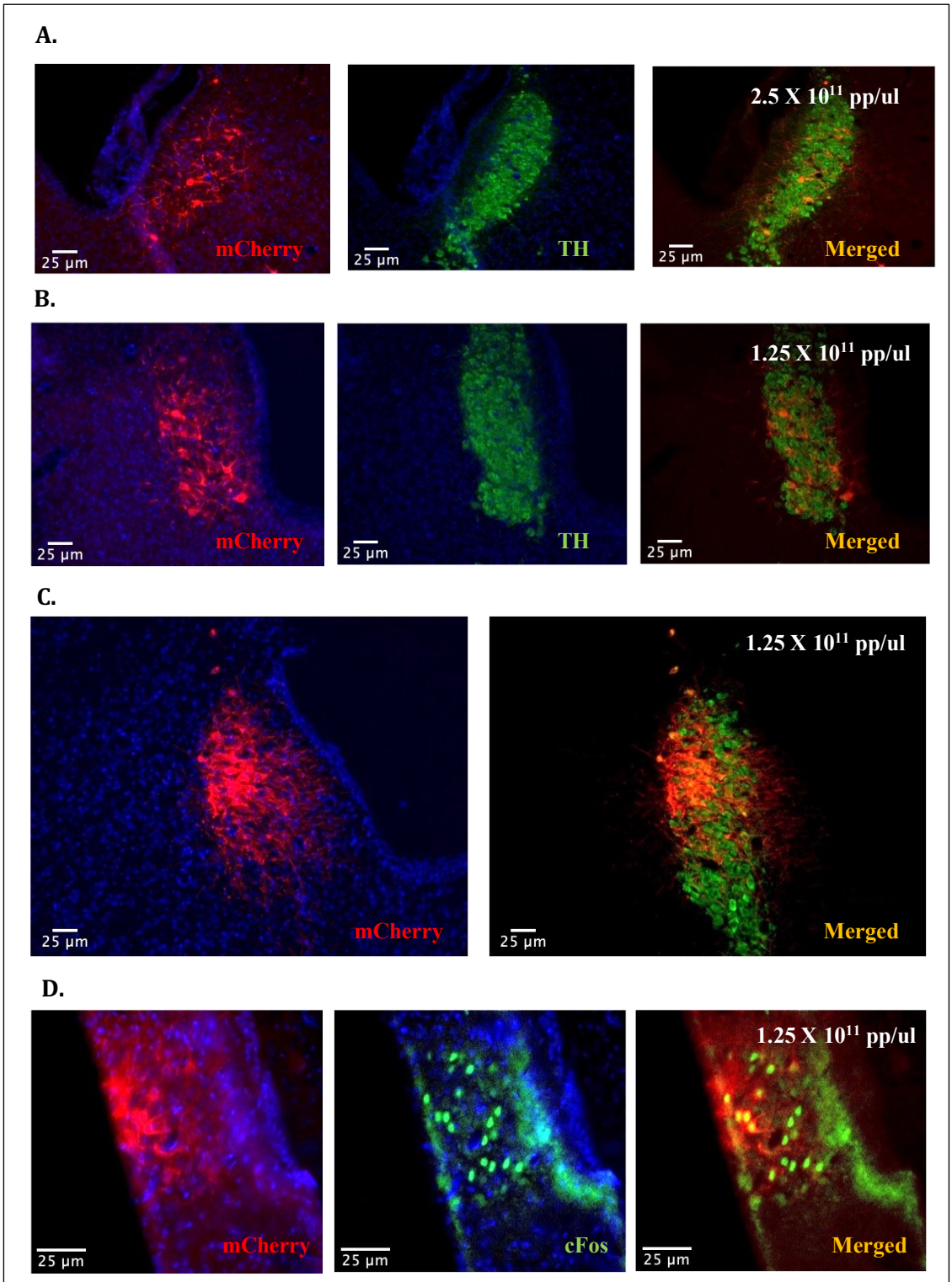

Figure 6.8. A. Representative images (10X magnification) of locus coeruleus (LC) transduction with the single CAV2 approach at 2.5X 10^{11} pp/ul (10X dilution): the transduced CAV2 is shown in red (mCherry) and tyrosine hydroxylase $(TH)^+$ cell bodies in green (AF 488). Merged mCherry and TH somas are shown orange. **B and C**: Representative images of LC transduction with the single CAV2 approach at 1.25 X 10^{11} pp/ul (20X dilution) (10X magnification): the transduced CAV2 is shown in red (mCherry) and TH^+ cell bodies in green (AF 488). Merged mCherry and TH somas are shown orange**. D**. Representative images of LC transduction and activation with the CAV2 approach at 1.25 X 10^{11} pp/ul (20X dilution): the transduced CAV2 is shown in red (mCherry) and c-Fos^+ cell bodies in green (AF 488). Merged mCherry and c-Fos somas are shown orange.

6.3.3. Locus Coeruleus *in vivo* activation post-CNO- LC electrophysiological recordings

As described in Chapter 2: Methods, for this procedure, animals were kept under general anaesthesia throughout, and the CO_2 levels and body temperature were continuously monitored. Both artery and vein cannulations were performed to monitor blood pressure and administer the anaesthetic. Orientation of the skull was set so that Bregma and Lambda were aligned, with no difference larger than 0.01 degrees. The skull was then drilled and dura carefully peeled off to insert the tungsten electrode (2 mΩ) into the LC, with coordinates: caudal from Lambda: - 2.20 mm, Medio-Lateral: 1.25mm, Dorso-Ventral: -5.60 mm (from the brain surface).

Noradrenergic neurons in the LC were identified as those responding immediately after the pinching (lasting 1 second) of the hindpaw. TH neurons were identified through their typical biphasic response: with an initial peak and followed inhibition. Filtering parameters: 300 - 6000 Hz bandpass filter. Once the LC nucleus was identified, five contralateral hind paw pinches (with 30 seconds in between) were performed as a baseline measure (**Figure 6.9.**). And after 10 minutes of rest, five ipsilateral hind paw pinches (also allowing 30 seconds between each) were measured. CNO (# C0832, Merck) was then administered intravenously (1 mg/kg). No statistical analysis was applied here as this was only a preliminary recording.

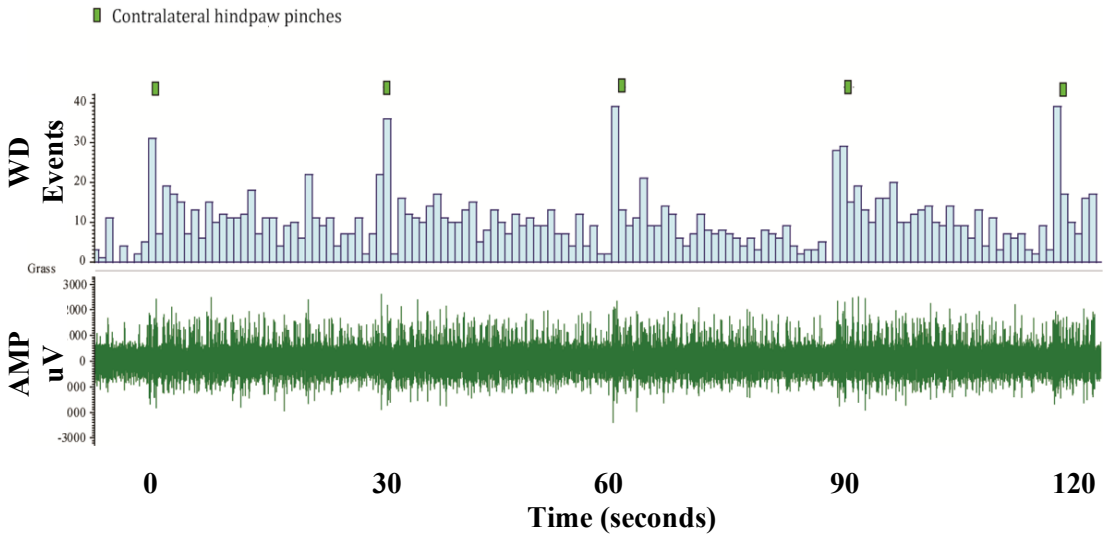

Figure 6.9. Example of an electrophysiological recording on Spike, labelled with five marks representing each of the contralateral hindpaw pinches. X-axis represents the time (in seconds), with the marked contralateral hind-paw pinches occurring every thirty seconds. The waveform channel (WD) clearly shows the characteristic TH-specific response of a group of cells by which there is a biphasic response: with an initial peak after the pinching of the contralateral hindpaw, followed by a sudden inhibition. The bottom channel (AMP) represents the continuous spike activity.

Changes in spontaneous activity were measured for 90 minutes post-CNO administration. There was an increase in spontaneous activity (Hz) as early as 12 minutes post-CNO, which continued to increase and remain sustained for the remaining 90 minutes. The firing rate of spikes (Hz) was continuously plotted on the Y-axis against time on the X-axis in the WD (Window Discriminator: total number of units responding above a set threshold of: 20.3) channel, and the average firing frequency of cell clusters was then measured by manually setting time cursors are different time points within the window discriminator (WD). The spontaneous activity at 2 min post-CNO was: 4Hz, and then increased to: 32Hz at 12 min post-CNO, to 60; 22 min post-CNO and 80; 32 min post-CNO (**Figure 6.10.**). Hind paw pinches were performed every 10 minutes however the increase in spontaneous activity became too high to identify hind paw-associated biphasic responses. Tissue was then collected 1h and 35 minutes' post CNO to check for viral transduction and c-Fos expression (**Figure 6.11.**).

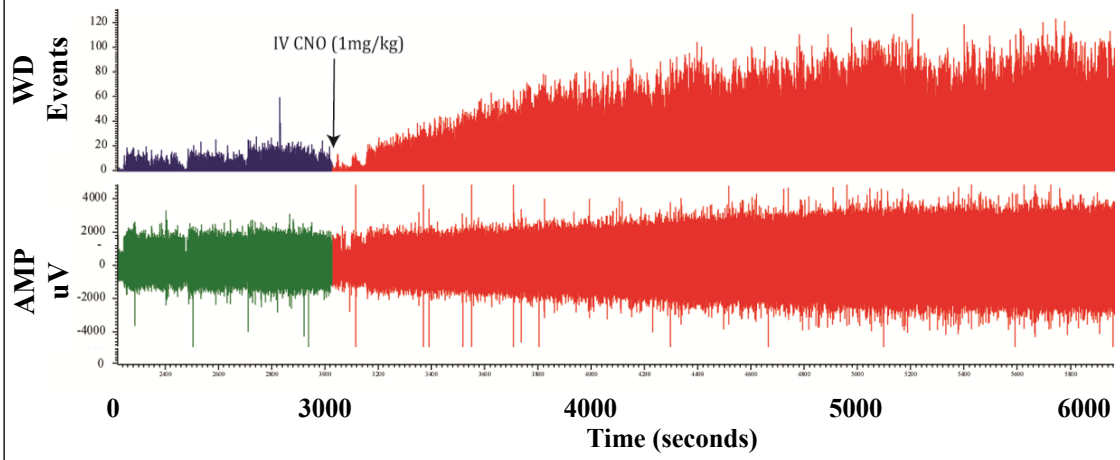

Figure 6.10. Example of the electrophysiological recording throughout a period of 60 minutes. Having identified tyrosine hydroxylase-responding cells within the locus coeruleus, CNO was given intravenously (1 mg/kg) and there was a rapid increase in spontaneous cell firing (Hz), which increased from 4 to 80 Hz throughout this period. Window Discriminator (WD)

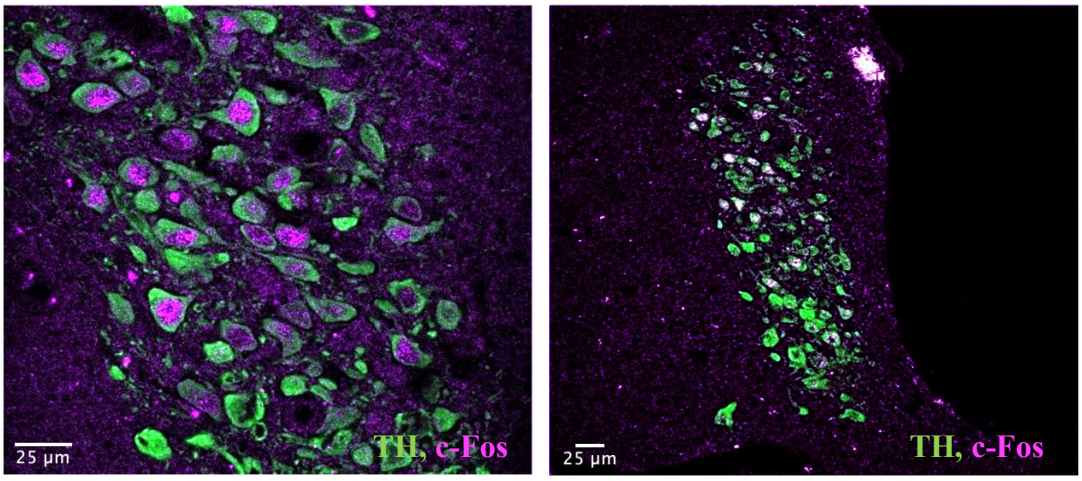

Figure 6.11. Example of c-Fos expression in the locus coeruleus of this CAV-transduced animal (n=1) following CNO administration at 20X (left) and 10X (right) magnification. Tissue was perfused and collected once the LC *in vivo* electrophysiological recordings were finalised. TH, tyrosine hydroxylase. Images taken with a A1R Confocal microscope.

6.3.4. Electrophysiological determination of noradrenergic regulation of trigeminal nociception using chemogenetics

6.3.4.1. Confirmation of noradrenergic specific activation

Once the electrophysiological recordings were completed, animals were perfused and the tissue processed as detailed. A total of 5 - 6 sections of the LC were stained for c-Fos and mCherry, and only those with successful transduction and activation (for the CAV-Active group), were included in the analysis. A total of n = 18 animals were initially injected with the active CAV2, from which n = 3 were excluded due to no transduction, n = 1 due to having transduction but no c-Fos activation, and n = 3 were not recorded due to complications during surgery or lack of cells found. A total of n =13 animals were injected with CAV-Inactive, but n = 1 was excluded due to no transduction in the LC, and n = 3 due to no cells found or surgery complications. With this, n = 11 animals from the CAV-Active group and n = 9 from the CAV-Inactive groups were analysed. Representative images of the approach taken are shown in **Figure 6.12. and 6.13.**

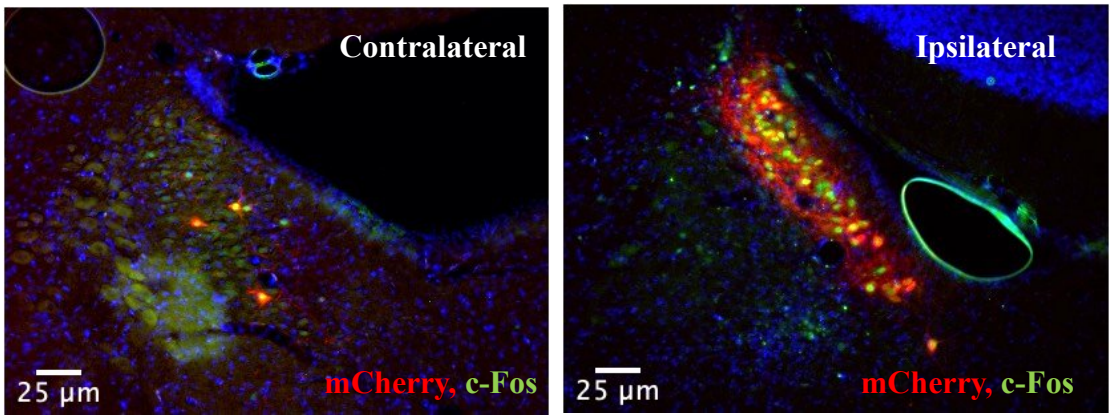

Figure 6.12. Representative images showing CAV2-transduced cell bodies in the locus coeruleus (mCherry), stained for c-Fos (green) and DAPI for nuclei (blue). Interestingly, there is a clear transduction and activation in the ipsilateral side (right image), but also in the contralateral side (left image).

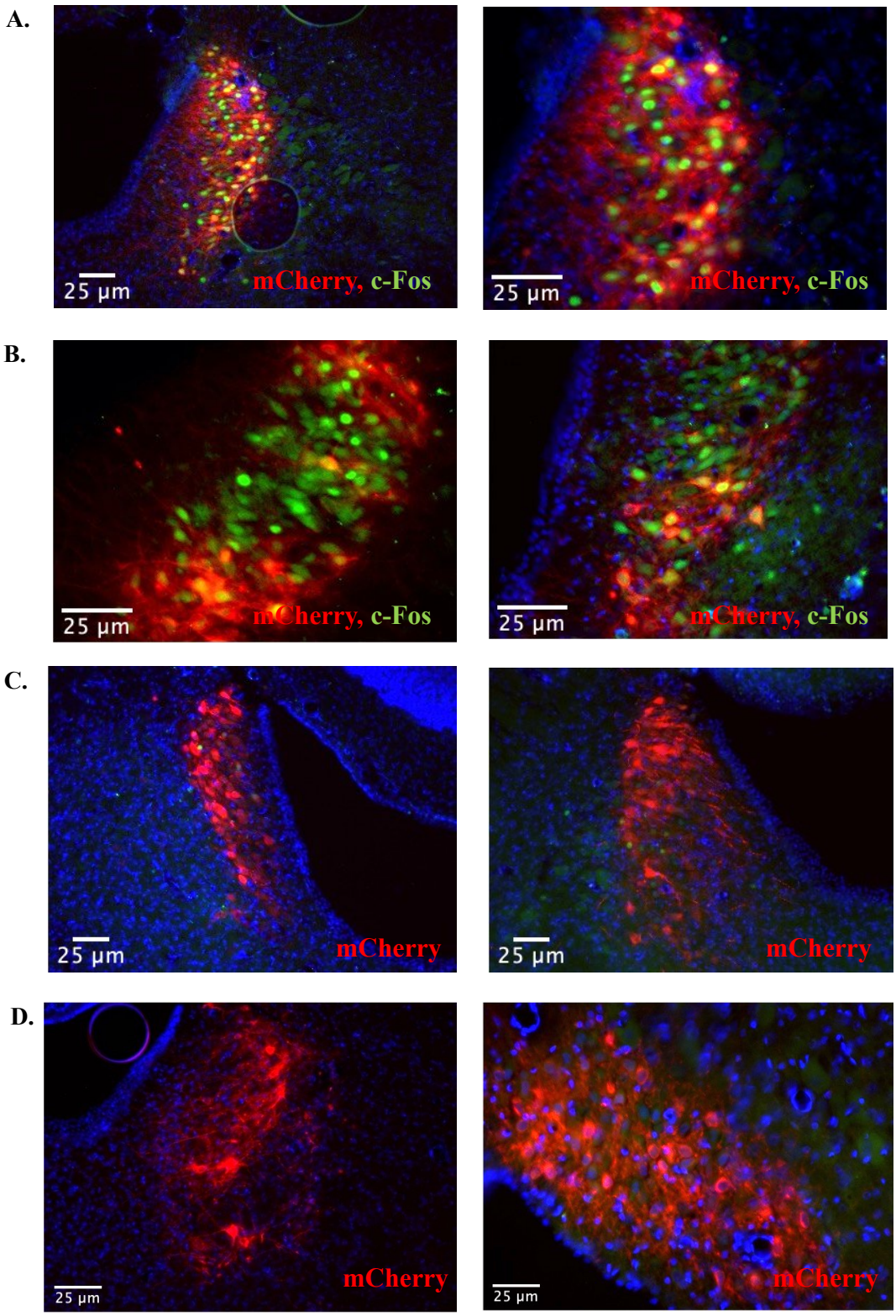

Figure 6.13. Once *in vivo* electrophysiolglical recordings finalised; every animal was perfused and the tissue was collected and fixed to then be cut at 40 µm and stained accordingly. A. **Representative images of cre-active injected rats, with co-localisation of mCherry (CAV2 vector, in red) and c-Fos as a marker of neural activation (in green), and cell nuclei as DAPI (in blue).** B. Examples of cre-inactive injected rats, with co-localisation of mCherry (CAV2 control, in red) and c-Fos (in green) and DAPI (in blue) in comparison.

6.3.4.2. Noradrenergic-mediated spontaneous activity in the TCC

Having established the optimal volume and titre of the novel NA-specific CAV, we examined the role of this pathway in modulating trigeminal nociception at the level of the trigeminocervical complex. Allowing 3-4 weeks for full viral transduction, both groups: inactive (injected with the control inactive vector: CAV2-CMV-mCherry) and active (injected with the experimental active vector: CAV2-PRS-hM3Dq-mCherry) groups underwent surgery to measure noradrenergic-specific electrophysiological responses. On the experimental day, once V1-specific and MMA-evoked cells were identified, three baseline responses were acquired to ensure these were stable, and their average was used as the pre-CNO measure. CNO was then given i.p. (3 mg/kg) and cells were followed for 210 minutes. Baseline spontaneous activity was measured as the average cell firing within 10 seconds prior to each MMA stimulation.

There was a significant 53% reduction in spontaneous activity within the active group over time, ($F_{(3.11,\ 30.65)} = 3.452$, $F_{(DFn,\ DFd)}$, $p = 0.027$), specifically at 210 minutes post-CNO (4.425 ± 1.023), $q_{(9)} = 3.694$, ($p = 0.034$) **Figure. 6.14.A**), suggesting a nociceptive-specific action of noradrenergic modulation over the TCC. Whereas, the control group had no significant changes in spontaneous activity over time: pre- and post-CNO ($F_{(2.02,\ 15.88)} = 0.341$, $p= 0.718$). Comparison of spontaneous activity at different time points within each group was analysed through a one-way ANOVA (mixed-effects analysis) **(Figure. 6.14.B**).

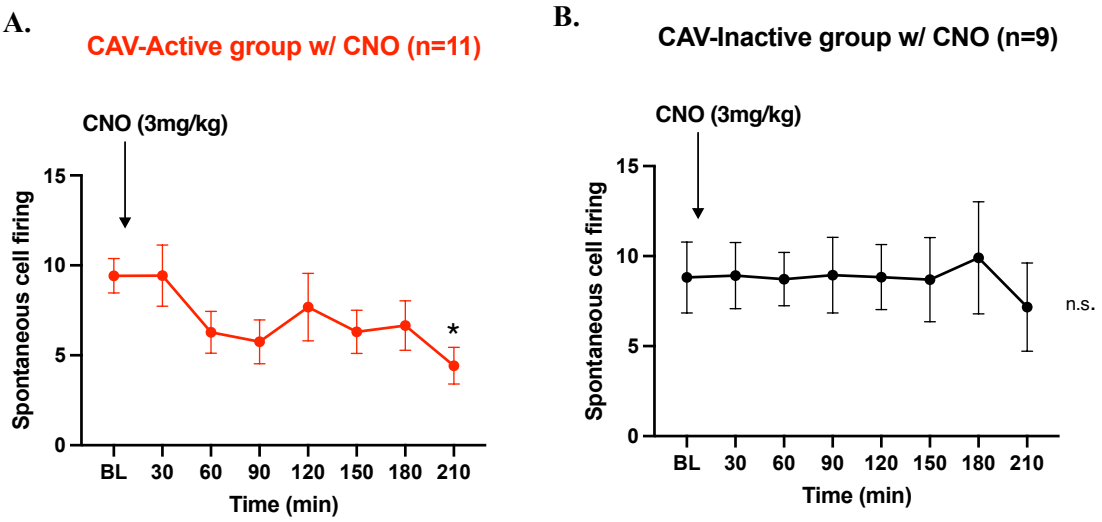

Figure 6.14. Changes in spontaneous activity (Hz) in the TCC pre and post-CNO in the active and inactive groups. A. *In vivo* noradrenergic activation resulted in a significant decrease in spontaneous activity between baseline (BL) (pre-CNO) and post-CNO (from 30 to 210 min; p = 0.039), specificially at time point 210 minutes. **B.** In comparison, the CAV-inactive control group showed no significant changes in spontaneous background activity from baseline to 210 minutes post-CNO (p = 0.718). Y-axis represents sponatenous cell firing which is the average amount/number of spikes (cell cluster) in a predefined time window (10 seconds), and X-axis the time (in minutes) *p ≤ 0.05, n.s. non-significant.

6.3.4.3. Noradrenergic-mediated durovascular nociceptive-evoked responses in the trigeminocervical complex

Changes in durovascular-evoked (MMA stimulation) responses were measured in the trigeminocervical complex: pre-CNO (baseline: average of three PSTHs), and post-CNO at different time points: from 30 to 210 minutes. There was a significant decrease in durovascular-evoked responses post-CNO ($F_{(2.15,\ 21.17)}$ = 6.923, $F_{(DFn,\ DFd)}$, p = 0.004; **Figure 6.15.**). Specifically, this reduction was significant at: 60 (68.05 ± 9.903, $q_{(10)}$ = 3.063, p= 0.047), 90 (63.32 ± 9.609, $q_{(10)}$ = 3.385, p= 0.041), 150 (65.41 ± 9.609, $q_{(10)}$ = 3.301, p= 0.041) and 210 (61.50 ± 8.892, $q_{(9)}$ = 3.731, p= 0.032) minutes post-CNO administration. In comparison, there was no change in rats injected with the inactive CAV post-CNO ($F_{(1.56,\ 12.28)}$ = 2.959, p = 0.098). Comparison of dural-evoked responses at different time points within each group were analysed through a one-way ANOVA (mixed-effects analysis).

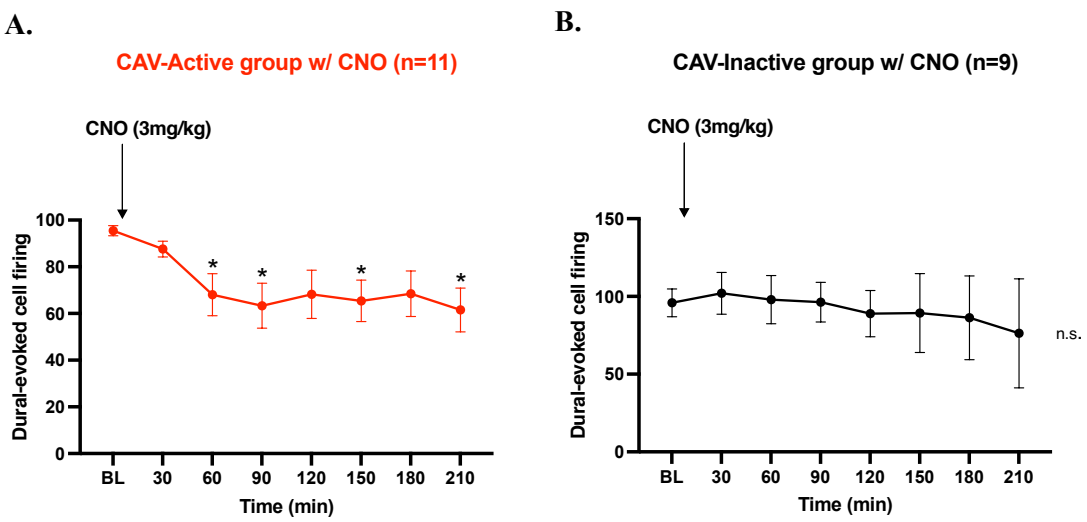

Figure 6.15. Changes in dural-evoked responses pre and post-CNO in the active and inactive groups. A. *In vivo* noradrenergic activation resulted in a significant decrease in durovascular-evoked responses between baseline (BL, pre-CNO) and post-CNO (from 30 to 210min; $p = 0.004$), specifically at time points: 60, 90, 150 and 210. **B.** In comparison, the CAV-inactive control group showed no significant changes in dural-evoked responses from BL to 210 minutes post-CNO ($p = 0.098$). *$p \leq 0.05$ compred to baseline. n.s. non-significant.

6.3.4.4. Brush and pinch-evoked responses in the trigeminocervical complex

Mechanical non-noxious (brush) and noxious (pinch) periorbital responses were measured every 30 minutes pre and post-CNO. Two brush and pinch responses were taken pre-CNO as baseline measures (BL). To account for any changes in spontaneous activity; the analysed data corresponds to the ratio of the brush or pinch-evoked response over the baseline spontaneous activity previous to that time point. Increases in the resulting ratio thus are representative of rather decreases of the raw data.

Despite an observed trend increase in the ratio of brush-evoked responses, there was no significant change within the active group over time ($F_{(2.6, 23.39)} = 2.389$, $F_{(DFn, DFd)}$, $p = 0.102$). There were additionally no significant changes within the control group over time ($F_{(1.69, 11.35)} = 1.691$, $p = 0.479$). The ratio of pinch-evoked responses within the active group also showed a trend towards an increase over time that was not significant ($F_{(3.48, 31.31)} = 2.034$, $p = 0.122$). There were no significant changes in pinch-evoked ratio within the control group over time ($F_{(1.3, 8.72)} = 1.110$, $p = 0.341$).

6.3.4.5. Significant reduction in periorbital mechanical withdrawal thresholds following CAV2-mediated noradrenergic activation in the LC

Having allowed two weeks for the rats to fully recover from surgery; baseline measures of periorbital mechanical sensitivity were taken on a day separate from the experimental day. On the day of the experiment, another baseline measure was taken at 9 a.m., prior to administering CNO. In accordance to the peak time point in which noradrenergic activation induced a significant decrease in dural-evoked responses after giving CNO; periorbital mechanical thresholds were measured again after 90 minutes. Given the observed variability in baseline measures in both groups, an average of the two baselines was used for the analysis. One animal in the CAV-Active was excluded from the study due to very high baseline periorbital mechanical thresholds, making the CAV-Active group n = 6 and CAV-Inactive n = 7.

Due to final COVID-related time constrains a preliminary run of immunohistochemical staining was performed over a selection of LC sections from each animal to allow a rapid assessment of transfection and activation. These were stained for c-Fos to confirm the successful activation of transduced cell bodies, as well as CAV-transduction. While the CAV-inactive animals remain to be processed, the CAV-Active group showed a degree of transduction in all animals (**Figure 6.16. (A)**). When exploring periorbital mechanical withdrawal thresholds, there was a significant interaction between time and group between pre and post-CNO in the active group ($F_{(1, 12)} = 12.11$, $F_{(DFn, DFd)}$, $p = 0.045$). Further post-hoc multiple comparisons (Sidak's) among groups also uncovered a significant difference between the CAV-inactive and CAV-active groups ($t_{(14)} = 2.677$, $p = 0.0262$).

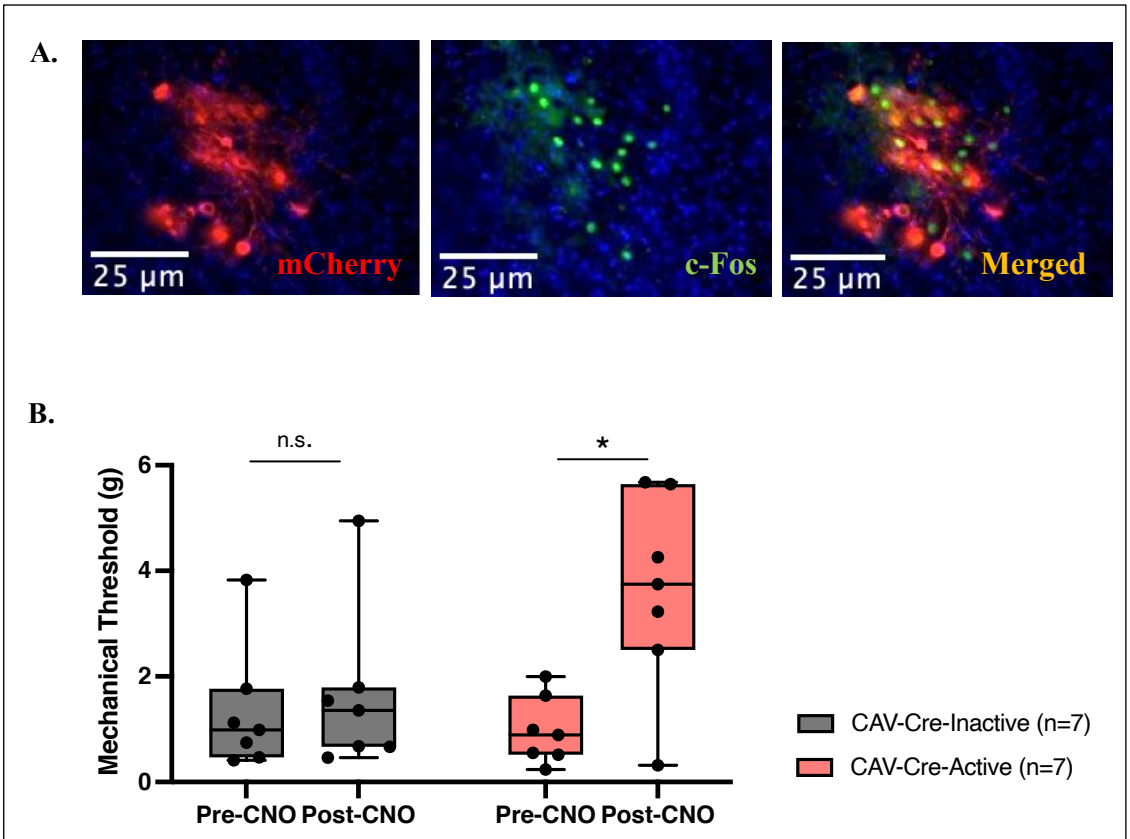

Figure 6.16. A. Representative images of a CAV-Active animal with locus coeruleus transduction of the CAV-PRS-Cre-hM3Dq-mCherry (mCherry) and c-Fos activation (green), with co-localisation indicative of a successful activation of TH-transduced cell bodies. **B.** Periorbital mechanical sensitivity was measured before and after CNO and compared among both groups: CAV-Inactive and CAV-Active. There was a significant effect of time and group ($p = 0.0045$) on periorbital mechanical withdrawal thresholds.

In this study, the use of a PRS-promoter enabled specific targeting of noradrenergic projections and permitted us to explore the function of the brainstem LC in the regulation of periorbital sensory thresholds in rats. Making it a key translational assay to explore the impact of LC noradrenergic function on trigeminal nociceptive processing. Although not fully powered, we uncovered a net inhibitory action of LC activation: measured as an increase in periorbital sensory thresholds. Suggesting that activation of LC noradrenergic neurons inhibit sensory processing in the absence of a noxious stimuli, which is of key relevance to migraine as a disorder of sensory processing (Goadsby, Holland et al. 2017).

6.4. DISCUSSION

The complexity of migraine and its associated symptoms, including alterations in cognitive, emotional and appetite functions in tandem with hypersensitivity to multimodal stimuli including light, sound, smell and touch make it a complex disorder to model (Giffin, Ruggiero et al. 2003, Pareja-Angel and Campo-Arias 2004, Schulte, Jurgens et al. 2015, Gil-Gouveia, Oliveira et al. 2016, Viana, Linde et al. 2016, Peres, Mercante et al. 2017, Buse, Reed et al. 2020, Karsan, Bose et al. 2020, Pearl, Dumkrieger et al. 2020). Much of the significant progress that has been made to date focusses on migraine-related pain and while this has heralded therapeutic success (Diener, Charles et al. 2015) it has failed to address the wider symptomatology of migraine. Of the more recently developed therapies, only lasmiditan (5-HT_{1F} receptor agonist, (Vila-Pueyo, Page et al. 2021)) readily crosses the blood brain barrier; however, the debate regarding the central actions of largely peripherally acting therapies continues. For example, large molecular weight monoclonal antibodies targeting CGRP or its receptor are considered too large to access the central nervous system, yet there is a clear central signature of decreased central activation in key hubs including the thalamus and hypothalamus, the latter of which was only present in responders (Ziegeler, Mehnert et al. 2020). Thus alterations in hypothalamic function may represent a biological readout of disease state, alteration of which has previously been shown to correlate with attack chronification (Schulte, Allers et al. 2017).

As such, migraine is a disorder of altered sensory and homeostatic regulation, one which is able to function relatively normally, then rapidly switches into a state of multimodal hypersensitivity with parallel dysfunctions in associated higher order processing. In order to understand this complexity, it is essential that we explore new methods to enable us to model migraine-related symptomatology in conjunction with the headache. In our earlier chapters we explored the impact of orexin-ablation in the open field test, highlighting a potential alteration in locomotor function, that is in agreement with initial studies exploring the open field test as a potential migraine-relevant behavioural readout (Greco, Demartini et al. 2021), while had time permitted we sought to develop and test an orofacial pain related device (Anderson, Mills et al. 2013) that could be adapted to record reward-related orofacial sensory thresholds while recording

spontaneous facial pain behaviours such as the rodent grimace scale (Akintola, Raver et al. 2017). The ability to model these more complex pain behaviours in parallel with other migraine-related readouts in freely behaving rodents requires the ability to relatively non-invasively regulate neural circuits in a time-dependent manner.

The current study aimed to start this journey by optimising a newly developed CAV2 vector coupled to a specific promotor that enables targeted expression in neurons based on a specific promoter (Li, Hickey et al. 2016), negates the need for complex Cre-expressing lines and importantly can be conducted in rats. In this case the PRS-promoter enables specific targeting of noradrenergic projections, which permitted us to explore the function of the brainstem LC in the regulation of trigeminal nociceptive processing. Initial optimisation confirmed successful and specific transfection of noradrenergic fibres using a dual viral approach of CAV-Cre-PRS-V5 with pAAV-hSyn-DIO-hM3D(G_q)-mCherry (#44361, Addgene) (Hayat, Regev et al. 2020). The rationale being that future studies could take advantage of the retrograde properties to specifically transfect functional output units in the LC as oppose to a pan-LC modulation (Poe, Foote et al. 2020). Following this we optimized a single viral approach using CAV2-PRSx8-hM3Dq-mCherry, that once the correct titre had been identified, demonstrated successful transfection and activation of LC noradrenergic neurons with no gross toxicity (Stevens, Larsen et al. 2021).

6.4.1. Successful use of the single viral approach: CAV2-PRS-hM3Dq-mCherry

Having optimised the CAV2, we transitioned to test its ability to modulate trigeminal nociceptive processing. Demonstrating using *in vivo* electrophysiology in the trigeminocervical complex that durovascular-evoked neuronal responses were significantly inhibited in rats injected with the active-CAV2 compared to the inactive form. Spontaneous neuronal activity was further reduced, suggesting that gross activation of noradrenergic neurons from the LC to the trigeminocervical complex is inhibitory. This is in agreement with previous studies (Sasa and Takaori 1973); however, a recent study from our laboratory demonstrated that acute and chronic ablation of the LC also produces inhibition (Vila-Pueyo, Strother et al. 2018), acutely this may be due to electrolytic lesioning releasing noradrenaline in the spinal cord, in agreement with our results;

however, the impact of chronic ablation suggests a complex interplay. The LC, does not function independently, but instead forms a modular hub, with segregated output channels that can regulate diverse functions including cognition, emotion, stress and pain responses (Chandler, Jensen et al. 2019, Likhtik and Johansen 2019, Totah, Logothetis et al. 2019). As such, chronic ablation of noradrenergic efferent likely alters the function of several neural networks that themselves have the potential to modulate trigeminal pain processing.

Importantly, we were able to conduct initial pilot studies that explored the impact of altered LC noradrenergic function on periorbital sensory thresholds in rats. Although not fully powered, we uncovered a net inhibitory action of LC activation, increasing sensory thresholds in rats. The LC is considered to alter nociceptive processing and respond more robustly to prolonged noxious stimuli. Herein, our results suggest that activation of LC noradrenergic neurons inhibits sensory processing in the absence of a noxious stimuli, this is of relevance to migraine as a disorder of sensory processing (Goadsby, Holland et al. 2017). It is clear that migraine results from the abnormal processing of sensory information, therefore the LC may play an integrative role, linking abnormal spinal processing, thalamic gating, altered arousal and migraine. How and where this occurs, will be the subject of future studies, catalysed by our optimization of the dual viral approach that will enable targeted labelling and manipulation of the modular efferent outputs of the LC and the characterization of their function.

7. General discussion

The aim of this thesis was to investigate the role of different networks underlying the migraine premonitory phase that might be involved in the underlying biology of migraine and influence the initiation of migraine attacks. Premonitory symptoms have long been reported by patients; however, their biological importance has until recently been unexplored (Husain Maniyar, Sprenger et al. , Giffin, Ruggiero et al. 2003, Maniyar, Sprenger et al. 2014, Schulte, Jurgens et al. 2015, Karsan, Bose et al. 2018, Karsan and Goadsby 2018, Karsan and Goadsby 2020). It is now clear that as the earliest identifiable attack feature (Giffin, Ruggiero et al. 2003) that can predict an ensuing acute attack, they represent an entirely new stream in migraine research. One that focuses on the underlying biology of migraine as oppose to treating the acute attack, moving away from migraine as a disorder of peripheral sensory afferents innervating the dural vasculature, to migraine as a systems disorder with an underlying inherent genetic susceptibility (Bron, Sutherland et al. 2021) whereby internal and external sensory information is abnormally processed (Schwedt 2013, Goadsby, Holland et al. 2017). This premise describes migraine as a whole nervous system disease, whereby acute attacks periodically arise with a characteristic throbbing, often unilateral pain and are accompanied by nausea, vomiting, cranial autonomic features and hypersensitivity to light, sound, smell and touch (2018, Headache Classification Committee of the International Headache Society (IHS)). These attacks are preceded by a set of symptoms that highlight a prominent role for dysfunctional homeostatic regulation in patients. This network wide approach is supported by neuroimaging studies that report abnormal activity and functional connectivity between several neuronal hubs prior, to during and across the entire migraine attack (Afridi, Kaube et al. 2005, Afridi, Giffin et al. 2005, Afridi and Goadsby 2006, Maniyar, Sprenger et al. 2014, Schulte and May 2016).

7.1. Hypothalamic and Locus Coeruleus Involvement in migraine

Progress to date has focused on the role of the hypothalamus in regulating trigeminal pain (Bartsch, Levy et al. 2004, Robert, Bourgeais et al. 2013) and to a lesser extent the LC (Vila-Pueyo, Strother et al. 2018). Migraine has several features that suggest a key role for the hypothalamus including a circadian periodicity, autonomic features, and the

association between hypothalamic regulation of sleep-wake, hunger and thirst and the premonitory symptoms (Giffin, Ruggiero et al. 2003, Alstadhaug 2009, Holland 2014, Holland 2017). With such a diverse set of symptoms, it is likely that several diverse networks, many of which are regulated/originate at the hypothalamic level are involved. For example, the hypothalamic paraventricular nucleus which is involved in the integration of sensory, affective and autonomic regulation of the autonomic nervous system has downstream effects on trigeminal pain processing (Robert, Bourgeais et al. 2013). A primary focus of this thesis, the lateral hypothalamic orexinergic system, similarly integrates homeostatic cues (e,g, arousal, energy metabolism), regulates sleep-wake cycles, disruption of which are known to trigger migraine attacks (Kelman 2007) and can bidirectionally modulate trigeminal pain processing (Bartsch, Levy et al. 2004). Hypothalamic activation is increased during the premonitory phase and in response to trigeminovascular activation during the pre-ictal phase as well as being linked to attack chronification (Maniyar, Sprenger et al. 2014, Schulte and May 2016, Schulte, Allers et al. 2017). It is reasonable to assume therefore that the hypothalamus represents a key hub that underlies migraine.

Specifically, they hypothalamic orexinergic system has received significant attention for its roles in the regulation of arousal, appetite, locomotion, stress responses and the modulation of trigeminal nociceptive processing (Bartsch, Levy et al. 2004, Holland, Akerman et al. 2005, Holland, Akerman et al. 2006, Hoffmann, Supronsinchai et al. 2015, Holland 2017). Herein the content of this thesis strengthens this association, demonstrating that loss of orexin tone is pronociceptive, with potential impacts on migraine-related symptoms (fatigue, measured as decreased locomotion). Importantly, targeted blockade of orexin signalling has proven to be ineffective as a clinical migraine therapeutic (Chabi, Zhang et al. 2015). Our data demonstrating a selective antinociceptive effect of intranasal or intra-LC OxA confirms initial studies which suggested that specific agonists of the OX_1R would represent the most viable target (Holland, Akerman et al. 2005, Holland, Akerman et al. 2006). While also proposing the intranasal route as a potential strategy to preferentially target the trigeminal nerve and hypothalamus (Dhuria, Hanson et al. 2009), an already approved administration route in humans (Weinhold, Seeck-Hirschner et al. 2014) with important implications in targeting migraine-related fatigue (Hagan, Leslie et al. 1999, Yamanaka, Beuckmann et al. 2003, Harris and Aston-Jones 2006, Tsujino and Sakurai 2013). Indeed, orexinergic regulation of arousal is state

dependent in rodents, whereby orexin neurons sense energy balance and adjust arousal to promote food seeking behaviours (Yamanaka, Beuckmann et al. 2003). It is striking in some ways how closely this mimics migraine, whereby altered appetite regulation, often observed as skipping meals/feelings of hunger are commonly reported before the onset of an attack and the presence of marked fatigue (Giffin, Ruggiero et al. 2003, Kelman 2007).

Considering how a hypothalamic dysfunction may regulate the diverse symptomatology of migraine, we next focused on the brainstem LC which forms a functional unit with the hypothalamus regulating, arousal, stress and cognitive functions as well as trigeminal nociceptive processing (Vila-Pueyo, Strother et al. 2018) and cortical excitability and the occurrence of cortical spreading depression, the electrophysiological correlate of migraine aura (Charles and Brennan 2009, Charles and Baca 2013).

The LC has a pivotal role in modulating arousal and sleep-wake transitions, as well as providing arousal-appropriate responses in response to nociceptive and stress-related stimuli (Sara and Segal 1991, Hagan, Leslie et al. 1999, Samuels and Szabadi 2008, Takahashi, Kayama et al. 2010, Vazey, Moorman et al. 2018, Breton-Provencher and Sur 2019, Morris, McCall et al. 2020, Poe, Foote et al. 2020). And importantly, in regulating the sensitivity to sensory-evoked stimuli during sleep (Hayat, Regev et al. 2020). Recent work has identified its role in maintaining high thresholds of sensitivity to sensory-evoked (i.e. auditory) stimuli during sleep to allow rest; with low baseline noradrenergic activity reducing the probability to wake up from these stimuli (Hayat, Regev et al. 2020). These sensory-auditory-evoked awakenings have been correlated with noradrenergic tonic, rather than phasic activity, which is in agreement with previously observed tonic activity in response to stress (McCall, Al-Hasani et al. 2015) as well as pain and anxiety (Waterhouse and Navarra 2019). This is extremely relevant in the context of migraine given the commonly reported rhythmic nature of the migraine attack; with most of the headache attacks being initiated during sleep and migraineurs being woken up by the excruciating pain. Prior and during to the acute attack; premonitory symptoms have also clearly suggested an underlying increased sensitivity to sensory evoked stimuli, as observed from increased hypothalamic to LC connectivity patterns during the interictal phase (Stankewitz, Aderjan et al. 2011, Schulte and May 2016), hypersensitivity to visual

and auditory stimuli during the premonitory phase (Schulte, Jurgens et al. 2015), which then exacerbate the ongoing pain during the acute attack and the same stimuli as worsening the pain during the attack (Schwedt 2013).

Noradrenergic and serotonergic networks are a crucial part of the brainstem descending regulatory control responsible for modulating 'diffuse noxious inhibitory control (DNIC)', which underlie the 'pain inhibits pain' phenomenon in the spinal cord (Le Bars, Dickenson and Besson, 1979). These two networks work in tandem through inhibitory (i.e. Noradrenaline via alpha2-adrenoreceptrors and Serotonin via 5HT7R) and excitatory (i.e. Serotonin via 5HT2/3Rs) mechanisms at the spinal cord level (Bannister & Dickenson, 2016).

The mechanism behind DNIC can be measured in patients through a Conditioned Pain Modulation (CPM) paradigm, which is defined as the decreased painful response to a noxious stimulus during or after the application of another noxious stimulus. Chronic pain disorders such as Fibromyalgia (Kosek & Hansson, 1997), tension-type headache (Pielsticker, Haag et al., 2005) (Buchgreitz, Egsgaard et al., 2008) (Cathcart, Winefield et al., 2010), and migraine (Sandrini, Rossi et al., 2006) (Nahman-Averbuch et al., 2013) have reported altered CPM responses, compared to healthy controls. In the context of migraine; the severity of CPM loss seems correlated with the chronicity, with episodic patients showing a reduction of CPM and chronic patients; rather a complete loss (Guy, Voisin et al.,, 2018). Whereas, cluster headache patients show an absence of CPM while being in-bout, but a full CPM remission when out-of-bout (Perrotta, Serrao et al., 2010).

Preclinical evidence has indeed identified noradrenergic (Bannister, Patel et al. 2015) modulation to be responsible for altering DNIC in neuropathic models. Importantly; the presence of intact descending modulatory pathways in these spinal ligated neuropathic models, allowed the recovery of DNIC through also serotonergic facilitation (i.e. spinal application of SSRIs) (Bannister and Dickenson, 2016). In line with the acknowledged central sensitisation of trigeminal pathways in migraine; the ability to record and recover CPM responses could normalise descending modulatory processes that are potentially dysregulated in a migrainous brain.

Parallel to the descending modulatory role of the LC; the thalamus receives dense noradrenergic innervation from the LC (Westlund, Sorkin et al. 1990, Westlund, Zhang et al. 1991). Thus the LC may regulate trigeminal nociceptive processing at several levels, including the thalamus which is a known hub for the integration of touch and light(Simpson, Altman et al. 1997, Allen, Procyk et al. 2017). In the context of migraine-

associated trigeminal modulation, as observed in this thesis; an engagement of such noradrenergic LC-mediated descending modulation has uncovered an analgesic effect over both trigeminal networks at the level of the trigeminocervical complex and migraine-associated symptoms (allodynia: increased sensitivity to touch), which is proposed to be α-2-adrenoreceptor-mediated (Vila-Pueyo, Strother et al. 2018). Overall, this fits into a hypothetical altered system in which an ongoing disruption in LC descending modulation might continuously decrease the thresholds for sensory-evoked signals (e.g. light, sound, smell, touch) and eventually be unable to hold the 'overwhelming' load of incoming stimuli, supporting the initiation of an acute migraine. In this context, it is interesting that patients report a variety of stimuli as migraine triggers (Kelman 2007) but in real terms the susceptibility to these triggers varies on a cyclic basis. Thus suggesting that cyclic variations in the response characteristics of this system, potentially in response to altered homeostatic signalling, can lead to a fluctuating state of acute attack susceptibility. This hypothesis predicts that a greater understanding of the network level dysfunctions would allow targeted interventions to stabilize the network and reduce the occurrence of attacks. While purely speculative, this is in keeping with the advice given to patients to maintain a regular lifestyle (e.g. sleep-wake time and eating habits) to prevent homeostatic alterations and an increased likelihood of an attack or the increased frequency of attacks (Bigal and Lipton 2006).

While the mechanisms behind maintaining an 'underwhelming' threshold are not fully understood; we have strong evidence to suggest that they are modulated by higher order systems such as the hypothalamic orexinergic system. As observed in this thesis; the orexinergic system holds a central role in modulating homeostatic changes in the body (Williams, Bing et al. 2001, Sakurai 2005, Coll and Yeo 2013). A lack of orexin modulation increases periorbital mechanical sensitivity in freely behaving mice (chapter 3), suggestive of an underlying hypersensitivity of the trigeminal system. Orexin A however, is able to rescue such sensitivity (chapter 4), potentially via an LC (chapter 5) and/or vlPAG (Kooshki, Abbasnejad et al. 2020) OX_1R-dependent analgesic pathway. This is in agreement with previous OxA-mediated analgesic effects over trigeminal nociception through direct (injected into the posterior hypothalamus; (Bartsch, Levy et al. 2004)) or systemic (Holland, Akerman et al. 2005, Holland, Akerman et al. 2006) administration. Having said that, the spinal trigeminal nucleus and trigeminal dorsal horns also receive direct orexinergic projections (van den Pol, 1999; Hervieu et al., 2001;

Marcus et al., 2001; Cluderay et al., 2002), suggesting a direct action of OxA. With this we have now highlighted various potential pathways; direct or indirect through the LC or vlPAG, through which orexinergic signalling can produce analgesic effects over trigeminal nociception. Having established a novel retrograde noradrenergic-specific CAV2 vector; further studies will benefit from applying its retrograde properties to target specific LC to migraine-relevant networks *in vivo.*

7.2. HOW DO THESE SYSTEMS FIT INTO THE MIGRAINE SYMPTOMATOLOGY?

The involvement of the orexinergic system extends beyond pain, from modulating: locomotion initiation and sleep-wake transitions, stress through the HPA axis, appetite, reward, among others (Hagan, Leslie et al. 1999, Bingham, Davey et al. 2001, Harris, Wimmer et al. 2005, Harris and Aston-Jones 2006, Gonzalez, Jensen et al. 2016, Inutsuka, Yamashita et al. 2016, Chieffi, Carotenuto et al. 2017, Karnani, Schone et al. 2020, Concetti and Burdakov 2021). It is considered to integrate internal and external cues essential for maintaining body homeostasis (Venner, Karnani et al. 2011, Coll and Yeo 2013), ensuring the most appropriate physiological response in a state-dependent manner. In agreement to this; both our model (initially through the open fields but more robustly through continuous 24hr monitoring of their sleep wake cycles) of orexinergic ablation and others observed disturbances in their locomotion profiles. Even though it is difficult to directly associate general locomotion to the marked fatigue commonly reported in patients, it certainly suggests a susceptibility to a decreased engagement and movement due to a potential increased sensitivity to external stimuli. Despite not having measured any recovery in these migraine associated phenotypes in our model, others have observed improvement in locomotor deficits in response to orexin. Further; OX_1R-antagonists are able to block hyperalgesia and light-aversion (Kooshki, Abbasnejad et al. 2020), in comparison to other approaches in which similar targeting of the endocannabinoid system is able to block hyperalgesia but not locomotor deficits and anxiety-like behaviours (Greco, Demartini et al. 2021). Having established these chemogenetic approaches which allow *in vivo* and temporally controlled modulation; in future work we hope to characterize other migraine-associated phenotypes such as fatigue (Greco, Demartini et al. 2021), photophobia (Wang, Mason et al. 2021) or anxiety-like behaviours (McCall, Al-Hasani et al. 2015, Seibenhener and Wooten 2015, Morris, McCall et al. 2020) and establish potential recovery mechanisms.

Hypothalamic orexinergic, and thus noradrenergic functions appear to be correlated with the range of interictal and premonitory symptoms ((Karsan and Goadsby 2018, Karsan and Goadsby 2021); **Figure 7.1**): increased fatigue, difficulty concentrating, neck stiffness, food cravings, repetitive yawning, photophobia, phonophobia, as well as changes in mood and activity (Giffin, Ruggiero et al. 2003, Maniyar, Sprenger et al. 2014). In agreement with the clinical imaging data; altered hypothalamic connectivity patterns throughout the interictal and premonitory phases of migraine suggest an already existing and ongoing alteration in these networks (Schulte and May 2016). The premonitory phase is thus often described as a period in which disruptions in these networks increase the susceptibility to any external homeostatic inputs (Schulte, Jurgens et al. 2015). Importantly, an increased likelihood to have one symptoms or another is associated with the hyperactive neural substrate during the attack, with for example, patients often reporting photophobia showing increased visual cortex activity (Stankewitz, Aderjan et al. 2011), suggesting an underlying hypersensitivity of the underlying neural networks that normally process light information.

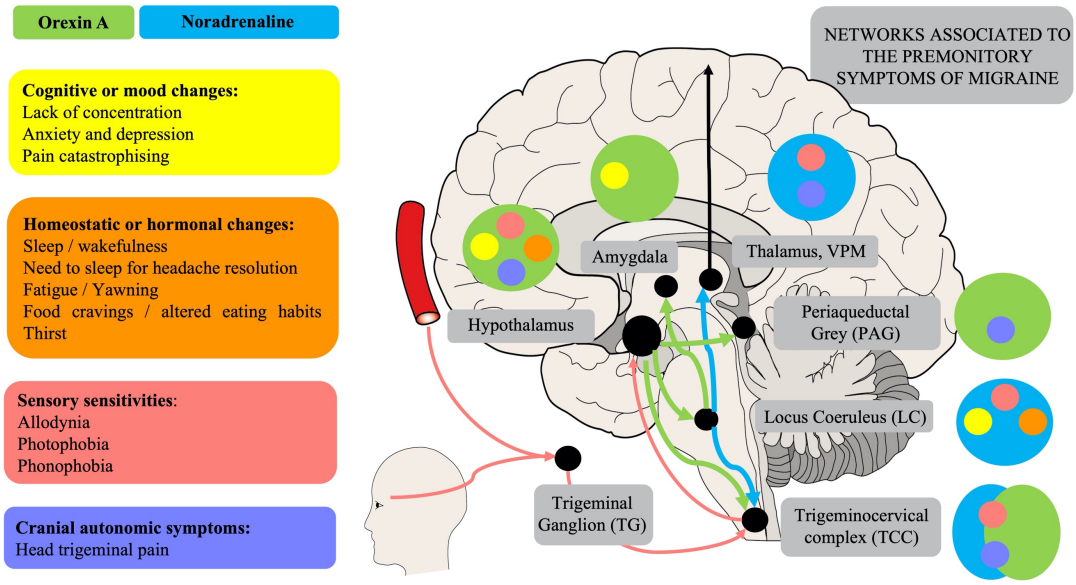

Figure 7.1. Summary of the main neural networks associated with the premonitory symptoms of migraine. According to the classification previously described (Chapter 1, Section 1.4), symptoms can be grouped into those referring to cognitive or mood changes (in yellow), homeostatic or hormonal changes (in orange), sensory hypersensitivity (in pink) and cranial autonomic symptoms (in purple). Each migraine-associated brain network is likely responsible for a set of functions which are associated to individual, or a combination of symptoms (small coloured circles). With this we aim to emphasize the importance of identifying potential connecting networks (arrows), whether they are orexin A (large green circles) or noradrenaline (large blue circles)-mediated, which we propose to be responsible for generating the migraine premonitory symptoms and trigeminal-associated pain (Adapted from Karsan and Goadsby, 2018).

7.3. PRECLINICAL BEHAVIOURAL MODELS OF MIGRAINE

An ongoing challenge in pain research is establishing accurate behavioural read-outs of pain. The perception of pain involves higher-order processing of a nociceptive stimulus to allow us to accurately define a painful experience. Measuring periorbital mechanical allodynia through von Frey approaches has proven key to translate basic discoveries into clinical translation (Saengjaroentham, Strother et al. 2020); and have in most cases accurately predicted the success of current therapies in targeting migraine headache. However, these measurements are fully dependent on spinal-reflex responses, which represent only a fraction of the processing of pain processing by only focusing at a nociceptor level and being localised to the spinal cord (Mogil 2009, Mogil, Davis et al. 2010, Klinck, Mogil et al. 2017). Being aware of this limitation; recent approaches have been developed which focus on spontaneous pain behaviours (Akintola, Raver et al.

2017), the rewarding component of the analgesic effect, or the freedom for the animal to choose whether to receive a reward or not depending on the underlying ongoing pain (Anderson, Mills et al. 2013). A review of multiple pain-related readouts has recently reviewed several options, highlighting some novel opportunities including cage hanging/climbing as a highly correlated pain measure (Zhang, Lecker et al. 2021); however, the complexity with migraine is transferring these readouts to the orofacial and ultimately the periorbital dermatome, given the role of the ophthalmic VI trigeminal afferents in migraine-related pain.

Based on the latter approach; we sought to utilise an orofacial pain assessment device (OPAD) which allows us to record the complex behaviour of choosing whether to receive a reward or not, based on the sensitivity to a nociceptive stimulus (Anderson, Mills et al. 2013). The OPAD system is a behavioural assay capable of measuring changes in pain perception in rodents. It provides a robust and objective measure of pain sensitivity based on the time spent being in contact with a pair of thermal/mechanical pads and licking from a condensed milk solution which sits just behind and in between the pads. Further, given that cold and hot thermal sensitivity has commonly been measured in whole-body assays such as the use of cold acetone, Hargreaves or tail flick tests in the hindpaw; this assay allows us to monitor changes in thermal sensitivity around the orofacial area. This assay thus allows rodents to have the choice on whether to engage with the reward or not, based on how noxious the thermal pads are considered. By measuring the result of a decision, rather than a spinal-reflex response localised to the spinal cord, we aim to get a step closer to the commonly clinically reported subjective levels of pain which have proven so challenging to represent. Preliminary work has investigated the utility of the OPAD as a sensitive tool to measure facial allodynia in freely behaving mice in a model of acute periorbital allodynia induced by nitroglycerin. Acute nitroglycerin administration caused a significant alteration in the number of licks at nociceptive temperatures (**see Figure 7.2.**). Sensitised mice demonstrated a significant decrease in licking at 55ºC, compared to 30ºC. This fits well with commonly reported acute mechanical and thermal hyperalgesic effects in the hindpaw post-nitroglycerin in mice (Holton, Strother et al. 2020, Bertels, Singh et al. 2021). It was ultimately our aim to integrate this model into the studies detailed in the thesis, testing our most interesting findings in a non-evoked pain assay. However, COVID-related delays prevented this with a focus instead on completing the core chapters outlined.

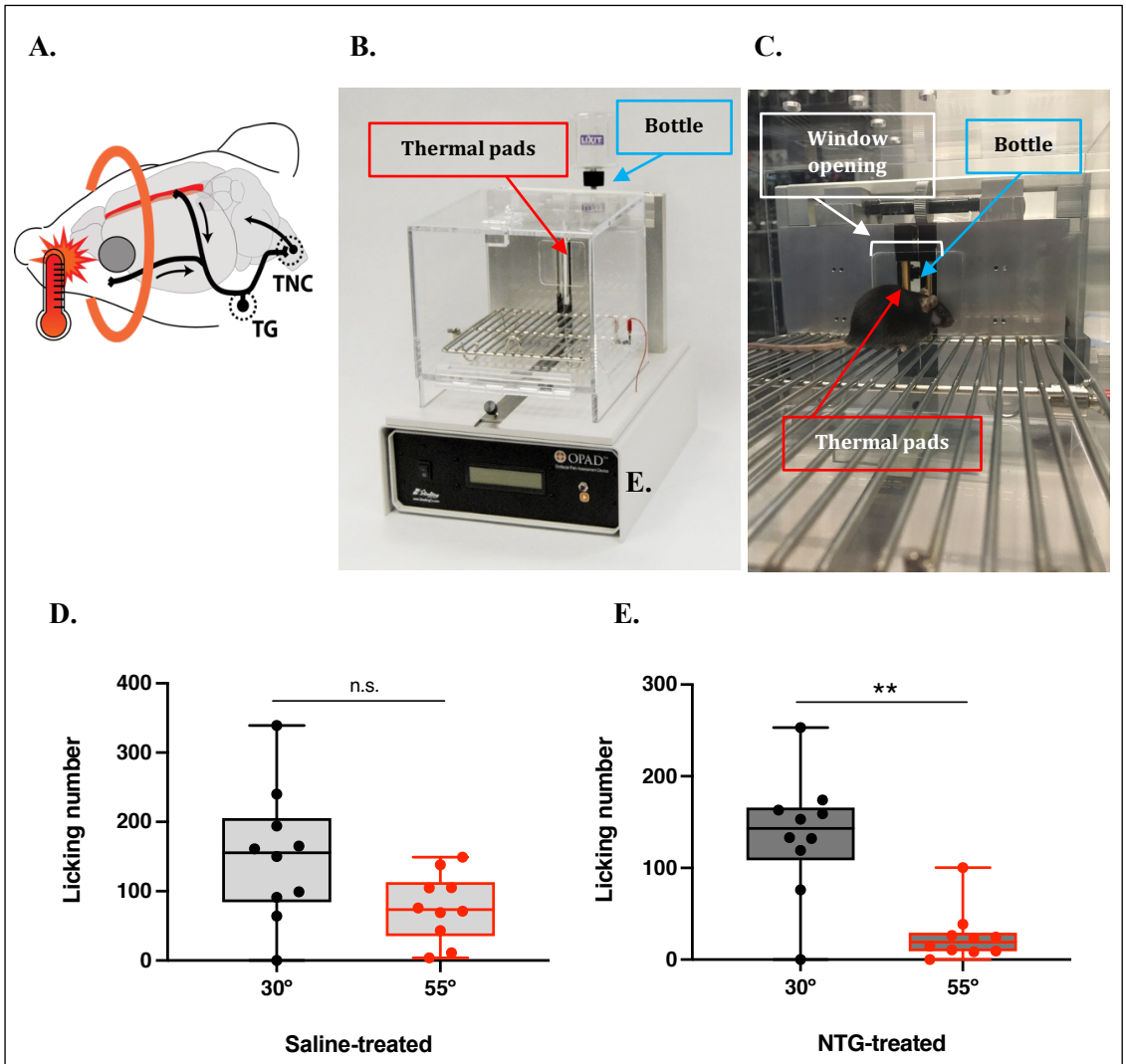

Figure 7.2. The orofacial pain assessment device (OPAD). A. With the OPAD device we aim to model the underlying sensitivity of trigeminal nociceptive pathways by applying heat around the orofacial area **B.** The OPAD device consists of a transparent box and mesh platform in which mice or rats are freely moving. Both thermal pads (labelled as red) lie vertically on both sides of the open 'window' (labelled as white) for the animal to access the bottle of condensed milk (labelled in blue) positioned just in between. Depending on the temperature of the pads and the underlying orofacial sensitivity: mice will choose whether to continue to drink from the rewarding condensed milk or not. Both the thermal pads and bottle of milk have embedded sensors of touch and movement, respectively, which connected to the OPAD panel and PC will record the amount of contact and licks **C.** Close up image of a mouse within the OPAD box approaching the bottle behind the thermal pads (yellow vertical metal pads). The cheek hair has been shaved off to increase the contact with the pads. Saline-treated mice showed no significant differences in orofacial thermal sensitivity (**D**, $p = 0.065$). Whereas, nitroglycerin (NTG)-treated mice showed a significant reduction (**E**, $p = 0.01$).

7.4. CHEMOGENETIC TECHNOLOGIES IN PRECLINICAL MIGRAINE MODELS

Cre-dependent AAV/CAV technology has opened a window of opportunities to modulate specific neuronal populations *in vivo*, in freely behaving animals and in a time controlled manner (Campbell and Marchant 2018). For the purpose of the initial work in this thesis; we made use of a Cre-dependent AAV coupled to a toxin to progressively ablate the orexinergic population in the lateral hypothalamus. This allowed us for the first time to understand the overall contribution of this population in migraine-associated behaviours in a freely behaving model of migraine and in a cell-specific manner.

Having said that, migraine has for a long time identified specific "neural hubs" as potential modulators and on occasion considered generators of the migraine headache (Schulte and May 2016). More recently, clinical imaging data has demonstrated continuous disrupted connectivity patterns throughout the whole brain in each of the migraine phases (Afridi, Giffin et al. 2005, Afridi, Matharu et al. 2005, Maniyar, Sprenger et al. 2014, Schulte and May 2016). Similarly, with preclinical locally-mediated pharmacological and/or ablation studies, one cannot be certain that the outcome is directly attributed to the result of the intervention, especially given the compensatory mechanisms potentially developed throughout a progressive ablation. Cre-dependent DREADD AAVs however represent a key technology to dissect the role of specific networks, and overcome any compensatory secondary effects. Their applications can vary based on the type of DREADD (mM3Dq or hM4Di) as well as AAV serotype used; whether that has higher transduction efficacy for neurons (AAV1, 5, 6 or AAV9), for astrocytes (AAV8) or for its retrograde properties (AAV2) (Aschauer, Kreuz et al. 2013). As briefly discussed; for the purpose of our work to investigate lateral hypothalamic to LC orexinergic projections, AAV2 serotypes coupled to hM3Dq receptors have been used to facilitate retrograde labelling and excitation of this pathway. While we are able to define the lateral hypothalamic pathways due to the relative restricted anatomical expression of orexin cell bodies; dual viral targeting strategies can also be implemented to map a pathway by injecting Cre-dependent and Cre-expressing vectors in different brain regions (Oguchi, Okajima et al. 2015).

In the context of migraine; these approaches hold great promise to investigate the roles of orexinergic and noradrenergic networks over many other migraine-associated

phenotypes. By use of retrograde AAV2 approaches (Tervo, Hwang et al. 2016) to delineate specific pathways it is then possible to characterize pathway-specific behavioural manifestations. Of particular interest to migraine, the combination of these approaches with behavioural readouts of photophobia (i.e. through light-dark box, (Wang, Mason et al. 2021)), fatigue (through in house circadian monitoring), reward (through pavlonian conditioning paradigms, (Lederle, Weber et al. 2011)) or even attention (through attentional-set-shifting tests, (Heisler, Morales et al. 2015)). Similarly, by combining nitroglycerin-induced allodynia models, one can test the predictive analgesic effects of these networks by modulating them and exploring restoration of normal sensory thresholds.

One more recent development that has the potential to aid in the understanding transection of migraine-related nociceptive processing and its associated symptoms in the novel c-Fos trap technology (Guenthner, Miyamichi et al. 2013). c-Fos has been extensively used to map brain regions activated by noxious stimuli (Hunt, Pini et al. 1987, Bullitt 1990). It has been instrumental in understanding the trigeminovascular system (Kaube, Hoskin et al. 1992, Strassman, Vos et al. 1993, Strassman, Mineta et al. 1994, Tassorelli and Joseph 1995, Sugimoto, He et al. 1998, Hoskin, Bulmer et al. 1999, Hoskin, Bulmer et al. 2001, Park, Moon et al. 2014), mapping diverse nuclei activated in response to trigeminal stimulation or the application of clinical migraine triggers (Tassorelli and Joseph 1995). Relevant to this thesis, trigeminovascular nociceptive activation elicits c-Fos expression in the trigeminocervical complex, the PAG (Hoskin, Bulmer et al. 2001), the LC (Tassorelli and Joseph 1995), thalamus (Park, Moon et al. 2014) and hypothalamus (Malick, Jakubowski et al. 2001), the latter of which highlighted a potential mechanism for pain-induced loss of appetite. As such, using c-Fos trap technology offers an important opportunity to further map and dissect these shared neural functions (**see Figure 7.1.**). This chemogenetic system is able to 'trap' the c-Fos induced from stimulation within a limited time window, so that the same active networks can then later be modulated *in vivo* (Guenthner, Miyamichi et al. 2013). By combination of a Cre-expressing AAV specific for the Fos promoter and a Cre-dependent AAV¡ expressing an inhibitory (hM4Di) or excitatory (hM3Dq) DREADD (Matos, Visser et al. 2019); one is able to induce and mimic the effects of specific active networks to understand how they may be involved in the wider migraine symptomatology.

The ability to translate the effect of single/group of activated neurons to the effects of an entire network, and associated behavioural representation will also enhance our understanding how these particular networks alter other more diverse networks in the brain. Similarly, to optogenetic approaches; combining DREADDs chemogenetic systems with functional MRI would offer an insight into the functional connectivity among networks with an increased spatial resolution. Given the high relevance of clinical imaging data in migraine; these technologies would help facilitate the translation from bench to the bedside and vice-versa. Given the overarching challenge of Cre-expressing transgenic mouse lines in maintaining Cre-expression through generations and the risk of developing tumours; great efforts have focused on developing Cre-expressing AAV-DREADDs which are already coupled to neural type specific promoters. An example introduced in this thesis are CAV2 vectors: which are known for their highly effective retrograde abilities as well as large vector sizes that enable the coupling of large promoters. The novel CAV2 vector optimized in this thesis contains a DREADD hM3Dq receptor as well as a noradrenergic-specific promoter (Stevens, Larsen et al. 2021): PRS, which allows for retrogradely excitation of noradrenergic pathways in freely behaving animals. This has proven highly effective in previous neuropathic pain models by LC-SC mapping and behavioural characterization (Hirschberg, Li et al. 2016). A prevailing issue with these DREADDs however is the use of the exogenous ligand: CNO; the partial conversion of which into clozapine is thought to act as an antipsychotic and have effects over startle responses and in amphetamine-induced hyper locomotion in rats (MacLaren, Browne et al. 2016). Despite this being taken into account by treating both active and inactive groups with CNO, recent work has developed a novel compound which we hope to implement in our future studies: deschloroclozapine which also seems to have has high-affinity and selectivity for DREADDs G-protein coupled receptors, as well as high brain permeability and rapid receptor activation within 10 minutes from systemic administration (Nagai, Miyakawa et al. 2020).

7.5. CONCLUSION

Overall, preclinical migraine research stands at a very exciting time in which cutting-edge technologies are available to dissect the underlying neural networks responsible for the diverse symptomatology that exists beyond migraine-related pain (Karsan and Goadsby 2021). It is often a challenge to be able to translate all the extremely relevant clinical information; whether that is imaging or symptomatology, to the bench due to the complexity of networks involved but also heterogeneity of the disorder; between and even within each patient. Similarly, with basic science focusing on dissecting very specific cellular and network processes; it often requires different read-outs and strategies to make a pathway/target translatable back to the clinic. Moving away from the previously recognized vascular nature of migraine; migraine is increasingly acknowledged as a multi-sensory pain disorder (Goadsby, Holland et al. 2017), with a vascular component. Preclinical applications of the previously described novel strategies have already started to unravel relevant similarities with other pain and sensory disorders, which is encouraging to continue to purse adaptable strategies and redefine what characterizes the migraine brain. With the initial studies presented in this thesis and the future use of revolutionary neuroscience technologies we aim to further dissect the structure/function relationship linking migraine-related pain with its associated symptomatology across the migraine attack. A particular focus is to understand the underlying premonitory symptoms and their biology, given that they are currently the earliest identifiable feature of an acute attack and therefore represent a potential novel therapeutic target to prevent the headache phase.

8. Glossary

5-HT: serotonin

AAV: adeno-associated virus

AChE: acetylcholine

ADP: Adenosine diphosphate

ANOVA: analysis of variance

ARRIVE: Animal Research: Reporting of In Vivo Experiments)

ATP: adenosine triphosphate

Au: auditory

BL: baseline measures

°C: Celsius

C1: first cervical level

C2: second cervical level

C57Bl6/J: C57 black 6

CAR: Chimeric antigen receptor

CART, cocaine- and amphetamine regulated transcript

CAV: canine-adenosine virus

CBT: cholera-B-toxin

CGRP: calcitonin gene-related peptide

CNO: Clozapine-N-oxide, CNO)

CNS: central nervous system

CO_2: carbon dioxide

CRH: corticotropin-releasing hormone

CSD: cortical spreading depression

CSF: cerebrospinal fluid

DHE: Dihydroergotamine

DAB: diaminobenzidine (DAB)

DBH: Dopamine beta-hydroxylase (DBH)

DIO: Double-floxed Inverted Open reading frame

dLGN: dorso-lateral geniculate nucleus

DNA: Deoxyribonucleic acid

DOX: doxycycline

DORA: dual orexin receptor antagonists (DORAs)

DREADDs: or a Designer Receptor Exclusively Activated by Designer Drugs

DRN: Dorsal Raphe Nucleus

dtA: diphtheria toxin A fragment (dtA)

Ect: ectorhinal

EF1a: elongation factor 1-alpha

ENK, enkephalin

fMRI: functional magnetic resonance imaging

GABA: gamma-aminobutyric acid

Gal: galanin

GFP: green fluorescent protein

G_q or $G_{i/o}$: G protein coupled-receptors

HD: Homeodomain (HD)

hM3Dq: human M3 muscarinic receptor

hM4Di: human M4 muscarinic receptor

IQR: interquartile range

INA: intranasal

Ins: insula

LC: locus coeruleus

LDT: laterodorsal tegmental nuclei

LH: lateral hypothalamus

LepRb: long-form of the leptin receptor

MC4R, melanocortin receptor 4

MCH: melanin-concentrating hormone (MCH

MMA: middle meningeal artery

NA: noradrenaline

NKA: neurokinin A

NOS: nitric oxide

NPY: neuropeptide Y

NSAIDS: Non-steroidal anti-inflammatory drugs

NTG: nitroglycerin

OX_1R: orexin 1 receptor

OX_2R: orexin 2 receptor

OxA: orexin A

OxB: orexin B

PACAP: pituitary adenylate-cyclase activating polypeptide

PAG: periaqueductal gray

PB: parabrachial nucleus

PBS: phosphate buffer solution (PBS).

PFA: paraformaldehyde (PFA)

PFC: prefrontal cortex (PFC)

PET: position emission tomography

PHM: peptide histidine methionine

PPT: pedunculopontine

PSEM308/PSAM: pharmacologically selective actuator module

PSTH: Post-stimulus histograms

PtA: parietal association

RVdG: Rabies viruses

ROI: region of interest (ROI)

RS: retrosplenial

SC: spinal cord (SC)

SP: substance P

SPG: sphenopalatine

SSS: superior sagittal sinus

SuS: the superior salivatory nucleus

Tet: tetracycline

TCC: trigeminocervical complex

TetO: tet operators

TF: transcription factors

TG: trigeminal ganglion

TH, tyrosine hydroxylase

TMN: tuberomammillary nucleus

TNC: trigeminal nucleus caudalis

TRH, thryotropin-releasing hormone

UCN3, urocortin-

V1: ophthalmic trigeminal branch

V2: maxillary trigeminal branch

V3: mandibular trigeminal branch

VIP: vasoactive intestinal peptide

VPM: ventroposteromedial nuclei

VPM: ventral posteriomedial nucleus (thalamus)

VTA: ventral tegmental area

9. References

(2018). "Headache Classification Committee of the International Headache Society (IHS) The International Classification of Headache Disorders, 3rd edition." Cephalalgia **38**(1): 1-211.

Abdallah, C. G. and P. Geha (2017). "Chronic Pain and Chronic Stress: Two Sides of the Same Coin?" Chronic Stress (Thousand Oaks)

Afridi, S., H. Kaube and P. J. Goadsby (2005). "Occipital activation in glyceryl trinitrate induced migraine with visual aura." J Neurol Neurosurg Psychiatry **76**(8): 1158-1160.

Afridi, S. K., N. J. Giffin, H. Kaube, K. J. Friston, N. S. Ward, R. S. Frackowiak and P. J. Goadsby (2005). "A positron emission tomographic study in spontaneous migraine." Arch Neurol **62**(8): 1270-1275.

Afridi, S. K. and P. J. Goadsby (2006). "Neuroimaging of migraine." Curr Pain Headache Rep **10**(3): 221-224.

Afridi, S. K., M. S. Matharu, L. Lee, H. Kaube, K. J. Friston, R. S. Frackowiak and P. J. Goadsby (2005). "A PET study exploring the laterality of brainstem activation in migraine using glyceryl trinitrate." Brain **128**(Pt 4): 932-939.

Aggarwal, M., Puri, V., Puri, S., (2012). "Serotonin and CGRP in Migraine." Annals of Neurosciences 19.

Ailani, J., Lipton, R.B., Goadsby, P.J., Guo, H., Miceli, R., Severt, L., Finnegan, M., Trugman, J.M., (2021) "Atogepant for the Preventive Treatment of Migraine" New England Journal of Medicine 385, 695–706.

Akintola, T., C. Raver, P. Studlack, O. Uddin, R. Masri and A. Keller (2017). "The grimace scale reliably assesses chronic pain in a rodent model of trigeminal neuropathic pain." Neurobiol Pain **2**: 13-17.

Alexander, G. M., S. C. Rogan, A. I. Abbas, B. N. Armbruster, Y. Pei, J. A. Allen, R. J. Nonneman, J. Hartmann, S. S. Moy, M. A. Nicolelis, J. O. McNamara and B. L. Roth (2009). "Remote control of neuronal activity in transgenic mice expressing evolved G protein-coupled receptors." Neuron 63(1): 27-39.

Allen, A. E., C. A. Procyk, T. M. Brown and R. J. Lucas (2017). "Convergence of visual and whisker responses in the primary somatosensory thalamus (ventral posterior medial region) of the mouse." J Physiol **595**(3): 865-881.

Alstadhaug, K. B. (2009). "Migraine and the hypothalamus." Cephalalgia **29**(8): 809-817.

Anderson, E. M., R. Mills, T. A. Nolan, A. C. Jenkins, G. Mustafa, C. Lloyd, R. M. Caudle and J. K. Neubert (2013). "Use of the Operant Orofacial Pain Assessment Device (OPAD) to measure changes in nociceptive behavior." J Vis Exp(76): e50336.

Anthony, M. (1968). "Plasma serotonin levels in migraine." Adv Pharmacol 6(Pt B): 203.Arima, Y., S. Yokota and M. Fujitani (2019). "Lateral parabrachial neurons innervate orexin neurons projecting to brainstem arousal areas in the rat." Sci Rep **9**(1): 2830.

Arendt-Nielsen L, Nie H, Laursen MB, Laursen BS, Madeleine P, Simonsen OH, Graven-Nielsen T (2010). "Sensitization in patients with painful knee osteoarthritis". Pain. 149(3):573-581.

Aschauer, D. F., S. Kreuz and S. Rumpel (2013). "Analysis of transduction efficiency, tropism and axonal transport of AAV serotypes 1, 2, 5, 6, 8 and 9 in the mouse brain." PLoS One **8**(9): e76310.

Ashina, M., J. M. Hansen, A. D. BO and J. Olesen (2017). "Human models of migraine - short-term pain for long-term gain." Nat Rev Neurol 13(12): 713-724.

Ashina, M., Z. Katsarava, T. P. Do, D. C. Buse, P. Pozo-Rosich, A. Özge, A. V. Krymchantowski, E. R. Lebedeva, K. Ravishankar, S. Yu, S. Sacco, S. Ashina, S. Younis, T. J. Steiner and R. B. Lipton (2021). "Migraine: epidemiology and systems of care." Lancet **397**(10283): 1485-1495.

Ashina, M., Saper, J., Cady, R., Schaeffler, B.A., Biondi, D.M., Hirman, J., Pederson, S., Allan, B., Smith, J., (2020.) "Eptinezumab in episodic migraine: A randomized, double-blind, placebo-controlled study (PROMISE-1)." Cephalalgia 40, 241–254..

Ashina, M., Cohen, J.M., Galic, M., Campos, V.R., Barash, S., Ning, X., Kessler, Y., Janka, L., Diener, H.-C., (2021). "Efficacy and safety of fremanezumab in patients with episodic and chronic migraine with documented inadequate response to 2 to 4 classes of migraine preventive medications over 6 months of treatment in the phase 3b FOCUS study." The Journal of Headache and Pain 22..

Ashkenazi, A., Schwedt, T., (2011). "Cluster Headache-Acute and Prophylactic Therapy." Headache: The Journal of Head and Face Pain 51, 272–286.

Aston-Jones, G., R. J. Smith, G. C. Sartor, D. E. Moorman, L. Massi, P. Tahsili-Fahadan and K. A. Richardson (2010). "Lateral hypothalamic orexin/hypocretin neurons: A role in reward-seeking and addiction." Brain Res **1314**: 74-90.

Ayata, C., H. Jin, C. Kudo, T. Dalkara and M. A. Moskowitz (2006). "Suppression of cortical spreading depression in migraine prophylaxis." Ann Neurol **59**(4): 652-661.

Bahra, A., M. S. Matharu, C. Buchel, R. S. Frackowiak and P. J. Goadsby (2001). "Brainstem activation specific to migraine headache." Lancet 357(9261): 1016-1017.

Bannister, Kirsty*; Patel, Ryan; Goncalves, Leonor; Townson, Louisa; Dickenson, Anthony H (2015) "Diffuse noxious inhibitory controls and nerve injury" PAIN. Volume 156 - Issue 9 - p 1803-1811

Bannister K, Dickenson AH. (2016) "What the brain tells the spinal cord." Pain. (10):2148-2151.

Barloese, M., P. Jennum, N. Lund, S. Knudsen, S. Gammeltoft and R. Jensen (2015). "Reduced CSF hypocretin-1 levels are associated with cluster headache." Cephalalgia **35**(10): 869-876.

Bartsch, T., Y. E. Knight and P. J. Goadsby (2004). "Activation of 5-HT(1B/1D) receptor in the periaqueductal gray inhibits nociception." Ann Neurol 56(3): 371-381.

Bartsch, T., M. J. Levy, Y. E. Knight and P. J. Goadsby (2004). "Differential modulation of nociceptive dural input to [hypocretin] orexin A and B receptor activation in the posterior hypothalamic area." Pain **109**(3): 367-378.

Bates, E., Nikai, T., Brennan, K., Fu, Y.-H., Charles, A., Basbaum, A., Ptáček, L., Ahn, A., (2010) "Sumatriptan alleviates nitroglycerin-induced mechanical and thermal allodynia in mice." Cephalalgia 30, 170–178..

Bayer, L., M. Serafin, E. Eggermann, B. Saint-Mleux, D. Machard, B. E. Jones and M. Muhlethaler (2004). "Exclusive postsynaptic action of hypocretin-orexin on sublayer 6b cortical neurons." J Neurosci **24**(30): 6760-6764.

Benjamin, L., M. J. Levy, M. P. Lasalandra, Y. E. Knight, S. Akerman, J. D. Classey and P. J. Goadsby (2004). "Hypothalamic activation after stimulation of the superior sagittal sinus in the cat: a Fos study." Neurobiol Dis 16(3): 500-505.

Berridge, C. W., B. E. Schmeichel and R. A. Espana (2012). "Noradrenergic modulation of wakefulness/arousal." Sleep Med Rev **16**(2): 187-197.

Bertels, Z., H. Singh, I. Dripps, K. Siegersma, A. F. Tipton, W. D. Witkowski, Z. Sheets, P. Shah, C. Conway, E. Mangutov, M. Ao, V. Petukhova, B. Karumudi, P. A. Petukhov, S. M. Baca, M. M. Rasenick and A. A. Pradhan (2021). "Neuronal

complexity is attenuated in preclinical models of migraine and restored by HDAC6 inhibition." Elife **10**.

Bhoi, S. K., J. Kalita and U. K. Misra (2012). "Metabolic syndrome and insulin resistance in migraine." J Headache Pain 13(4): 321-326.

Bigal, M. E. and R. B. Lipton (2006). "Modifiable risk factors for migraine progression." Headache **46**(9): 1334-1343.

Bingham, S., P. T. Davey, A. J. Babbs, E. A. Irving, M. J. Sammons, M. Wyles, P. Jeffrey, L. Cutler, I. Riba, A. Johns, R. A. Porter, N. Upton, A. J. Hunter and A. A. Parsons (2001). "Orexin-A, an hypothalamic peptide with analgesic properties." Pain **92**(1-2): 81-90.

Black, S. W., J. D. Sun, P. Santiago, A. Laihsu, N. Kimura, A. Yamanaka, R. Bersot and P. S. Humphries (2018). "Partial ablation of the orexin field induces a sub-narcoleptic phenotype in a conditional mouse model of orexin neurodegeneration." Sleep **41**(9).

Blanco, M., M. Lopez, T. Garcia-Caballero, R. Gallego, A. Vazquez-Boquete, G. Morel, R. Senaris, F. Casanueva, C. Dieguez and A. Beiras (2001). "Cellular localization of orexin receptors in human pituitary." J Clin Endocrinol Metab **86**(7): 3444-3447.

Bonaventure, P., S. Yun, P. L. Johnson, A. Shekhar, S. D. Fitz, B. T. Shireman, T. P. Lebold, D. Nepomuceno, B. Lord, M. Wennerholm, J. Shelton, N. Carruthers, T. Lovenberg and C. Dugovic (2015). "A selective orexin-1 receptor antagonist attenuates stress-induced hyperarousal without hypnotic effects." J Pharmacol Exp Ther **352**(3): 590-601.

Bonnavion, P., L. E. Mickelsen, A. Fujita, L. de Lecea and A. C. Jackson (2016). "Hubs and spokes of the lateral hypothalamus: cell types, circuits and behaviour." J Physiol **594**(22): 6443-6462.

Bose, P., N. Karsan and P. J. Goadsby (2018). "The Migraine Postdrome." Continuum (Minneap Minn) **24**(4, Headache): 1023-1031.

Boulaire, J., P. Balani and S. Wang (2009). "Transcriptional targeting to brain cells: Engineering cell type-specific promoter containing cassettes for enhanced transgene expression." Adv Drug Deliv Rev **61**(7-8): 589-602.

Bourgin, P., S. Huitron-Resendiz, A. D. Spier, V. Fabre, B. Morte, J. R. Criado, J. G. Sutcliffe, S. J. Henriksen and L. de Lecea (2000). "Hypocretin-1 modulates rapid eye movement sleep through activation of locus coeruleus neurons." J Neurosci 20(20): 7760-7765.

Brain SD, Grant AD. 2004.nVascular actions of calcitonin gene-related peptide and adrenomedullin. Physiol Rev. doi: 10.1152/physrev.00037.2003. PMID: 15269340.

Brennan, K. C., E. A. Bates, R. E. Shapiro, J. Zyuzin, W. C. Hallows, Y. Huang, H. Y. Lee, C. R. Jones, Y. H. Fu, A. C. Charles and L. J. Ptacek (2013). "Casein kinase idelta mutations in familial migraine and advanced sleep phase." Sci Transl Med **5**(183): 183ra156, 181-111.

Brennan, K. C. and D. Pietrobon (2018). "A Systems Neuroscience Approach to Migraine." Neuron **97**(5): 1004-1021.

Breton-Provencher, V. and M. Sur (2019). "Active control of arousal by a locus coeruleus GABAergic circuit." Nat Neurosci **22**(2): 218-228.

Brockschnieder, D., C. Lappe-Siefke, S. Goebbels, M. R. Boesl, K. A. Nave and D. Riethmacher (2004). "Cell depletion due to diphtheria toxin fragment A after Cre-mediated recombination." Mol Cell Biol **24**(17): 7636-7642.

Bron, C., H. G. Sutherland and L. R. Griffiths (2021). "Exploring the Hereditary Nature of Migraine." Neuropsychiatr Dis Treat **17**: 1183-1194.

Buchgreitz L, Egsgaard LL, Jensen R, Arendt-Nielsen L, Bendtsen L. (2008) Abnormal pain processing in chronic tension-type headache: a high-density EEG brain mapping study. Brain. 131(Pt 12):3232-8.

Bullitt, E. (1990). "Expression of c-fos-like protein as a marker for neuronal activity following noxious stimulation in the rat." J Comp Neurol **296**(4): 517-530.

Burdakov, D., O. Gerasimenko and A. Verkhratsky (2005). "Physiological changes in glucose differentially modulate the excitability of hypothalamic melanin-concentrating hormone and orexin neurons in situ." J Neurosci 25(9): 2429-2433.

Burstein, R., K. D. Cliffer and G. J. Giesler (1990). "Cells of Origin of the Spinohypothalamic Tract in the Rat." Journal of Comparative Neurology 291(3): 329-344.

Burstein, R., H. Yamamura, A. Malick and A. M. Strassman (1998). "Chemical stimulation of the intracranial dura induces enhanced responses to facial stimulation in brain stem trigeminal neurons." J-Neurophysiol. **79**(2): 964-982.

Burstein, R., D. Yarnitsky, I. Goor-Aryeh, B. J. Ransil and Z. H. Bajwa (2000). "An association between migraine and cutaneous allodynia." Ann Neurol **47**(5): 614-624.

Burstein, R., M. F. Cutrer and D. Yarnitsky (2000). "The development of cutaneous allodynia during a migraine attack clinical evidence for the sequential recruitment

of spinal and supraspinal nociceptive neurons in migraine." Brain **123 (Pt 8)**: 1703-1709.

Burstein, R., M. Jakubowski, E. Garcia-Nicas, V. Kainz, Z. Bajwa, R. Hargreaves, L. Becerra and D. Borsook (2010). "Thalamic Sensitization Transforms Localized Pain into Widespread Allodynia." Annals of Neurology **68**(1): 81-91.

Burstein, R., M. Jakubowski and S. D. Rauch (2011). "The science of migraine." J Vestib Res **21**(6): 305-314.

Burstein, R., R. Noseda and D. Borsook (2015). "Migraine: multiple processes, complex pathophysiology." J Neurosci **35**(17): 6619-6629.

Buse, D. C., R. B. Lipton, Y. Hallstrom, U. Reuter, S. J. Tepper, F. Zhang, S. Sapra, H. Picard, D. D. Mikol and R. A. Lenz (2018). "Migraine-related disability, impact, and health-related quality of life among patients with episodic migraine receiving preventive treatment with erenumab." Cephalalgia **38**(10): 1622-1631.

Buse, D. C., M. L. Reed, K. M. Fanning, R. Bostic, D. W. Dodick, T. J. Schwedt, S. Munjal, P. Singh and R. B. Lipton (2020). "Comorbid and co-occurring conditions in migraine and associated risk of increasing headache pain intensity and headache frequency: results of the migraine in America symptoms and treatment (MAST) study." J Headache Pain **21**(1): 23.

Cady, R. K., F. Sheftell, R. B. Lipton, S. O'Quinn, M. Jones, D. G. Putnam, A. Crisp, A. Metz and S. McNeal (2000). "Effect of early intervention with sumatriptan on migraine pain: retrospective analyses of data from three clinical trials." Clin Ther **22**(9): 1035-1048.

Campbell, E. J. and N. J. Marchant (2018). "The use of chemogenetics in behavioural neuroscience: receptor variants, targeting approaches and caveats." Br J Pharmacol **175**(7): 994-1003.

Carter, M. E., L. de Lecea and A. Adamantidis (2013). "Functional wiring of hypocretin and LC-NE neurons: implications for arousal." Front Behav Neurosci **7**: 43.

Cathcart S, Winefield AH, Lushington K, Rolan P (2010) "Stress and tension-type headache mechanisms." Cephalalgia. 30(10):1250-67.

Cedarbaum, J. M. and G. K. Aghajanian (1978). "Activation of locus coeruleus neurons by peripheral stimuli: modulation by a collateral inhibitory mechanism." Life Sci **23**(13): 1383-1392.

Chabi, A., Y. Zhang, S. Jackson, R. Cady, C. Lines, W. J. Herring, K. M. Connor and D. Michelson (2015). "Randomized controlled trial of the orexin receptor antagonist filorexant for migraine prophylaxis." Cephalalgia **35**(5): 379-388.

Chaplan, S. R., F. W. Bach, J. W. Pogrel, J. M. Chung and T. L. Yaksh (1994). "Quantitative assessment of tactile allodynia in the rat paw." J Neurosci Methods **53**(1): 55-63.

Charles, A. and K. Brennan (2009). "Cortical spreading depression-new insights and persistent questions." Cephalalgia **29**(10): 1115-1124.

Charles, A. C. and S. M. Baca (2013). "Cortical spreading depression and migraine." Nat Rev Neurol **9**(11): 637-644.

Chandler, D. J., P. Jensen, J. G. McCall, A. E. Pickering, L. A. Schwarz and N. K. Totah (2019). "Redefining Noradrenergic Neuromodulation of Behavior: Impacts of a Modular Locus Coeruleus Architecture." J Neurosci **39**(42): 8239-8249.

Cheng, J. K., R. C. Chou, L. L. Hwang and L. C. Chiou (2003). "Antiallodynic effects of intrathecal orexins in a rat model of postoperative pain." J Pharmacol Exp Ther **307**(3): 1065-1071.

Chieffi, S., M. Carotenuto, V. Monda, A. Valenzano, I. Villano, F. Precenzano, D. Tafuri, M. Salerno, N. Filippi, F. Nuccio, M. Ruberto, V. De Luca, L. Cipolloni, G. Cibelli, M. P. Mollica, D. Iacono, E. Nigro, M. Monda, G. Messina and A. Messina (2017). "Orexin System: The Key for a Healthy Life." Front Physiol **8**: 357.

Chillon, M. and E. J. Kremer (2001). "Trafficking and propagation of canine adenovirus vectors lacking a known integrin-interacting motif." Hum Gene Ther 12(14): 1815-1823.

Chou, T. C., C. E. Lee, J. Lu, J. K. Elmquist, J. Hara, J. T. Willie, C. T. Beuckmann, R. M. Chemelli, T. Sakurai, M. Yanagisawa, C. B. Saper and T. E. Scammell (2001). "Orexin (hypocretin) neurons contain dynorphin." J Neurosci **21**(19): RC168.

Christiansen I, Thomsen L, Daugaard D, Ulrich V, Olesen J. (1999) "Glyceryl Trinitrate Induces Attacks of Migraine Without Aura in Sufferers of Migraine with Aura." Cephalalgia. 19(7):660-667.

Coll, A. P. and G. S. Yeo (2013). "The hypothalamus and metabolism: integrating signals to control energy and glucose homeostasis." Curr Opin Pharmacol **13**(6): 970-976.

Collaborators, G. B. D. N. (2019). "Global, regional, and national burden of neurological disorders, 1990-2016: a systematic analysis for the Global Burden of Disease Study 2016." Lancet Neurol 18(5): 459-480.Concetti, C. and D. Burdakov (2021).

"Orexin/Hypocretin and MCH Neurons: Cognitive and Motor Roles Beyond Arousal." Front Neurosci **15**: 639313.

Coppola, G., A. Di Renzo, E. Tinelli, C. Di Lorenzo, G. Di Lorenzo, V. Parisi, M. Serrao, J. Schoenen and F. Pierelli (2016). "Thalamo-cortical network activity during spontaneous migraine attacks." Neurology **87**(20): 2154-2160.

Coppola, G., A. Di Renzo, E. Tinelli, C. Lepre, C. Di Lorenzo, G. Di Lorenzo, M. Scapeccia, V. Parisi, M. Serrao, C. Colonnese, J. Schoenen and F. Pierelli (2016). "Thalamo-cortical network activity between migraine attacks: Insights from MRI-based microstructural and functional resting-state network correlation analysis." J Headache Pain **17**(1): 100.

Croop R, Goadsby PJ, Stock DA, Conway CM, Forshaw M, Stock EG, Coric V, Lipton RB. (2019) "Efficacy, safety, and tolerability of rimegepant orally disintegrating tablet for the acute treatment of migraine: a randomised, phase 3, double-blind, placebo-controlled trial." Lancet. Aug 31;394(10200):737-745.

Croop R, Lipton RB, Kudrow D, Stock DA, Kamen L, Conway CM, Stock EG, Coric V, Goadsby PJ. (2021) "Oral rimegepant for preventive treatment of migraine: a phase 2/3, randomised, double-blind, placebo-controlled trial. Lancet." Jan 2;397(10268):51-60. Epub 2020 Dec 15. PMID: 33338437.

Cumberbatch, M. J., R. G. Hill and R. J. Hargreaves (1998). "Differential effects of the 5HT1B/1D receptor agonist naratriptan on trigeminal versus spinal nociceptive responses." Cephalalgia **18**(10): 659-663.

Curran, D. A., H. Hinterberger and J. W. Lance (1965). "Total plasma serotonin, 5-hydroxyindoleacetic acid and p-hydroxy-m-methoxymandelic acid excretion in normal and migrainous subjects." Brain **88**(5): 997-1010.

Cutler, D. J., R. Morris, V. Sheridhar, T. A. K. Wattam, S. Holmes, S. Patel, J. R. S. Arch, S. Wilson, R. E. Buckingham, M. L. Evans, R. A. Leslie and G. Williams (1999). "Differential distribution of orexin-A and orexin-B immunoreactivity in the rat brain and spinal cord." Peptides **20**(12): 1455-1470.

Dahmen, N., M. Kasten, S. Wieczorek, M. Gencik, J. T. Epplen and B. Ullrich (2003). "Increased frequency of migraine in narcoleptic patients: a confirmatory study." Cephalalgia **23**(1): 14-19.

Dahmen, N., K. Querings, B. Grun and J. Bierbrauer (1999). "Increased frequency of migraine in narcoleptic patients." Neurology **52**(6): 1291-1293.

Date, Y., M. S. Mondal, S. Matsukura and M. Nakazato (2000). "Distribution of orexin-A and orexin-B (hypocretins) in the rat spinal cord." Neurosci Lett **288**(2): 87-90.

Davies, P. (2011). "What has imaging taught us about migraine?" Maturitas **70**(1): 34-36.

Deadwyler, S. A., L. Porrino, J. M. Siegel and R. E. Hampson (2007). "Systemic and nasal delivery of orexin-A (Hypocretin-1) reduces the effects of sleep deprivation on cognitive performance in nonhuman primates." J Neurosci **27**(52): 14239-14247.

De Silva, K. L., M. A. Ron and J. Pearce (1974). "Blood sugar response to glucagon in migraine." J Neurol Neurosurg Psychiatry **37**(1): 105-107.

Demartini, C., R. Greco, A. M. Zanaboni, G. Sances, R. De Icco, D. Borsook and C. Tassorelli (2019). "Nitroglycerin as a comparative experimental model of migraine pain: From animal to human and back." Prog Neurobiol **177**: 15-32.

Detke, H.C., Goadsby, P.J., Wang, S., Friedman, D.I., Selzler, K.J., Aurora, S.K., (2018.) "Galcanezumab in chronic migraine". Neurology 91, e2211–e2221.

Dhuria, S. V., L. R. Hanson and W. H. Frey, 2nd (2009). "Intranasal drug targeting of hypocretin-1 (orexin-A) to the central nervous system." J Pharm Sci **98**(7): 2501-2515.

Dickenson, A.H., Le Bars, D. (1983) "Diffuse noxious inhibitory controls (DNIC) involve trigeminothalamic and spinothalamic neurones in the rat." Experimental Brain Research 49, 174–180.

Diener HC, Barbanti P, Dahlöf C, Reuter U, Habeck J, Podhorna J. (2011) "BI 44370 TA, an oral CGRP antagonist for the treatment of acute migraine attacks: results from a phase II study." Cephalalgia. (5):573-84.

Diener, H. C., A. Charles, P. J. Goadsby and D. Holle (2015). "New therapeutic approaches for the prevention and treatment of migraine." Lancet Neurol **14**(10): 1010-1022.

Dimitriadou, V., M. G. Buzzi, M. A. Moskowitz and T. C. Theoharides (1991). "Trigeminal sensory fiber stimulation induces morphological changes reflecting secretion in rat dura mater mast cells." Neuroscience **44**(1): 97-112.

Doods, H., Hallermayer, G., Wu, D., Entzeroth, M., Rudolf, K., Engel, W., Eberlein, W., (2000). "Pharmacological profile of BIBN4096BS, the first selective small molecule CGRP antagonist." British Journal of Pharmacology 129, 420–423..

Durham, P.L., Sharma, R.V., Russo, A.F., (1997) "Repression of the Calcitonin Gene-Related Peptide Promoter by 5-HT1Receptor Activation." The Journal of Neuroscience 17, 9545–9553.

Edelmayer, R. M., T. W. Vanderah, L. Majuta, E. T. Zhang, B. Fioravanti, M. De Felice, J. G. Chichorro, M. H. Ossipov, T. King, J. Lai, S. H. Kori, A. C. Nelsen, K. E. Cannon, M. M. Heinricher and F. Porreca (2009). "Medullary pain facilitating neurons mediate allodynia in headache-related pain." Ann Neurol **65**(2): 184-193.

Edvinsson, L. and P. J. Goadsby (1995). "Neuropeptides in the cerebral circulation: relevance to headache." Cephalalgia **15**(4): 272-276.

Edvinsson, L. and P. Tfelt-Hansen (2008). "The blood-brain barrier in migraine treatment." Cephalalgia **28**(12): 1245-1258.

Ehrstrom, M., E. Naslund, F. Levin, R. Kaur, A. L. Kirchgessner, E. Theodorsson and P. M. Hellstrom (2004). "Pharmacokinetic profile of orexin A and effects on plasma insulin and glucagon in the rat." Regul Pept **119**(3): 209-212.

Ellrich, J., K. Messlinger, C. Y. Chiang and J. W. Hu (2001). "Modulation of neuronal activity in the nucleus raphe magnus by the 5-HT(1)-receptor agonist naratriptan in rat." Pain **90**(3): 227-231.

Enger, R., W. Tang, G. F. Vindedal, V. Jensen, P. Johannes Helm, R. Sprengel, L. L. Looger and E. A. Nagelhus (2015). "Dynamics of Ionic Shifts in Cortical Spreading Depression." Cereb Cortex **25**(11): 4469-4476.

Estabrooke, I. V., M. T. McCarthy, E. Ko, T. C. Chou, R. M. Chemelli, M. Yanagisawa, C. B. Saper and T. E. Scammell (2001). "Fos expression in orexin neurons varies with behavioral state." J Neurosci **21**(5): 1656-1662.

Evans, B.N., Rosenblatt, M.I., Mnayer, L.O., Oliver, K.R., Dickerson, I.M., (2000) "CGRP-RCP, a Novel Protein Required for Signal Transduction at Calcitonin Gene-related Peptide and Adrenomedullin Receptors". Journal of Biological Chemistry 275, 31438–31443.

Evers, S., F. Quibeldey, K. H. Grotemeyer, B. Suhr and I. W. Husstedt (1999). "Dynamic changes of cognitive habituation and serotonin metabolism during the migraine interval." Cephalalgia **19**(5): 485-491.

Felgenhauer, K., (1974) "Protein size and cerebrospinal fluid composition." Klinische Wochenschrift 52, 1158–1164.

Ferrari MD, Diener HC, Ning X, Galic M, Cohen JM, Yang R, Mueller M, Ahn AH, Schwartz YC, Grozinski-Wolff M, Janka L, Ashina M. (2019) "Fremanezumab

versus placebo for migraine prevention in patients with documented failure to up to four migraine preventive medication classes (FOCUS): a randomised, double-blind, placebo-controlled, phase 3b trial." Lancet. Sep 21;394(10203):1030-1040.

Ferrari, M.D., Reuter, U., Goadsby, P.J., Paiva Da Silva Lima, G., Mondal, S., Wen, S., Tenenbaum, N., Pandhi, S., Lanteri-Minet, M., Stites, T.,)2021). "Two-year efficacy and safety of erenumab in participants with episodic migraine and 2–4 prior preventive treatment failures: results from the LIBERTY study". Journal of Neurology, Neurosurgery & Psychiatry jnnp-2021-32748..

Fields HL, Basbaum AI, Clanton CH, Anderson SD. (1977) Nucleus raphe magnus inhibition of spinal cord dorsal horn neurons. Brain Res. 126(3):441-53.

Filiz A, Tepe N, Eftekhari S, Boran HE, Dilekoz E, Edvinsson L, Bolay H. (2019) "CGRP receptor antagonist MK-8825 attenuates cortical spreading depression induced pain behavior." Cephalalgia. (3):354-365.

Flores, A., V. Valls-Comamala, G. Costa, R. Saravia, R. Maldonado and F. Berrendero (2014). "The hypocretin/orexin system mediates the extinction of fear memories." Neuropsychopharmacology **39**(12): 2732-2741.

Foord, S. M., T. I. Bonner, R. R. Neubig, E. M. Rosser, J. P. Pin, A. P. Davenport, M. Spedding and A. J. Harmar (2005). "International Union of Pharmacology. XLVI. G protein-coupled receptor list." Pharmacol Rev **57**(2): 279-288.

Furutani, N., M. Hondo, H. Kageyama, N. Tsujino, M. Mieda, M. Yanagisawa, S. Shioda and T. Sakurai (2013). "Neurotensin co-expressed in orexin-producing neurons in the lateral hypothalamus plays an important role in regulation of sleep/wakefulness states." PLoS One **8**(4): e62391.

Gamble, M. C., F. Katsuki, J. G. McCoy, R. E. Strecker and J. T. McKenna (2020). "The dual orexinergic receptor antagonist DORA-22 improves the sleep disruption and memory impairment produced by a rodent insomnia model." Sleep **43**(3).

Gelfand, A. A., A. C. Reider and P. J. Goadsby (2013). "Cranial autonomic symptoms in pediatric migraine are the rule, not the exception." Neurology **81**(5): 431-436.

Ghanizada, H., M. A. Al-Karagholi, C. S. Walker, N. Arngrim, T. Rees, J. Petersen, A. Siow, M. Morch-Rasmussen, S. Tan, S. J. O'Carroll, P. Harris, L. T. Skovgaard, N. R. Jorgensen, M. Brimble, J. S. Waite, B. J. Rea, L. P. Sowers, A. F. Russo, D. L. Hay and M. Ashina (2021). "Amylin Analog Pramlintide Induces Migraine-like Attacks in Patients." Ann Neurol **89**(6): 1157-1171.

Ghasemi, H., B. Khaledi-Paveh, A. Abdi, R. Jalali, N. Salari, A. Vaisi-Raygani and M. Mohammadi (2020). "The Prevalence of Restless Legs Syndrome in Patients with Migraine: A Systematic Review and Meta-Analysis." Pain Res Manag **2020**: 2763808.

Giardino, W. J., A. Eban-Rothschild, D. J. Christoffel, S. B. Li, R. C. Malenka and L. de Lecea (2018). "Parallel circuits from the bed nuclei of stria terminalis to the lateral hypothalamus drive opposing emotional states." Nat Neurosci **21**(8): 1084-1095.

Giffin, N. J., L. Ruggiero, R. B. Lipton, S. D. Silberstein, J. F. Tvedskov, J. Olesen, J. Altman, P. J. Goadsby and A. Macrae (2003). "Premonitory symptoms in migraine: an electronic diary study." Neurology **60**(6): 935-940.

Gil-Gouveia, R., A. G. Oliveira and I. P. Martins (2016). "The impact of cognitive symptoms on migraine attack-related disability." Cephalalgia **36**(5): 422-430.

Goadsby, P. J. and K. L. Hoskin (1997). "The distribution of trigeminovascular afferents in the nonhuman primate brain Macaca nemestrina: A c-fos immunocytochemical study." Journal of Anatomy **190**: 367-375.

Goadsby, P. J., L. Edvinsson and R. Ekman (1988). "Release of vasoactive peptides in the extracerebral circulation of humans and the cat during activation of the trigeminovascular system." Ann Neurol **23**(2): 193-196.

Goadsby, P. J. and J. W. Duckworth (1989). "Low frequency stimulation of the locus coeruleus reduces regional cerebral blood flow in the spinalized cat." Brain Res **476**(1): 71-77.

Goadsby, P. J., L. Edvinsson and R. Ekman (1990). "Vasoactive peptide release in the extracerebral circulation of humans during migraine headache." Ann Neurol **28**(2): 183-187.

Goadsby, P. J., S. Akerman and R. J. Storer (2001). "Evidence for postjunctional serotonin (5-HT1) receptors in the trigeminocervical complex." Ann Neurol **50**(6): 804-807.

Goadsby, P. J., R. B. Lipton and M. D. Ferrari (2002). "Migraine--current understanding and treatment." N Engl J Med **346**(4): 257-270.

Goadsby, P. J. and S. Akerman (2012). "The trigeminovascular system does not require a peripheral sensory input to be activated--migraine is a central disorder. Focus on 'Effect of cortical spreading depression on basal and evoked traffic in the trigeminovascular sensory system'." Cephalalgia **32**(1): 3-5.

Goadsby, P. J., P. R. Holland, M. Martins-Oliveira, J. Hoffmann, C. Schankin and S. Akerman (2017). "Pathophysiology of Migraine: A Disorder of Sensory Processing." Physiol Rev **97**(2): 553-622.

Goadsby, P.J., Silberstein, S.D., Yeung, P.P., Cohen, J.M., Ning, X., Yang, R., Dodick, D.W., (2020). "Long-term safety, tolerability, and efficacy of fremanezumab in migraine." Neurology 95, e2487–e2499..

Goadsby, P.J., Reuter, U., Lanteri-Minet, M., Paiva Da Silva Lima, G., Hours-Zesiger, P., Fernandes, C., Wen, S., Tenenbaum, N., Kataria, A., Ferrari, M.D., Klatt, J., (2021). "Long-term Efficacy and Safety of Erenumab." Neurology 96, e2724–e2735..

Gomez, J. L., J. Bonaventura, W. Lesniak, W. B. Mathews, P. Sysa-Shah, L. A. Rodriguez, R. J. Ellis, C. T. Richie, B. K. Harvey, R. F. Dannals, M. G. Pomper, A. Bonci and M. Michaelides (2017). "Chemogenetics revealed: DREADD occupancy and activation via converted clozapine." Science **357**(6350): 503-507.

Gonzalez, J. A., L. T. Jensen, L. Fugger and D. Burdakov (2012). "Convergent inputs from electrically and topographically distinct orexin cells to locus coeruleus and ventral tegmental area." Eur J Neurosci **35**(9): 1426-1432.

Gonzalez, J. A., L. T. Jensen, P. Iordanidou, M. Strom, L. Fugger and D. Burdakov (2016). "Inhibitory Interplay between Orexin Neurons and Eating." Curr Biol **26**(18): 2486-2491.

Goutaudier, R., V. Coizet, C. Carcenac and S. Carnicella (2020). "Compound 21, a two-edged sword with both DREADD-selective and off-target outcomes in rats." PLoS One **15**(9): e0238156.

Greco, R., C. Demartini, M. Francavilla, A. M. Zanaboni and C. Tassorelli (2021). "Dual Inhibition of FAAH and MAGL Counteracts Migraine-like Pain and Behavior in an Animal Model of Migraine." Cells **10**(10).

Guenthner, C. J., K. Miyamichi, H. H. Yang, H. C. Heller and L. Luo (2013). "Permanent genetic access to transiently active neurons via TRAP: targeted recombination in active populations." Neuron **78**(5): 773-784.

Gursoy-Ozdemir, Y., Qiu, J., Matsuoka, N., Bolay, H., Bermpohl, D., Jin, H., Wang, X., Rosenberg, G.A., Lo, E.H., Moskowitz, M.A., (2004) "Cortical spreading depression activates and upregulates MMP-9". Journal of Clinical Investigation 113, 1447–1455.

Guy N, Voisin D, Mulliez A, Clavelou P, Dallel R. (2008) "Medication overuse reinstates conditioned pain modulation in women with migraine." Cephalalgia. 38(6):1148-1158.

Hadjikhani, N., M. Sanchez Del Rio, O. Wu, D. Schwartz, D. Bakker, B. Fischl, K. K. Kwong, F. M. Cutrer, B. R. Rosen, R. B. Tootell, A. G. Sorensen and M. A. Moskowitz (2001). "Mechanisms of migraine aura revealed by functional MRI in human visual cortex." Proc Natl Acad Sci U S A **98**(8): 4687-4692.

Han JS, Li W, Neugebauer V. (2005) "Critical role of calcitonin gene-related peptide 1 receptors in the amygdala in synaptic plasticity and pain behavior." J Neurosci.Nov 16;25(46):10717-28.

Hansen JM (2010). "Familial hemiplegic migraine." Dan Med Bull. Sep;57(9):B4183. PMID: 20816023.

Hansen, J. M., A. W. Hauge, J. Olesen and M. Ashina (2010). "Calcitonin gene-related peptide triggers migraine-like attacks in patients with migraine with aura." Cephalalgia **30**(10): 1179-1186.

Hanson, L. R., J. M. Fine, A. L. Svitak and K. A. Faltesek (2013). "Intranasal administration of CNS therapeutics to awake mice." J Vis Exp(74).

Hagan, J. J., R. A. Leslie, S. Patel, M. L. Evans, T. A. Wattam, S. Holmes, C. D. Benham, S. G. Taylor, C. Routledge, P. Hemmati, R. P. Munton, T. E. Ashmeade, A. S. Shah, J. P. Hatcher, P. D. Hatcher, D. N. Jones, M. I. Smith, D. C. Piper, A. J. Hunter, R. A. Porter and N. Upton (1999). "Orexin A activates locus coeruleus cell firing and increases arousal in the rat." Proc Natl Acad Sci U S A **96**(19): 10911-10916.

Hara, J., C. T. Beuckmann, T. Nambu, J. T. Willie, R. M. Chemelli, C. M. Sinton, F. Sugiyama, K. Yagami, K. Goto, M. Yanagisawa and T. Sakurai (2001). "Genetic ablation of orexin neurons in mice results in narcolepsy, hypophagia, and obesity." Neuron **30**(2): 345-354.

Harriott, A. M., L. C. Strother, M. Vila-Pueyo and P. R. Holland (2019). "Animal models of migraine and experimental techniques used to examine trigeminal sensory processing." J Headache Pain **20**(1): 91.

Harris, G. C. and G. Aston-Jones (2006). "Arousal and reward: a dichotomy in orexin function." Trends Neurosci **29**(10): 571-577.

Harris, G. C., M. Wimmer and G. Aston-Jones (2005). "A role for lateral hypothalamic orexin neurons in reward seeking." Nature **437**(7058): 556-559.

Hastings, M. H., E. S. Maywood and M. Brancaccio (2018). "Generation of circadian rhythms in the suprachiasmatic nucleus." Nat Rev Neurosci **19**(8): 453-469.

Hayat, H., N. Regev, N. Matosevich, A. Sales, E. Paredes-Rodriguez, A. J. Krom, L. Bergman, Y. Li, M. Lavigne, E. J. Kremer, O. Yizhar, A. E. Pickering and Y. Nir (2020). "Locus coeruleus norepinephrine activity mediates sensory-evoked awakenings from sleep." Sci Adv **6**(15): eaaz4232.

Haynes, A. C., B. Jackson, H. Chapman, M. Tadayyon, A. Johns, R. A. Porter and J. R. Arch (2000). "A selective orexin-1 receptor antagonist reduces food consumption in male and female rats." Regul Pept **96**(1-2): 45-51.

Heidari-Oranjaghi, N., H. Azhdari-Zarmehri, E. Erami and A. Haghparast (2012). "Antagonism of orexin-1 receptors attenuates swim- and restraint stress-induced antinociceptive behaviors in formalin test." Pharmacol Biochem Behav **103**(2): 299-307.

Heinricher, M.M., Tavares, I., Leith, J.L., Lumb, B.M., (2009). "Descending control of nociception: Specificity, recruitment and plasticity". Brain Research Reviews 60, 214–225..

Heisler, J. M., J. Morales, J. J. Donegan, J. D. Jett, L. Redus and J. C. O'Connor (2015). "The attentional set shifting task: a measure of cognitive flexibility in mice." J Vis Exp(96).

Hernández-Cáceres J, Macias-González R, Brozek G, Bures J. Systemic ketamine blocks cortical spreading depression but does not delay the onset of terminal anoxic depolarization in rats (1987). Brain Res. Dec 29;437(2):360-4. doi: 10.1016/0006-8993(87)91652-0. PMID: 3435842.

Herrera, D. G., D. Maysinger, R. Gadient, C. Boeckh, U. Otten and A. C. Cuello (1993). "Spreading depression induces c-fos-like immunoreactivity and NGF mRNA in the rat cerebral cortex." Brain Res **602**(1): 99-103.

Herreras, O. and G. G. Somjen (1993). "Analysis of potential shifts associated with recurrent spreading depression and prolonged unstable spreading depression induced by microdialysis of elevated K+ in hippocampus of anesthetized rats." Brain Research **610**(2): 283-294.

Hickey, L., Y. Li, S. J. Fyson, T. C. Watson, R. Perrins, J. Hewinson, A. G. Teschemacher, H. Furue, B. M. Lumb and A. E. Pickering (2014). "Optoactivation of locus ceruleus neurons evokes bidirectional changes in thermal nociception in rats." J Neurosci **34**(12): 4148-4160.

Hirschberg, S., Y. Li, A. Randall, E. J. Kremer and A. E. Pickering (2017). "Functional dichotomy in spinal- vs prefrontal-projecting locus coeruleus modules splits descending noradrenergic analgesia from ascending aversion and anxiety in rats." Elife **6**.

Ho TW, Mannix LK, Fan X, Assaid C, Furtek C, Jones CJ, Lines CR, Rapoport AM (2008). "MK-0974 Protocol 004 study group. Randomized controlled trial of an oral CGRP receptor antagonist, MK-0974, in acute treatment of migraine". Neurology. 70(16):1304-12.

Ho, Y. C., H. J. Lee, L. W. Tung, Y. Y. Liao, S. Y. Fu, S. F. Teng, H. T. Liao, K. Mackie and L. C. Chiou (2011). "Activation of orexin 1 receptors in the periaqueductal gray of male rats leads to antinociception via retrograde endocannabinoid (2-arachidonoylglycerol)-induced disinhibition." J Neurosci **31**(41): 14600-14610.

Ho AP, Dahlöf CG, Silberstein SD, Saper JR, Ashina M, Kost JT, Froman S, Leibensperger H, Lines CR, Ho TW (2010) "Randomized, controlled trial of telcagepant over four migraine attacks." Cephalalgia. (12):1443-57.

Hoffmann, J., W. Supronsinchai, S. Akerman, A. P. Andreou, C. J. Winrow, J. Renger, R. Hargreaves and P. J. Goadsby (2015). "Evidence for orexinergic mechanisms in migraine." Neurobiology of Disease **74**: 137-143.

Hoffmann, J. and A. Charles (2018). "Glutamate and Its Receptors as Therapeutic Targets for Migraine." Neurotherapeutics **15**(2): 361-370.

Holland, P. R., S. Akerman and P. J. Goadsby (2005). "Orexin 1 receptor activation attenuates neurogenic dural vasodilation in an animal model of trigeminovascular nociception." J Pharmacol Exp Ther **315**(3): 1380-1385.

Holland, P. R., S. Akerman and P. J. Goadsby (2006). "Modulation of nociceptive dural input to the trigeminal nucleus caudalis via activation of the orexin 1 receptor in the rat." Eur J Neurosci **24**(10): 2825-2833.

Holland, P. R. and P. J. Goadsby (2009). "Cluster headache, hypothalamus, and orexin." Curr Pain Headache Rep **13**(2): 147-154.

Holland, P. R. (2014). "Headache and sleep: shared pathophysiological mechanisms." Cephalalgia **34**(10): 725-744.

Holland, P. R. (2017). "Biology of Neuropeptides: Orexinergic Involvement in Primary Headache Disorders." Headache **57 Suppl 2**: 76-88.

Holland, P. R. and P. J. Goadsby (2018). "Targeted CGRP Small Molecule Antagonists for Acute Migraine Therapy." Neurotherapeutics **15**(2): 304-312.

Holland, P. R., P. Sureda-Gibert and M. Vila-Pueyo (2020). "Rapid uptake of sumatriptan into the brain: An ongoing question of blood-brain barrier permeability." Cephalalgia **40**(4): 327-329.

Holton, C. M., L. C. Strother, I. Dripps, A. Pradhan, P. J. Goadsby and P. R. Holland (2020). "ASIC3 blockade inhibits durovascular and nitric oxide-mediated trigeminal pain." British journal of pharmacology: 10.1111/bph.14990.

Horvath, T. L., C. Peyron, S. Diano, A. Ivanov, G. Aston-Jones, T. S. Kilduff and A. N. van Den Pol (1999). "Hypocretin (orexin) activation and synaptic innervation of the locus coeruleus noradrenergic system." J Comp Neurol **415**(2): 145-159.

Hoskin, K. L., H. Kaube and P. J. Goadsby (1996). "Central activation of the trigeminovascular pathway in the cat is inhibited by dihydroergotamine. A c-Fos and electrophysiological study." Brain **119 (Pt 1)**: 249-256.

Hoskin, K. L., D. C. Bulmer and P. J. Goadsby (1999). "Fos expression in the trigeminocervical complex of the cat after stimulation of the superior sagittal sinus is reduced by L-NAME." Neurosci Lett **266**(3): 173-176.

Hoskin, K. L., D. C. Bulmer, M. Lasalandra, A. Jonkman and P. J. Goadsby (2001). "Fos expression in the midbrain periaqueductal grey after trigeminovascular stimulation." J Anat **198**(Pt 1): 29-35.

Howorth, P. W., S. R. Thornton, V. O'Brien, W. D. Smith, N. Nikiforova, A. G. Teschemacher and A. E. Pickering (2009). "Retrograde viral vector-mediated inhibition of pontospinal noradrenergic neurons causes hyperalgesia in rats." J Neurosci **29**(41): 12855-12864.

Hughes, S.W., Hickey, L., Hulse, R.P., Lumb, B.M., Pickering, A.E., (2013)."Endogenous analgesic action of the pontospinal noradrenergic system spatially restricts and temporally delays the progression of neuropathic pain following tibial nerve injury". Pain 154, 1680–1690.

Hunt, S. P., A. Pini and G. Evan (1987). "Induction of c-fos-like protein in spinal cord neurons following sensory stimulation." Nature **328**(6131): 632-634.

Husain Maniyar, F., T. Sprenger, T. Monteith, C. Schankin and P. James Goadsby "Brain activations in the premonitory phase of nitroglycerin-triggered migraine attacks." A JOURNAL OF NEUROLOGY.

Hwang, C. K., U. M. D'Souza, A. J. Eisch, S. Yajima, C. H. Lammers, Y. Yang, S. H. Lee, Y. M. Kim, E. J. Nestler and M. M. Mouradian (2001). "Dopamine receptor

regulating factor, DRRF: a zinc finger transcription factor." Proc Natl Acad Sci U S A **98**(13): 7558-7563.

Ilg, A. K., T. Enkel, D. Bartsch and F. Bahner (2018). "Behavioral Effects of Acute Systemic Low-Dose Clozapine in Wild-Type Rats: Implications for the Use of DREADDs in Behavioral Neuroscience." Front Behav Neurosci **12**: 173.

Inutsuka, A., A. Inui, S. Tabuchi, T. Tsunematsu, M. Lazarus and A. Yamanaka (2014). "Concurrent and robust regulation of feeding behaviors and metabolism by orexin neurons." Neuropharmacology **85**: 451-460.

Inutsuka, A., A. Yamashita, S. Chowdhury, J. Nakai, M. Ohkura, T. Taguchi and A. Yamanaka (2016). "The integrative role of orexin/hypocretin neurons in nociceptive perception and analgesic regulation." Sci Rep **6**: 29480.

Ishiguro, H., K. S. Kim and T. H. Joh (1995). "Identification of a negative regulatory element in the 5'-flanking region of the human dopamine beta-hydroxylase gene." Brain Res Mol Brain Res **34**(2): 251-261.

Ivanov, A. and G. Aston-Jones (2000). "Hypocretin/orexin depolarizes and decreases potassium conductance in locus coeruleus neurons." Neuroreport **11**(8): 1755-1758.

Jacobs, B. L. (1986). "Single unit activity of locus coeruleus neurons in behaving animals." Prog Neurobiol **27**(2): 183-194.

Janitzky, K., M. T. Lippert, A. Engelhorn, J. Tegtmeier, J. Goldschmidt, H. J. Heinze and F. W. Ohl (2015). "Optogenetic silencing of locus coeruleus activity in mice impairs cognitive flexibility in an attentional set-shifting task." Front Behav Neurosci **9**: 286.

Janss, A. J. and G. F. Gebhart (1988). "Brainstem and spinal pathways mediating descending inhibition from the medullary lateral reticular nucleus in the rat." Brain Res **440**(1): 109-122.

Jendryka, M., M. Palchaudhuri, D. Ursu, B. van der Veen, B. Liss, D. Katzel, W. Nissen and A. Pekcec (2019). "Pharmacokinetic and pharmacodynamic actions of clozapine-N-oxide, clozapine, and compound 21 in DREADD-based chemogenetics in mice." Sci Rep **9**(1): 4522.

Johren, O., S. J. Neidert, M. Kummer, A. Dendorfer and P. Dominiak (2001). "Prepro-orexin and orexin receptor mRNAs are differentially expressed in peripheral tissues of male and female rats." Endocrinology **142**(8): 3324-3331.

Johren, O., S. J. Neidert, M. Kummer and P. Dominiak (2002). "Sexually dimorphic expression of prepro-orexin mRNA in the rat hypothalamus." Peptides **23**(6): 1177-1180.

Kajiyama, S., M. Kawamoto, S. Shiraishi, S. Gaus, A. Matsunaga, H. Suyama and O. Yuge (2005). "Spinal orexin-1 receptors mediate anti-hyperalgesic effects of intrathecally-administered orexins in diabetic neuropathic pain model rats." Brain Res **1044**(1): 76-86.

Karatas, H., S. E. Erdener, Y. Gursoy-Ozdemir, S. Lule, E. Eren-Kocak, Z. D. Sen and T. Dalkara (2013). "Spreading depression triggers headache by activating neuronal Panx1 channels." Science **339**(6123): 1092-1095.

Karnani, M. M., C. Schone, E. F. Bracey, J. A. Gonzalez, P. Viskaitis, H. T. Li, A. Adamantidis and D. Burdakov (2020). "Role of spontaneous and sensory orexin network dynamics in rapid locomotion initiation." Prog Neurobiol **187**: 101771.

Karsan, N., P. Bose and P. J. Goadsby (2018). "The Migraine Premonitory Phase." Continuum (Minneap Minn) **24**(4, Headache): 996-1008.

Karsan, N. and P. J. Goadsby (2018). "Biological insights from the premonitory symptoms of migraine." Nat Rev Neurol **14**(12): 699-710.

Karsan, N., P. R. Bose, C. Thompson, J. Newman and P. J. Goadsby (2020). "Headache and non-headache symptoms provoked by nitroglycerin in migraineurs: A human pharmacological triggering study." Cephalalgia **40**(8): 828-841.

Karsan, N. and P. J. Goadsby (2020). "Imaging the Premonitory Phase of Migraine." Front Neurol **11**: 140.

Karsan, N. and P. J. Goadsby (2021). "Migraine: beyond pain." Pract Neurol **21**(6): 475-480.

Karsan, N., P. Bose, J. Newman and P. J. Goadsby (2021). "Are some patient-perceived migraine triggers simply early manifestations of the attack?" J Neurol **268**(5): 1885-1893.

Karsan, N., A. Perez-Rodriguez, K. Nagaraj, P. R. Bose and P. J. Goadsby (2021). "The migraine postdrome: Spontaneous and triggered phenotypes." Cephalalgia **41**(6): 721-730.

Kastin, A. J. and V. Akerstrom (1999). "Orexin A but not orexin B rapidly enters brain from blood by simple diffusion." J Pharmacol Exp Ther **289**(1): 219-223.

Kaube, H., K. L. Hoskin and P. J. Goadsby (1992). "Activation of the trigeminovascular system by mechanical distension of the superior sagittal sinus in the cat." Cephalalgia **12**(3): 133-136.

Kaube, H., K. A. Keay, K. L. Hoskin, R. Bandler and P. J. Goadsby (1993). "Expression of C-Fos-Like Immunoreactivity in the Caudal Medulla and Upper Cervical Spinal-Cord Following Stimulation of the Superior Sagittal Sinus in the Cat." Brain Research **629**(1): 95-102.

Kaushik, M. K., K. Aritake, A. Imanishi, T. Kanbayashi, T. Ichikawa, T. Shimizu, Y. Urade and M. Yanagisawa (2018). "Continuous intrathecal orexin delivery inhibits cataplexy in a murine model of narcolepsy." Proc Natl Acad Sci U S A **115**(23): 6046-6051.

Kayaba, Y., A. Nakamura, Y. Kasuya, T. Ohuchi, M. Yanagisawa, I. Komuro, Y. Fukuda and T. Kuwaki (2003). "Attenuated defense response and low basal blood pressure in orexin knockout mice." Am J Physiol Regul Integr Comp Physiol **285**(3): R581-593.

Kelman, L. (2007). "The triggers or precipitants of the acute migraine attack." Cephalalgia **27**(5): 394-402.

Khatami, R., S. Birkmann and C. L. Bassetti (2007). "Amygdala dysfunction in narcolepsy-cataplexy." J Sleep Res **16**(2): 226-229.

Kim, H. S., H. Seo, C. Yang, J. F. Brunet and K. S. Kim (1998). "Noradrenergic-specific transcription of the dopamine beta-hydroxylase gene requires synergy of multiple cis-acting elements including at least two Phox2a-binding sites." J Neurosci **18**(20): 8247-8260.

Kim, S. H., J. Y. Park, H. E. Shin, S. B. Lee, D. W. Ryu, T. W. Kim and J. W. Park (2019). "The influence of rapid eye movement sleep deprivation on nociceptive transmission and the duration of facial allodynia in rats: a behavioral and Fos immunohistochemical study." J Headache Pain **20**(1): 21.

Klinck, M. P., J. S. Mogil, M. Moreau, B. D. X. Lascelles, P. A. Flecknell, T. Poitte and E. Troncy (2017). "Translational pain assessment: could natural animal models be the missing link?" Pain **158**(9): 1633-1646.

Knight, Y.E., Bartsch, T., Kaube, H., Goadsby, P.J., (2002)." P/Q-Type Calcium-Channel Blockade in the Periaqueductal Gray Facilitates Trigeminal Nociception: A Functional Genetic Link for Migraine?". The Journal of Neuroscience 22, RC213–RC213.

Knight, Y. E., J. D. Classey, M. P. Lasalandra, S. Akerman, F. Kowacs, K. L. Hoskin and P. J. Goadsby (2005). "Patterns of fos expression in the rostral medulla and caudal pons evoked by noxious craniovascular stimulation and periaqueductal gray stimulation in the cat." Brain Res **1045**(1-2): 1-11.

Knight, Y. E. and P. J. Goadsby (2001). "The periaqueductal grey matter modulates trigeminovascular input: a role in migraine?" Neuroscience **106**(4): 793-800.

Kremer, E. J., S. Boutin, M. Chillon and O. Danos (2000). "Canine adenovirus vectors: an alternative for adenovirus-mediated gene transfer." J Virol **74**(1): 505-512.

Kooshki, R., M. Abbasnejad, S. Esmaeili-Mahani, M. Raoof and V. Sheibani (2020). "Activation orexin 1 receptors in the ventrolateral periaqueductal gray matter attenuate nitroglycerin-induced migraine attacks and calcitonin gene related peptide up-regulation in trigeminal nucleus caudalis of rats." Neuropharmacology **178**: 107981.

Kosek E, Hansson P. (1997) Modulatory influence on somatosensory perception from vibration and heterotopic noxious conditioning stimulation (HNCS) in fibromyalgia patients and healthy subjects. Pain. 70(1):41-51.

Kudrow, D., Cady, R.K., Allan, B., Pederson, S.M., Hirman, J., Mehta, L.R., Schaeffler, B.A., (2021). "Long-term safety and tolerability of eptinezumab in patients with chronic migraine: a 2-year, open-label, phase 3 trial." BMC Neurology 21..

Lambert G, Michalicek J. Cortical Spreading Depression Reduces Dural Blood Flow a Possible Mechanism for Migraine Pain? (1994) *Cephalalgia*. 14(6):430-436.

Lambert, G. A., L. Truong and A. S. Zagami (2011). "Effect of cortical spreading depression on basal and evoked traffic in the trigeminovascular sensory system." Cephalalgia **31**(14): 1439-1451.

Lauritzen, M., Hansen, A.J., (1992). The Effect of Glutamate Receptor Blockade on Anoxic Depolarization and Cortical Spreading Depression. Journal of Cerebral Blood Flow & Metabolism 12, 223–229.

Lauritzen, M., Dreier, J.P., Fabricius, M., Hartings, J.A., Graf, R., Strong, A.J (2011). Clinical Relevance of Cortical Spreading Depression in Neurological Disorders: Migraine, Malignant Stroke, Subarachnoid and Intracranial Hemorrhage, and Traumatic Brain Injury. Journal of Cerebral Blood Flow & Metabolism 31, 17–35.

Lavoie, A. and B. H. Liu (2020). "Canine Adenovirus 2: A Natural Choice for Brain Circuit Dissection." Front Mol Neurosci **13**: 9.

Le Bars D, Dickenson AH, Besson JM. (1979) "Diffuse noxious inhibitory controls (DNIC). II. Lack of effect on non-convergent neurones, supraspinal involvement and theoretical implications". Pain. 3):305-327.

Leao, A. A. (1944). "Spreading depression of activity in the cerebral cortex." Journal of Neurophysiology **7**: 359-390.

Leao, A. A. (1947). "Further observations on the spreading depression of activity in the cerebral cortex." J Neurophysiol **10**(6): 409-414.

Lederle, L., S. Weber, T. Wright, M. Feyder, J. L. Brigman, H. S. Crombag, L. M. Saksida, T. J. Bussey and A. Holmes (2011). "Reward-related behavioral paradigms for addiction research in the mouse: performance of common inbred strains." PLoS One **6**(1): e15536.

Lee, J. H., E. Bang, K. J. Chae, J. Y. Kim, D. W. Lee and W. Lee (1999). "Solution structure of a new hypothalamic neuropeptide, human hypocretin-2/orexin-B." Eur J Biochem **266**(3): 831-839.

Li, W., X. Diao, C. Chen, C. Li, Y. Zhang and Y. Li (2018). "Changes in hormones of the hypothalamic-pituitary-gonadal axis in migraine patients." J Clin Neurosci **50**: 165-171.

Lipton, R. B., M. E. Bigal, M. Diamond, F. Freitag, M. L. Reed, W. F. Stewart and A. A. Group (2007). "Migraine prevalence, disease burden, and the need for preventive therapy." Neurology **68**(5): 343-349.

Lipton, R. B., M. E. Bigal, S. Ashina, R. Burstein, S. Silberstein, M. L. Reed, D. Serrano, W. F. Stewart and G. American Migraine Prevalence Prevention Advisory (2008). "Cutaneous allodynia in the migraine population." Ann Neurol **63**(2): 148-158.

Lipton, R. B., D. C. Buse, C. B. Hall, H. Tennen, T. A. Defreitas, T. M. Borkowski, B. M. Grosberg and S. R. Haut (2014). "Reduction in perceived stress as a migraine trigger: testing the "let-down headache" hypothesis." Neurology **82**(16): 1395-1401.

Lipton, R.B., Croop, R., Stock, E.G., Stock, D.A., Morris, B.A., Frost, M., Dubowchik, G.M., Conway, C.M., Coric, V., Goadsby, P.J., (2019). "Rimegepant, an Oral Calcitonin Gene–Related Peptide Receptor Antagonist, for Migraine." New England Journal of Medicine 381, 142–149.

Lipton, R.B., Goadsby, P.J., Smith, J., Schaeffler, B.A., Biondi, D.M., Hirman, J., Pederson, S., Allan, B., Cady, R., (2020) "Efficacy and safety of eptinezumab in patients with chronic migraine." Neurology 94, e1365–e1377..

Li, Y., L. Hickey, R. Perrins, E. Werlen, A. A. Patel, S. Hirschberg, M. W. Jones, S. Salinas, E. J. Kremer and A. E. Pickering (2016). "Retrograde optogenetic characterization of the pontospinal module of the locus coeruleus with a canine adenoviral vector." Brain Res **1641**(Pt B): 274-290.

Li, Z., L. Kelly, M. Heiman, P. Greengard and J. M. Friedman (2015). "Hypothalamic Amylin Acts in Concert with Leptin to Regulate Food Intake." Cell Metab **22**(6): 1059-1067.

Likhtik, E. and J. P. Johansen (2019). "Neuromodulation in circuits of aversive emotional learning." Nat Neurosci **22**(10): 1586-1597.

Liu, Y., J. Broman and L. Edvinsson (2008). "Central projections of the sensory innervation of the rat middle meningeal artery." Brain Res **1208**: 103-110.

Liu, Y., J. Broman, M. Zhang and L. Edvinsson (2009). "Brainstem and thalamic projections from a craniovascular sensory nervous centre in the rostral cervical spinal dorsal horn of rats." Cephalalgia **29**(9): 935-948.

Llorca-Torralba, M., G. Borges, F. Neto, J. A. Mico and E. Berrocoso (2016). "Noradrenergic Locus Coeruleus pathways in pain modulation." Neuroscience **338**: 93-113.

Lui, J. Z., N. P. Young, J. O. Ebbert, J. K. Rosedahl and L. M. Philpot (2020). "Loneliness and Migraine Self-Management: A Cross-Sectional Assessment." J Prim Care Community Health **11**: 2150132720924874.

MacLaren, D. A., R. W. Browne, J. K. Shaw, S. Krishnan Radhakrishnan, P. Khare, R. A. Espana and S. D. Clark (2016). "Clozapine N-Oxide Administration Produces Behavioral Effects in Long-Evans Rats: Implications for Designing DREADD Experiments." eNeuro **3**(5).

Magon, S., A. May, A. Stankewitz, P. J. Goadsby, A. R. Tso, M. Ashina, F. M. Amin, C. L. Seifert, M. M. Chakravarty, J. Muller and T. Sprenger (2015). "Morphological Abnormalities of Thalamic Subnuclei in Migraine: A Multicenter MRI Study at 3 Tesla." J Neurosci **35**(40): 13800-13806.

Mahler, S. V. and G. Aston-Jones (2018). "CNO Evil? Considerations for the Use of DREADDs in Behavioral Neuroscience." Neuropsychopharmacology **43**(5): 934-936.

Mahoney, C. E., A. Cogswell, I. J. Koralnik and T. E. Scammell (2019). "The neurobiological basis of narcolepsy." Nat Rev Neurosci **20**(2): 83-93.

Malick, A. and R. Burstein (1998). "Cells of origin of the trigeminohypothalamic tract in the rat." J Comp Neurol **400**(1): 125-144.

Malick, A., R. M. Strassman and R. Burstein (2000). "Trigeminohypothalamic and reticulohypothalamic tract neurons in the upper cervical spinal cord and caudal medulla of the rat." J Neurophysiol **84**(4): 2078-2112.

Malick, A., M. Jakubowski, J. K. Elmquist, C. B. Saper and R. Burstein (2001). "A neurohistochemical blueprint for pain-induced loss of appetite." Proc Natl Acad Sci U S A **98**(17): 9930-9935.

Maniyar, F. H., T. Sprenger, T. Monteith, C. Schankin and P. J. Goadsby (2014). "Brain activations in the premonitory phase of nitroglycerin-triggered migraine attacks." Brain **137**(Pt 1): 232-241.

Manoukian, R., Sun, H., Miller, S., Shi, D., Chan, B., Xu, C., (2019). "Effects of monoclonal antagonist antibodies on calcitonin gene-related peptide receptor function and trafficking". The Journal of Headache and Pain 20.

Maolood, N. and B. Meister (2010). "Nociceptin/orphanin FQ peptide in hypothalamic neurones associated with the control of feeding behaviour." J Neuroendocrinol **22**(2): 75-82.

Marcus R, Goadsby PJ, Dodick D, Stock D, Manos G, Fischer TZ. (2014) "BMS-927711 for the acute treatment of migraine: a double-blind, randomized, placebo controlled, dose-ranging trial." Cephalalgia. Feb;34(2):114-25. Epub 2013 Aug 21. PMID: 23965396.

Marrannes R, Willems R, De Prins E, Wauquier A. Evidence for a role of the N-methyl-D-aspartate (NMDA) receptor in cortical spreading depression in the rat (1988). Brain Res. 457(2):226-40.

Marcus, J. N., C. J. Aschkenasi, C. E. Lee, R. M. Chemelli, C. B. Saper, M. Yanagisawa and J. K. Elmquist (2001). "Differential expression of orexin receptors 1 and 2 in the rat brain." Journal of Comparative Neurology **435**(1): 6-25.

Martins-Oliveira, M., S. Akerman, P. R. Holland, J. R. Hoffmann, I. Tavares and P. J. Goadsby (2017). "Neuroendocrine signaling modulates specific neural networks relevant to migraine." Neurobiol Dis **101**: 16-26.

Martins-Oliveira, M., I. Tavares and P. J. Goadsby (2021). "Was it something I ate? Understanding the bidirectional interaction of migraine and appetite neural circuits." Brain Res **1770**: 147629.

Mathew, P. G., F. M. Cutrer and I. Garza (2016). "A touchy subject: an assessment of cutaneous allodynia in a chronic migraine population." J Pain Res **9**: 101-104.

Matos, M. R., E. Visser, I. Kramvis, R. J. van der Loo, T. Gebuis, R. Zalm, P. Rao-Ruiz, H. D. Mansvelder, A. B. Smit and M. C. van den Oever (2019). "Memory strength gates the involvement of a CREB-dependent cortical fear engram in remote memory." Nat Commun **10**(1): 2315.

Matsushita, M., M. Ikeda and N. Okado (1982). "The cells of origin of the trigeminothalamic, trigeminospinal and trigeminocerebellar projections in the cat." Neuroscience **7**(6): 1439-1454.

McCall, J. G., R. Al-Hasani, E. R. Siuda, D. Y. Hong, A. J. Norris, C. P. Ford and M. R. Bruchas (2015). "CRH Engagement of the Locus Coeruleus Noradrenergic System Mediates Stress-Induced Anxiety." Neuron **87**(3): 605-620.

McCrone, P., P. T. Seed, A. J. Dowson, L. V. Clark, L. H. Goldstein, M. Morgan and L. Ridsdale (2011). "Service use and costs for people with headache: a UK primary care study." J Headache Pain **12**(6): 617-623.

McNaughton, F. L. and W. Feindel (1977). Innervation of intracranial structures: a reappraisal. Physiological aspects of clinical neurology. F. C. Rose. Oxford, Blackwell Scientific**:** 279-293.

Messina, G., C. Dalia, D. Tafuri, V. Monda, F. Palmieri, A. Dato, A. Russo, S. De Blasio, A. Messina, V. De Luca, S. Chieffi and M. Monda (2014). "Orexin-A controls sympathetic activity and eating behavior." Front Psychol **5**: 997.

Mieda, M., J. T. Willie, J. Hara, C. M. Sinton, T. Sakurai and M. Yanagisawa (2004). "Orexin peptides prevent cataplexy and improve wakefulness in an orexin neuron-ablated model of narcolepsy in mice." Proc Natl Acad Sci U S A **101**(13): 4649-4654.

Mieda, M., N. Tsujino and T. Sakurai (2013). "Differential roles of orexin receptors in the regulation of sleep/wakefulness." Front Endocrinol (Lausanne) **4**: 57.

Millan, M. J. (2002). "Descending control of pain." Prog Neurobiol **66**(6): 355-474.

Mintz, E. M., A. N. van den Pol, A. A. Casano and H. E. Albers (2001). "Distribution of hypocretin-(orexin) immunoreactivity in the central nervous system of Syrian hamsters (Mesocricetus auratus)." J Chem Neuroanat **21**(3): 225-238.

Mobarakeh, J. I., K. Takahashi, S. Sakurada, S. Nishino, H. Watanabe, M. Kato and K. Yanai (2005). "Enhanced antinociception by intracerebroventricularly and

intrathecally-administered orexin A and B (hypocretin-1 and -2) in mice." Peptides **26**(5): 767-777.

Mogil, J. S. (2009). "Animal models of pain: progress and challenges." Nat Rev Neurosci **10**(4): 283-294.

Mogil, J. S., K. D. Davis and S. W. Derbyshire (2010). "The necessity of animal models in pain research." Pain **151**(1): 12-17.

Mondal, M. S., M. Nakazato, Y. Date, N. Murakami, M. Yanagisawa and S. Matsukura (1999). "Widespread distribution of orexin in rat brain and its regulation upon fasting." Biochem Biophys Res Commun **256**(3): 495-499.

Moreno-Ajona, D., A. Perez-Rodriguez and P. J. Goadsby (2020). "Gepants, calcitonin-gene-related peptide receptor antagonists: what could be their role in migraine treatment?" Curr Opin Neurol **33**(3): 309-315.

Moulton, E. A., L. Becerra, A. Johnson, R. Burstein and D. Borsook (2014). "Altered hypothalamic functional connectivity with autonomic circuits and the locus coeruleus in migraine." PloS one **9**: e95508.

Moulton, E. A., R. Burstein, S. Tully, R. Hargreaves, L. Becerra and D. Borsook (2008). "Interictal dysfunction of a brainstem descending modulatory center in migraine patients." PLoS One **3**(11): e3799.

Morris, L. S., J. G. McCall, D. S. Charney and J. W. Murrough (2020). "The role of the locus coeruleus in the generation of pathological anxiety." Brain Neurosci Adv **4**: 2398212820930321.

Murphy, P., M. Moline, D. Mayleben, R. Rosenberg, G. Zammit, K. Pinner, S. Dhadda, Q. Hong, L. Giorgi and A. Satlin (2017). "Lemborexant, A Dual Orexin Receptor Antagonist (DORA) for the Treatment of Insomnia Disorder: Results From a Bayesian, Adaptive, Randomized, Double-Blind, Placebo-Controlled Study." J Clin Sleep Med **13**(11): 1289-1299.

Muschamp, J. W., J. A. Hollander, J. L. Thompson, G. Voren, L. C. Hassinger, S. Onvani, T. M. Kamenecka, S. L. Borgland, P. J. Kenny and W. A. Carlezon, Jr. (2014). "Hypocretin (orexin) facilitates reward by attenuating the antireward effects of its cotransmitter dynorphin in ventral tegmental area." Proc Natl Acad Sci U S A **111**(16): E1648-1655.

Nagai, Y., N. Miyakawa, H. Takuwa, Y. Hori, K. Oyama, B. Ji, M. Takahashi, X. P. Huang, S. T. Slocum, J. F. DiBerto, Y. Xiong, T. Urushihata, T. Hirabayashi, A. Fujimoto, K. Mimura, J. G. English, J. Liu, K. I. Inoue, K. Kumata, C. Seki, M.

Ono, M. Shimojo, M. R. Zhang, Y. Tomita, J. Nakahara, T. Suhara, M. Takada, M. Higuchi, J. Jin, B. L. Roth and T. Minamimoto (2020). "Deschloroclozapine, a potent and selective chemogenetic actuator enables rapid neuronal and behavioral modulations in mice and monkeys." Nat Neurosci **23**(9): 1157-1167.

Nahman-Averbuch, H., Granovsky, Y., Coghill, R.C., Yarnitsky, D., Sprecher, E., Weissman-Fogel, I., (2013). "Waning of "Conditioned Pain Modulation": A Novel Expression of Subtle Pronociception in Migraine." Headache: The Journal of Head and Face Pain 53, 1104–1115.

Navratilova, E., S. Behravesh, J. Oyarzo, D. W. Dodick, P. Banerjee and F. Porreca (2020). "Ubrogepant does not induce latent sensitization in a preclinical model of medication overuse headache." Cephalalgia **40**(9): 892-902.

Negro, A., J. L. Seidel, T. Houben, E. S. Yu, I. Rosen, A. J. Arreguin, N. Yalcin, L. Shorser-Gentile, L. Pearlman, H. Sadhegian, R. Vetrivelan, N. L. Chamberlin, C. Ayata, P. Martelletti, M. A. Moskowitz and K. Eikermann-Haerter (2020). "Acute sleep deprivation enhances susceptibility to the migraine substrate cortical spreading depolarization." J Headache Pain **21**(1): 86.

Nellgård B, Wieloch T. NMDA-receptor blockers but not NBQX, an AMPA-receptor antagonist, inhibit spreading depression in the rat brain. Acta Physiol Scand. 1992 Dec;146(4):497-503.

Nixon, J. P., V. Mavanji, T. A. Butterick, C. J. Billington, C. M. Kotz and J. A. Teske (2015). "Sleep disorders, obesity, and aging: the role of orexin." Ageing Res Rev **20**: 63-73.

Noseda, R., M. Jakubowski, V. Kainz, D. Borsook and R. Burstein (2011). "Cortical projections of functionally identified thalamic trigeminovascular neurons: implications for migraine headache and its associated symptoms." J Neurosci **31**(40): 14204-14217.

Noseda, R., V. Kainz, M. Jakubowski, J. J. Gooley, C. B. Saper, K. Digre and R. Burstein (2010). "A neural mechanism for exacerbation of headache by light." Nat Neurosci **13**(2): 239-245.

Nygren, L. G. and L. Olson (1977). "A new major projection from locus coeruleus: the main source of noradrenergic nerve terminals in the ventral and dorsal columns of the spinal cord." Brain Res **132**(1): 85-93.

Oguchi, M., M. Okajima, S. Tanaka, M. Koizumi, T. Kikusui, N. Ichihara, S. Kato, K. Kobayashi and M. Sakagami (2015). "Double Virus Vector Infection to the Prefrontal Network of the Macaque Brain." PLoS One **10**(7): e0132825.

O'Hare, L. (2017). "Multisensory Integration in Migraine: Recent Developments." Multisens Res **30**(6): 549-563.

Olesen J, Friberg L, Olsen TS, Iversen HK, Lassen NA, Andersen AR, Karle A. (1990) "Timing and topography of cerebral blood flow, aura, and headache during migraine attacks." Ann Neurol. Dec;28(6):791-8.

Olesen, J., Diener, H.-C., Husstedt, I.W., Goadsby, P.J., Hall, D., Meier, U., Pollentier, S., Lesko, L.M., (2004) "Calcitonin Gene–Related Peptide Receptor Antagonist BIBN 4096 BS for the Acute Treatment of Migraine." New England Journal of Medicine 350, 1104–1110.

Oppenheimer, N. J. and J. W. Bodley (1981). "Diphtheria toxin. Site and configuration of ADP-ribosylation of diphthamide in elongation factor 2." J Biol Chem **256**(16): 8579-8581.

Ozcan, R. K. and S. G. Ozmen (2019). "The Association Between Migraine, Metabolic Syndrome, Insulin Resistance, and Obesity in Women: A Case-Control Study." Sisli Etfal Hastan Tip Bul **53**(4): 395-402.

Pantazis, C. B., M. H. James, S. O'Connor, N. Shin and G. Aston-Jones (2021). "Orexin-1 receptor signaling in ventral tegmental area mediates cue-driven demand for cocaine." Neuropsychopharmacology.

Pareja-Angel, J. and A. Campo-Arias (2004). "[The prevalence of symptoms of anxiety and depression in female migraine sufferers]." Rev Neurol **39**(8): 711-714.

Pavlovic, J. M., D. Akcali, H. Bolay, C. Bernstein and N. Maleki (2017). "Sex-related influences in migraine." J Neurosci Res **95**(1-2): 587-593.

Park, J., H. Moon, S. Akerman, P. R. Holland, M. P. Lasalandra, A. P. Andreou, M. D. Ferrari, A. M. van den Maagdenberg and P. J. Goadsby (2014). "Differential trigeminovascular nociceptive responses in the thalamus in the familial hemiplegic migraine 1 knock-in mouse: a Fos protein study." Neurobiol Dis **64**: 1-7.

Paxinos, G. and C. Watson (1986). The Rat Brain in Stereotaxic Coordinates. London, Academic Press.

Pearl, T. A., G. Dumkrieger, C. D. Chong, D. W. Dodick and T. J. Schwedt (2020). "Impact of Depression and Anxiety Symptoms on Patient-Reported Outcomes in

Patients With Migraine: Results From the American Registry for Migraine Research (ARMR)." Headache **60**(9): 1910-1919.

Penfield, W. and F. McNAUGHTON (1940). "Dural headache and innervation of the dura mater." Archives of Neurology & Psychiatry **44**(1): 43-75.

Peres, M. F., M. A. Stiles, H. C. Siow and S. D. Silberstein (2005). "Excessive daytime sleepiness in migraine patients." J Neurol Neurosurg Psychiatry **76**(10): 1467-1468.

Peres, M. F. P., J. P. P. Mercante, P. R. Tobo, H. Kamei and M. E. Bigal (2017). "Anxiety and depression symptoms and migraine: a symptom-based approach research." J Headache Pain **18**(1): 37.

Percie du Sert, N., V. Hurst, A. Ahluwalia, S. Alam, M. T. Avey, M. Baker, W. J. Browne, A. Clark, I. C. Cuthill, U. Dirnagl, M. Emerson, P. Garner, S. T. Holgate, D. W. Howells, N. A. Karp, S. E. Lazic, K. Lidster, C. J. MacCallum, M. Macleod, E. J. Pearl, O. H. Petersen, F. Rawle, P. Reynolds, K. Rooney, E. S. Sena, S. D. Silberberg, T. Steckler and H. Wurbel (2020). "The ARRIVE guidelines 2.0: updated guidelines for reporting animal research." BMJ Open Sci **4**(1): e100115.

Perrotta A, Serrao M, Sandrini G, Burstein R, Sances G, Rossi P, Bartolo M, Pierelli F, Nappi G. (2010) "Sensitisation of spinal cord pain processing in medication overuse headache involves supraspinal pain control." Cephalalgia.30(3):272-84.

Peters, C.M., Hayashida, K.-I., Suto, T., Houle, T.T., Aschenbrenner, C.A., Martin, T.J., Eisenach, J.C., (2015). "Individual Differences in Acute Pain-induced Endogenous Analgesia Predict Time to Resolution of Postoperative Pain in the Rat." Anesthesiology 122, 895–907..

Peyron, C., D. K. Tighe, A. N. van den Pol, L. de Lecea, H. C. Heller, J. G. Sutcliffe and T. S. Kilduff (1998). "Neurons containing hypocretin (orexin) project to multiple neuronal systems." J Neurosci **18**(23): 9996-10015.

Pielsticker A, Haag G, Zaudig M, Lautenbacher S. (2005) "Impairment of pain inhibition in chronic tension-type headache." Pain. 118(1-2):215-23.

Podvin, S., T. Yaksh and V. Hook (2016). "The Emerging Role of Spinal Dynorphin in Chronic Pain: A Therapeutic Perspective." Annu Rev Pharmacol Toxicol **56**: 511-533.

Poe, G. R., S. Foote, O. Eschenko, J. P. Johansen, S. Bouret, G. Aston-Jones, C. W. Harley, D. Manahan-Vaughan, D. Weinshenker, R. Valentino, C. Berridge, D. J. Chandler, B. Waterhouse and S. J. Sara (2020). "Locus coeruleus: a new look at the blue spot." Nat Rev Neurosci **21**(11): 644-659.

Porcaro, C., G. Di Lorenzo, S. Seri, F. Pierelli, F. Tecchio and G. Coppola (2017). "Impaired brainstem and thalamic high-frequency oscillatory EEG activity in migraine between attacks." Cephalalgia **37**(10): 915-926.

Porreca F, Ossipov MH, Gebhart GF (2002). "Chronic pain and medullary descending facilitation. Trends Neurosci." (6):319-25.

Raddant, A.C., Russo, A.F., 2011. Calcitonin gene-related peptide in migraine: intersection of peripheral inflammation and central modulation. Expert Reviews in Molecular Medicine 13.. doi:10.1017/s1462399411002067

Rainero, I., S. Gallone, E. Rubino, P. Ponzo, W. Valfre, E. Binello, P. Fenoglio, S. Gentile, M. Anoaica, M. Gasparini and L. Pinessi (2008). "Haplotype analysis confirms the association between the HCRTR2 gene and cluster headache." Headache **48**(7): 1108-1114.

Rainero, I., E. Rubino, S. Gallone, P. Fenoglio, L. R. Picci, L. Giobbe, L. Ostacoli and L. Pinessi (2011). "Evidence for an association between migraine and the hypocretin receptor 1 gene." J Headache Pain **12**(2): 193-199.

Randeva, H. S., E. Karteris, D. Grammatopoulos and E. W. Hillhouse (2001). "Expression of orexin-A and functional orexin type 2 receptors in the human adult adrenals: Implications for adrenal function and energy homeostasis." Journal of Clinical Endocrinology and Metabolism **86**(10): 4808-4813.

Rapoport, A. M., M. E. Bigal, S. J. Tepper and F. D. Sheftell (2004). "Intranasal medications for the treatment of migraine and cluster headache." CNS Drugs **18**(10): 671-685.

Rau, J. C., E. Navratilova, J. Oyarzo, K. W. Johnson, S. K. Aurora, T. J. Schwedt, D. W. Dodick and F. Porreca (2020). "Evaluation of LY573144 (lasmiditan) in a preclinical model of medication overuse headache." Cephalalgia **40**(9): 903-912.

Ray, B. S. and H. G. Wolff (1940). "Experimental studies on headache: pain-sensitive structures of the head and their significance in headache." Archives of Surgery **41**(4): 813-856.

Ray, B. S. and H. G. Wolff (1940). "Experimental studies on headache: pain-sensitive structures of the head and their significance in headache." Archives of Surgery **41**: 813-856.

Recober, A., Russo, A.F., 2009. Calcitonin gene-related peptide: an update on the biology. Current Opinion in Neurology 22, 241–246.. doi:10.1097/wco.0b013e32832b2427

Recober, A., Kuburas, A., Zhang, Z., Wemmie, J.A., Anderson, M.G., Russo, A.F., 2009. Role of Calcitonin Gene-Related Peptide in Light-Aversive Behavior: Implications for Migraine. The Journal of Neuroscience 29, 8798–8804.. doi:10.1523/jneurosci.1727-09.2009

Recober, A., Kaiser, E.A., Kuburas, A., Russo, A.F., 2010. Induction of multiple photophobic behaviors in a transgenic mouse sensitized to CGRP. Neuropharmacology 58, 156–165.. doi:10.1016/j.neuropharm.2009.07.009

Reuter, U., Ehrlich, M., Gendolla, A., Heinze, A., Klatt, J., Wen, S., Hours-Zesiger, P., Nickisch, J., Sieder, C., Hentschke, C., Maier-Peuschel, M., (2022.) "Erenumab versus topiramate for the prevention of migraine – a randomised, double-blind, active-controlled phase 4 trial." Cephalalgia 42, 108–118..

Rivera-Mancilla, E., L. Al-Hassany, C. M. Villalon and A. MaassenVanDenBrink (2021). "Metabolic Aspects of Migraine: Association With Obesity and Diabetes Mellitus." Front Neurol **12**: 686398.

Robert, C., L. Bourgeais, C. D. Arreto, M. Condes-Lara, R. Noseda, T. Jay and L. Villanueva (2013). "Paraventricular hypothalamic regulation of trigeminovascular mechanisms involved in headaches." J Neurosci **33**(20): 8827-8840.

Rodriguez, E., K. Sakurai, J. Xu, Y. Chen, K. Toda, S. Zhao, B. X. Han, D. Ryu, H. Yin, W. Liedtke and F. Wang (2017). "A craniofacial-specific monosynaptic circuit enables heightened affective pain." Nat Neurosci **20**(12): 1734-1743.

Roh, J. H., H. Jiang, M. B. Finn, F. R. Stewart, T. E. Mahan, J. R. Cirrito, A. Heda, B. J. Snider, M. Li, M. Yanagisawa, L. de Lecea and D. M. Holtzman (2014). "Potential role of orexin and sleep modulation in the pathogenesis of Alzheimer's disease." J Exp Med **211**(13): 2487-2496.

Ross, S.B., Stenfors, C., (2015) "DSP4, a Selective Neurotoxin for the Locus Coeruleus Noradrenergic System. A Review of Its Mode of Action." Neurotoxicity Research 27, 15–30.

Russell, F. A., R. King, S. J. Smillie, X. Kodji and S. D. Brain (2014). "Calcitonin gene-related peptide: physiology and pathophysiology." Physiol Rev **94**(4): 1099-1142.

Russo, A.F., Dickerson, I.M., 2006. CGRP: a Multifunctional Neuropeptide, in: . pp. 391–426.. doi:10.1007/978-0-387-30381-9_19

Saengjaroentham, C., L. C. Strother, I. Dripps, M. R. Sultan Jabir, A. Pradhan, P. J. Goadsby and P. R. Holland (2020). "Differential medication overuse risk of novel anti-migraine therapeutics." Brain **143**(9): 2681-2688.

Sakurai, T., A. Amemiya, M. Ishii, I. Matsuzaki, R. M. Chemelli, H. Tanaka, S. C. Williams, J. A. Richardson, G. P. Kozlowski, S. Wilson, J. R. S. Arch, R. E. Buckingham, A. C. Haynes, S. A. Carr, R. S. Annan, D. E. McNulty, W. S. Liu, J. A. Terrett, N. A. Elshourbagy, D. J. Bergsma and M. Yanagisawa (1998). "Orexins and orexin receptors: A family of hypothalamic neuropeptides and G protein-coupled receptors that regulate feeding behavior (vol 92, pg 573, 1998)." Cell **92**(5): U29-U29.

Sakurai, T. (2005). "Reverse pharmacology of orexin: from an orphan GPCR to integrative physiology." Regul Pept **126**(1-2): 3-10.

Sakurai, T. (2005). "Roles of orexin/hypocretin in regulation of sleep/wakefulness and energy homeostasis." Sleep Med Rev **9**(4): 231-241.

Sakurai, T. (2007). "The neural circuit of orexin (hypocretin): maintaining sleep and wakefulness." Nat Rev Neurosci **8**(3): 171-181.

Sakurai, T., (2014). "The role of orexin in motivated behaviours." Nature Reviews Neuroscience 15, 719–731.

Samuels, E. R. and E. Szabadi (2008). "Functional neuroanatomy of the noradrenergic locus coeruleus: its roles in the regulation of arousal and autonomic function part I: principles of functional organisation." Curr Neuropharmacol **6**(3): 235-253.

Samuels, E. R. and E. Szabadi (2008). "Functional neuroanatomy of the noradrenergic locus coeruleus: its roles in the regulation of arousal and autonomic function part II: physiological and pharmacological manipulations and pathological alterations of locus coeruleus activity in humans." Curr Neuropharmacol **6**(3): 254-285.

Sanchez-Garcia, A., G. A. Cabral-Pacheco, V. C. Zomosa-Signoret, R. Ortiz-Lopez, A. Camacho, P. M. Tabera-Tarello, J. A. Garnica-Lopez and R. Vidaltamayo (2018). "Modular organization of a hypocretin gene minimal promoter." Mol Med Rep **17**(2): 2263-2270.

Sand, T., N. Zhitniy, L. R. White and L. J. Stovner (2008). "Visual evoked potential latency, amplitude and habituation in migraine: a longitudinal study." Clin Neurophysiol **119**(5): 1020-1027.

Sandrini G, Rossi P, Milanov I, Serrao M, Cecchini A, Nappi G. (2006) "Abnormal Modulatory Influence of Diffuse Noxious Inhibitory Controls in Migraine and Chronic Tension-Type Headache Patients."Cephalalgia. 26(7):782-789.

Santangelo, G., A. Russo, L. Trojano, F. Falco, L. Marcuccio, M. Siciliano, F. Conte, F. Garramone, A. Tessitore and G. Tedeschi (2016). "Cognitive dysfunctions and

psychological symptoms in migraine without aura: a cross-sectional study." J Headache Pain **17**(1): 76.

Sara, S. J. and M. Segal (1991). "Plasticity of sensory responses of locus coeruleus neurons in the behaving rat: implications for cognition." Prog Brain Res **88**: 571-585.

Sasa, M. and S. Takaori (1973). "Influence of the locus coeruleus on transmission in the spinal trigeminal nucleus neurons." Brain Res **55**(1): 203-208.

Schone, C., J. Apergis-Schoute, T. Sakurai, A. Adamantidis and D. Burdakov (2014). "Coreleased orexin and glutamate evoke nonredundant spike outputs and computations in histamine neurons." Cell Rep **7**(3): 697-704.

Schulte, L. H., T. P. Jurgens and A. May (2015). "Photo-, osmo- and phonophobia in the premonitory phase of migraine: mistaking symptoms for triggers?" J Headache Pain **16**: 14.

Schulte, L. H. and A. May (2016). "The migraine generator revisited: continuous scanning of the migraine cycle over 30 days and three spontaneous attacks." Brain **139**(Pt 7): 1987-1993.

Schulte, L. H., A. Allers and A. May (2017). "Hypothalamus as a mediator of chronic migraine: Evidence from high-resolution fMRI." Neurology **88**(21): 2011-2016.

Schwedt, T. J. (2013). "Multisensory integration in migraine." Curr Opin Neurol **26**(3): 248-253.

Seibenhener, M. L. and M. C. Wooten (2015). "Use of the Open Field Maze to measure locomotor and anxiety-like behavior in mice." J Vis Exp(96): e52434.

Shrewsbury, S. B., M. Jeleva, K. H. Satterly, J. Lickliter and J. Hoekman (2019). "STOP 101: A Phase 1, Randomized, Open-Label, Comparative Bioavailability Study of INP104, Dihydroergotamine Mesylate (DHE) Administered Intranasally by a I123 Precision Olfactory Delivery (POD((R))) Device, in Healthy Adult Subjects." Headache **59**(3): 394-409.

Schwedt, T. J. (2013). "Multisensory integration in migraine." Curr Opin Neurol **26**(3): 248-253.

Shields, K. G. and P. J. Goadsby (2006). "Serotonin receptors modulate trigeminovascular responses in ventroposteromedial nucleus of thalamus: a migraine target?" Neurobiol Dis **23**(3): 491-501.

Shigenaga, Y., Z. Nakatani, T. Nishimori, S. Suemune, R. Kuroda and S. Matano (1983). "The cells of origin of cat trigeminothalamic projections: especially in the caudal medulla." Brain Res **277**(2): 201-222.

Sicuteri, F., P. Periti, B. Anselmi and M. Fanciullacci (1965). "[Tryptaminuria and serotonin and catecholamine catabolism in the course of migraine]." Boll Soc Ital Biol Sper **41**(9): 474-475.

Siemian, J. N., M. A. Arenivar, S. Sarsfield, C. B. Borja, L. J. Erbaugh, A. L. Eagle, A. J. Robison, G. Leinninger and Y. Aponte (2021). "An excitatory lateral hypothalamic circuit orchestrating pain behaviors in mice." Elife **10**.

Simpson, K. L., D. W. Altman, L. Wang, M. L. Kirifides, R. C. Lin and B. D. Waterhouse (1997). "Lateralization and functional organization of the locus coeruleus projection to the trigeminal somatosensory pathway in rat." J Comp Neurol **385**(1): 135-147.

Skljarevski, V., Matharu, M., Millen, B.A., Ossipov, M.H., Kim, B.-K., Yang, J.Y., (2018.) "Efficacy and safety of galcanezumab for the prevention of episodic migraine: Results of the EVOLVE-2 Phase 3 randomized controlled clinical trial." Cephalalgia 38, 1442–1454..

Sofia Beas, B., X. Gu, Y. Leng, O. Koita, S. Rodriguez-Gonzalez, M. Kindel, B. A. Matikainen-Ankney, R. S. Larsen, A. V. Kravitz, M. A. Hoon and M. A. Penzo (2020). "A ventrolateral medulla-midline thalamic circuit for hypoglycemic feeding." Nat Commun **11**(1): 6218.

Soudais, C., C. Laplace-Builhe, K. Kissa and E. J. Kremer (2001). "Preferential transduction of neurons by canine adenovirus vectors and their efficient retrograde transport in vivo." FASEB J **15**(12): 2283-2285.

Soya, S., H. Shoji, E. Hasegawa, M. Hondo, T. Miyakawa, M. Yanagisawa, M. Mieda and T. Sakurai (2013). "Orexin receptor-1 in the locus coeruleus plays an important role in cue-dependent fear memory consolidation." J Neurosci **33**(36): 14549-14557.

Soya, S., T. M. Takahashi, T. J. McHugh, T. Maejima, S. Herlitze, M. Abe, K. Sakimura and T. Sakurai (2017). "Orexin modulates behavioral fear expression through the locus coeruleus." Nat Commun **8**(1): 1606.

Soya, S. and T. Sakurai (2020). "Orexin as a modulator of fear-related behavior: Hypothalamic control of noradrenaline circuit." Brain Res **1731**: 146037.

Sprenger, T., M. Viana and C. Tassorelli (2018). "Current Prophylactic Medications for Migraine and Their Potential Mechanisms of Action." Neurotherapeutics **15**(2): 313-323.

Stankewitz, A., D. Aderjan, F. Eippert and A. May (2011). "Trigeminal nociceptive transmission in migraineurs predicts migraine attacks." J Neurosci **31**(6): 1937-1943.

Stanyer, E. C., H. Creeney, A. D. Nesbitt, P. R. Holland and J. Hoffmann (2021). "Subjective Sleep Quality and Sleep Architecture in Patients With Migraine: A Meta-analysis." Neurology **97**(16): e1620-e1631.

Stauffer, V.L., Dodick, D.W., Zhang, Q., Carter, J.N., Ailani, J., Conley, R.R., (2018.) "Evaluation of Galcanezumab for the Prevention of Episodic Migraine". JAMA Neurology 75, 1080.

Steiner, T. J., L. J. Stovner, Z. Katsarava, J. M. Lainez, C. Lampl, M. Lanteri-Minet, D. Rastenyte, E. Ruiz de la Torre, C. Tassorelli, J. Barre and C. Andree (2014). "The impact of headache in Europe: principal results of the Eurolight project." J Headache Pain **15**: 31.

Steiner, T. J., L. J. Stovner, R. Jensen, D. Uluduz, Z. Katsarava and H. Lifting The Burden: the Global Campaign against (2020). "Migraine remains second among the world's causes of disability, and first among young women: findings from GBD2019." J Headache Pain **21**(1): 137.

Sternson, S. M. and B. L. Roth (2014). "Chemogenetic tools to interrogate brain functions." Annu Rev Neurosci **37**: 387-407.

Stevens, L., L. E. Larsen, W. Van Lysebettens, E. Carrette, P. Boon, R. Raedt and K.

Totah, N. K. B., N. K. Logothetis and O. Eschenko (2019). "Noradrenergic ensemble-based modulation of cognition over multiple timescales." Brain Res **1709**: 50-66.

Stevens, L., L. E. Larsen, W. Van Lysebettens, E. Carrette, P. Boon, R. Raedt and K. Vonck (2021). "Optimized Parameters for Transducing the Locus Coeruleus Using Canine Adenovirus Type 2 (CAV2) Vector in Rats for Chemogenetic Modulation Research." Front Neurosci **15**: 663337.

Strassman, A. M., B. P. Vos, Y. Mineta, S. Naderi, D. Borsook and R. Burstein (1993). "Fos-like immunoreactivity in the superficial medullary dorsal horn induced by noxious and innocuous thermal stimulation of facial skin in the rat." J Neurophysiol **70**(5): 1811-1821.

Strassman, A. M., Y. Mineta and B. P. Vos (1994). "Distribution of fos-like immunoreactivity in the medullary and upper cervical dorsal horn produced by stimulation of dural blood vessels in the rat." J Neurosci **14**(6): 3725-3735.

Strassman, A. M., S. A. Raymond and R. Burstein (1996). "Sensitization of meningeal sensory neurons and the origin of headaches." Nature **384**(6609): 560-564.

Sugimoto, T., Y. F. He, C. Xiao and H. Ichikawa (1998). "c-fos induction in the subnucleus oralis following trigeminal nerve stimulation." Brain Res **783**(1): 158-162.

Summ, O., Charbit, A.R., Andreou, A.P., Goadsby, P.J., 2010. Modulation of nocioceptive transmission with calcitonin gene-related peptide receptor antagonists in the thalamus. Brain 133, 2540–2548.. doi:10.1093/brain/awq224

Suyama, H., M. Kawamoto, S. Shiraishi, S. Gaus, S. Kajiyama and O. Yuge (2004). "Analgesic effect of intrathecal administration of orexin on neuropathic pain in rats." In Vivo **18**(2): 119-123.

Suzuki R, Rygh LJ, Dickenson AH (2004)."Bad news from the brain: descending 5-HT pathways that control spinal pain processing". Trends Pharmacol Sci.(12):613-7.

Takahashi, K., Y. Kayama, J. S. Lin and K. Sakai (2010). "Locus coeruleus neuronal activity during the sleep-waking cycle in mice." Neuroscience **169**(3): 1115-1126.

Takeuchi, T., A. J. Duszkiewicz, A. Sonneborn, P. A. Spooner, M. Yamasaki, M. Watanabe, C. C. Smith, G. Fernandez, K. Deisseroth, R. W. Greene and R. G. Morris (2016). "Locus coeruleus and dopaminergic consolidation of everyday memory." Nature **537**(7620): 357-362.

Tassorelli, C. and S. A. Joseph (1995). "Systemic nitroglycerin induces Fos immunoreactivity in brainstem and forebrain structures of the rat." Brain Res **682**(1-2): 167-181.

Tejeda, H. A. and A. Bonci (2019). "Dynorphin/kappa-opioid receptor control of dopamine dynamics: Implications for negative affective states and psychiatric disorders." Brain Res **1713**: 91-101.

Ter Horst, G. J., W. J. Meijler, J. Korf and R. H. Kemper (2001). "Trigeminal nociception-induced cerebral Fos expression in the conscious rat." Cephalalgia **21**(10): 963-975.

Tervo, D. G., B. Y. Hwang, S. Viswanathan, T. Gaj, M. Lavzin, K. D. Ritola, S. Lindo, S. Michael, E. Kuleshova, D. Ojala, C. C. Huang, C. R. Gerfen, J. Schiller, J. T. Dudman, A. W. Hantman, L. L. Looger, D. V. Schaffer and A. Y. Karpova (2016).

"A Designer AAV Variant Permits Efficient Retrograde Access to Projection Neurons." Neuron **92**(2): 372-382.

Tiseo, C., A. Vacca, A. Felbush, T. Filimonova, A. Gai, T. Glazyrina, I. A. Hubalek, Y. Marchenko, L. H. Overeem, S. Piroso, A. Tkachev, P. Martelletti, S. Sacco and S. European Headache Federation School of Advanced (2020). "Migraine and sleep disorders: a systematic review." J Headache Pain **21**(1): 126.

Trivedi, P., H. Yu, D. J. MacNeil, L. H. Van der Ploeg and X. M. Guan (1998). "Distribution of orexin receptor mRNA in the rat brain." FEBS Lett **438**(1-2): 71-75.

Tso, A. R. and P. J. Goadsby (2017). "Anti-CGRP Monoclonal Antibodies: the Next Era of Migraine Prevention?" Curr Treat Options Neurol **19**(8): 27.

Tsujino, N. and T. Sakurai (2013). "Role of orexin in modulating arousal, feeding, and motivation." Frontiers in behavioral neuroscience **7**: 28.

Vaiva, G., F. Ducrocq, K. Jezequel, B. Averland, P. Lestavel, A. Brunet and C. R. Marmar (2003). "Immediate treatment with propranolol decreases posttraumatic stress disorder two months after trauma." Biol Psychiatry **54**(9): 947-949.

van den Pol, A. N. (1999). "Hypothalamic hypocretin (orexin): Robust innervation of the spinal cord." Journal of Neuroscience **19**(8): 3171-3182.

van Oosterhout, W., E. van Someren, G. G. Schoonman, M. A. Louter, G. J. Lammers, M. D. Ferrari and G. M. Terwindt (2018). "Chronotypes and circadian timing in migraine." Cephalalgia **38**(4): 617-625.

Vazey, E. M., D. E. Moorman and G. Aston-Jones (2018). "Phasic locus coeruleus activity regulates cortical encoding of salience information." Proc Natl Acad Sci U S A **115**(40): E9439-E9448.

Veinante, P., M. F. Jacquin and M. Deschenes (2000). "Thalamic projections from the whisker-sensitive regions of the spinal trigeminal complex in the rat." J Comp Neurol **420**(2): 233-243.

Venner, A., M. M. Karnani, J. A. Gonzalez, L. T. Jensen, L. Fugger and D. Burdakov (2011). "Orexin neurons as conditional glucosensors: paradoxical regulation of sugar sensing by intracellular fuels." J Physiol **589**(Pt 23): 5701-5708.

Vetvik, K. G. and E. A. MacGregor (2017). "Sex differences in the epidemiology, clinical features, and pathophysiology of migraine." Lancet Neurol **16**(1): 76-87.

Viana, M., F. Khaliq, C. Zecca, M. D. L. Figuerola, G. Sances, V. Di Piero, B. Petolicchio, M. Alessiani, P. Geppetti, C. Lupi, S. Benemei, R. Iannacchero, F. Maggioni, M.

E. Jurno, S. Odobescu, E. Chiriac, A. Marfil, F. Brighina, N. Barrientos Uribe, C. Perez Lago, C. Bordini, F. Lucchese, V. Maffey, G. Nappi, G. Sandrini and C. Tassorelli (2020). "Poor patient awareness and frequent misdiagnosis of migraine: findings from a large transcontinental cohort." Eur J Neurol **27**(3): 536-541.

Viana, M., M. Linde, G. Sances, N. Ghiotto, E. Guaschino, M. Allena, S. Terrazzino, G. Nappi, P. J. Goadsby and C. Tassorelli (2016). "Migraine aura symptoms: Duration, succession and temporal relationship to headache." Cephalalgia **36**(5): 413-421.

Viana, M., G. Sances, M. Linde, N. Ghiotto, E. Guaschino, M. Allena, S. Terrazzino, G. Nappi, P. J. Goadsby and C. Tassorelli (2017). "Clinical features of migraine aura: Results from a prospective diary-aided study." Cephalalgia **37**(10): 979-989.

Vila-Pueyo, M., L. C. Strother, M. Kefel, P. J. Goadsby and P. R. Holland (2018). "Divergent influences of the locus coeruleus on migraine pathophysiology." Pain.

Vila-Pueyo, M., K. Page, P. R. Murdock, H. J. Loraine, A. J. Woodrooffe, K. W. Johnson, P. J. Goadsby and P. R. Holland (2021). "The selective 5-HT1F receptor agonist lasmiditan inhibits trigeminal nociceptive processing: Implications for migraine and cluster headache." Br J Pharmacol.

Viana, M., M. Linde, G. Sances, N. Ghiotto, E. Guaschino, M. Allena, S. Terrazzino, G. Nappi, P. J. Goadsby and C. Tassorelli (2016). "Migraine aura symptoms: Duration, succession and temporal relationship to headache." Cephalalgia **36**(5): 413-421.

Vonck (2021). "Optimized Parameters for Transducing the Locus Coeruleus Using Canine Adenovirus Type 2 (CAV2) Vector in Rats for Chemogenetic Modulation Research." Front Neurosci **15**: 663337.

Voss T, Lipton RB, Dodick DW, Dupre N, Ge JY, Bachman R, et al. A phase IIb randomized, double-blind, placebo-controlled trial of ubrogepant for the acute treatment of migraine. Cephalalgia. 2016;3

Waeber, C. and M. A. Moskowitz (1995). "[3H]sumatriptan labels both 5-HT1D and 5-HT1F receptor binding sites in the guinea pig brain: an autoradiographic study." Naunyn Schmiedebergs Arch Pharmacol **352**(3): 263-275.

Wang, T., N. Chen, W. Zhan, J. Liu, J. Zhang, Q. Liu, H. Huang, L. He, J. Zhang and Q. Gong (2015). "Altered effective connectivity of posterior thalamus in migraine with cutaneous allodynia: a resting-state fMRI study with Granger causality analysis." J Headache Pain **17**: 17.

Wang, M., B. N. Mason, L. P. Sowers, A. Kuburas, B. J. Rea and A. F. Russo (2021). "Investigating Migraine-Like Behavior using Light Aversion in Mice." J Vis Exp(174).

Watanabe, S., T. Kuwaki, M. Yanagisawa, Y. Fukuda and M. Shimoyama (2005). "Persistent pain and stress activate pain-inhibitory orexin pathways." Neuroreport **16**(1): 5-8.

Waterhouse, B. D. and R. L. Navarra (2019). "The locus coeruleus-norepinephrine system and sensory signal processing: A historical review and current perspectives." Brain Res **1709**: 1-15.

Waters, K. (2021). "Review of the Efficacy and Safety of Lemborexant, a Dual Receptor Orexin Antagonist (DORA), in the Treatment of Adults With Insomnia Disorder." Ann Pharmacother: 10600280211008492.

Wei, H. and A. Pertovaara (2006). "Spinal and pontine alpha2-adrenoceptors have opposite effects on pain-related behavior in the neuropathic rat." Eur J Pharmacol **551**(1-3): 41-49.

Weiller, C., A. May, V. Limmroth, M. Juptner, H. Kaube, R. V. Schayck, H. H. Coenen and H. C. Diener (1995). "Brain stem activation in spontaneous human migraine attacks." Nat Med **1**(7): 658-660.

Weinhold, S. L., M. Seeck-Hirschner, A. Nowak, M. Hallschmid, R. Goder and P. C. Baier (2014). "The effect of intranasal orexin-A (hypocretin-1) on sleep, wakefulness and attention in narcolepsy with cataplexy." Behav Brain Res **262**: 8-13.

Welander, N. Z., J. Mwinyi, S. Asif, H. B. Schioth, A. Skalkidou and E. Fransson (2021). "Migraine as a risk factor for mixed symptoms of peripartum depression and anxiety in late pregnancy: A prospective cohort study." J Affect Disord **295**: 733-739.

Westlund, K. N., L. S. Sorkin, D. G. Ferrington, S. M. Carlton, H. H. Willcockson and W. D. Willis (1990). "Serotoninergic and noradrenergic projections to the ventral posterolateral nucleus of the monkey thalamus." J Comp Neurol **295**(2): 197-207.

Westlund, K. N., D. Zhang, S. M. Carlton, L. S. Sorkin and W. D. Willis (1991). "Noradrenergic innervation of somatosensory thalamus and spinal cord." Prog Brain Res **88**: 77-88.

W. D. Willis (1990). "Serotoninergic and noradrenergic projections to the ventral posterolateral nucleus of the monkey thalamus." J Comp Neurol **295**(2): 197-207.

Wilcox, S. L., R. Veggeberg, J. Lemme, D. J. Hodkinson, S. Scrivani, R. Burstein, L. Becerra and D. Borsook (2016). "Increased Functional Activation of Limbic Brain Regions during Negative Emotional Processing in Migraine." Front Hum Neurosci **10**: 366.

Williams, G., C. Bing, X. J. Cai, J. A. Harrold, P. J. King and X. H. Liu (2001). "The hypothalamus and the control of energy homeostasis: different circuits, different purposes." Physiol Behav **74**(4-5): 683-701.

Williams, M. N., D. S. Zahm and M. F. Jacquin (1994). "Differential foci and synaptic organization of the principal and spinal trigeminal projections to the thalamus in the rat." Eur J Neurosci **6**(3): 429-453.

Willie, J. T., R. M. Chemelli, C. M. Sinton, S. Tokita, S. C. Williams, Y. Y. Kisanuki, J. N. Marcus, C. Lee, J. K. Elmquist, K. A. Kohlmeier, C. S. Leonard, J. A. Richardson, R. E. Hammer and M. Yanagisawa (2003). "Distinct narcolepsy syndromes in Orexin receptor-2 and Orexin null mice: molecular genetic dissection of Non-REM and REM sleep regulatory processes." Neuron **38**(5): 715-730.

Wolff, B. S., S. A. Raheem and L. N. Saligan (2018). "Comparing passive measures of fatigue-like behavior in mice." Sci Rep **8**(1): 14238.

Xie, J. Y., M. De Felice, C. M. Kopruszinski, N. Eyde, J. LaVigne, B. Remeniuk, P. Hernandez, X. Yue, N. Goshima, M. Ossipov, T. King, J. M. Streicher, E. Navratilova, D. Dodick, H. Rosen, E. Roberts and F. Porreca (2017). "Kappa opioid receptor antagonists: A possible new class of therapeutics for migraine prevention." Cephalalgia **37**(8): 780-794.

Xu M, Kontinen VK, Kalso E. (1999) Endogenous noradrenergic tone controls symptoms of allodynia in the spinal nerve ligation model of neuropathic pain. Eur J Pharmacol. ;366(1):41-5.

Yamamoto, T., N. Nozaki-Taguchi and T. Chiba (2002). "Analgesic effect of intrathecally administered orexin-A in the rat formalin test and in the rat hot plate test." Br J Pharmacol **137**(2): 170-176.

Yamamoto, T., O. Saito, K. Shono, T. Aoe and T. Chiba (2003). "Anti-mechanical allodynic effect of intrathecal and intracerebroventricular injection of orexin-A in the rat neuropathic pain model." Neurosci Lett **347**(3): 183-186.

Yamamoto, T., O. Saito, K. Shono and S. Hirasawa (2003). "Activation of spinal orexin-1 receptor produces anti-allodynic effect in the rat carrageenan test." Eur J Pharmacol **481**(2-3): 175-180.

Yamanaka, A., C. T. Beuckmann, J. T. Willie, J. Hara, N. Tsujino, M. Mieda, M. Tominaga, K. Yagami, F. Sugiyama, K. Goto, M. Yanagisawa and T. Sakurai (2003). "Hypothalamic orexin neurons regulate arousal according to energy balance in mice." Neuron **38**(5): 701-713.

Yang, C., H. S. Kim, H. Seo, C. H. Kim, J. F. Brunet and K. S. Kim (1998). "Paired-like homeodomain proteins, Phox2a and Phox2b, are responsible for noradrenergic cell-specific transcription of the dopamine beta-hydroxylase gene." J Neurochem **71**(5): 1813-1826.

Yang, Y. C., C. C. Hu and Y. C. Lai (2015). "Non-additive modulation of synaptic transmission by serotonin, adenosine, and cholinergic modulators in the sensory thalamus." Front Cell Neurosci **9**: 60.

Yang, C. P., M. L. Hsieh, J. H. Chiang, H. Y. Chang and V. C. Hsieh (2017). "Migraine and risk of narcolepsy in children: A nationwide longitudinal study." PLoS One **12**(12): e0189231.

Zagami, A. S. and G. A. Lambert (1990). "Stimulation of cranial vessels excites nociceptive neurones in several thalamic nuclei of the cat." Exp Brain Res **81**(3): 552-566.

Zagami, A. S. and G. A. Lambert (1991). "Craniovascular application of capsaicin activates nociceptive thalamic neurones in the cat." Neurosci Lett **121**(1-2): 187-190.

Ziegeler, C., J. Mehnert, K. Asmussen and A. May (2020). "Central effects of erenumab in migraine patients: An event-related functional imaging study." Neurology **95**(20): e2794-e2802.

Zhang, H., I. Lecker, C. Collymore, A. Dokova, M. C. Pham, S. F. Rosen, H. Crawhall-Duk, M. Zain, M. Valencia, H. F. Filippini, J. Li, A. J. D'Souza, C. Cho, V. Michailidis, P. D. Whissell, I. Patel, H. W. Steenland, W. J. Virginia Lee, M. Moayedi, T. L. Sterley, J. S. Bains, J. A. Stratton, J. R. Matyas, J. Biernaskie, D. Dubins, I. Vukobradovic, A. Bezginov, A. M. Flenniken, L. J. Martin, J. S. Mogil and R. P. Bonin (2021). "Cage-lid hanging behavior as a translationally relevant measure of pain in mice." Pain **162**(5): 1416-1425.

Zhang, J., S. Sampogna, F. R. Morales and M. H. Chase (2002). "Hypocretin (orexin)-like immunoreactivity in the central nervous system of the guinea pig." Sleep **25**: 402.

Zhang, J. H., S. Sampogna, F. R. Morales and M. H. Chase (2001). "Orexin (hypocretin)-like immunoreactivity in the cat hypothalamus: A light and electron microscopic study." Sleep **24**(1): 67-76.

Zhang, J. H., S. Sampogna, F. R. Morales and M. H. Chase (2002). "Co-localization of hypocretin-1 and hypocretin-2 in the cat hypothalamus and brainstem." Peptides **23**(8): 1479-1483.

Zhang, J. H., S. Sampogna, F. R. Morales and M. H. Chase (2004). "Distribution of hypocretin (orexin) immunoreactivity in the feline pons and medulla." Brain Res **995**(2): 205-217.

Zhang, X., D. Levy, V. Kainz, R. Noseda, M. Jakubowski and R. Burstein (2011). "Activation of central trigeminovascular neurons by cortical spreading depression." Ann Neurol **69**(5): 855-865.

Zhou, W., K. Cheung, S. Kyu, L. Wang, Z. Guan, P. A. Kurien, P. E. Bickler and L. Y. Jan (2018). "Activation of orexin system facilitates anesthesia emergence and pain control." Proc Natl Acad Sci U S A **115**(45): E10740-E10747.

Zhu, H. and B. L. Roth (2014). "Silencing synapses with DREADDs." Neuron **82**(4): 723-725.

Zhu, H. and B. L. Roth (2014). "DREADD: a chemogenetic GPCR signaling platform." Int J Neuropsychopharmacol **18**(1).

Zou Q, Long X, Zuo X, Yan C, Zhu C, Yang Y, Liu D, He Y, Zang Y (2009). "Functional connectivity between the thalamus and visual cortex under eyes closed and eyes open conditions: a resting-state fMRI study". Hum Brain Mapp. (9):3066-78.